UNIVERSITY OF CALIFORNIA, SAN DIEGO

Characterization of new roles for the glucanosyltransferase Gas1 and other carbohydrate modifying enzymes in transcriptional silencing in the yeast *Saccharomyces cerevisiae*

A dissertation submitted in partial satisfaction of the requirements for the degree Doctor of Philosophy

in

Biology

by

Melissa R. Koch

Committee in charge:

Professor Lorraine Pillus, Chair
Professor Richard Gallo
Professor Tracy Johnson
Professor James Kadonaga
Professor James Wilhelm

2009

The Dissertation of Melissa R. Koch is approved, and it is acceptable in quality and form for publication on microfilm and electronically:

Chair

University of California, San Diego

2009

To my husband, Tyree Koch, and my parents, Fred and Terri Krick

TABLE OF CONTENTS

Signature Page……...iii

Dedication……..iv

Table of Contents……v

List of Abbreviations……..x

List of Figures……xi

List of Tables……..xvii

Acknowledgements……..xix

Vita and Publications……...xxi

Abstract of Dissertation……..xxii

Chapter 1 Introduction: Silent chromatin formation and regulation in the yeast *S. cerevisiae*……1

Silencer elements and silencer-binding proteins……6

The SIR and RENT silencing complexes……...8

The role of histone modifications in silent chromatin formation……...10

Assembly of the SIR complex and silent chromatin formation……16

Regulation of silent chromatin spreading……19

The nuclear periphery and silent chromatin formation……22

Conclusions……...23

Chapter 2 The glucanosyltransferase Gas1 functions in transcriptional silencing

INTRODUCTION……25

RESULTS…….28

Deletion of *GAS1* causes decreased telomeric silencing and increased rDNA silencing…….28

Telomeric silencing function is not a general property of proteins with roles in cell wall biogenesis……..35

Well-defined hallmarks of silent chromatin are intact in *gas1*Δ……...36

Gas1 silencing function is potentially mediated through its interaction with Sir2……46

Gas1's enzymatic activity is required for transcriptional silencing…..54

DISCUSSION……...56

A distinct role for *GAS1* in transcriptional silencing……61

A role for carbohydrate modification in chromatin function……62

MATERIALS AND METHODS……..66

Chapter 3 Genetic analyses in the characterization of *GAS1* functions……...77

INTRODUCTION……77

RESULTS…….80

Simultaneous expression of *MAT*a and *MAT*α suppresses *gas1*Δ temperature sensitivity……..80

The *gas1*Δ telomeric silencing defect is suppressed by DNA tethering of Sir1 and Sir2, *SIR2* and *SIR3* overexpression, and *SIR1* deletion…89

Reciprocal effects of *GAS5* on *gas1*Δ temperature sensitivity and telomeric silencing defects……94

GAS1 deletion displays synthetic growth defects with *eaf1*Δ, *orc2-1*, and *rpd3*Δ strains……..99

DISCUSSION…….119

Cell type-specific suppression of *gas1*Δ temperature sensitivity……124

SIR-specific effects on the *gas1*Δ telomeric silencing defect…….125

Effects of other *GAS* genes on *gas1*Δ phenotypes……..127

Synthetic genetic interactions between *GAS1* and other silencing genes……129

MATERIALS AND METHODS……134

Chapter 4 Biochemical and cell biological investigation of Gas1 function in transcriptional silencing……..141

INTRODUCTION……..141

RESULTS……...143

Further investigation of silent chromatin and silent chromatin factors in *gas1*Δ mutants…….143

Purified Gas1 did not alter Sir2 activity *in vitro*…….151

β-1,3-glucanase treatments of protein extracts for analysis of the potentially β -glucan-modified Sir2……161

Unresolved tests of protein-protein interactions between Gas1 and the SIR complex members Sir2 and Sir3……..162

DISCUSSION…….180

MATERIALS AND METHODS……184

Chapter 5 The Sir2-interacting protein Kre6 functions in transcriptional silencing..191

INTRODUCTION……..191

RESULTS……...193

Deletion of *KRE6* results in a defect in telomeric silencing……...193

Slow growth and temperature sensitivity was observed in *kre6*Δ *sir2*Δ mutants……198

DISCUSSION…….205

MATERIALS AND METHODS……214

Chapter 6 Initial dissection of carbohydrate modification pathways in transcriptional silencing……..218

INTRODUCTION……..218

RESULTS……...223

Deletion of *FKS1* leads to a defect in silencing telomeres……..223

Deletion of *PMT1* decreases telomeric silencing and enhances *gas1*Δ phenotypes, including its defect in telomeric silencing……..228

DISCUSSION…….235

MATERIALS AND METHODS……239

Chapter 7 Future Directions……...242

The function of *GAS1* in transcriptional silencing……..242

Other carbohydrate modification enzymes are involved in transcriptional silencing……..245

Appendix A Two-hybrid analysis of Sir2-interacting proteins with Sir2 family members and catalytically inactive sir2-H364Y…….249

Two-hybrid analysis of Hst2 with Sir2-interacting proteins: Gas1 and Dps1 interact with full-length Hst2……..249

Two-hybrid analysis of Sir2 family members with Sir2-interacting proteins: Luc7 interacts specifically with the core domain of Sir2……253

Two-hybrid analysis of catalytically inactive sir2-H364Y with Sir2-interacting proteins: Ktr4's interaction with Sir2 is dependent on Sir2's deacetylase activity…….……261

MATERIALS AND METHODS……269

Appendix B Slx5 interacts with Sir2 by GST affinity binding……..273

Slx5 interacts with Sir2 by GST affinity binding……...273

Slx5 interacts with Sir2 in the absence of Slx8 and the SIR complex……273

MATERIALS AND METHODS……280

Appendix C Cell type specific defects in telomeric silencing……...283

Wild-type pseudodiploids are defective in telomeric silencing……..283

Wild-type diploids are defective in telomeric silencing…….283

Understanding the molecular basis for the telomeric silencing defect seen upon simultaneous expression of *MAT***a** and *MAT*α……....290

MATERIALS AND METHODS……293

REFERENCES……295

LIST OF ABBREVIATIONS

5-FOA	5-fluoroorotic acid
AAR	O-acetyl-ADP-ribose
ARS	autonomous replicating sequence
ChIP	chromatin immunoprecipitation
DAPI	4',6-diamidino-2-phenylindole
dSLAM	diploid-based synthetic lethality analysis on microarray
GAD	Gal4 activation domain
GBD	Gal4 binding domain
GFP	green fluorescent protein
GST	glutathione S-transferase
FT	flow-through
IN	input
IP	immunoprecipitation
NAD^+	nicotinamide adenine dinucleotide
NTS	non-transcribed spacer
NuA4	nucleosomal acetylation of histone H4
O-GlcNAc	O-linked beta-N acetylglucosamine
ORC	origin recognition complex
ORF	open reading frame
rDNA	ribosomal DNA
RENT	regulator of nucleolar silencing and telophase exit
SC	synthetic complete
SGA	synthetic genetic array
SIR	silent information regulator
SRR	Sir2 responsive region
WT	wild-type
YPD	yeast extract-peptone-dextrose

LIST OF FIGURES

Page

Figure 1-1. A SIR-centric view of three major silenced regions in *S. cerevisiae*…..3

Figure 1-2. Sites of acetylation, methylation, and ubiquitination of histone residues implicated in transcriptional silencing……...12

Figure 2-1. *GAS1* functions in transcriptional silencing……..30

Figure 2-2. Silencing of *HMR* and 25S rDNA is unaffected in *gas1*Δ mutants…..32

Figure 2-3. The *gas1*Δ telomeric silencing defect is not telomere or promoter specific……..34

Figure 2-4. The *GAS1* telomeric silencing function is not shared with other cell wall genes……..38

Figure 2-5. Sir2 and Sir3 levels are unchanged in *gas1*Δ mutants……..40

Figure 2-6. Key features of silent chromatin are unaltered in *gas1*Δ mutants…….42

Figure 2-7. Sir3 binds to the telomere and localizes to telomeric foci in *gas1*Δ; the *in vitro* histone deacetylase activity of Sir2 is unaffected by Gas1…..44

Figure 2-8. GFP-Gas1 localizes to the nuclear periphery and is functional in telomeric silencing……49

Figure 2-9. Sir2 interacts with Gas1 by two-hybrid and GST affinity binding…...51

Figure 2-10. Catalytically inactive versions of Sir2 and Gas1 interact by GST affinity binding; *GAS1* function in telomeric silencing is separable from its role at the cell wall; Sir2 is immunoprecipitated by anti-β-1,3-glucan in *sir3*Δ *sir4*Δ strains…….53

Figure 2-11. Gas1 enzymatic activity is required for transcriptional silencing and is linked to Sir2……58

Figure 2-12. A model summarizing Gas1 effects on transcriptional silencing……..60

Figure 2-13. Genome-wide acetylation of histone H3K9,K14, H4K5, and H4K16 is not controlled by *GAS1*……64

Figure 3-1. The temperature sensitivity of *gas1*Δ is suppressed by deletion of any of the four *SIR* genes……82

Figure 3-2. The temperature sensitivity of *gas1*Δ on synthetic medium is only partially suppressed by combined deletion of multiple *SIR* genes in the same strain……84

Figure 3-3. The temperature sensitivity of *gas1*Δ on rich medium is only partially suppressed by combined deletion of multiple *SIR* genes in the same strain……..86

Figure 3-4. Overexpression of *SIR* genes does not affect *gas1*Δ temperature sensitivity……..88

Figure 3-5. Simultaneous expression of *MAT***a** and *MAT*α in the same strain suppresses *gas1*Δ temperature sensitivity……91

Figure 3-6. DNA tethering of Sir1 or Sir2 to a telomeric reporter gene rescues the *gas1*Δ telomeric silencing defect……..93

Figure 3-7. Overexpression of *SIR2* and *SIR3* partially suppresses the *gas1*Δ telomeric silencing defect……96

Figure 3-8. Deletion of *SIR1* suppresses the *gas1*Δ telomeric silencing defect…...98

Figure 3-9. *GAS5* overexpression rescues *gas1*Δ temperature sensitivity…….101

Figure 3-10. *GAS5* overexpression rescues the *gas1*Δ telomeric silencing defect..103

Figure 3-11. Deletion of *GAS5* exacerbates *gas1*Δ slow growth on rich media and sensitivity to elevated temperature……..105

Figure 3-12. Deletion of *GAS3* and/or *GAS5* does not alter the *gas1*Δ silencing defect at telomere V-R……107

Figure 3-13. Deletion of *GAS5* exacerbates the *gas1*Δ telomeric silencing defect at telomere VII-L……109

Figure 3-14. Deletion of *GAS1* is not synthetically sick in combination with *dot1*Δ in the W303 genetic background…….112

Figure 3-15. Deletion of *GAS1* is not synthetically sick in combination with *dot1*Δ in the BY4741 genetic background…….114

Figure 3-16. Deletion of *GAS1* is synthetically lethal in combination with *orc2-1* in the W303 genetic background…….116

Figure 3-17. Deletion of *GAS1* is synthetically lethal in combination with *eaf1*Δ in the W303 genetic background…….118

Figure 3-18. Deletion of *GAS1* is synthetically lethal in combination with *rpd3*Δ in the W303 genetic background…….121

Figure 3-19. Deletion of *GAS1* is synthetically sick in combination with *rpd3*Δ at high temperature in the BY4741 genetic background…….123

Figure 4-1. Sir4 binds to the telomere in *gas1*Δ mutants……...146

Figure 4-2. Gas1 does not bind to the telomere…….148

Figure 4-3. Sir2 and Sir4 co-immunoprecipitate when Sir4 is immunoprecipitated in a *gas1*Δ strain……..150

Figure 4-4. Sir3 may be hyperphosphorylated in *gas1*Δ mutants……..153

Figure 4-5. GFP-Yku70 localization may be more diffuse in *gas1*Δ mutants…...155

Figure 4-6. GFP-Yku80 localization may be more diffuse in *gas1*Δ mutants…...157

Figure 4-7. Sir2 deacetylase activity is not enhanced in the presence of Gas1 or laminarin in NAD^+ hydrolysis assays…….160

Figure 4-8. Zymolyase treatment of whole cell extracts leads to disappearance of Sir2 and appearance of a novel band in only *gas1*Δ and *gas1*Δ *gas3*Δ *gas5*Δ strains……...164

Figure 4-9. Zymolyase treatment leads to some degradation of β-tubulin and phosphoglycerate kinase but not complete loss of either protein…...166

Figure 4-10. Purified glucanase treatment does not degrade or alter Sir2……..…168

Figure 4-11. The band that appears in zymolyase-treated whole-cell extracts from *gas1*Δ strains on the Sir2 immunoblot is not Sir2-specific…….170

Figure 4-12. Sir2 and Gas1 do not co-immunoprecipiate……172

Figure 4-13. Gas1 and Sir2 may interact by GST affinity binding……..175

Figure 4-14. Sir3 and Gas1 may co-immunoprecipitate……..177

Figure 4-15. Gas1 may interact with Sir3 fragments by GST affinity binding…...179

Figure 5-1. Deletion of *KRE6* causes defects in transcriptional silencing at telomeres…….195

Figure 5-2. The *kre6*Δ telomeric silencing defect is partially complemented by *KRE6*, and *KRE6* overexpression interferes with telomeric silencing in wild-type cells…….197

Figure 5-3. Sir2 remains enriched at telomeres in *kre6*Δ mutants……..200

Figure 5-4. Deletion of *KRE6* does not affect 5S ribosomal DNA silencing……202

Figure 5-5. Multiple isolates of *kre6*Δ *sir2*Δ strains are temperature sensitive….204

Figure 5-6. The temperature sensitivity of *kre6*Δ *sir2*Δ is not complemented by *SIR2* and is partially complemented by *KRE6* overexpression……...207

Figure 5-7. A model for Gas1 and Kre6 contributions to telomeric silencing through Sir2, or a Sir2-interacting factor……211

Figure 6-1. Fks1 and Pmt1 function in the same pathway as Gas1 to modify cell wall proteins……220

Figure 6-2. Deletion of *FKS1* leads to defects in transcriptional silencing at telomeres…….225

Figure 6-3. Deletion of *FKS1* partially suppresses *gas1*Δ temperature sensitivity but does not alter *gas1*Δ's telomeric silencing defect……..227

Figure 6-4. Deletion of *FKS1* or *PMT1* does not increase silencing in the rDNA……...230

Figure 6-5. Deletion of *PMT1* leads to slight, variable, telomeric silencing defects.....232

Figure 6-6. Deletion of *PMT1* exacerbates *gas1*Δ slow growth, temperature sensitivity, and telomeric silencing defects…….234

Figure 6-7. A model for how Fks1 and Pmt1 function with Gas1 to strengthen telomeric silencing through modification of Sir2 or a Sir2-interacting factor……...237

Figure A-1. Full-length Hst2 interacts with Gas1 and Dps1 by two-hybrid……..252

Figure A-2. Gas1 interacts with specific Sir2 family members……..256

Figure A-3. Pat1 interacts with all Sir2 family members……...258

Figure A-4. Luc7 interacts specifically with Sir2……...260

Figure A-5. Ktr4 fails to interact with catalytically inactive sir2-H364Y……..264

Figure A-6. Pph22 interacts weakly with catalytically inactive sir2-H364Y…….266

Figure A-7. Pho11 interacts weakly with catalytically inactive sir2-H364Y…….268

Figure B-1. Slx5 interacts with Sir2 by GST affinity binding……...275

Figure B-2. Slx5 interacts with Sir2 in the absence of Slx8……...277

Figure B-3. Slx5 interacts with Sir2 in the absence of Slx8 and the SIR complex members Sir3 and Sir4……279

Figure C-1. Simultaneous expression of *MAT***a** and *MAT*α creates a telomeric silencing defect in wild-type cells……...285

Figure C-2. Wild-type diploids are defective in telomeric silencing…….287

Figure C-3. *MAT***a**/*MAT***a** and *MAT*α/*MAT*α diploids partially silence telomeres…….289

Figure C-4. Telomeric silencing is more defective in wild-type *MAT***a**/*MAT*α diploids when they are homozygous for the TELV-R::*ADE2* reporter……292

LIST OF TABLES

Page

Table 1-1. *Saccharomyces cerevisiae* silencing genes……4

Table 2-1. Yeast strains used in Chapter 2……67

Table 2-2. Oligonucleotides used in Chapter 2……..70

Table 2-3. Plasmids used in Chapter 2……...72

Table 3-1. Effects of *SIR* gene dosage on *gas1*Δ telomeric silencing defect and temperature sensitivity……128

Table 3-2. Effects of *GAS* gene dosage on *gas1*Δ telomeric silencing defect and temperature sensitivity……....128

Table 3-3. Yeast strains used in Chapter 3……...135

Table 3-4. Plasmids used in Chapter 3…….....139

Table 3-5. Oligonucleotides used in Chapter 3……....140

Table 4-1. Yeast strains used in Chapter 4……...186

Table 4-2. Plasmids used in Chapter 4……187

Table 5-1. Yeast strains used in Chapter 5……...215

Table 5-2. Oligonucleotides used in Chapter 5……216

Table 5-3. Plasmids used in Chapter 5……217

Table 6-1. Yeast strains used in Chapter 6……...240

Table 6-2. Oligonucleotides used in Chapter 6……241

Table A-1. Two-hybrid analysis of Sir2-interacting proteins with full-length Hst2……250

Table A-2. Two-hybrid analysis of Sir2-interacting proteins with Sir2 family members……..254

Table A-3. Two-hybrid analysis of Sir2-interacting proteins with sir2-H364Y...262

Table A-4. Plasmids used in Appendix A…….270

Table A-5. Oligonucleotides used in Appendix A……271

Table B-1. Yeast strains used in Appendix B……...282

Table C-1. Yeast strains used in Appendix C……...294

ACKNOWLEDGEMENTS

I would especially like to thank Lorraine Pillus for the opportunity to complete my thesis research in her lab. I thank her for her guidance and support of this project. Her encouragement through every step of this project was critical for my success.

Thanks to my family, my husband Tyree Koch, and my parents, Fred and Terri Krick, for being supportive throughout graduate school. Ty, you have been with me through this journey and I appreciate your willingness to come to the lab at odd hours. Mom and Dad, you encouraged me to go to graduate school to further my education, and I could not be happier with the decision I made to pursue a Biology Ph.D.

Thanks to Erin Scott and Christie Chang, fellow graduate students in the lab, who have made this experience memorable, in and outside of lab, from lunchtime conversations, to weekend hikes, to dinner parties. I thank current and former lab members for their advice to help progress this project, including Erin, Christie, Sandi Jacobson, Sandy Garcia, Russell Darst, Eric Gamache, Erik Spedale, Sunny Lo, Anne Lafon, Stephen Gilmore, Renee Garza, Tricia Laurenson, Jeanne Wilson, Myriam Ruault, Viet Le, Cara Cast, Anna Shemorry, and Eva Samal.

I especially thank Sandy for early contributions to this work and observations included in Chapter 2. Thanks to Young Chun and Rei Otsuka, undergraduate students I worked with who contributed strains used in Chapter 2. I also thank rotation students I worked with, Julia Claggett, Jesse Vargas, Anne Lamsa, and Moriah Eustice, who all contributed to this project. Thanks to Frank Solomon for advice on NAD^+ hydrolysis assays and Alicia Bicknell for microscopy advice. Thanks to the following people who

supplied reagents/advice: C. Sütterlin, A. Conzelmann, J. Rine, R. Schekman, S. Berger, M. Grunstein, F.Winston, P. Layborne, J. Thorner, J. Wilhelm, and R. Dutnall. Thanks to Sandi, Tricia, Jeanne, Erin, and Christie for Chapter 1 comments. Thanks to the following people for Chapter 2 comments: Christie, Russell, Sandy, Sandi, Erin, Jeanne, Jenny DuRose, Jim Kadonaga, and Frank Solomon. Thanks to Erin and Christie for careful reading of other thesis chapters.

I am grateful for the support of the UCSD School of Medicine Molecular Endocrinology training grant (Michael Rosenfeld, principal investigator). Also, this thesis research could not have been carried out without the support of the NIH.

Chapter 1, in full, is a book review chapter as it will appear in *Handbook of Cell Signaling*, Silent chromatin formation and regulation in the yeast *Saccharomyces cerevisiae* (in press, 2009, 2nd Ed., Eds. R. A. Bradshaw and E. A. Dennis, Elsevier, Inc.). In this publication, Lorraine Pillus and I are authors.

Chapter 2, in full, is a manuscript accepted for publication in *Proceedings of the National Academy of Sciences USA*, The glucanosyltranferase Gas1 functions in transcriptional silencing (in press, 2009). In this publication, I am the primary researcher and author. Lorraine Pillus directed and supervised the research that forms the basis of this chapter.

Appendix B contains data (Figure B-3) that appears in *Molecular and Cellular Biology*, Slx5 promotes transcriptional silencing and is required for robust growth in the absence of Sir2 (2008, 28(4):1361-1372). Russell P. Darst is the primary author of this publication and Sandra N. Garcia is a secondary author. I am also an author and Lorraine Pillus directed and supervised the research appearing in this publication.

VITA

2001	Internship, Howard Hughes Medical Institute
	Fred Hutchinson Cancer Research Center, Seattle, WA
2002	B.S., Biology
	University of Puget Sound, Tacoma, WA
2002-2009	Graduate Student Researcher
	University of California, San Diego, La Jolla, CA
2009	Ph.D., Biology
	University of California, San Diego, La Jolla, CA

PUBLICATIONS

Darst, R.P., Garcia, S.N., **Koch, M.R.,** and Pillus, L. 2008. Slx5 promotes transcriptional silencing and is required for robust growth in the absence of Sir2. *Molecular and Cellular Biology* **28**(4):1361-1372.

Koch, M.R. and Pillus, L. Silent chromatin formation and regulation in the yeast *Saccharomyces cerevisiae*. Handbook of Cell Signaling, Elsevier, Inc., in press.

Koch, M.R. and Pillus, L. The glucanosyltransferase Gas1 functions in transcriptional silencing. *Proceedings of the National Academy of Sciences USA*, in press.

ABSTRACT OF THE DISSERTATION

Characterization of new roles for the glucanosyltransferase Gas1 and other carbohydrate modifying enzymes in transcriptional silencing in the yeast *Saccharomyces cerevisiae*

by

Melissa R. Koch

Doctor of Philosophy in Biology

University of California, San Diego, 2009

Professor Lorraine Pillus, Chair

Transcriptional silencing is a crucial process that is mediated through chromatin structure. The histone deacetylase Sir2 silences genomic regions that include telomeres, ribosomal DNA, and the cryptic mating-type loci. The formation and regulation of silent chromatin has been much studied but remains incompletely understood. Additional factors controlling silent chromatin were suggested by a previously completed Sir2 two-hybrid screen. In this screen, Gas1 was identified as a Sir2-interacting protein. In the research reported here, an unsuspected role for the enzyme Gas1 in locus-specific transcriptional silencing is presented using genetic and

biochemical methods. *GAS1* encodes a β-1,3-glucanosyltransferase previously characterized for its role in cell wall biogenesis. In *gas1*Δ mutants, telomeric silencing is defective and rDNA silencing is enhanced. The catalytic activity of Gas1 is required for normal silencing, established through analysis of *gas1* catalytically inactive mutants. Gas1's role in silencing is distinct from its role in cell wall biogenesis.

Established hallmarks of silent chromatin, such as Sir2 binding and H4K16 and H3K56 deacetylation, appear unaffected in *gas1* mutants in chromatin immunoprecipitation analysis. Thus, another event required for telomeric silencing must be influenced by *GAS1*. Sir2 itself is present in immunoprecipitations of β-1,3-glucan, the substrate of Gas1 activity. This points to the possibility that Sir2 may be modified by β-1,3-glucan, or β-1,3-glucan is linked to Sir2 through interacting chromatin proteins.

Since the catalytic activity of Gas1 is required for telomeric silencing and Gas1 and Sir2 physically interact, a model is proposed in which carbohydrate post-translational modification of chromatin components provides a new regulatory element that may be critical for chromatin function. Other proteins contributing to steps upstream of Gas1 in carbohydrate modification pathways are also newly identified as necessary for silencing. These include Kre6, another Sir2-interacting protein and a β-1,6-glucan synthase, Fks1, a β-1,3-glucan synthase, and Pmt1, a mannosyltransferase. The initial genetic characterization of *KRE6*, *FKS1*, and *PMT1* demonstrates that these genes are also required for telomeric silencing and further reinforces the potentially crucial roles of *GAS1* and carbohydrate modification in transcriptional silencing.

Chapter 1

Introduction: Silent chromatin formation and regulation in the yeast *S. cerevisiae*

Cellular signaling occurs both between and within cells, and may stimulate responses in all cellular compartments. Within the nucleus, signaling mediates effects on gene expression through transcription that can range from highly induced, to constitutive, to repressed, to transcriptional states that are epigenetically regulated. One well-studied example of transcriptional regulation is silencing in budding yeast.

Chromatin-mediated silencing represses transcription from large genomic regions by altering chromatin structure into heterochromatin. In *Saccharomyces cerevisiae* (*S. cerevisiae*) or budding yeast, silent chromatin is cytologically distinct from heterochromatin in other eukaryotes, but many of the proteins and histone modifications involved are conserved. In particular, the process of silent chromatin formation and its regulation in yeast has led to an increased understanding of how chromosomal position can affect gene expression. Known as position effect variegation, this phenomenon has also been observed in many other organisms, including fission yeast, fruit flies, and humans (reviewed in Grewal and Elgin 2007).

The three silenced regions in the yeast genome lie at the core of a broad field of research into how silent chromatin is formed and regulated (Figure 1-1). Four *S*ilent *I*nformation *R*egulator (*SIR*) genes (*SIR1*, *SIR2*, *SIR3*, and *SIR4*) were initially found to control expression of *HML* and *HMR* (*HM* loci). *HML* contains a cryptic copy of the *MAT*α mating type gene whereas *HMR* contains a cryptic copy of the *MAT***a** mating type gene. *SIR1* is required for establishment of silencing at the *HM* loci,

Figure 1-1. A SIR-centric view of three major silenced regions in *S. cerevisiae*. Many proteins have been implicated in chromatin-mediated silencing (see Table 1-1). These diagrams highlight only the most characterized silencing proteins. Not shown is the underlying nucleosomal chromatin structure, nor histone modifications that have been mapped genome-wide (Millar and Grunstein 2006; Schones and Zhao 2008). *(A)* Chromosome III contains the transcribed *MAT* locus and the silenced mating-type loci, *HML*α and *HMR***a**. The E silencer (E), I silencer (I), and tRNA gene near *HMR* (tRNA) which function in boundary formation are indicated. The SIR complex, including Sir2, Sir3, and Sir4, is required to silence the *HM* loci. Additional proteins, including Rap1, Abf1, ORC, and Sir1, contribute to *HM* loci repression and SIR complex binding. *(B)* A representative yeast telomere is shown, including the repetitive telomeric sequence TG_{1-3}/$C_{1-3}A$ and X and Y' elements. The SIR complex is required to silence telomeric genes. Rap1, a major component of telomeric chromatin, positively influences silencing at telomeres, and is necessary for SIR complex binding. Distinct sequences for Rap1 binding at telomeres and at a genome-wide level have been established (Lieb et al. 2001). *(C)* Chromosome XII contains the 9.1 kilobase ribosomal DNA (rDNA) locus, repeated 100-200 times, that encodes the 5S and 35S ribosomal RNAs. The origin of replication (ARS) and non-transcribed spacers that separate the sequences encoding 5S and 35S (NTS1, NTS2) are indicated. The RENT complex, composed of Sir2, Net1, and Cdc14, is required for rDNA silencing. The rDNA also has other cryptic RNA Polymerase II-driven transcripts (not depicted) that are subject to Sir2-dependent regulation (Coelho et al. 2002; Kobayashi and Ganley 2005; Li et al. 2006; Vasiljeva et al. 2008). There is evidence for a Rap1 consensus rDNA sequence, but further experiments are necessary to determine if Rap1 binding recruits Sir2 or other chromatin-modifying enzymes to the rDNA.

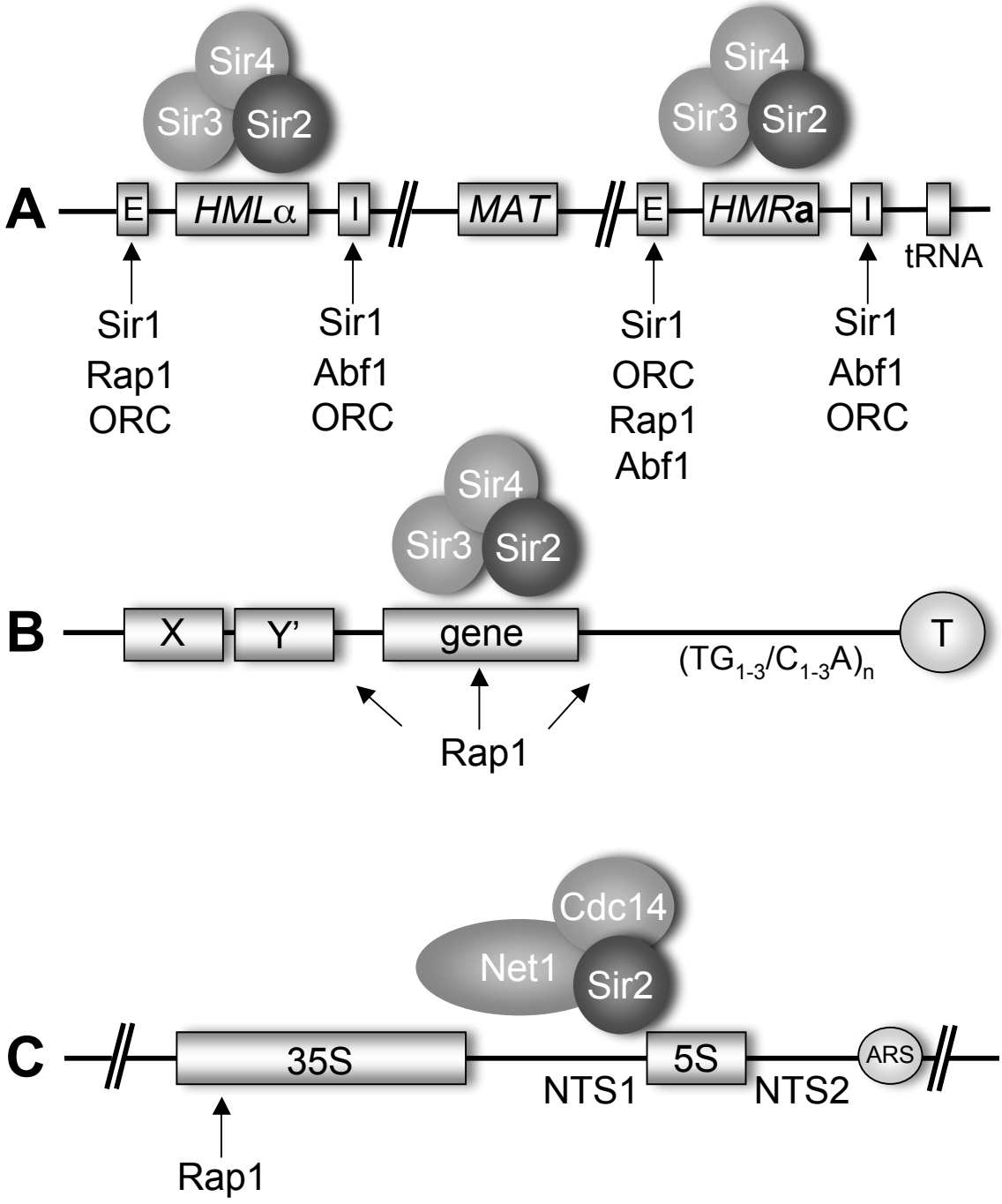
A
Sir4
Sir3
Sir2
E
HMLα
I
MAT
E
HMRa
I
tRNA
Sir1
Rap1
ORC
Sir1
Abf1
ORC
Sir1
ORC
Rap1
Abf1
Sir1
Abf1
ORC
B
Sir4
Sir3
Sir2
X
Y'
gene
T
(TG1-3/C1-3A)n
Rap1
C
Cdc14
Net1
Sir2
35S
5S
ARS
NTS1
NTS2
Rap1

Table 1-1. *Saccharomyces cerevisiae* silencing genes.[a]

Cellular role	Genes
Cell-cycle progression	*CHL1, CIN8, CLB1, CLB2, CLN3, DUN1, ELG1, HSL7, MBP1, MCD1, MND2, MPS3,* ***NET1****, PCH2, RNR1, SIT4, SWI4, SWI5, SWI6, UME1, UME6, WTM1, WTM2, YCS4*
Chromatin structure	*ARP4, ARP5, ASF1, ASF2, CAC2, DLS1,* ***HHF1****,* ***HHF2****, HHO1,* ***HHT1****,* ***HHT2****, HIF1, HIR1, HIR2, HIR3,* ***HTA1****,* ***HTA2****,* ***HTB1****,* ***HTB2****,* ***HTZ1****, IES3, INO80, ISW1, ISW2, ITC1, MSI1,* ***RAP1****, RIF1, RIF2, RLF2, RSC1, RSC2,* ***SIR1****,* ***SIR3****,* ***SIR4****, SNF2, SNF5, SNF6*
DNA repair	***ABF1****, MEC1, MEC3, MMS21, MSH2, RAD7, RAD18, RAD53, RTT107, SGS1, TDP1*
DNA replication	*CDC6, CDC7, CDC45, DNA2, DPB2, DPB3, DPB4, DPB11, FOB1, MCM5, MCM10, MRC1,* ***ORC1****,* ***ORC2****,* ***ORC3****,* ***ORC4****,* ***ORC5****,* ***ORC6****, POL1, POL2, POL30, POL32, RFC1, TOP1*
(De)acetylation[b]	***ARD1****, EPL1,* ***ESA1****,* ***GCN5****, HAT1, HAT2, HDA1, HDA2, HDA3, HST1, HST2,* ***HST3****,* ***HST4****,* ***NAT1****, PHO23, RPD3,* ***RTT109****, RXT3, SAP30,* ***SAS2****, SAS3, SAS4, SAS5, SDS3, SIN3,* ***SIR2****, YAF9, YNG1*
(De)methylation[b]	*BRE2,* ***DOT1****, HMT1,* ***JHD2****, SDC1,* ***SET1****,* ***SET2****, SHG2, SPP1, SWD1, SWD2, SWD3*
(De)ubiquitination[b] ***UBP10****, ULP2, ULS1*	*BRE1,* ***RAD6****, RKR1, SAN1, SLX5, SLX8, UBP3,*
MAP kinase signaling	*BCK1, FUS3, KSS1,* ***SLT2****, YKL161C*
NAD^+ biosynthesis	*BNA1, NMA1, NMA2, NPT1, NRK1, PNC1, TNA1*
Nuclear pore *SEH1, THP1*	*NUP2, NUP60, NUP84, NUP120, NUP133, NUP145,*
Sister chromatid cohesion	*CTF4, CTF18, DCC1*
Telomere maintenance	*EST1, EST2, STN1, TLC1, YKU70, YKU80*
Transcription	*ACA1, ADA2, AHC2, BDF1, CTI6, CUP2, FKH1, FKH2, GAL11, HFI1, HSF1, IFH1, LEU3, MED2, MED6, MED8, MGA2, NGG1, PAF1, PGD1, PPR1, RGT1, ROX3, RPA34, RPB4, RTF1, SFP1, SGF29, SGF73, SPT3, SPT4, SPT6, SPT10, SPT15, SPT20, SPT21, SPT23, TAF3, TAF5, TAF6, TAF9, TAF12, TAF14, TFA2*
Transcription repression	*CRF1, HMRA1, SIF2, SUM1, TUP1*

Table 3-1. *Saccharomyces cerevisiae* silencing genes. (continued)

Other[c]	*COG2, CPR1, DOT5, DOT6, EMP46, ESC1, ESC2, ESC8, ESS1, FPR4, GDS1, GRE2, GSP1, GTR1, GTR2, HEK2, ICY1, IRA1, IRS4, LGE1, LRS4, LSM1, LYS5, MIC14, MPT5, MRS6, NAM7, NMD2, NNT1, NPL3, NRD1, PAP2, PBP2, PEX1, PTK2, PUF4, REP1, REP2, RFM1, RNA1, RPL32, RPT4, RPT6, RRP6, RTT106, SAC7, SAS10, SCP160, SCS2, SCS22, SPB1, SRM1, SSH1, SUB2, SWA2, UPF3, UTH1, VAC8, YAP1802, YHC3, YRB2, YTA7, ZDS1, ZDS2*
Unknown[d]	*YBL081W, YBR271W, YCR076C*

[a]These genes have been linked to silencing or silent chromatin through a variety of studies, including overexpression, mutant phenotype, and biochemical analyses. In many cases the gene's function in silencing is not yet defined. For example, many of these may function indirectly, or even antagonize silencing. For references and descriptions, consult the *Saccharomyces* Genome Database (http://www.yeastgenome.org). Genes in **bold** are noted in the text.

[b]These classes of post-transcriptional modifiers include enzymes and complex components catalyzing both addition and removal of the modification. They have been grouped to simplify major categories.

[c]This category includes a broad range of genes functioning in diverse processes or cellular structures; several were first identified in screens to identify genes affecting silencing.

[d]This category includes genes without a defined function.

whereas the other three *SIR* genes are required for silent chromatin maintenance. *SIR*-dependent epigenetic silencing was also discovered at yeast telomeres, through the observation that reporter genes integrated at subtelomeric repetitive regions are silenced. The *SIR2*, *SIR3*, and *SIR4* genes also control telomeric silencing, whereas *SIR1* is specific to *HM* loci silencing. The third silenced region is found at ribosomal DNA (rDNA) repeats. Here, both silencing of reporter genes and suppression of recombination is observed and is distinct from the other two silenced regions due to its requirement for only one of the *SIR* genes, *SIR2* (reviewed in Rusche et al. 2003).

Much progress has been made identifying additional genes that enhance or interfere with silencing, and these link transcriptional silencing to various other cellular processes (Table 1-1). The diverse functions of proteins involved in silencing these three genomic regions also point to the complex post-translational histone modifications that mediate chromatin dynamics.

This chapter highlights key findings concerning the assembly of silent chromatin and the regulation of silent chromatin spreading in budding yeast, focusing on the function of Sir proteins in silencing. In particular, the proteins and histone modifications that positively influence silent chromatin formation or restrict silent chromatin spreading are discussed.

Silencer elements and silencer-binding proteins

DNA sequences and DNA binding proteins functioning in silent chromatin formation have been identified (Figure 1-1). DNA sequences termed silencers, by

analogy with enhancers, have been identified at the *HM* loci. These sequence elements recruit DNA binding proteins that in turn recruit chromatin-modifying factors to modify the local chromatin structure. The silent mating type loci consists of cryptic copies of mating type information, *HML*a and *HMR***a**, flanked by the DNA silencer elements E and I (Figure 1-1*A*). These silencer sequences consist of a combination of binding sites for Abf1, Rap1, and the origin recognition complex (ORC). All four silencers confer replication functions to a plasmid and are able to bind ORC *in vitro*, but only *HMR*-E and *HMR*-I act as chromosomal origins of replication (Rusche et al. 2003).

Directly analogous silencer sequences have not been identified at telomeres or rDNA. However, sequences that recruit DNA binding proteins have been identified at telomeres and rDNA. Telomeres consist of repetitive sequences, X and Y' elements, and $C_{1-3}A$ terminal telomeric repeats which foster silencing at the telomeres and contain binding sites for Rap1 (Figure 1-1*B*) (reviewed in Mondoux and Zakian 2006; Lundblad 2006). As of yet, no specific sequences recruiting DNA binding proteins to promote silencing have been identified in the rDNA, however experiments that shifted a reporter gene to different locations within the rDNA identified specific sequences within the rDNA subject to Sir2-dependent silencing (Buck et al. 2002).

Rap1 influences both the activation and repression of transcription. Rap1 functions in silencing at both the silent mating type loci and telomeres. Rap1 initiates silent chromatin formation by binding DNA at silencers or telomeric repetitive elements and interacting with the SIR complex (reviewed in Shore 1994). A genome-wide binding analysis found Rap1 localized to most telomeres and the *HM* loci, in

addition to other regions of the genome (Lieb et al. 2001). A protein with similarity to Rap1, Abf1 is an autonomously replicating sequence (ARS)-binding factor. Mutant alleles of this essential gene are defective in silencing the *HM* loci (reviewed in Loo and Rine 1995).

The origin recognition complex (ORC), critical for DNA replication, participates in silencing at the *HM* loci, and may influence silencing at the telomeres. Intriguingly, ORC's function in silencing can be separated from its role in replication based on analysis of conditional *orc* mutants that only display defects in silencing (Loo and Rine 1995). At the *HM* loci silencers, ORC and Sir4 recruit a common domain of Sir1 to initially establish silencing (Bose et al. 2004; Gardner and Fox 2001). However, tethering of Sir1 to *HMR* and telomeres establishes silencing and bypasses the requirement for ORC. ORC function in telomeric silencing is independent of Sir1, although ORC interactions with silencing proteins at telomeres are currently undefined (Rusche et al. 2003).

The SIR and RENT silencing complexes

Several multimeric protein complexes participate in the initiation, establishment, and maintenance of heterochromatic structures. Silencing mechanisms at the cryptic mating type loci and telomeres share the requirement for the heterotrimeric SIR complex, comprised of the proteins Sir2, Sir3, and Sir4 (Rusche et al. 2003). Whereas Sir3 and Sir4 are considered structural components of silent chromatin, Sir2 alters chromatin structure enzymatically through NAD^+-dependent

deacetylase activity (reviewed in Blander and Guarente 2004). Sir2 has homologs in every biological kingdom, and some of these homologs function in transcriptional repression through the conserved NAD^+-dependent deacetylase activity (Brachmann et al. 1995; Blander and Guarente 2004). Evidence for conservation of Sir2 silencing function comes from studies showing that Sir2 homologs can function in silencing, suggesting that the conserved deacetylase domain has a similar function in other organisms (Freeman-Cook et al. 2005; Sherman et al. 1999).

Post-translational modifications regulate the silencing function of Sir3. Acetylation of the Sir3 amino terminal bromo-adjacent homology (BAH) domain by NatA promotes Sir3 binding within silent chromatin (Wang et al. 2004; Geissenhoner et al. 2004). In addition, phosphorylation of Sir3 by the MAP kinase Slt2 (Ai et al. 2002; Ray et al. 2003), strengthens telomeric silencing (Stone and Pillus 1996). Sir3 phosphorylation by the MAP kinase signal transduction pathway, in response to stress, heat shock, starvation, and other environmental changes likewise affects silencing strength (Ai et al. 2002; Stone and Pillus 1996). It has also been reported that Sir3 and Sir4 are sumoylated, but this observation and its role in silencing awaits validation and further study (Denison et al. 2005; Wohlschlegel et al. 2004).

A second silencing complex, RENT, functions at the rDNA repeats. The Regulator of Nucleolar silencing and Telophase exit (RENT) complex is comprised of Sir2, Net1, and Cdc14. It is a nucleolar complex with two separable functions: silencing within the rDNA array and regulating mitotic exit (reviewed in Garcia and Pillus 1999). The rDNA array contains 100 to 200 tandem repeats of a 9.1-kilobase-pair cassette that encodes two precursor rRNA transcripts (Figure 1-1*C*).

Nontranscribed spacers, NTS1 and NTS2, separate these two genes, with NTS1 being an example of a Sir2 responsive region (SRR) in the rDNA (Huang and Moazed 2003). Net1 binds to the rDNA, tethering RENT to the rDNA repeat (Garcia and Pillus 1999). A direct role in rDNA silencing for the Cdc14 component of RENT has not been reported.

Additional chromatin modifying and remodeling complexes have been implicated in silencing, including methyltransferase, acetyltransferase, and deacetylase complexes (reviewed in Lafon et al. 2007; Shilatifard 2006). The role of these other complexes in silencing is not yet as well defined as the SIR and RENT complexes, but some clearly contribute directly to chromatin regulation as described below.

The role of histone modifications in silent chromatin formation

Many different co- and post-translational modifications of histones and other chromatin components appear critical for diverse biological processes. Much progress in understanding the roles of individual histone residues and modifications comes from studies in yeast. This is because, uniquely among most eukaryotes, the histone gene families are small and are amenable to genetic manipulation. Histones and histone modifications are intimately linked to the formation of transcriptionally silent chromatin (Figure 1-2). The silenced *HM* loci and telomeres are associated with reduced nucleosomal acetylation, primarily hypoacetylated histone H3 and H4, which are required for efficient silencing (Rusche et al. 2003). Indeed, the amino termini of histone H3 and histone H4 are required for silencing at *HM* loci and telomeres

Figure 1-2. Sites of acetylation, methylation, and ubiquitination of histone residues implicated in transcriptional silencing. Histones H2A, H2B, H3, and H4 and histone variant H2A.Z are indicated. Globular histone domains are distinguished from amino-terminal tails by a thicker line. Histone H2A residues implicated in only telomeric silencing include lysines 4 (K4) and 7 (K7) when they are jointly mutated, lysine 21 (K21) which may contribute structurally to telomeric silencing, and threonine 125 (T125), which is phosphorylated (Wyatt et al. 2003). Histone H2B is ubiquitinated at lysine 123 (K123) by Rad6. This modification is removed by Ubp10. Deubiquitinated H2BK123 helps maintain low levels of H3K4 and H3K79 methylation in silent chromatin. Histone H3K4 is methylated by Set1 (COMPASS complex), H3K36 by Set2, and H3K79 by Dot1. H3 methylation restricts silent chromatin spreading. Trimethylated H3K4 is demethylated by Jhd2. H3K56 is acetylated by Rtt109. The modification is removed by Sir2 at silenced loci, but global deacetylation of this residue is regulated by Hst3 and Hst4. Deacetylated H3K56 is required for silent chromatin formation. Histone H4 is acetylated at K16 by Sas2 (SAS complex) and deacetylated by Sir2 at silent loci. This deacetylation promotes silencing whereas acetylation restricts the spread of silencing. H4 is also acetylated at K91, but the enzymes responsible for addition or removal of this modification are currently unknown. So far H4K91 has only been implicated in silencing of the cryptic mating-type loci. H4 is methylated at K59, again, by unknown enzymes. H4K59 methylation is essential for silencing at telomeres and *HM* loci. The histone variant H2A.Z is acetylated at K14 by Esa1 (NuA4 complex) and Gcn5 (SAGA complex) and helps form the barrier between silent chromatin and euchromatin.

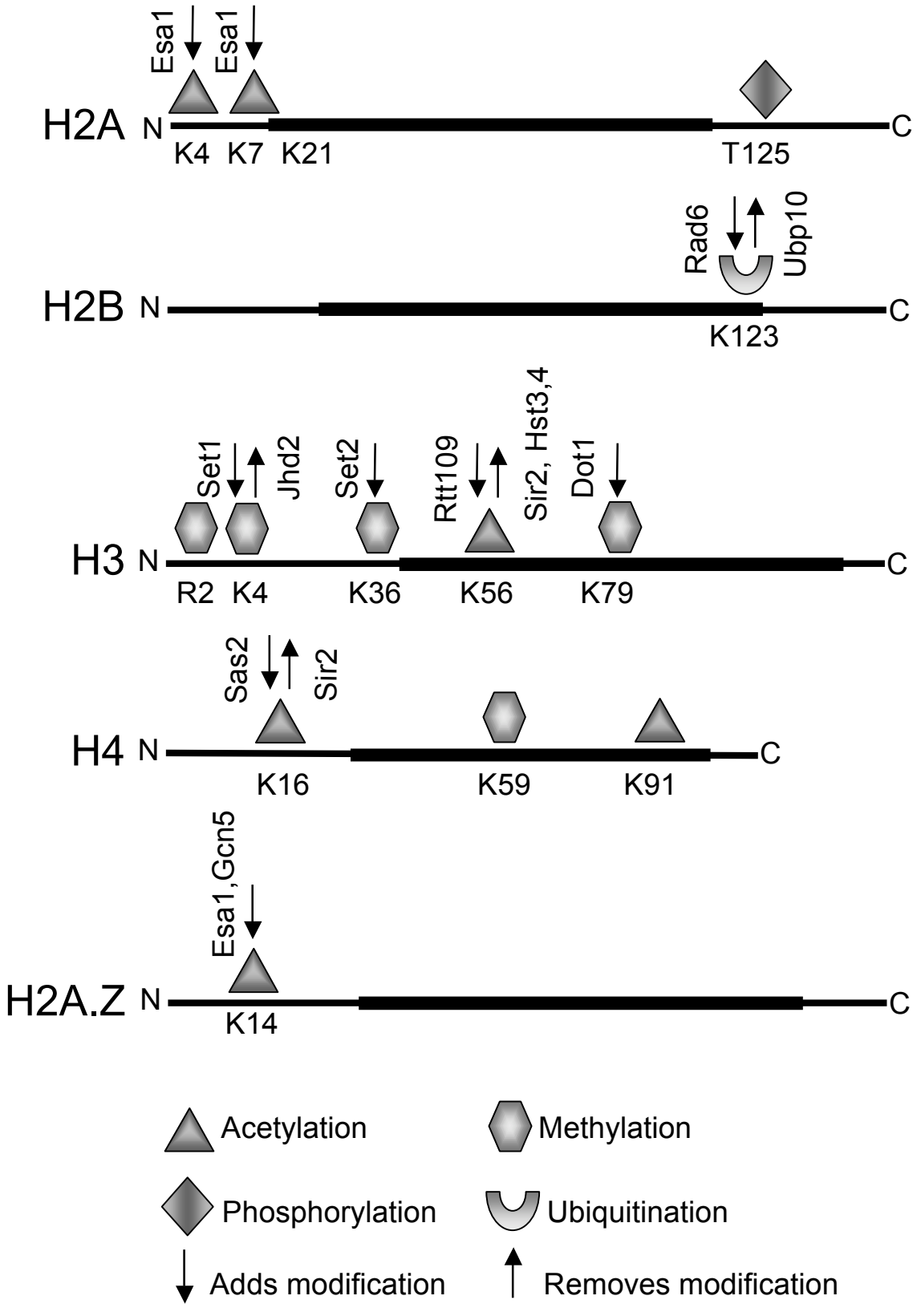
Esa1
Esa1
H2A
N
C
K4
K7
K21
T125
Rad6
Ubp10
H2B
N
C
K123
Set1
Jhd2
Set2
Rtt109
Sir2, Hst3,4
Dot1
H3
N
C
R2
K4
K36
K56
K79
Sas2
Sir2
H4
N
C
K16
K59
K91
Esa1,Gcn5
H2A.Z
N
C
K14
Acetylation
Methylation
Phosphorylation
Ubiquitination
Adds modification
Removes modification

(reviewed in Shahbazian and Grunstein 2007). Point mutations in the genes encoding histone H3 and histone H4 that affect their acetylation state often result in silencing defects (reviewed in Smith 1991). Furthermore, Sir3 and Sir4 physically interact with the hypoacetylated amino-terminal tails of histone H3 and histone H4, suggesting a mechanism in which these proteins interact during the formation of silent chromatin (Shahbazian and Grunstein 2007).

Lysine 16 within the amino-terminal tail of histone H4 (H4K16) is a target of reversible acetylation and has the most clearly established silencing function of the histone H3 and H4 residues. Early studies showed that substitution of the H4K16 lysine residue with alanine caused derepression of *HM* loci, whereas mutation of the other three amino terminal tail lysine residues with alanine, glutamine, or glycine residues showed only minor phenotypic changes (Smith 1991). Sir2 deacetylates H4K16 *in vitro*, resulting in a critical modification for the assembly of silent chromatin. *In vivo* evidence shows that silenced DNA is deacetylated at H4K16 and the deacetylation of H4K16 is lost in *sir2*Δ mutants (Blander and Guarente 2004).

An acetylatable lysine residue in the nucleosome core has recently been implicated in silencing. Histone H3 lysine 56 (H3K56), a target of Sir2, is hypoacetylated at telomeres and at the *HM* loci, and its deacetylated state has been postulated to enable the compaction of chromatin (Xu et al. 2007). The Sir2 homologs Hst3 and Hst4 also affect H3K56 acetylation, and when jointly mutated result in defective telomeric silencing (Brachmann et al. 1995; Ozdemir et al. 2006). Substitution of H3K56 by glycine, glutamine, or arginine led to defects in telomeric silencing and rDNA silencing (Xu et al. 2007; Hyland et al. 2005). Loss of Rtt109-

mediated H3K56 acetylation restored silencing to a crippled *HMR* locus (Miller et al. 2008). Acetylation of histone H4 lysine 91 (H4K91) is also implicated in silencing. A mutation altering H4K91 leads to phenotypes which suggest derepression of the silent mating-type loci and altered silent chromatin structure (Ye et al. 2005), but the enzymes responsible for acting on H4K91 have not been identified. Acetylation of H2AK4 and H2AK7 has been implicated in telomeric silencing because the combined substitution of these two residues results in defective silencing at telomeres (Wyatt et al. 2003). Acetylation of these two residues may be mediated by the histone acetyltransferase Esa1 (Lafon et al. 2007).

Histone methylation has also been linked to transcriptional silencing. Simultaneous substitution with arginine of three methylatable lysine residues of histone H3—K4, K36, and K79—results in a lethal phenotype and is associated with increased gene silencing that initiates at and spreads out from the telomeres, suggesting that methylation of histone H3 is critical for silencing (Jin et al. 2007). Set1, the catalytic subunit of the COMPASS complex, methylates H3K4. Strains with mutations in *SET1* are defective in rDNA, telomeric, and *HM* silencing. Importantly, Set1 functions independently of Sir2 when silencing within the rDNA array. Methylation of H3K4 in euchromatin promotes Sir3 association with heterochromatic regions containing unmethylated H3K4, therefore concentrating it at these sites (reviewed in Dehé and Géli 2006). Jhd2, a demethylase, contributes to telomeric silencing regulation by demethylation of trimethylated H3K4 (Liang et al. 2007). Recently, methylation of histone H3 arginine 2 (H3R2) has been shown to prevent

trimethylation of H3K4 by Set1, suggesting that arginine methylation of histone H3 promotes silencing (Kirmizis et al. 2007).

H3K36 is methylated by Set2 (Briggs et al. 2002) and substitution of H3K36 with glutamic acid or methionine causes ectopic spreading of silencing from a heterochromatin reporter at the *HM* loci and telomeres (Tompa and Madhani 2007). H3K79 is another histone methylation target linked to silencing. In the nucleosome core, Dot1 methylates H3K79. H3K79 is hypomethylated at *HM* loci and telomeres, where the Sir proteins appear to block its methylation (reviewed in Wood et al. 2005). A fourth lysine residue, histone H4 lysine 59, is a methylation target and is essential for silencing at *HM* loci and telomeres (Zhang et al. 2003), but the enzymes that target this residue have not been identified.

Phosphorylation is a common modification of histones, but is not usually connected to silencing. An exception is a study implicating a phosphorylated residue of H2A, T125, in telomeric silencing (Wyatt et al. 2003).

A fourth histone modification with connections to silencing is ubiquitination. Histone H2B is ubiquitinated at lysine 123 (H2BK123) by Rad6 (Wood et al. 2005). Ubp10 targets this site for deubiquitination and through crosstalk between modifications, maintains low levels of H3K4 and H3K79 methylation in silent chromatin (reviewed in Weake and Workman 2008; Wood et al. 2005). Ubp10 localizes to the silent chromatin regions at *HM* and telomeric loci and disrupts silencing when overexpressed. Loss of Ubp10 activity results in decreased binding of Sir2 and Sir3 to telomeres. Ubp10 also physically interacts with Sir4 and regulates its abundance (Weake and Workman 2008).

Lastly, sumoylation is also associated with transcriptional repression. All four histones are sumoylated, and some of the sites of sumoylation have been reported (Nathan et al. 2006). Further research will be required to identify the proteins responsible for sumoylation of histones, its functional significance in silencing, and any potential crosstalk between histone sumoylation and other modifications involved in transcriptional silencing.

Assembly of the SIR complex and silent chromatin formation

The process of silent chromatin formation is complex and has generated intense study on how it becomes assembled and how it inhibits transcription. Silent chromatin formation occurs via the assembly of the SIR complex, modifications to histones, and the spreading of silent chromatin. It is recognized that passage through S phase is required for silencing, but that DNA replication *per se* is not necessary for silencing to be established at the *HM* loci (Rusche et al. 2003). However, how cell cycle progression exactly contributes to silencing is unclear. At the *HM* loci, there is a need to re-create the silent state after replication to ensure the ability of a haploid cell to mate. At the telomeres, silencing is relatively stable after establishment, yet after DNA replication, there is competition between proteins involved in establishing the silenced state and the active state, leading to the stochastic nature of silencing at telomeres.

The binding of the SIR complex appears critical to the initial stage of silent chromatin formation. Studies examining the *HM* loci and telomeres have contributed

to understanding how the SIR complex and silent chromatin form. DNA-bound Rap1 and Abf1 recruit Sir4 to initiate the formation of silent chromatin at *HM* loci (Luo et al. 2002), which is required for the other Sir proteins to associate with silencers (Rusche et al. 2002). Rap1 physically interacts with both Sir4 and Sir3, and may stabilize SIR complex-nucleosome interactions (Moretti and Shore 2001). *In vitro* evidence suggests that a complex composed solely of Sir2 and Sir4 may initially associate with chromatin and begin deacetylation independently of Sir3 (Hoppe et al. 2002). The role of Sir3 as a structural chromatin component is demonstrated by the protein's ability to bind to a variety of DNA templates, and to form a condensed higher order chromatin structure (McBryant et al. 2008). Also, the synthesis of O-acetyl-ADP-ribose (AAR), an evolutionarily conserved metabolite produced during the Sir2 deacetylation reaction (Borra et al. 2002; Tanner et al. 2000), promotes Sir3 association with Sir2/Sir4 complex and induces a SIR complex structural rearrangement (Liou et al. 2005). Nonetheless, histone deacetylation alone does not appear sufficient for full recruitment of silencing proteins to chromatin (Rudner et al. 2005), although histone hypoacetylation is sufficient for Sir protein spreading (Yang and Kirchmaier 2006). Interactions between all members of the SIR complex appear important for silent chromatin formation since silencing is disrupted even when Sir3 assembly into the complex is disrupted (Rudner et al. 2005). The cycle of nucleosome deacetylation by Sir2 is followed by recruitment of additional Sir2, Sir3, and Sir4 to deacetylate adjacent nucleosomes and spread silent chromatin (Rusche et al. 2002). Loss of acetylation but not methylation appears to facilitate recruitment and spreading of Sir proteins (Yang et al. 2008a).

There is less known about the formation of silent chromatin in the rDNA. The rDNA is distinct from the other silent loci because of the repetitive nature of rDNA and the fact that the RNA Polymerase I and III transcribed genes are actively expressed in the rDNA, yet endogenous RNA Polymerase II genes and reporter genes are silenced when integrated (Coelho et al. 2002; Kobayashi and Ganley 2005; Li et al. 2006; Vasiljeva et al. 2008; Rusche et al. 2003). It is known that histone H3 and histone H4 amino terminal tails are required for rDNA silencing, and that histone H4 in the rDNA is hypo-acetylated in a Sir2-dependent manner (Hoppe et al. 2002). Spontaneous changes in the number of rDNA copies alters Sir2 levels and silencing strength at telomeres and *HM* loci, suggesting that silencing is dependent on the balance between the pools of nucleolar and non-nucleolar Sir2 (Michel et al. 2005). Prior to its identification as an rDNA silencing factor, Sir2 was implicated in the rDNA for its role in suppressing recombination and promoting longevity by recombination-dependent rDNA circle formation (reviewed in Guarente 2000). Set1 functions independently of Sir2 in rDNA silencing, and its methylation of H3K4 is necessary for silencing (Dehé and Géli 2006).

Other chromatin-related proteins have been implicated in rDNA silencing (Table 1-1). Further, a screen for genes that when mutated have altered rDNA silencing, uncovered a number of additional factors, many of which are not well studied. Among them, *SIR4* deletion indirectly results in increased silencing by disrupting Sir2 association at *HM* and telomeric loci, thereby making more Sir2 available for rDNA silencing in the nucleolus (Smith et al. 1998). Further research will be necessary to identify steps in silent chromatin assembly in the rDNA and to

highlight differences between silent chromatin formation in the rDNA, telomeres, and silent mating type loci.

Regulation of silent chromatin spreading

Spreading of the proteins that constitute silent chromatin is crucial for formation of silenced domains, however, it is necessary to restrict spreading from the regions of chromatin that require expression (reviewed in Donze and Kamakaka 2002). Spreading was observed early on in position effect variegation in fruit flies (reviewed in Ebert et al. 2006), so there was an expectation a similar phenomenon might be found in yeast. Sir3 overexpression provided just such an early example. Sir3 is a crucial component of silent chromatin, which initiates at the telomere and assembles inward along the chromosome. When overexpressed, Sir3 spreads from telomeric regions and represses adjacent genes as it invades the chromosome, even into regions depleted of Sir2 and Sir4 (Donze and Kamakaka 2002). It is thought that Sir3 spreading recruits Sir2 to these telomere-proximal regions, as hypoacetylation is sufficient for the spread of silent chromatin, even in the absence of Sir2 histone deacetylation activity and AAR production (Yang and Kirchmaier 2006).

Although it is likely to be regulated differently than spreading at telomeres and the silent mating-type locus, spreading has also been observed in the rDNA. Within the rDNA array, silent chromatin spreading is promoted by *SIR2* overexpression and requires deacetylation of histone H3 and histone H4. Surprisingly, rDNA silencing

required RNA Polymerase I transcription and the direction of silent chromatin spreading was controlled by the direction of transcription (Buck et al. 2002).

DNA elements, proteins, and histone modifications have been identified that contribute to boundaries between active and silent chromatin. The first silent chromatin domain boundary elements were discovered at the silent mating-type loci. It was recognized that the upstream activation sequence of ribosomal protein genes, which includes binding sites for Rap1, physically blocked the spread of silent chromatin initiated at an *HM* locus silencer. In addition, deletion of boundary elements flanking the *HMR***a** locus caused silent chromatin spreading. The boundary element at *HMR***a** contains a Ty1 long terminal repeat (LTR) retrotransposon and a transfer RNA (tRNA) gene. The transcriptional potential of the tRNA gene is critical for its function as a barrier since tRNA promoter mutation or inhibition of RNA Polymerase III complex assembly decreases barrier activity (Donze and Kamakaka 2002). Further, silent chromatin spreading can also be blocked by tethering the *HML* locus to the nuclear pore complex (Ishii et al. 2002).

Histone modifications can antagonize the spread of silent chromatin. One clear example is the acetylation of H4K16 by Sas2 (Kimura et al. 2002; Shia et al. 2005; Suka et al. 2002). There is a gradient of acetylation along the chromosome, starting with hypoacetylated H4K16 at the telomeric end of the chromosome changing to hyperacetylated H4K16 at more distant locations, suggesting that Sir2 and Sas2 opposingly regulate silent chromatin since they target the same histone residue (Kimura et al. 2002; Suka et al. 2002).

Histone methylation also contributes to boundaries. Strains lacking the methyltransferases Set1, Set2, and Dot1, which target H3K4, H3K36, and H3K79, respectively, show evidence of spreading at *HM* loci and telomeres, suggesting that H3 methylation inhibits silencing (Katan-Khaykovich and Struhl 2005; Tompa and Madhani 2007). Dot1 and Sir3 compete for binding at the same region of the histone H4 N-terminal tail (Altaf et al. 2007). Acetylation of H4K16 displaces Sir3, enabling methylation of H3K79 by Dot1 and inhibiting further binding and spreading by Sir3 (Altaf et al. 2007).

A variant histone, H2A.Z, has been implicated in forming the boundary between euchromatin and silent chromatin. H2A.Z is enriched in euchromatin and prevents the spread of heterochromatin (Meneghini et al. 2003). H4K16 acetylation by Sas2 is required for H2A.Z incorporation into telomeric nucleosomes (Shia et al. 2006). Acetylation of lysine 14 of H2A.Z by Esa1 and Gcn5 is critical for its boundary function since an unacetylatable H2A.Z substitution mutant is enriched at heterochromatin boundaries and is unable to block silent chromatin spreading (Babiarz et al. 2006). Indeed, recent results implicate collaboration between Set1 and H2A.Z in optimally balancing chromatin modifications to restrict silencing not just to classically defined regions, but throughout the genome (Venkatasubrahmanyam et al. 2007).

The process of forming barriers between active and silent chromatin involves several other proteins that may have redundant functions. A screen was used to identify proteins responsible for blocking the spread of silencing at *HMR***a**. This screen identified many chromatin modifying enzymes and complexes, including Dot1, SAS,

SAGA, NuA3, and NuA4, as well as the chromatin remodelers SWI/SNF (Oki et al. 2004).

The proteins discussed above antagonize the formation and spreading of silent chromatin, yet counterintuitively many display silencing defects when the gene encoding the protein is deleted. Together, the data suggest that the silencing defects result from binding of Sir proteins to non-silent regions, diluting the effective concentration of Sir proteins in silent chromatin. Some Sir proteins are known to be limiting for silencing, and silent loci are in competition for the limited pool of Sir proteins (Rusche et al. 2003).

The nuclear periphery and silent chromatin formation

Over the last decade, an ongoing debate has focused on whether localization to the nuclear periphery is critical in formation of silent chromatin. Although early studies showed that anchoring a defective *HMR* locus to the periphery could establish silencing of the locus, other studies found that localization of silent loci to the nuclear periphery is not sufficient for transcriptional repression and that repression can be sustained without perinuclear anchoring. In other instances, the nuclear periphery is associated with transcriptional activation, but the anchoring sites for active genes are distinct from those for silent genes (reviewed in Akhtar and Gasser 2007). The exact contribution of nuclear periphery localization to silent chromatin formation thus remains an area of active investigation.

Conclusions

Knowledge of silent chromatin formation in *S. cerevisiae* has increased significantly since the initial discovery of the *SIR* genes and silenced loci. Numerous proteins have been implicated in silencing, linking diverse cellular processes to silencing, including cell-cycle progression, DNA repair, and DNA replication, among other functions. Sir proteins themselves have also been implicated in other processes, including aging, chromosome stability, DNA repair, and DNA replication (reviewed in Buck et al. 2004; Blander and Guarente 2004). Many recent studies have addressed the establishment and maintenance of silent chromatin and the control of silent chromatin spreading. Histone modifications and histone-modifying enzymes have been identified that are required for promoting or restricting silent chromatin spreading.

Early studies provided evidence that silent chromatin can prevent accessibility of some enzymes in a *SIR*-dependent fashion (reviewed in Chen and Widom 2004). However, defining the stage of transcription affected by silent chromatin remains a topic of debate. Silencing was shown to act downstream of gene activator binding to reduce occupancy of pre-initiation factors at *HM* loci and telomeres (Chen and Widom 2005). However, further investigation will be necessary to identify whether blocking the transition from transcription initiation to elongation is the universal method of silencing transcription in chromatin (Gao and Gross 2008) or whether different mechanisms function at different loci.

Silencing in yeast is required for more than just repression of transcription. Recently, silent chromatin has been linked to cohesion of sister chromatids during cell

division (Chang et al. 2005; Dubey and Gartenberg 2007; Suter et al. 2004). A model for this connection proposes that cohesin binds silent chromatin through linkages to chromatids (Chang et al. 2005). The role of silencing in cohesion is an area open for further study.

Silent chromatin in yeast shares similar chromatin modification and heterochromatin formation mechanisms with many organisms, making budding yeast an exceptional model for studying formation and regulation of a repressed chromatin structure. The absence of heterochromatin protein 1 (HP1) and histone H3 lysine 9 (H3K9) methylation in budding yeast silent chromatin is a distinct difference between yeast and other organisms. Another, more recently recognized distinction is the apparent absence of the RNA interference (RNAi) pathway in budding yeast silencing. RNAi functions in heterochromatin formation in many other organisms, including fission yeast and fruit flies (reviewed in Grewal and Elgin 2007). However, clear roles for RNA in silencing have been documented in budding yeast (Berretta et al. 2008; Camblong et al. 2007), showing that RNA can promote physiologically relevant silencing, even in the absence of many components of RNAi machinery. The active field of silent chromatin research in budding yeast promises to contribute significant discoveries in the future.

The text of this Chapter appears in a review chapter, Koch, M. R. and Pillus, L. 2009. Silent chromatin formation and regulation in the yeast *Saccharomyces cerevisiae*. Handbook of Cell Signaling, Elsevier, Inc., in press.

Chapter 2

The glucanosyltransferase Gas1 functions in transcriptional silencing

INTRODUCTION

The formation of silent chromatin leads to the transcriptional repression of regions of the genome. In the yeast *Saccharomyces cerevisiae* these regions include the telomeres, ribosomal DNA (rDNA), and the cryptic mating-type loci (the *HM* loci, *HML* and *HMR*), all of which require the Silent Information Regulator 2 protein (Sir2), an NAD^+-dependent protein deacetylase (reviewed in Rusche et al. 2003). Sir2 is the founding member of the conserved sirtuin deacetylase family (Brachmann et al. 1995), with Sir2 directing its activity toward lysine 16 of histone H4 (H4K16) to promote silent chromatin formation (reviewed in Buck et al. 2004). There is also evidence that deacetylation of lysine 56 of histone H3 (H3K56) by Sir2 (Xu et al. 2007), or the sirtuins Hst3 and Hst4 (Yang et al. 2008b), enables silencing at the telomeres and *HM* loci. Sir2 functions in the SIR complex with Sir3 and Sir4 to silence at telomeres, and also at the *HM* loci, where an additional protein, Sir1, also participates (Rusche et al. 2003). However, within the rDNA, the Sir2-containing RENT complex acts independently of the other Sir proteins (Rusche et al. 2003). Distinctions among the three silenced regions led to the hypothesis that different mechanisms of silent chromatin formation and regulation exist for each region.

The basic model for silent chromatin formation at telomeres and *HM* loci involves recruitment of the SIR complex by DNA binding proteins, followed by Sir2-

mediated histone deacetylation and additional SIR complex spreading. Hypoacetylation of histones enables silent chromatin spreading in the absence of Sir2 deacetylase activity, but is not sufficient for full silencing (Yang and Kirchmaier 2006). Instead, deacetylase activity must be targeted to the silenced loci through Sir3 or some other means (Chou et al. 2008). Although early studies focused on Sir2-mediated histone deacetylation, silent chromatin formation is also regulated through histone methylation and ubiquitination (reviewed in Shilatifard 2006), indicating that histone deacetylation alone is not sufficient for silencing. Multiple biochemical activities are recognized to contribute to chromatin function, and more are likely to emerge. The identification of *GAS1* by synthetic genetic array (SGA) analysis as an interactor with genes encoding nuclear functions provides one such new candidate activity.

In the cell wall, Gas1 is an abundant protein anchored via glycophosphatidylinositol (GPI) (Nuoffer et al. 1991). Gas1 β-1,3-glucanosyltransferase activity catalyzes formation and maintenance of chains of β-1,3-glucan (reviewed in Popolo and Vai 1999). The modification occurs on proteins to which mannose residues have first been attached through serine or threonine residues (Popolo and Vai 1999). *GAS1* deletion mutants have cell wall defects, including reduced viability, thermal sensitivity, and sensitivity to cell wall disrupting compounds (Popolo et al. 1993). *GAS1* is broadly conserved in fungi and has four homologs in yeast (Popolo and Vai 1999). *GAS1*, *GAS3*, and *GAS5* are expressed in vegetatively growing cells, whereas *GAS2* and *GAS4* are expressed meiotically during sporulation (Ragni et al. 2007a).

GAS1 surfaced in SGA screens using mutants with established nuclear functions. For example, a conditional allele of *ORC2* uncovered synthetic sickness with *gas1*Δ (Suter et al. 2004). *ORC2* encodes a component of the DNA replication Origin Recognition Complex that has a separable function in promoting silencing of the *HM* loci (reviewed in Loo and Rine 1995). *GAS1* also exhibited a growth defect with deletion of *EAF1* or a conditional allele of *ESA1* (Mitchell et al. 2008), which both encode subunits of the Nucleosomal Acetylation of H4 (NuA4) complex (reviewed in Lafon et al. 2007) that functions in silencing at the telomeres and rDNA (Clarke et al. 2006). The basis for these interactions has not been pursued, but they suggest that *GAS1* and *ORC2*, *ESA1*, and *EAF1* may contribute to parallel processes that are critical for cellular function and viability. These might involve Gas1's established role at the cell wall, or may point to a previously unsuspected role for Gas1 in nuclear or chromatin function.

We show here that Gas1 participates in transcriptional silencing in a manner separable from its established function at the cell wall. In *gas1*Δ mutants, no change in silencing was observed at the *HM* loci, telomeric silencing was disrupted, and rDNA silencing was enhanced. Key features of silent chromatin, including Sir2 and Sir3 binding at telomeres and deacetylation of H4K16 and H3K56, are comparable in wild-type and *gas1*Δ strains. Analysis of enzymatically inactive *gas1* mutants showed that β-1,3-glucanosyltransferase activity itself is required for transcriptional silencing at the telomeres. Further analysis demonstrated that Gas1 may act through modification of Sir2 or other interacting factors. These results thus reveal a new nuclear role for a carbohydrate modification enzyme in transcriptional silencing.

RESULTS

Deletion of *GAS1* causes decreased telomeric silencing and increased rDNA silencing. Based on the interactions between *GAS1* and transcriptional silencing genes, we tested if *GAS1* participated in silencing. Assays of *HM* loci silencing in *gas1*Δ strains with *TRP1* reporters integrated at *HML* (Figure 2-1*A*) and *HMR* (Figure 2-1*B*) showed no defect in silencing compared to *sir1*Δ or *sir2*Δ strains, which are defective in *HM* silencing. Likewise, silencing of an independent reporter gene, *ADE2*, integrated at *HMR* was comparable in wild-type and *gas1*Δ strains (Figure 2-2*A*).

To determine whether *GAS1* influenced silencing in the rDNA, strains with reporters integrated within the rDNA repeat were constructed. A *gas1*Δ strain with a *URA3* reporter integrated at non-transcribed spacer 1 (NTS1) near the 5S rRNA gene of a single rDNA repeat (Smith and Boeke 1997) had enhanced silencing compared to wild-type (Figure 2-1*C*). This effect is Sir2-dependent since *gas1*Δ *sir2*Δ was as defective as *sir2*Δ in silencing of the rDNA (Figure 2-1*C*). The increase in silencing seen in *gas1*Δ is specific for the NTS1 region, as an *ADE2-CAN1* reporter in the 25S rRNA gene, which is only moderately subject to Sir2-dependent silencing (Fritze et al. 1997), did not show any change in silencing (Figure 2-2*B*).

To assess telomeric silencing in *gas1*Δ mutants, a *URA3* telomeric reporter on chromosome V-R (Renauld et al. 1993) was evaluated. In this assay, *URA3* expression is monitored on medium containing 5-FOA, a suicide substrate for cells expressing

Figure 2-1. *GAS1* functions in transcriptional silencing. *(A)* Deletion of *GAS1* does not affect *HML* silencing. All growth plates in *(A)*-*(D)* are synthetic complete (SC) medium. Wild-type (WT) (LPY13659), *sir1*Δ (LPY13660), and *gas1*Δ (LPY13661) strains with a *HML*::*TRP1* reporter were plated on SC lacking tryptophan (SC-trp). Increased growth on SC-trp indicates defective silencing. *(B)* Deletion of *GAS1* does not affect *HMR* silencing. WT (LPY4912), *sir1*Δ (LPY4958), *sir2*Δ (LPY4980) and *gas1*Δ (LPY13665) strains with a *hmr*Δ*E*::*TRP1* reporter were assayed as in *(A)*. Levels of wild-type silencing differ at these *TRP1 HM* loci reporters due to differences in the structure of the reporter. The *HML::TRP1* reporter (Le et al. 1997) contains a *TRP1* reporter at *HML* whereas *hmr*Δ*E::TRP1* contains a mutated silencer (Enomoto and Berman 1998). *(C)* Deletion of *GAS1* causes increased silencing at the rDNA. WT (LPY2446), *sir2*Δ (LPY2447), *gas1*Δ (LPY10074), and *gas1*Δ *sir2*Δ (LPY10078) with an m*URA3* NTS1 rDNA reporter were assayed for silencing on SC plates lacking uracil (SC-ura). Increased growth on SC-ura indicates defective silencing. (See Figure 2-6*A* for location of this reporter in the rDNA repeat). *(D)* Deletion of *GAS1* causes a telomeric silencing defect. WT (LPY4916), *sir2*Δ (LPY10397), and *gas1*Δ (LPY10362) with a *URA3* telomeric reporter on chromosome V-R, and a *gas1*Δ control strain (LPY10129) with no telomeric reporter (*gas1*Δ *ura3-1*), to monitor *gas1*Δ 5-FOA sensitivity, were plated on SC containing 5-FOA. Decreased growth on 5-FOA indicates defective silencing. *(E)* Expression of an endogenous telomeric gene, *YFR057W*, is increased in *gas1*Δ. cDNAs from WT (LPY1029), *sir2*Δ (LPY12660), and *gas1*Δ (LPY10358) strains were analyzed by quantitative PCR, with the bars representing *YFR057W* cDNA signal minus control reactions without reverse transcriptase, normalized to *ACT1*.

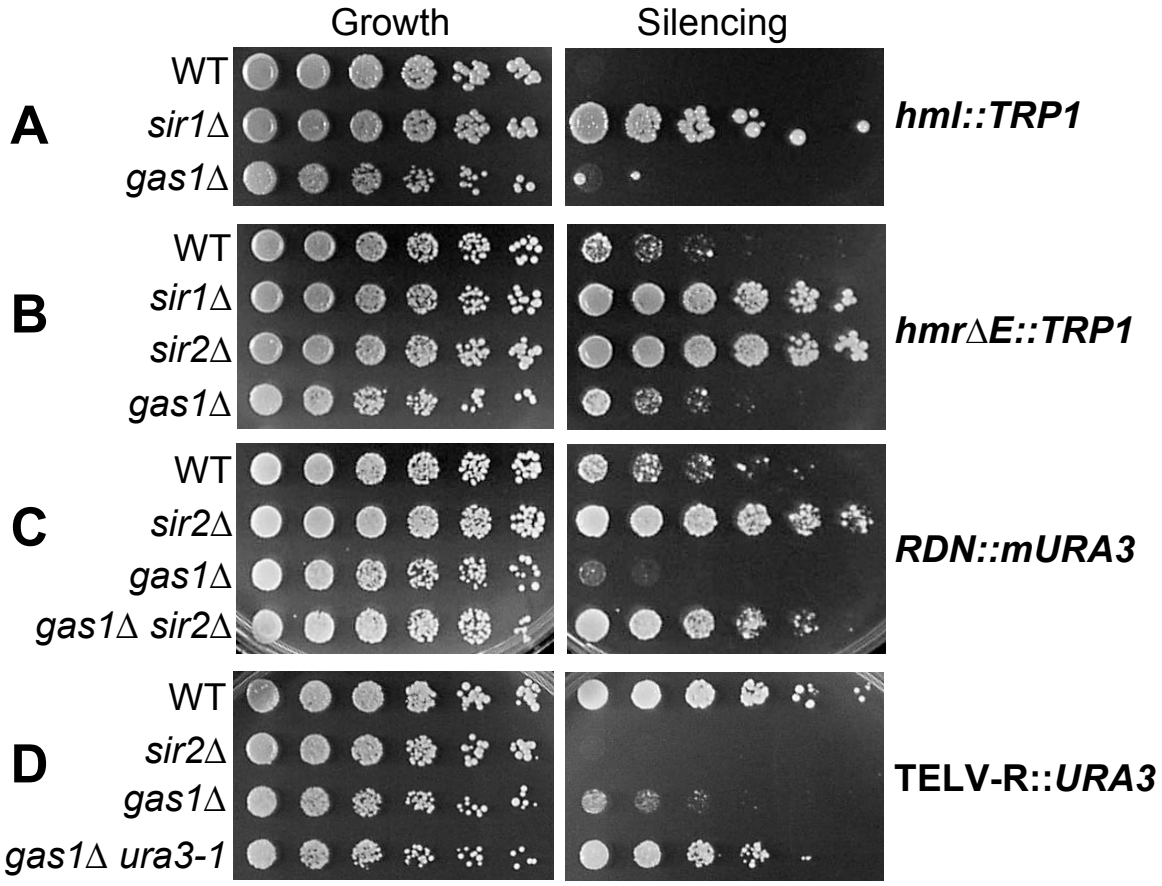
Growth
Silencing
A
WT
sir1Δ
gas1Δ
hml::TRP1
B
WT
sir1Δ
sir2Δ
gas1Δ
hmrΔE::TRP1
C
WT
sir2Δ
gas1Δ
gas1Δ sir2Δ
RDN::mURA3
D
WT
sir2Δ
gas1Δ
gas1Δ ura3-1
TELV-R::URA3

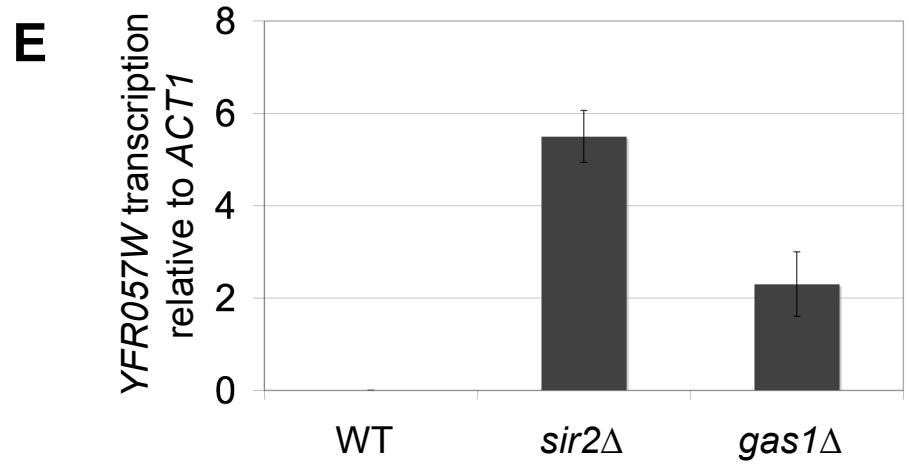
E
YFR057W transcription relative to ACT1
8
6
4
2
0
WT
sir2Δ
gas1Δ

Figure 2-2. Silencing of *HMR* and 25S rDNA is unaffected in *gas1*Δ mutants. (A) Deletion of *GAS1* does not affect *HMR* silencing. WT (LPY14324, LPY14235), *sir2*Δ (LPY11551, LPY11552), and *gas1*Δ (LPY14328, LPY14329) strains with a *hmr::ADE2* reporter in the context of a wild-type silencer (Sussel et al. 1993) were struck on a YPD plate and incubated at 30˚C for 4 days. Plate was placed at 4˚C for 4 days prior to image capture. Note smaller colony formation of *gas1*Δ cells, representative of their growth defect. White colony color (*ADE2* expression) indicates defective silencing. Complete repression of *ADE2* gives rise to pink colonies. *(B)* rDNA silencing at the 25S locus is not enhanced in *gas1*Δ mutants. WT (LPY4908), *esa1-*Δ*414* (LPY4910), *sir2*Δ (LPY4978), and *gas1*Δ (LPY14408) strains with a rDNA::*ADE2-CAN1* reporter at 25S (Fritze et al. 1997) (see Figure 2-6*A* for location of reporter in rDNA) were plated on SC plates lacking adenine and arginine (SC-ade-arg) to monitor growth and SC-ade-arg containing 32 μg/ml canavanine (CAN) to monitor silencing. Decreased growth on canavanine plate indicates defective silencing. Note that the wild-type and *sir2*Δ strains show silencing of the reporter gene whereas the *esa1-*Δ*414* mutant displays a prominent defect in silencing. *ESA1* contributes significantly to 25S rDNA silencing whereas *SIR2*'s contribution is negligible (Clarke et al. 2006). This is consistent with the observation that different genes have different contributions to rDNA silencing, depending on the location of the reporter. For *gas1*Δ, in contrast to the reporter at the 5S rDNA (Figure 2-1*C*), there is no increase in silencing for this 25S reporter. Note that in this control plating, *gas1*Δ growth is reduced therefore the observation that its growth is comparable to *sir2*Δ on the canavanine plate underscores the conclusion that there is no influence on silencing at this locus.

A

hmr::ADE2

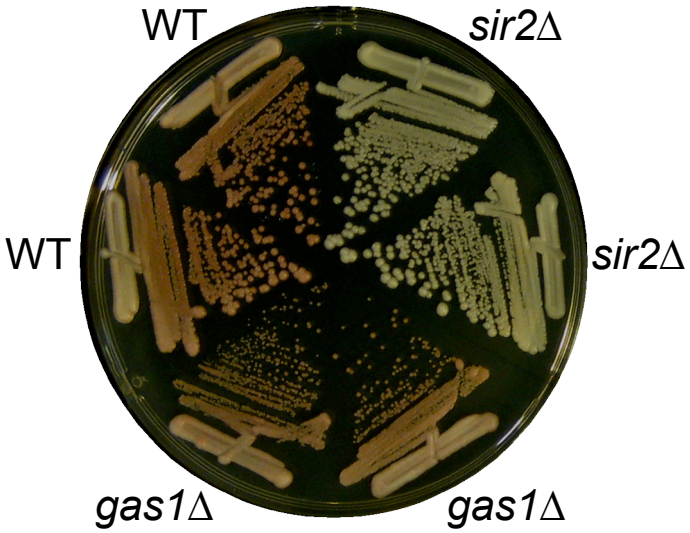

B

rDNA::*ADE2-CAN1*

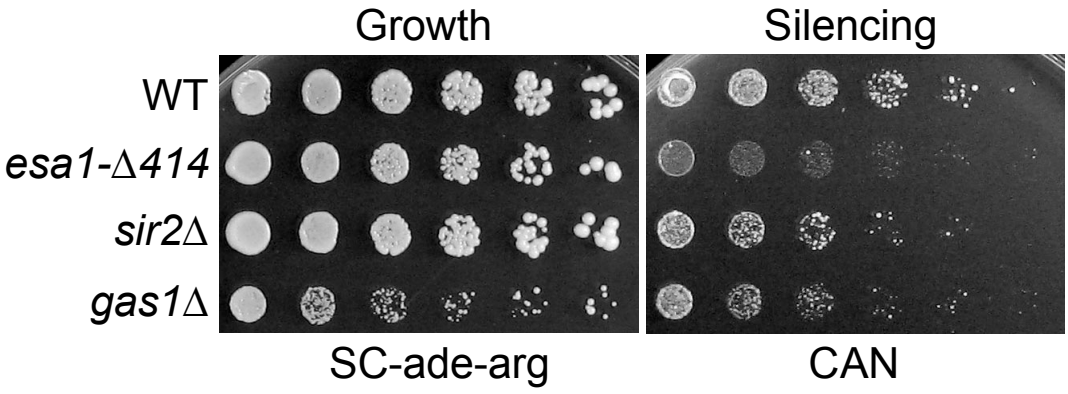

Figure 2-3. The *gas1*Δ telomeric silencing defect is not telomere or promoter specific. *(A)* The *gas1*Δ telomeric silencing defect is observed at chromosome VII-L. WT (LPY1029), *sir2*Δ (LPY12660), and *gas1*Δ (LPY10358) strains with the *URA3* telomeric reporter on chromosome VII-L (Chien et al. 1993) were plated on SC to assay growth and SC containing 5-FOA to assay silencing. Decreased growth on 5-FOA indicates defective silencing. *(B)* The *gas1*Δ telomeric silencing defect is observed with a chromosome V-R *ADE2* telomeric reporter. WT (LPY9911), *sir2*Δ (LPY9961), and *gas1*Δ (LPY14400) strains were grown in YPD overnight and plated for single colonies on YPD. WT and *sir2*Δ plates were incubated at 30˚C for 3 days, and *gas1*Δ plates for 5 days. Plates were placed at 4˚C for 1 month, for red/pink color development, prior to image capture. White colony color (*ADE2* expression) indicates defective silencing.

A

TELVII-L::*URA3*

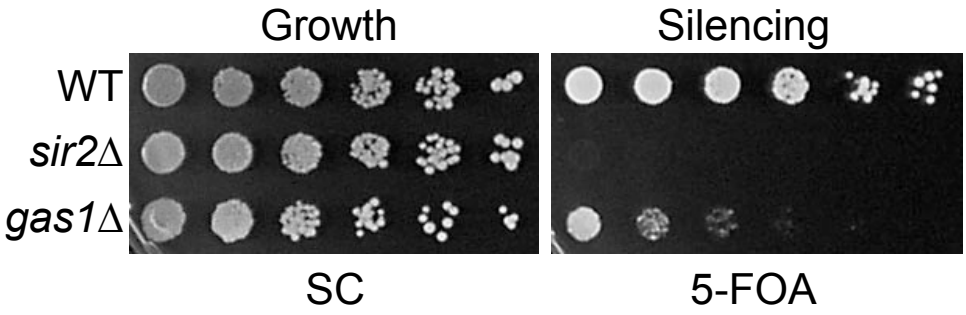

B

TELVR::*ADE2*

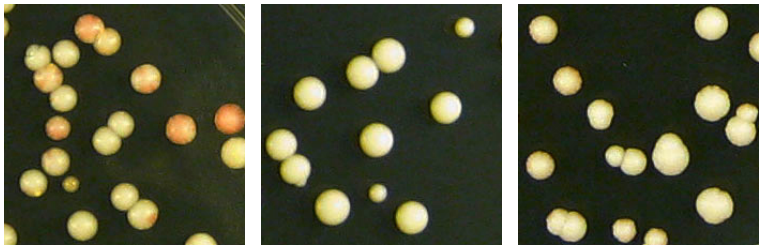

URA3. Both *sir2*Δ and *gas1*Δ mutants expressed this telomeric reporter gene, whereas wild-type cells had intact telomeric silencing (Figure 2-1*D*). In control *gas1*Δ strains lacking the reporter, no 5-FOA sensitivity was seen (Figure 2-1*D*). The *gas1*Δ silencing defect was also observed with a chromosome VII-L *URA3* telomeric reporter (Figure 2-3*A*) and with a chromosome V-R *ADE2* telomeric reporter (Figure 2-3*B*), indicating that the silencing defect occurs at multiple telomeres and is promoter- and gene-independent.

In addition to the reporter assays, transcription of the normally silenced *YFR057W* gene at telomere VI-R was assayed by reverse transcription-coupled quantitative PCR. *YFR057W* RNA was undetectable in wild-type cells whereas transcription was readily detected in both the *gas1*Δ mutant and *sir2*Δ control (Figure 2-1*E*). Thus telomeric silencing in *gas1*Δ is defective compared to wild-type by two independent assays. Yet, some telomeric silencing must be intact since the defects of *gas1*Δ mutants are less somewhat severe than for *sir2*Δ mutants.

The locus-specific silencing phenotypes of *gas1*Δ cells are unusual in that loss of *GAS1* function causes loss of silencing at telomeres, but increased silencing at the rDNA, with no effect on *HM* silencing. This constellation of phenotypes is atypical of the nearly 300 genes previously reported to influence silencing. Thus, *GAS1*'s functions may represent a molecular contribution not yet studied in silent chromatin.

Telomeric silencing function is not a general property of proteins with roles in cell wall biogenesis. In the same way that multiple proteins have roles in silencing, many different enzymes also function in cell wall formation. To determine whether the *gas1*Δ defect in telomeric silencing is a general property of proteins with

these functions, deletions of three genes that contribute enzymatically to the cell wall were constructed with the telomeric reporter. *BGL2* encodes an endo-β-1,3-glucanase involved in cell wall construction and remodeling (Mrsa et al. 1993), and *GAS3* and *GAS5* are homologs of *GAS1* that also encode β-1,3-glucanosyltransferases (Popolo and Vai 1999). Not one of these mutants disrupted telomeric silencing (Figure 2-4). Thus, telomeric silencing defects are not a general characteristic of genes involved in maintenance of the cell wall, including those encoding comparable enzymatic activities, but instead are specific to *gas1*Δ mutants.

Well-defined hallmarks of silent chromatin are intact in *gas1*Δ mutants. The telomeric silencing defect in *gas1*Δ may be caused by a defect in the amount or formation of silent chromatin. At the molecular level, the *gas1*Δ telomeric silencing defect is not a consequence of Sir expression since *gas1*Δ microarray expression analysis reveals normal transcription of *SIR2*, *SIR3*, and *SIR4* (Lagorce et al. 2003), and direct immunoblotting showed that Sir2 and Sir3 levels were not decreased in *gas1*Δ (Figure 2-5).

A distinct possibility was that the silencing phenotypes result from a change in Sir protein occupancy at the silenced region. To test this, Sir2 binding in *gas1*Δ strains was evaluated by chromatin immunoprecipitation (ChIP) experiments using telomere VI-R and rDNA-specific primers (Figure 2-6*A*). We observed that Sir2 occupancy at telomere VI-R in *gas1*Δ was marginally increased relative to wild-type (Figure 2-6*B*). Therefore, decreased Sir2 occupancy does not explain the defective telomeric silencing seen in *gas1*Δ mutants. Likewise, Sir3 occupancy at the telomeres is

Figure 2-4. The *GAS1* telomeric silencing function is not shared with other cell wall genes. WT (LPY4916), *sir2*Δ (LPY10397), *gas1*Δ (LPY10362), *bgl2*Δ (LPY13094), *gas3*Δ (LPY12337) and *gas5*Δ (LPY12348) strains were assayed for telomeric silencing as in Figure 2-1*D*.

TELV-R::*URA3*

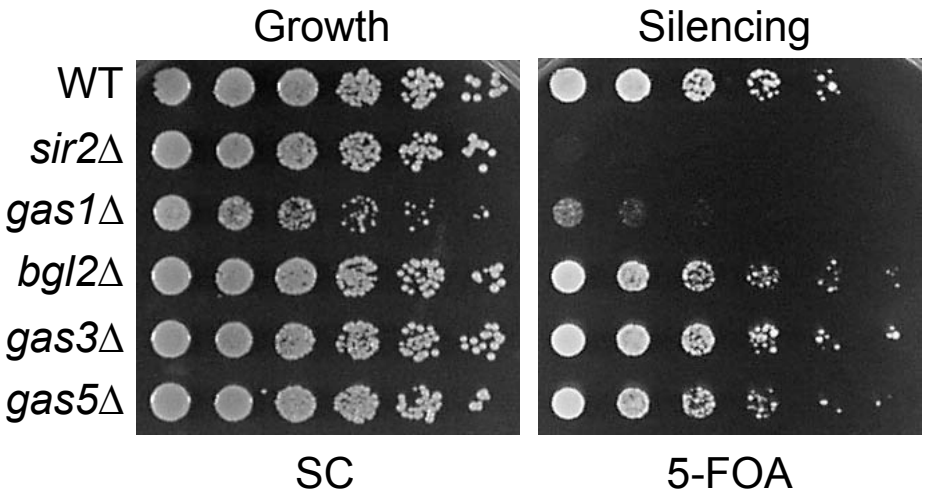

Figure 2-5. Sir2 and Sir3 levels are unchanged in *gas1*Δ mutants. *(A)* Sir2 levels are unaltered in *gas1*Δ mutants. Whole cell protein extracts from WT (LPY5), *gas1*Δ (LPY10129), and *sir2*Δ (LPY11) strains were separated by SDS-PAGE. Immunoblot analysis of Sir2 (65 kDa) was performed with anti-Sir2. Immunoblot analysis of tubulin (50 kDa) was performed with anti-β-tubulin. Images were captured on the Typhoon Trio Variable Mode Imager (GE Healthcare, Piscataway, NJ) and analyzed using ImageQuant TL software. Quantification with normalization to amount of tubulin is shown below Sir2 image, with WT set to 1. *(B)* Sir3 levels are unaltered in *gas1*Δ mutants. Whole cell protein extracts from WT (LPY5), *gas1*Δ (LPY10129) and *sir3*Δ (LPY10) strains were separated by SDS-PAGE. Immunoblot analysis of Sir3 (116 kDa) was performed with anti-Sir3. Immunoblot analysis of tubulin (50 kDa) was performed with anti-β-tubulin. Images were captured as in *(A)*. Quantification with normalization to amount of tubulin is shown below Sir3 image, with WT set to 1.

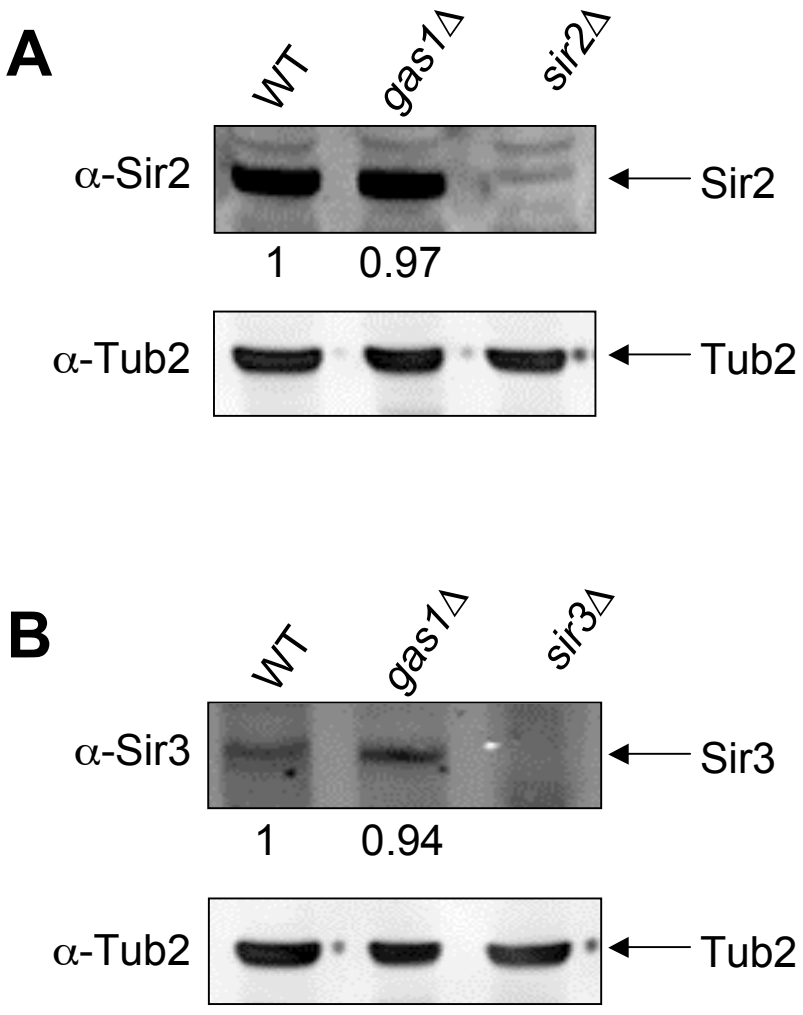
A
WT
gas1Δ
sir2Δ
α-Sir2
Sir2
1
0.97
α-Tub2
Tub2
B
WT
gas1Δ
sir3Δ
α-Sir3
Sir3
1
0.94
α-Tub2
Tub2

Figure 2-6. Key features of silent chromatin are unaltered in *gas1*Δ mutants. *(A)* Map of primer sites used for ChIP. Chromosome VI-R primers amplify regions 0.2 kb and 1 kb from the end of the telomere. Chromosome XII primers amplify regions near the 25S rRNA and 5S rRNA genes. Also shown are *ADE2-CAN1* and *URA3* reporter locations for rDNA silencing assays. *(B)* Sir2 occupancy in *gas1*Δ is increased slightly at the telomere and 5S rDNA. ChIP of Sir2 was done in WT (LPY5), *sir2*Δ (LPY11), and *gas1*Δ (LPY10129) strains. Input and IP DNA were analyzed with primers shown in *(A)* and the non-specific locus *ACT1*. Sir2 enrichment at the telomere and rDNA was normalized to *ACT1*. *(C)* H4K16 is deacetylated at the telomere and rDNA in *gas1*Δ. ChIP of acetylated H4K16 (AcH4K16) was done in the same strains as *(B)*. AcH4K16 enrichment at the telomere and rDNA was normalized to the Chr. V intergenic region. *(D)* H3K56 is deacetylated at the telomere in *gas1*Δ. ChIP of acetylated H3K56 (AcH3K56) was done in the same strains as *(B)*, and as a negative control, *hht2-K56Q* (LPY13166). AcH3K56 enrichment at the telomere was normalized to the intergenic region.

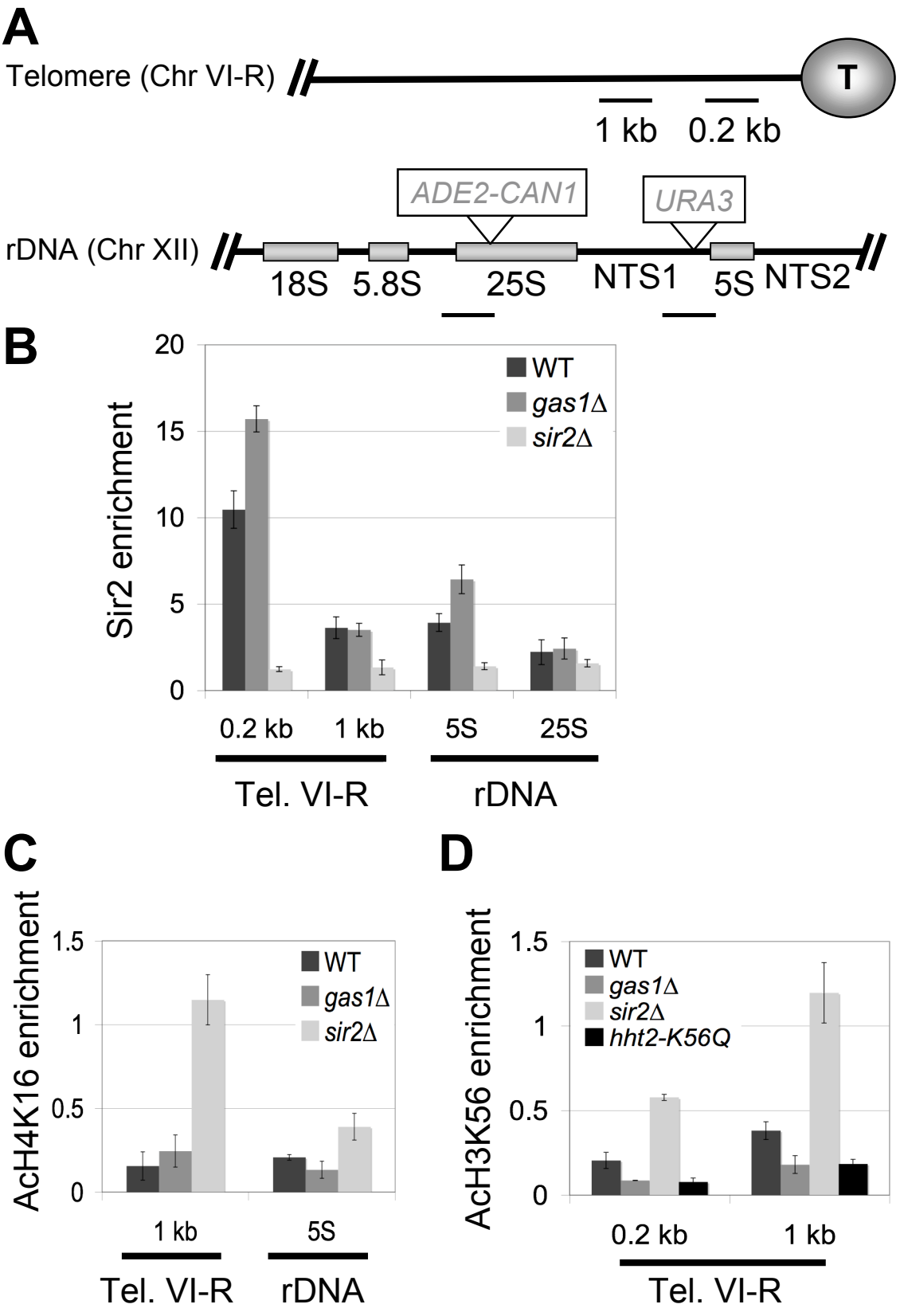
A
Telomere (Chr VI-R)
T
1 kb
0.2 kb
ADE2-CAN1
URA3
rDNA (Chr XII)
18S
5.8S
25S
NTS1
5S
NTS2
B
Sir2 enrichment
20
15
10
5
0
WT
gas1Δ
sir2Δ
0.2 kb
1 kb
5S
25S
Tel. VI-R
rDNA
C
AcH4K16 enrichment
1.5
1
0.5
0
WT
gas1Δ
sir2Δ
1 kb
5S
Tel. VI-R
rDNA
D
AcH3K56 enrichment
1.5
1
0.5
0
WT
gas1Δ
sir2Δ
hht2-K56Q
0.2 kb
1 kb
Tel. VI-R

Figure 2-7. Sir3 binds to the telomere and localizes to telomeric foci in *gas1*Δ; the *in vitro* histone deacetylase activity of Sir2 is unaffected by Gas1. *(A)* Levels of Sir3 occupancy in *gas1*Δ strains overlap those of wild-type cells at the telomere. ChIP of Sir3 was done in WT (LPY5), *sir3*Δ (LPY10), and *gas1*Δ (LPY10129) strains. Input and IP DNA were analyzed with primers shown in Figure 2-6*A* and the non-specific locus *ACT1*. Sir3 enrichment at the telomere was normalized to *ACT1*. (B) GFP-Sir3 localizes to telomeric foci in *gas1*Δ mutants. GFP-Sir3 was visualized in live cells in wild-type diploid (LPY12401) and *gas1*Δ diploid (LPY12462) strains. Three dimensional deconvolution was used to resolve telomeric GFP-Sir3 foci. Each image is a representative nucleus containing GFP-Sir3 foci. *(C)* GST (pLP1302), GST-Sir2 (pLP1275), GST-Gas1 (pLP2087), and GST-Gas1 E161Q, E262Q (pLP2119) were expressed in and purified from bacteria. Purified proteins were added to NAD^+ hydrolysis assays containing ^{3}H-NAD^+. GST-Sir2 activity shown correlates with the conversion of ^{3}H-NAD^+ to ^{3}H-nicotinamide. Sir2 activity was monitored over a 5-hr time period. Addition of wild-type Gas1 or enzymatically inactive Gas1 to these assays neither enhanced nor inhibited Sir2 deacetylase activity.

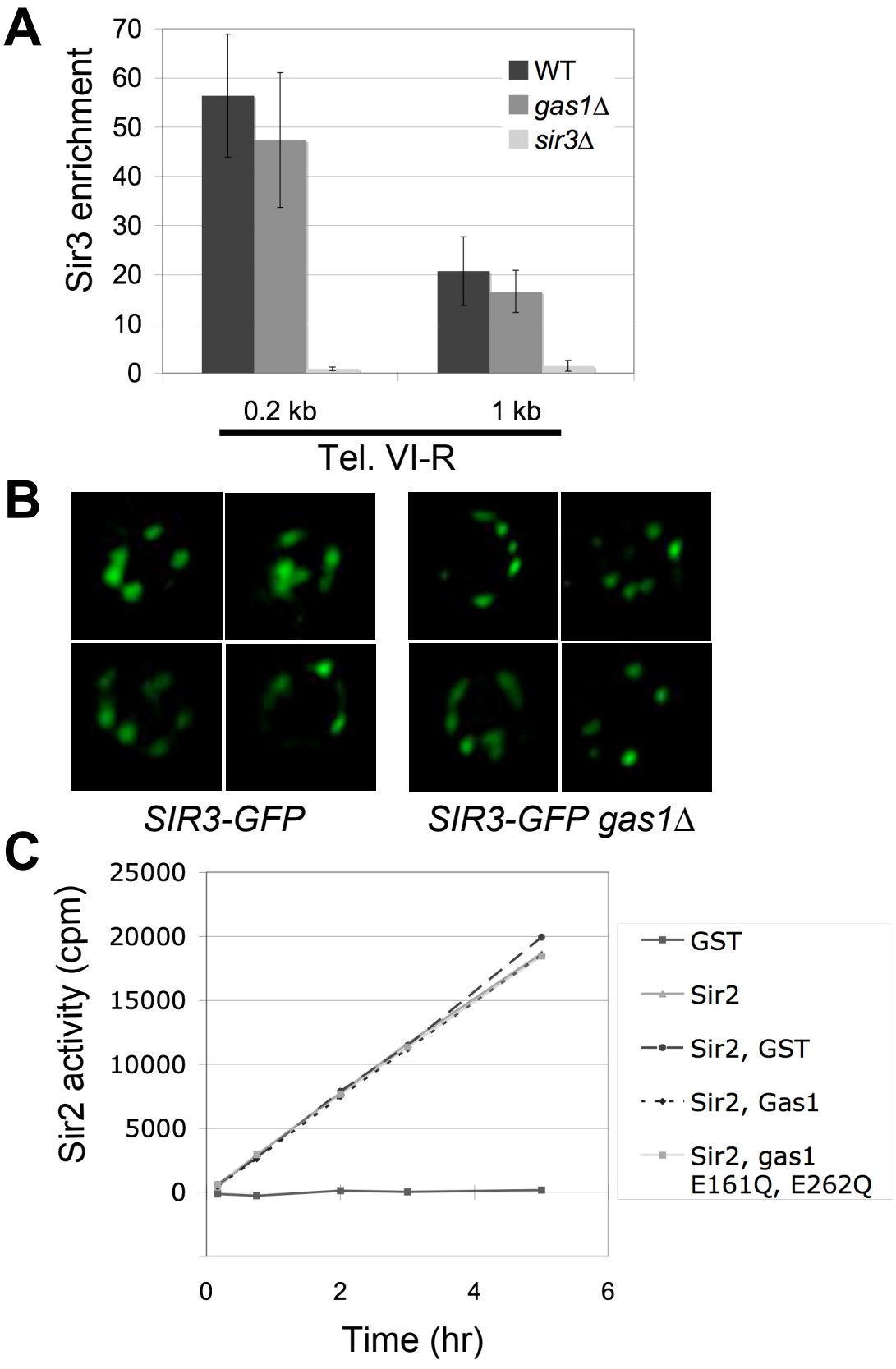
A
Sir3 enrichment
70
60
50
40
30
20
10
0
WT
gas1Δ
sir3Δ
0.2 kb
1 kb
Tel. VI-R
B
SIR3-GFP
SIR3-GFP gas1Δ
C
Sir2 activity (cpm)
25000
20000
15000
10000
5000
0
0
2
4
6
Time (hr)
GST
Sir2
Sir2, GST
Sir2, Gas1
Sir2, gas1
E161Q, E262Q

unaffected in *gas1*Δ mutants (Figure 2-7*A*). Furthermore, Sir3 localizes to telomeric foci in *gas1*Δ mutants, indicating that telomere clustering is normal (Figure 2-7*B*).

An increase in Sir2 binding may explain *gas1*Δ's increase in rDNA silencing. Modestly elevated Sir2 binding was seen near 5S in the rDNA (Figure 2-6*B*), a region of the rDNA repeat including *NTS1* where the increase in silencing was observed (Figure 2-1*B*). At the 25S rDNA, there was no change in Sir2 occupancy (Figure 2-6*B*), a location in the rDNA that showed no difference in rDNA silencing for *gas1*Δ mutants (Figure 2-2*B*). Therefore, occupancy of Sir2 in the rDNA parallels the strength of rDNA silencing observed in *gas1*Δ mutants.

Because a modest increase of Sir2 occupancy in *gas1*Δ was also observed at telomeres, but yielded defective silencing, we considered the possibility that histone acetylation profiles were altered in *gas1*Δ. To address this, ChIP experiments were performed for acetylation of the Sir2 histone targets H4K16 and H3K56 at silenced loci. No increase in H4K16 acetylation was observed in *gas1*Δ at the telomere or 5S rRNA gene (Figure 2-6*C*). Further, no increase in H3K56 acetylation was detected in *gas1*Δ (Figure 2-6*D*). In contrast, the *sir2*Δ mutant displayed increased levels of acetylation at both sites (Figure 2-6*C*, 2-6*D*). Consistent with these results, *in vitro* NAD^+-dependent deacetylase assays with purified GST-Sir2 showed that deacetylase activity was unaffected by addition of purified Gas1 (Figure 2-7*C*). Thus five well-established molecular criteria for telomeric silencing are intact in *gas1*Δ: Sir2 and Sir3 remain telomere bound, Sir3 localizes to telomeric foci, and both H4K16 and H3K56 remain deacetylated. Therefore, a different *GAS1*-dependent event in silent chromatin must be disrupted.

Gas1 silencing function is potentially mediated through its interaction with Sir2. In a genome-wide survey, it was reported that GFP-Gas1 surprisingly localizes to the nuclear periphery in addition to its more expected localization at the cell wall, mitochondria, and endoplasmic reticulum (Huh et al. 2003). Direct examination of GFP-Gas1 showed staining within each cell that coincided with the outer edge of the DAPI nuclear staining, confirming the genome-wide result (Figure 2-8*A*). The nuclear periphery is a clearly relevant location for a fraction of the protein to reside for its function in transcriptional silencing, potentially as a nuclear membrane associated protein.

Because in the localization study GFP was fused to the Gas1 C-terminus, proximal to the GPI anchoring position, we tested whether the tag interfered with proper function of the protein. We found that GFP-Gas1 strains were fully competent for telomeric silencing and had no growth defects at high temperature (Figure 2-8*B*). Therefore it appeared that the tagged protein was functional and there was no reason to consider the reported localization to be spurious.

Two converging observations of Gas1-SIR complex physical interactions prompted us to further examine Gas1's connection with the nuclear Sir2 protein. First, in a high-throughput identification of protein complexes by mass spectrometry, Gas1 associated with the SIR complex component Sir3 (Ho et al. 2002). Second, in a Sir2 two-hybrid screen, Gas1 was found as an interacting protein (Garcia 2003).

Two-hybrid analysis demonstrated an interaction between a GBD-core Sir2 construct containing the catalytic deacetylase domain (residues 244-457) and a GAD-Gas1 construct containing a portion of its catalytic domain (residues 163-407) (Figure

2-9*A*). These constructs contained only a portion of Sir2 and Gas1 to accommodate the possibility that full-length Sir2 bait protein can be repressive (Garcia 2003) and because smaller domain-based protein fragments are observed to increase detection and sensitivity of two-hybrid interactions (Boxem et al. 2008). No interaction was seen when GAD-Gas1 was co-transformed with a GBD vector or GBD-Sir2 construct containing nearly full-length Sir2 (Figure 2-9*A*). Thus, two-hybrid analysis revealed a specific interaction between constructs containing the catalytic domains of Sir2 and Gas1. Previous studies demonstrated that neither *SIR3* nor *SIR4* were required for the Sir2-Gas1 interaction (Garcia 2003). Of note, however, is that the Sir2-Gas1 interaction was enhanced in the *sir4*Δ two-hybrid strain (Garcia 2003). These observations suggest competition between Gas1 and Sir4 for Sir2 binding and indicate that the interaction does not require integrity of the SIR complex.

GST affinity experiments were performed to validate the Sir2-Gas1 two-hybrid interaction with full-length proteins. Recombinant GST-Sir2 was incubated with whole cell extracts from wild-type, *sir2*Δ, or *gas1*Δ yeast strains. GST-Sir2 specifically bound Gas1 both in the presence and absence of endogenous Sir2 (Figure 2-9*B*). A catalytically inactive Sir2, Sir2-H364Y, also interacted with Gas1 by GST affinity binding, showing that the proteins interact despite the loss of Sir2 deacetylase activity (Figure 2-10*A*). This confirmation of the Sir2-Gas1 physical interaction with full-length proteins implies that the effect of Gas1 on silencing may be mediated through its interaction with members of the SIR complex, especially Sir2. It should be noted that GST-Sir2 pulled down only a fraction of Gas1, indicating that both proteins participate in other complexes independently of one another, consistent with Gas1's

Figure 2-8. GFP-Gas1 localizes to the nuclear periphery and is functional in telomeric silencing. *(A)* GFP-Gas1 localizes to the nuclear periphery. GFP-Gas1 (green) was visualized in live wild-type diploid cells (LPY14311). DNA was stained with DAPI (blue). Images shown are representative of nonbudded and budding cells. *(B) GAS1-GFP* functions in telomeric silencing. WT (LPY4916), *sir2*Δ (LPY10397), *gas1*Δ (LPY10362), and *GAS1-GFP* (LPY13691) with a *URA3* telomeric reporter on chromosome V-R were assayed for silencing as in Figure 2-1*D*. To monitor growth (SC) and silencing (5-FOA), plates were incubated at 30˚C, and to monitor temperature sensitivity on SC, plates were incubated at 37˚C.

A

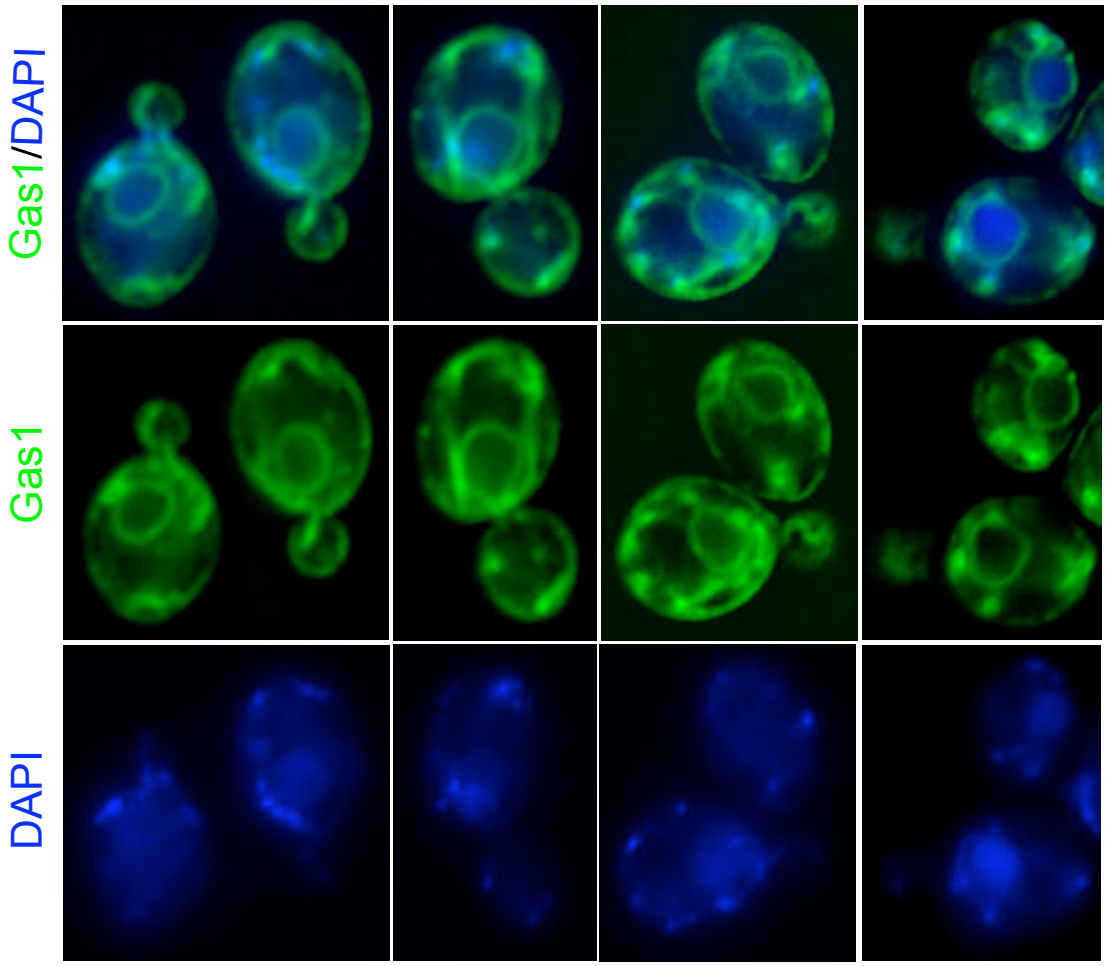

B

TELV-R::*URA3*

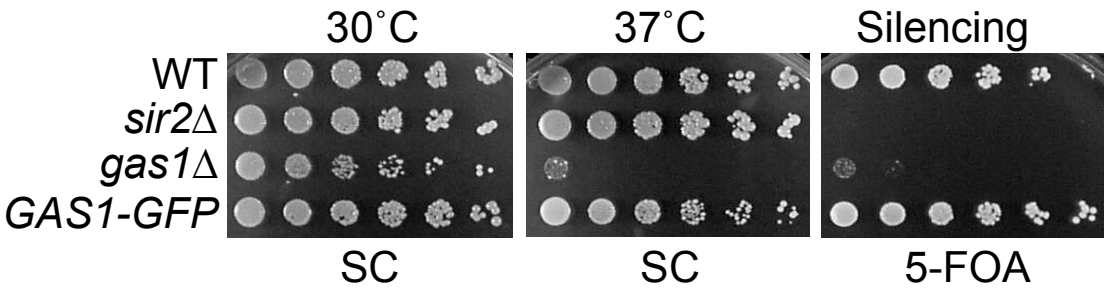

Figure 2-9. Sir2 interacts with Gas1 by two-hybrid and GST affinity binding. *(A)* GBD-core Sir2 interacts with GAD-Gas1. The constructs GBD vector (pLP956), GBD-core Sir2 (pLP1073), and GBD-Sir2 (pLP1074) were expressed from 2μ *TRP1* plasmids. GAD-Gas1 (pLP1205) was expressed from a 2μ *LEU2* plasmid. The two-hybrid strain (LPY3374) was transformed with pairs of these plasmids to form LPY7251 (with pLP956, pLP1205), LPY7251 (with pLP1073, pLP1205), and LPY7253 (with pLP1074, 1205). The growth control plate is SC-leu-trp medium. The interaction plate is this medium also lacking histidine and adenine, to simultaneously monitor for *GAL1-HIS3* and *GAL2-ADE2* reporter activation. Growth on this plate indicates a physical interaction between GBD-core Sir2 and GAD-Gas1. *(B)* GST-Sir2 physically interacts with Gas1. GST (pLP1302) and GST-Sir2 (pLP1275) were purified and incubated with whole-cell extracts from strains used in Figure 2-6*B*. Bound protein was analyzed by immunobloting for Gas1 (125 kDa).

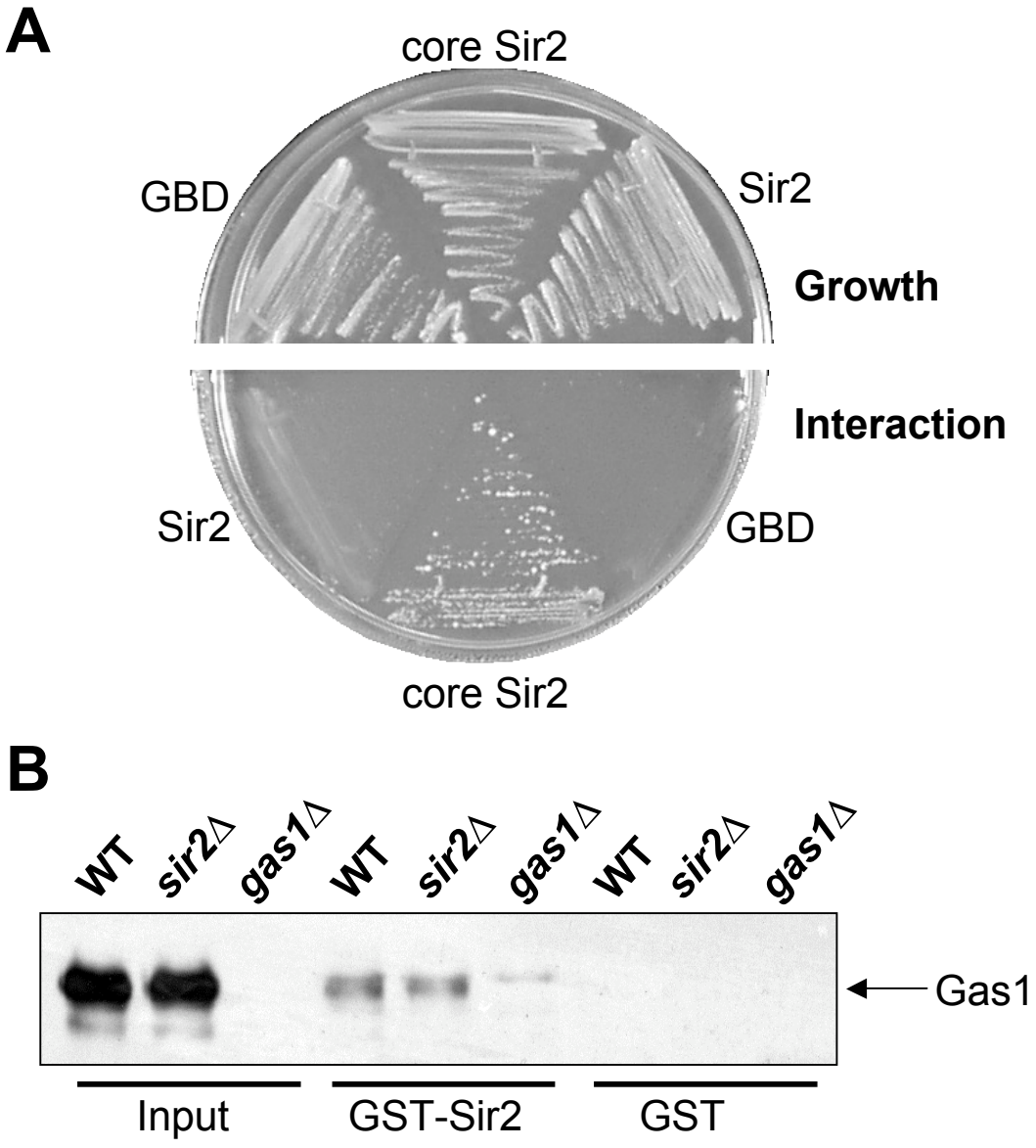
A
core Sir2
GBD
Sir2
Growth
Interaction
Sir2
GBD
core Sir2
B
WT
sir2Δ
gas1Δ
WT
sir2Δ
gas1Δ
WT
sir2Δ
gas1Δ
Gas1
Input
GST-Sir2
GST

Figure 2-10. Catalytically inactive versions of Sir2 and Gas1 interact by GST affinity binding; *GAS1* function in telomeric silencing is separable from its role at the cell wall; Sir2 is immunoprecipitated by anti-β-1,3-glucan in *sir3*Δ *sir4*Δ strains. (A) sir2-H364Y and gas1-E161Q, E262Q physically interact by GST affinity binding. GST (pLP1302), GST-Sir2 (pLP1275), and GST-sir2-H364Y (pLP1276) were purified and incubated with whole-cell extracts from WT (LPY5), *sir2*Δ (LPY11), *gas1-E161Q, E262Q* (LPY12251), and *gas1*Δ (LPY10129) strains. Bound protein was analyzed by immunobloting for Gas1 (125 kDa). *(B)* Sorbitol addition to growth medium suppresses *gas1*Δ temperature sensitivity but does not affect *gas1*Δ telomeric silencing. WT (LPY4916), *sir2*Δ (LPY10397), and *gas1*Δ (LPY10362) strains were plated on SC, with and without 1 M sorbitol, to assay growth at 30˚C and growth at elevated temperature, 37˚C. 5-FOA plates, with and without 1 M sorbitol, were used to assay silencing at 30˚C. *(C)* β-1-3-glucan immunoprecipitations were performed in extracts from wild-type (LPY5), *gas1*Δ (LPY10129), *gas1*Δ *gas3*Δ *gas5*Δ (LPY13543), *sir3*Δ *sir4*Δ (LPY12625) strains overexpressing *SIR2* (pLP349) and from *sir2*Δ (LPY11) expressing a vector construct (pLP135). Transformed strains are LPY13545, LPY13549, LPY13553, LPY13653, and LPY13546, respectively. Immunoprecipitated material was analyzed by immunoblot for Sir2 (65 kDa). Right panel shows a separate immunoblot comparing input levels from *sir3*Δ *sir4*Δ strains to the other strains expressing *SIR2*. Note that input levels of Sir2 are elevated in *sir3*Δ *sir4*Δ, which is likely to result in the increased signal observed in the IP for the *sir3*Δ *sir4*Δ strain.

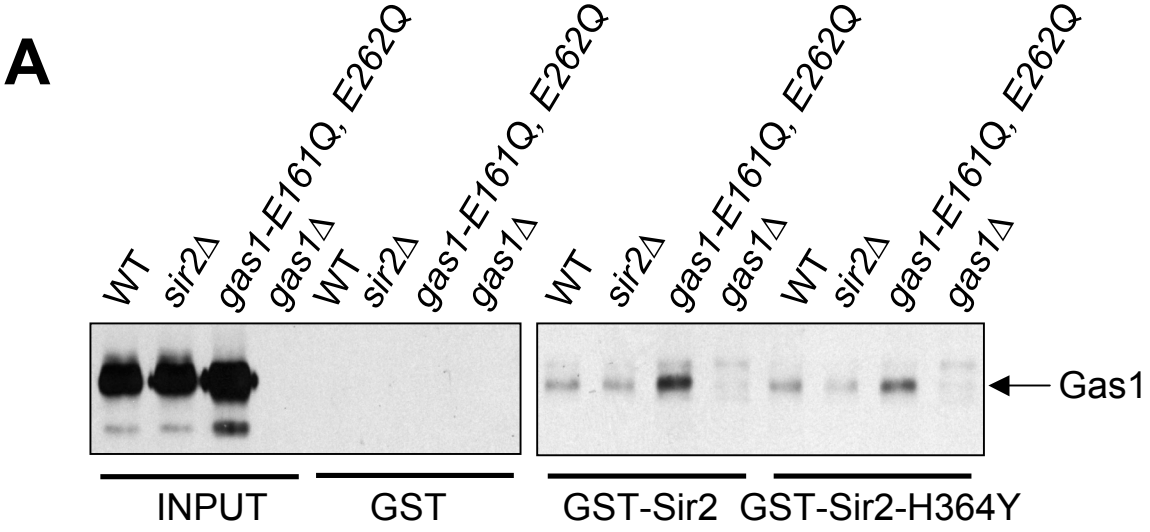
A
WT
sir2Δ
gas1-E161Q, E262Q
gas1Δ
Gas1
INPUT
GST
GST-Sir2
GST-Sir2-H364Y

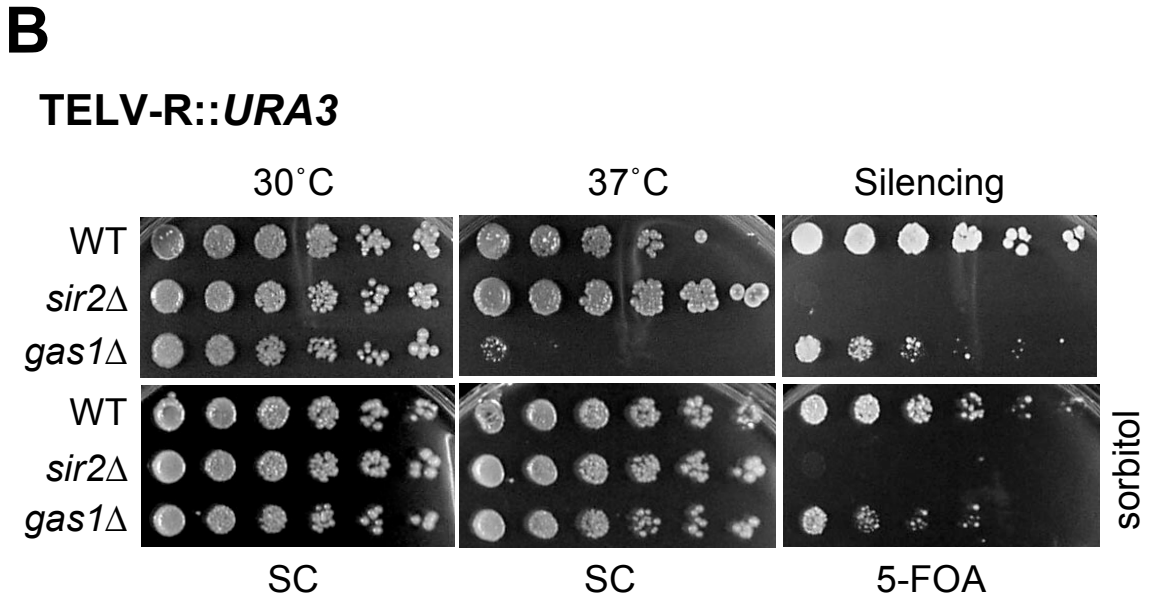
B
TELV-R::URA3
30˚C
37˚C
Silencing
WT
sir2Δ
gas1Δ
sorbitol
SC
SC
5-FOA

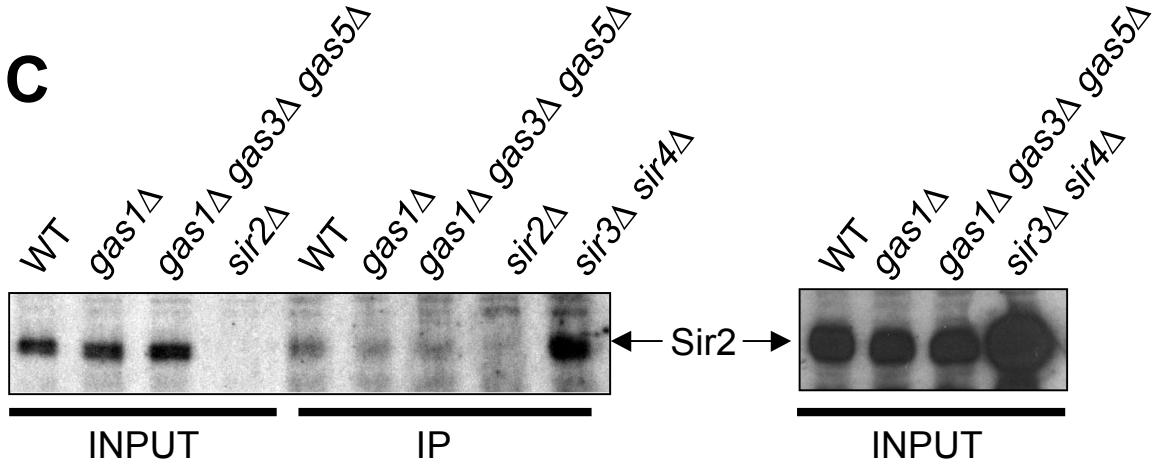
C
WT
gas1Δ
gas1Δ gas3Δ gas5Δ
sir2Δ
sir3Δ sir4Δ
Sir2
INPUT
IP
INPUT

additional localization beyond the nuclear periphery and the previous characterization of Sir2 as a member of the SIR and RENT complexes.

Gas1's enzymatic activity is required for transcriptional silencing. Gas1's physical association with Sir2 suggested a direct role for Gas1 in silencing. Therefore, we tested whether the enzymatic activity of Gas1 contributes to silencing. Previous studies identified two amino acid residues critical for Gas1 β-1,3-glucanosyltransferase activity, E161 and E262, that map to its catalytic domain (Carotti et al. 2004; Papaleo et al. 2006). Importantly, Gas1 protein with glutamine substitutions of these two catalytic residues remains structurally intact, yet its enzymatic activity is destroyed (Carotti et al. 2004).

The *gas1-E161Q* and *gas1-E262Q* mutants were assayed for growth and telomeric silencing. Sensitivity to high temperature was observed in the mutant strains, confirming that the enzymatically inactive *gas1* mutants exhibited the classic cell wall defect of *gas1*Δ (Figure 2-11*A*). The catalytically inactive Gas1 mutant proteins were also completely defective in telomeric silencing, indicating that the enzymatic activity is necessary for silencing (Figure 2-11*A*). When the double point mutant (*gas1-E161Q, E262Q*) was expressed in a wild-type background, growth at high temperature and telomeric silencing was not compromised, demonstrating that the mutations were not dominant (Figure 2-11*A*). Further, the Gas1-Sir2 interaction was not disrupted in the *gas1* catalytically inactive mutant, as demonstrated by GST affinity (Figure 2-10*A*). Thus, although Gas1's catalytic activity is required for its silencing function, it does not promote interaction with Sir2.

To determine if Gas1's established function in cell wall biogenesis is separable from its role in silencing, telomeric silencing of *gas1*Δ was examined in the presence of sorbitol. Sorbitol is an osmotic stabilizing agent capable of rescuing many types of mutants with thermosensitive cell lytic phenotypes (Cid et al. 1995; Hampsey 1997). Sorbitol rescues the temperature sensitivity of *gas1*Δ mutants (Figure 2-10*B*). However, sorbitol did not rescue *gas1*Δ telomeric silencing, demonstrating a separation of function between Gas1 actions at the cell wall and silencing (Figure 2-10*B*). The inability of sorbitol to rescue *gas1*Δ telomeric silencing defects supports the idea that *GAS1*'s effect on transcriptional silencing is not a simple consequence of its role in the cell wall and provides evidence that silencing is a separate nuclear role for Gas1.

The observations that Gas1 enzymatic activity is required for silencing (Figure 2-11*A*) and that GFP-Gas1 localizes to the nuclear periphery (Huh et al. 2003) (Figure 2-8*A*) raise the possibility that Gas1 enzymatically modifies chromatin factors, such as Sir proteins or histones. This would result in attachment and elongation of β-1,3-glucan to nuclear protein substrates, which has not previously been observed. To probe for cellular substrates involved in silencing, an antibody directed against β-1,3-glucan (Meikle et al. 1991) was used in immunoprecipitations that were then analyzed for the presence of Sir2 protein. No signal was observed in the *sir2*Δ control strain yet Sir2 was immunoprecipitated by anti-β-1,3-glucan, demonstrating that endogenous Sir2 or proteins with which it is complexed were recognized (Figure 2-11*B*). Importantly, in *gas1*Δ cells, significantly less Sir2 was pulled down, and Sir2 was undetectable in the *gas1*Δ *gas3*Δ *gas5*Δ strain that is likely to have no residual β-1,3-

glucanosyltranferase activity (Figure 2-11*B*). Sir2 was also detected in β-1,3-glucan immunoprecipitations in a *sir3*Δ *sir4*Δ strain, suggesting that the SIR complex was not required for this potential Sir2 modification or association with other substrate (Figure 2-10*C*). These results support the possibility that post-translational modification by β-1,3-glucan of Sir2 or other chromatin components may provide a new mechanism for regulation of locus-specific transcriptional silencing.

DISCUSSION

We report here that the glucanosyltransferase Gas1 participates in locus-specific transcriptional silencing. The role of Gas1 in silencing is mediated by its β-1,3-glucanosyltransferase activity and may act through its physical interaction with Sir2 or other bridging partners (Figure 2-12). Importantly, Gas1's function in silencing is separable from its previously described role in cell wall biogenesis, demonstrating an unsuspected nuclear function for this enzyme.

The surprising, yet compelling observations that Gas1 is enzymatically active in the nucleus and functions in transcriptional silencing are supported by several independent lines of evidence. First, the β-1,3-glucanosyltranferase activity of Gas1 is required for silencing (Figure 2-11*A*). In addition, sorbitol rescues *gas1*Δ osmotic sensitivity, but not silencing defects (Figure 2-10*B*), consistent with a role for Gas1 beyond cell wall biogenesis, such as in the nucleus where silencing occurs. Gas1 localization to the nuclear periphery (Huh et al. 2003) (Figure 2-8*A*) strengthens the notion that the Sir2-Gas1 physical interaction is relevant *in vivo* since a subset of

Figure 2-11. Gas1 enzymatic activity is required for transcriptional silencing and is linked to Sir2. *(A) gas1* enzymatically inactive point mutants are defective in telomeric silencing. The diagram of Gas1 shows the location of the E161Q and E262Q mutations in the catalytic domain. Dark bar at the C-terminus of Gas1 indicates GPI anchor position. WT (LPY4916) strains were transformed with the 2µ *HIS3* plasmids: vector (pLP359), *GAS1* (pLP2091), and *gas1-E161Q, E262Q* (pLP2117). Transformed WT strains are LPY13554, LPY13559, and LPY13562. The *gas1*Δ strain (LPY10362) was transformed with 2µ *HIS3* plasmids: pLP359, pLP2091, pLP2093 (*gas1-E161Q*), pLP2094 (*gas1-E262Q*), and pLP2117. Transformed *gas1*Δ strains are LPY13563 and LPY13568-LPY13571. Growth was examined on SC plates lacking histidine (SC-his). Silencing was examined on SC-his containing 5-FOA (SC-his 5-FOA). Growth at elevated temperature was examined at 37˚C. *(B)* Anti-β-1,3-glucan immunoprecipitates Sir2. β-1-3-glucan immunoprecipitations were performed in extracts from wild-type (LPY5), *gas1*Δ (LPY10129), and *gas1*Δ *gas3*Δ *gas5*Δ (LPY13543) strains overexpressing *SIR2* (pLP349) and from *sir2*Δ (LPY11) expressing a vector construct (pLP135). Transformed strains are LPY13545, LPY13549, LPY13553, and LPY13546, respectively. Immunoprecipitated material was analyzed by immunoblot for Sir2 (65 kDa).

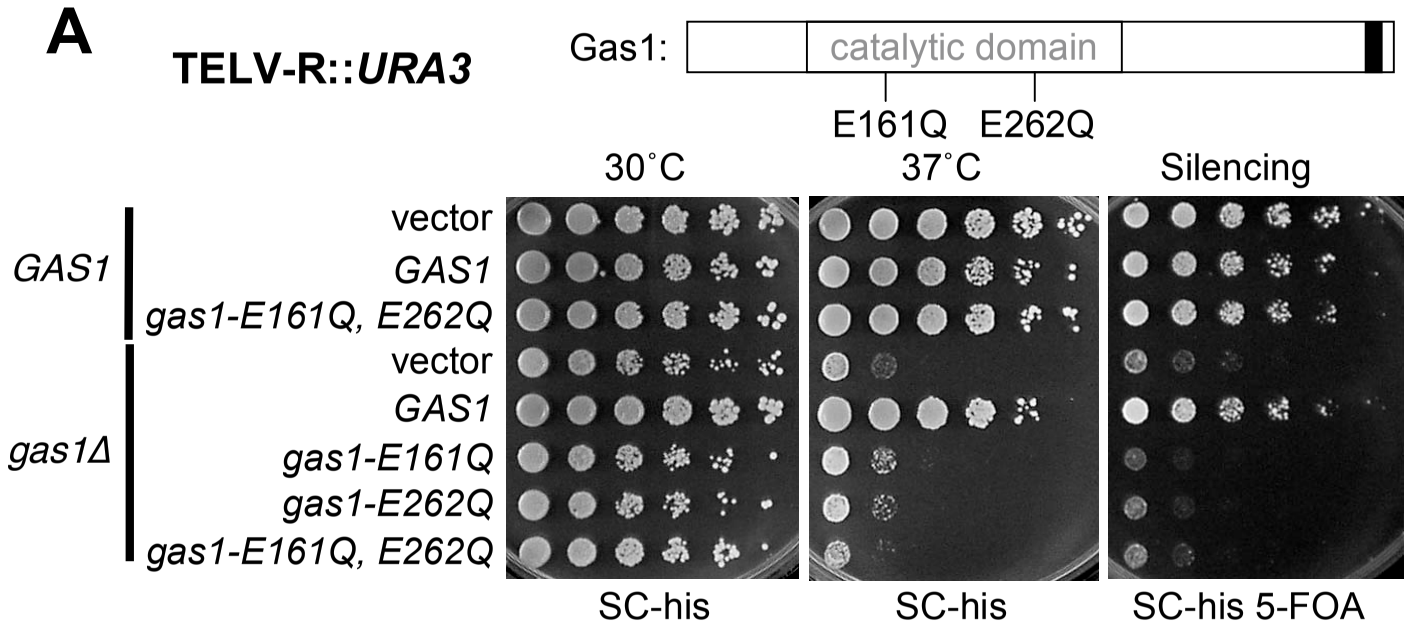
A
TELV-R::URA3
Gas1:
catalytic domain
E161Q
E262Q
30˚C
37˚C
Silencing
GAS1
vector
GAS1
gas1-E161Q, E262Q
gas1Δ
vector
GAS1
gas1-E161Q
gas1-E262Q
gas1-E161Q, E262Q
SC-his
SC-his
SC-his 5-FOA

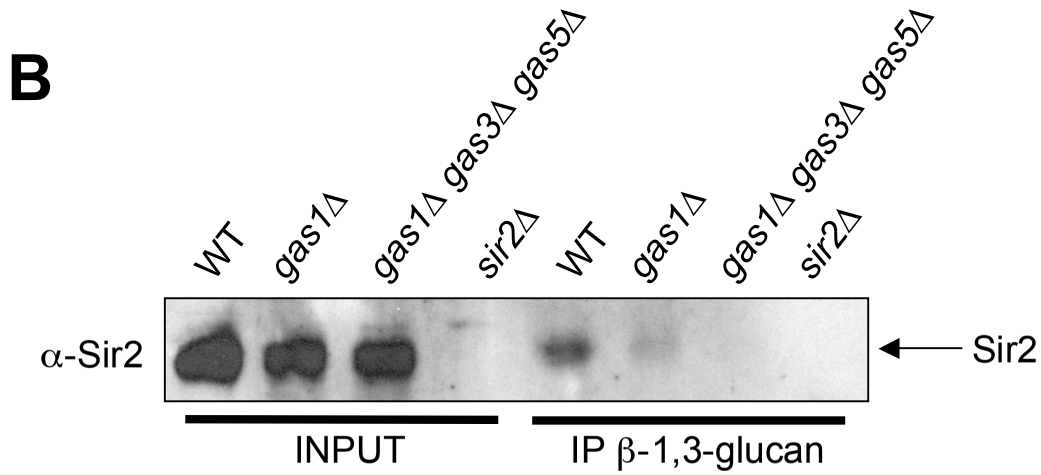
B
WT
gas1Δ
gas1Δ gas3Δ gas5Δ
sir2Δ
WT
gas1Δ
gas1Δ gas3Δ gas5Δ
sir2Δ
α-Sir2
Sir2
INPUT
IP β-1,3-glucan

Figure 2-12. A model summarizing Gas1 effects on transcriptional silencing. In wild-type cells, Sir2 functions in robust silencing of the rDNA. In the absence of Gas1 nuclear function, Sir2 can also weakly contribute to telomeric silencing. Gas1 physically interacts with Sir2 to alter the β-1,3-glucan modification state of Sir2, or other chromatin factors that Sir2 contacts, thereby strengthening Sir2 function in telomeric silencing, and inhibiting Sir2 function in rDNA silencing. When *GAS1* function is lost, the modification to Sir2 (or other factors) is also lost, resulting in decreased telomeric silencing and increased rDNA silencing. Note that β-1-3,glucan is modeled as a single residue here (hexagon), yet Gas1 contributes to both β-1,3-glucan chain elongation and branching. The structure of any carbohydrate modification is likely to be more complex than that modeled here (Popolo and Vai 1999).

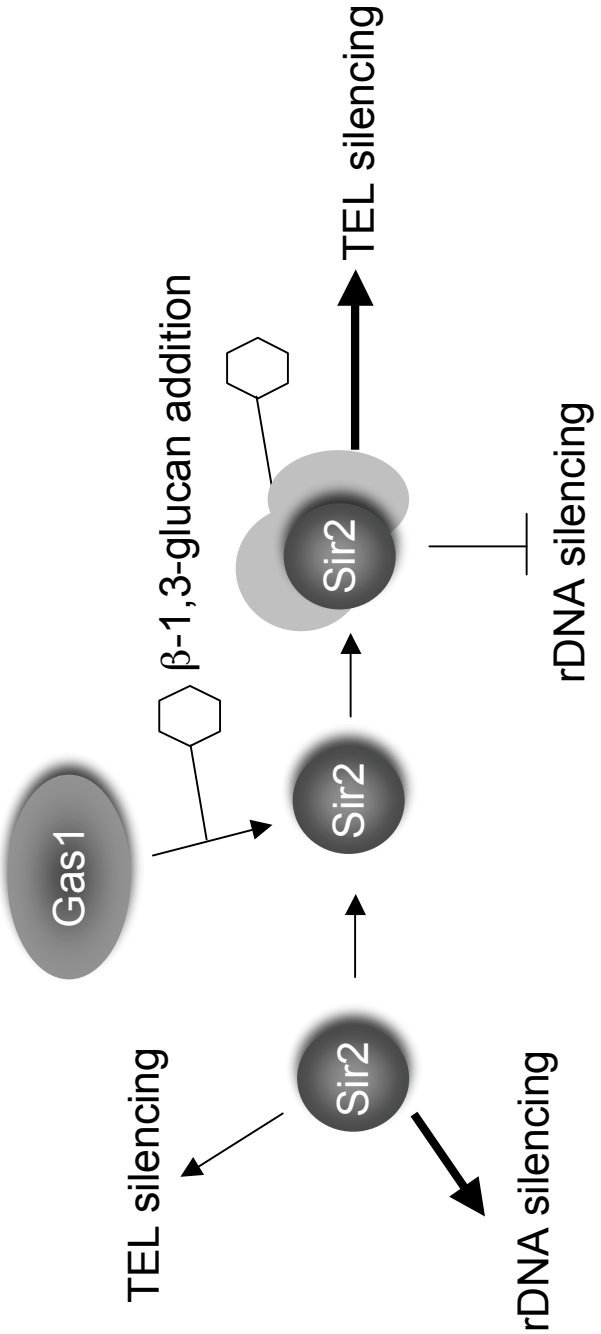
TEL silencing
Sir2
rDNA silencing
Gas1
β-1,3-glucan addition
Sir2
Sir2
TEL silencing
rDNA silencing

silencing proteins reside in the same nuclear compartment. Indeed, Sir2 was found in immunoprecipitates with an antibody directed against β-1,3-glucan, the subunit transferred by Gas1 catalysis (Figure 2-11*B*), demonstrating that the modification is physically associated with Sir2, either directly or bridged through other substrate proteins.

The regulation of transcriptional silencing is complex, with numerous proteins implicated in the processes of forming silent chromatin and restricting its spread into euchromatic regions. Modifications of histones and other chromatin proteins are fundamental for the appropriate regulation of silent chromatin (reviewed in Rusche et al. 2003; Shilatifard 2006; Berger 2007). Post-translational modifications of non-histone silencing proteins have also been observed. For example, the SIR complex structural component Sir3 is acetylated and phosphorylated, and these modifications contribute to its function in transcriptional silencing (Wang et al. 2004; Stone and Pillus 1996). Other less well-studied post-translational modifications are likely to contribute to transcriptional silencing. The discovery of such modifications will be facilitated by the characterization of new catalytically active proteins with roles in silencing, as reported here.

A distinct role for *GAS1* in transcriptional silencing. Silencing assays in *gas1*Δ mutants revealed telomeric silencing defects, increased rDNA silencing, and intact *HM* silencing. This combination of phenotypes is unique. Deletion of the MAP kinase pathway genes *BCK1* and *SLT2* results in defective telomeric silencing and enhanced rDNA silencing, but also causes enhanced *HMR* silencing (Ray et al. 2003). Slt2 phosphorylates Sir3 (Ai et al. 2002; Ray et al. 2003). During stress response,

hyperphosphorylation of Sir3 can decrease telomeric silencing (Ai et al. 2002) and under normal conditions, Sir3 phosphorylation strengthens telomeric silencing (Stone and Pillus 1996). Our data point to modification of the SIR complex by a previously unsuspected activity.

A recent study provides another link between Gas1 and chromatin modification since *gas1*Δ and a number of other mutants are implicated in regulation of total acetylation levels of histone H3 and H4 (Peng et al. 2008). Decreased levels of tetraacetylated H3 and H4 were reported for *gas1*Δ mutants when assayed by mass spectrometry (Peng et al. 2008). However, in directed studies with isoform specific histone antibodies for multiple acetylated lysines including H4K16, which is required for telomeric silencing, we detected no differences in acetylation in *gas1*Δ mutants (Figure 2-13). Therefore, it remains unresolved if specific changes in acetylation or other histone modifications underlie the silencing phenotypes of *gas1*Δ mutants.

A role for carbohydrate modification in chromatin function. The modification of Sir2 or other chromatin components by Gas1 raises a new possibility for regulating Sir2 enzymatic activity downstream of Sir2 binding and histone deacetylation, perhaps by influencing the recruitment of other factors crucial for silent chromatin formation. It is possible that the interaction between Sir2, Gas1, and β-1,3-glucan is bridged by another factor that Sir2 contacts, yet it is unlikely that such bridging factors are solely members of the SIR complex because Sir2 was also recovered in β-1,3-glucan immunoprecipitations in *sir3*Δ *sir4*Δ strains (Figure 2-10*C*). Future studies should establish whether other Sir2-interacting proteins, such as

Figure 2-13. Genome-wide acetylation of histone H3K9,K14, H4K5, and H4K16 is not controlled by *GAS1*. Whole cell protein extracts from WT (LPY5), *gas1*Δ (LPY10129), *gas1-E161Q, E262Q* (LPY12251), *gas1*Δ *gas3*Δ *gas5*Δ (LPY13543), *hht2-K14A* (LPY13654), *hhf2-K5A* (LPY13656), and *hhf2-K16A* (LPY11509) were separated by SDS-PAGE. Immunoblot analysis was performed with antiserum specific to acetylated H3K9,K14 (AcH3K9,K14), acetylated H4K5 (AcH4K5), acetylated H4K16 (AcH4K16), and the C-terminus of histone H3. Images were captured on the Typhoon Trio Variable Mode Imager (GE Healthcare, Piscataway, NJ).

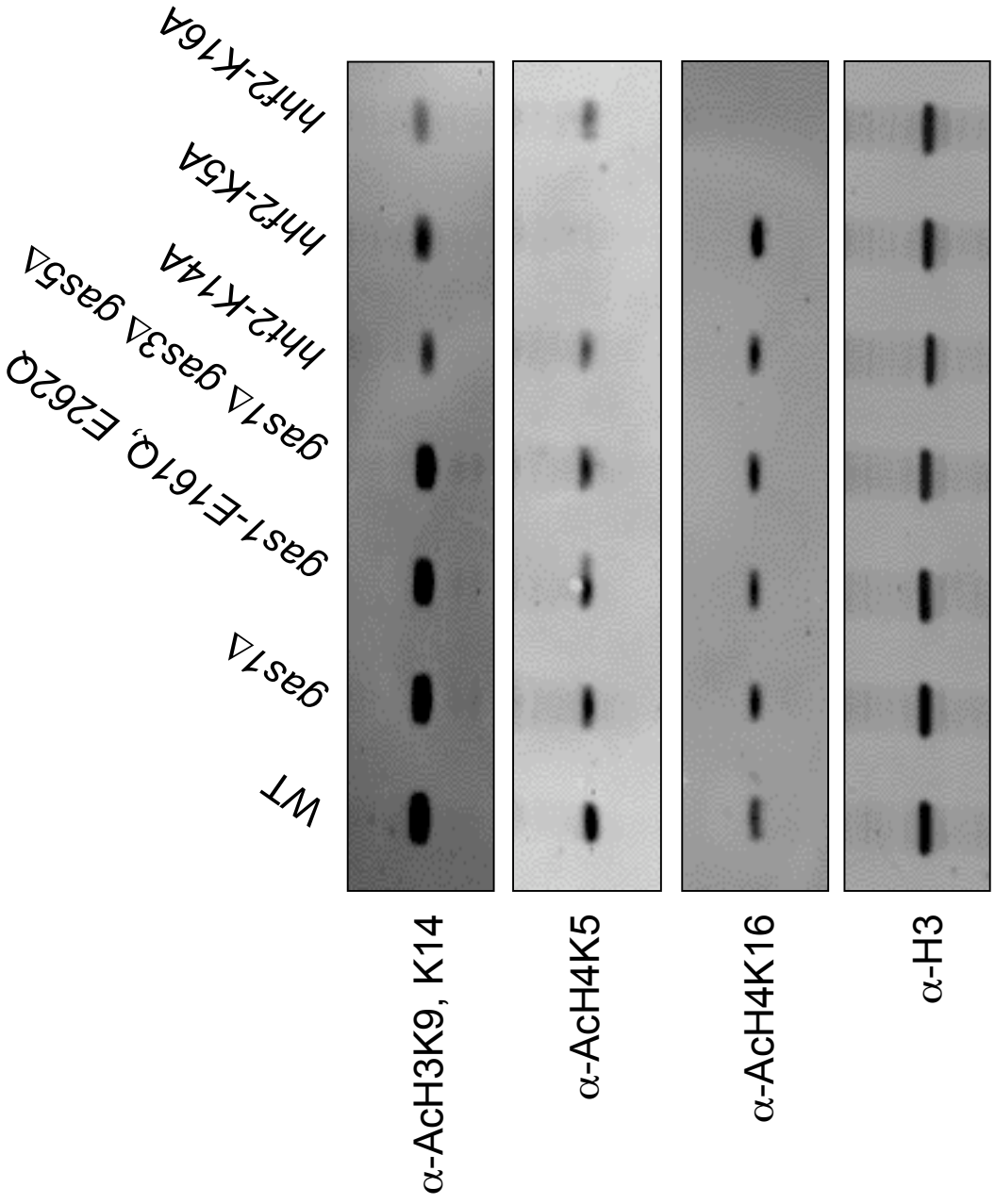
α-AcH3K9, K14
α-AcH4K5
α-AcH4K16
α-H3
WT
gas1Δ
gas1-E161Q, E262Q
gas1Δ gas3Δ gas5Δ
hht2-K14A
hht2-K5A
hht2-K16A

histones and other chromatin components, mediate the interaction between Sir2 and β-1,3-glucan, or are themselves substrates for Gas1.

Precedents are known for post-translational carbohydrate modifications of proteins that affect transcription. Early studies demonstrated glycosylation of histones in Tetrahymena (Levy-Wilson 1983) and complex carbohydrate modification of vertebrate high mobility group proteins (Reeves et al. 1981). More recently O-linked beta-N-acetylglucosamine (O-GlcNAc) modification at serine and threonine residues has been found on both cytoplasmic and nuclear proteins in all plants and animals. Indeed, in mammalian cells, O-GlcNAcylation of nuclear proteins is critical to cellular processes including signaling, cell cycle progression, and transcription, and these O-GlcNAcylated proteins are tied to diabetes and neurodegeneration (reviewed in Hart et al. 2007). Furthermore, the RNA polymerase II transcription factor Sp1 is O-GlcNAcylated (Jackson and Tjian 1988). *In vitro* studies established that Sp1's modification appeared required for its role in transcriptional activation, but not in template loading, analogous to the *in vivo* observations reported here for chromatin in *GAS1*-dependent silencing. A number of Sp1-related DNA-binding factors are also glycosylated, illustrating a potentially common mode of regulation (reviewed in Bouwman and Philipsen 2002). Further exploration of the *in vivo* roles of carbohydrate modifying enzymes in transcriptional silencing should provide new insights into the diverse regulatory mechanisms for silencing and other chromatin-dependent processes.

MATERIALS AND METHODS

Yeast strains and methods. Strains are listed in Table 2-1. Yeast strains were constructed with standard methods (Amberg et al. 2005), (Darst et al. 2008) with deletions using oligonucleotides in Table 2-2.

Plasmid construction. Plasmids described below are listed in Table 2-3. The plasmid pLP1951 was constructed by inserting the *Eag*I *GAS1* fragment from YEpBS6 (pLP1823; gift from A. Conzelmann) (Vai et al. 1991) into pRS425 (pLP1623, 2µ *LEU2* vector). pLP2001 was obtained by direct PCR mutagenesis (Wang and Malcolm 1999) of pLP1951 with oligonucleotides oLP818 and oLP819. The *gas1-E161Q* mutation in pLP2001 was verified by sequencing using oLP822, oLP823, and oLP824. pLP2002 was obtained by PCR mutagenesis of pLP1951 with oLP820 and oLP821. The *gas1-E262Q* mutation in pLP2002 was verified by sequencing using oLP822, oLP823, and oLP824. The plasmid pLP2114 was obtained by PCR mutagenesis of pLP2002 using the primers oLP818 and oLP819, with *gas1-E161Q* mutation verified by sequencing with oLP823. The plasmids pLP2091, pLP2093, and pLP2094 resulted from ligating the *Spe*I-*Sac*II fragment of pLP1951, pLP2001, and pLP2002 to *Spe*I-*Sac*II digested pRS423 (pLP359, 2µ *HIS3* vector). pLP2117 was obtained by PCR mutagenesis on pLP2094 with oLP818 and oLP819, with *gas1-E161Q* mutation verified by sequencing with oLP823. The plasmid pLP2087 was obtained by ligating the *Dra*I fragment of pLP1951 to *Sma*I digested pGEX-4T-2 (pLP2057), to create an in frame GST tagged Gas1 construct, verified by sequencing with oLP847. pLP2099 was obtained by PCR mutagenesis of pLP2087

Table 2-1. Yeast strains used in Chapter 2.[a]

Strain	Genotype	Source/Reference
LPY5	W303-1a *MAT***a** *ade2-1 can1-100 his3-11,15 leu2-3,112 trp1-1 ura3-1*	R. Rothstein
LPY10	W303-1a *sir3::TRP1*	
LPY11	W303-1a *sir2::HIS3*	
LPY79	W303-1b *MAT*α *ade2-1 can1-100 his3-11,15 leu2-3,112 trp1-1 ura3-1*	R. Rothstein
LPY1029	YDS631 W303-1b *adh4::URA3-*$(C_{1\text{-}3}A)_n$	Chien et al. 1993
LPY2446	JS128 *MAT*α *his3*Δ*200 leu2*Δ*1 ura3-167 RDN::Ty1-mURA3*	Smith and Boeke 1997
LPY2447	JS163 *MAT*α *his3*Δ*200 leu2*Δ*1 ura3-167 sir2*Δ*2::HIS3 RDN::Ty1-mURA3*	
LPY3374	PJ69-4A *MAT***a** *gal4*Δ *gal80*Δ *his3-200 leu2-3,112 trp1-901 ura3-52 GAL2-ADE2 LYS2::GAL1-HIS3 met2::GAL7-lacZ*	James et al. 1996
LPY4908	W303-1a rDNA::*ADE2-CAN1*	
LPY4910	W303-1a *esa1-*Δ*414* rDNA::*ADE2-CAN1*	
LPY4912	W303-1a *hmr*Δ*E::TRP1*	
LPY4916	W303-1a TELVR*::URA3*	
LPY4958	W303-1a *sir1::LEU2 hmr*Δ*E::TRP1*	
LPY4978	W303-1b *sir2::HIS3* rDNA::*ADE2-CAN1*	
LPY4980	W303-1a *sir2::HIS3 hmr*Δ*E::TRP1*	
LPY7251	LPY3374 + pLP956, pLP1205	
LPY7252	LPY3374 + pLP1073, pLP1205	
LPY7253	LPY3374 + pLP1074, pLP1205	
LPY9046	W303-1a *hht1-hhf1*Δ*::kanMX hht2-hhf2*Δ*::kanMX hta2-htb2*Δ*::HPH* + pJH33	
LPY9911	W303-1a TELVR::*ADE2*	
LPY9961	W303-1b *sir2::HIS3* TELVR::*ADE2*	
LPY10074	*MAT*α *his3*Δ*200 leu2*Δ*1 ura3-167 gas1*Δ*::kanMX RDN::Ty-1-mURA3*	
LPY10078	*MAT*α *his3*Δ*200 leu2*Δ*1 ura3-167 gas1*Δ*::kanMX sir2*Δ*2::HIS3 RDN::Ty-1-mURA3*	

Table 2-1. Yeast strains used in Chapter 2. (continued)

LPY10129	W303-1a *gas1Δ::kanMX*
LPY10358	W303-1a *gas1Δ::kanMX trp1Δ0 ura3Δ0 adh4::URA3-UAS$_G$*
LPY10362	W303-1a *gas1Δ::kanMX* TELVR*::URA3*
LPY10397	W303-1a *sir2::HIS3* TELVR*::URA3*
LPY11509	LPY9046 + pLP1990
LPY11551	W303-1a *sir2::HIS3 hmr::ADE2*
LPY11552	W303-1b *sir2::HIS3 hmr::ADE2*
LPY12232	W303-1a *hht1-hhf1Δ::kanMX hht2-hhf2Δ::kanMX hta2-htb2Δ::HPH* + pJH33
LPY12251	LPY10129 + pLP2114
LPY12337	W303-1a *gas3Δ::kanMX* TELVR::*URA3*
LPY12348	W303-1a *gas5Δ::kanMX* TELVR::*URA3*
LPY12401	*MAT***a**/*MATα his3Δ1/his3Δ1 leu2Δ0/leu2Δ0 LYS2/LYS2 met15Δ0/met15Δ0 ura3Δ0/ura3Δ0 GFP-SIR3-HIS3MX6/GFP-SIR3-HIS3MX6*
LPY12462	*MAT***a**/*MATα his3Δ1/his3Δ1 leu2Δ0/leu2Δ0 lys2Δ0/LYS2 MET15/met15Δ0 ura3Δ0/ura3Δ0 GFP-SIR3-HIS3MX6/GFP-SIR3-HIS3MX6 gas1Δ::kanMX/gas1Δ::kanMX*
LPY12625	W303-1b *sir3::TRP1 sir4::HIS3*
LPY12660	W303-1b *sir2::HIS3 ura3Δ0 adh4::URA3-UAS$_G$*
LPY13094	W303-1a *bgl2Δ::kanMX* TELVR::*URA3*
LPY13166	LPY9046 + pLP2282 (pFX05)
LPY13543	W303-1b *gas1Δ::kanMX gas3Δ::kanMX gas5Δ::kanMX*
LPY13545	LPY5 + pLP349
LPY13546	LPY11 + pLP135
LPY13549	LPY10129 + pLP349
LPY13553	LPY13543 + pLP349
LPY13554	LPY4916 + pLP359

Table 2-1. Yeast strains used in Chapter 2. (continued)

LPY13559	LPY4916 + pLP2091
LPY13562	LPY4916 + pLP2117
LPY13563	LPY10362 + pLP359
LPY13568	LPY10362 + pLP2091
LPY13569	LPY10362 + pLP2093
LPY13570	LPY10362 + pLP2094
LPY13571	LPY10362 + pLP2117
LPY13653	LPY12625 + pLP349
LPY13654	LPY9046 + pLP1777
LPY13656	LPY12232 + pLP2181
LPY13659	W303-1b *hml::TRP1*
LPY13660	W303-1a *sir1::LEU2 hml::TRP1*
LPY13661	W303-1a *gas1*Δ*::kanMX hml::TRP1*
LPY13665	W303-1a *gas1*Δ*::kanMX hmr*Δ*E::TRP1*
LPY13691	*MAT***a** *ade2-1 his3*Δ*1* or *his3-11,15 leu2*Δ*0* or *leu2-3,112 ura3*Δ*0* or *ura3-1 GFP-GAS1-HIS3MX6* TELVR::*URA3*
LPY14311	*MAT***a**/*MAT*α *his3*Δ*1/his3*Δ*1 leu2*Δ*0/leu2*Δ*0 LYS2/LYS2 met15*Δ*0/MET15 ura3*Δ*0/ura3*Δ*0 GFP-GAS1-HIS3MX6/GFP-GAS1-HIS3MX6*
LPY14324	W303-1a *hmr::ADE2*
LPY14325	W303-1b *hmr::ADE2*
LPY14328	W303-1a *gas1*Δ*::kanMX hmr::ADE2*
LPY14329	W303-1b *gas1*Δ*::kanMX hmr::ADE2*
LPY14400	W303-1a *gas1*Δ*::kanMX* TELVR::*ADE2*
LPY14408	W303-1b *gas1*Δ*::kanMX* rDNA::*ADE2-CAN1*

[a]Unless otherwise noted, strains were constructed during the course of this study or are part of the standard lab collection.

Table 2-2. Oligonucleotides used in Chapter 2.

Oligo	Name	Sequence (5' to 3')[a]	Source/Reference
oLP416	*GAS1*-F2	ATAAAGCGAGCTGGTGCCTATCATAGCCG	
oLP417	*GAS1*-R2	AATTGTGTGTGCTCAATCTAATATCTCCGC	
oLP675	*GAS3*-F	TCTTTCTGCTGCGGAAGCGCTATACGGC	
oLP676	*GAS3*-R	CCATGGCTCAAGGATCCCTTGGGTATGG	
oLP766	TEL6R-1 kb-F	GGACCTACTAGTGTCTATAGTAAGTG	Darst et al. 2008
oLP767	TEL6R-1 kb-R	CTCTAACATAACTTTGATCCTTACTCG	Darst et al. 2008
oLP774	25S-F	TGTTGAAAGGGAAGGGCATT	Emre et al. 2005
oLP775	25S-R	AGCAGAGGGCACAAAACACC	Emre et al. 2005
oLP776	5S-R	CATGGAGCAGTTTTTTCCGC	Emre et al. 2005
oLP777	5S-F	TACAAGCACTCATGTTTGCCG	Emre et al. 2005
oLP778	TEL6R-0.2 kb-F	AAATGGCAAGGGTAAAAACCG	Emre et al. 2005
oLP779	TEL6R-0.2 kb-R	TCGGATCACTACACACGGAAAT	Emre et al. 2005
oLP798	*ACT1*-F1	GGTGGTTCTATCTTGGCTTC	Darst et al. 2005
oLP799	*ACT1*-R1	ATGGACCACTTTCGTCGTAT	Darst et al. 2005
oLP815	*GAS5*-F *Eag*I	CTTCGATCTGCGG**C**CGTTACTTCTAACG	
oLP816	*GAS5*-R *Bam*HI	TGAGGAT**C**CAACTTCGATCTCATCAGCG	
oLP818	*GAS1-E161Q*-F	GGTTTCTTCGCCGGTAAT**C**AAGTTACTAACAATTACACC	

Table 2-2. Oligonucleotides used in Chapter 2. (continued)

oLP819	*GAS1-E161Q*-R	GGTGTAATTGTTAGTAACTT**G**ATTACCGGCGAAGAAACC	
oLP820	*GAS1-E262Q*-F	CCTGTTTTCTTCTCT**C**AATACGGTTGTAACG	
oLP821	*GAS1-E262Q*-R	CGTTACAACCGTATT**G**AGAGAAGAAAACAGG	
oLP822	*GAS1*_seq_1	CCTCTACTACTGTTGACACG	
oLP823	*GAS1*_seq_2	AGCTCCAGCCACCTCTATC	
oLP824	*GAS1*_seq_3	GCTACTGGTAAGTACTGGTC	
oLP847	pGEX-F	GGGCTGGCAAGCCACGTTTGGTG	
oLP871	INT-ChrV_sense	GTGTTTGACCCGAGGGTATG	F. Winston/V. Cheung
oLP872	INT-ChrV_antisense	TAAGGTCCACACCGTCATCA	F. Winston/V. Cheung
oLP1010	*BGL2*-F	CAGTGGTGACTTCCACTACG	
oLP1011	*BGL2*-R	TGGACTACGAAACGGATGGC	

[a]Nucleotides in **bold** in the above sequences are mutagenic, compared to the wild-type sequence.

Table 2-3. Plasmids used in Chapter 2.[a]

Plasmid (alias)	Description	Source/Reference
pLP135 (YEp351)	vector *LEU2* 2μ	Hill et al. 1986
pLP349	*SIR2 LEU2* 2μ	Sherman et al. 1999
pLP359 (pRS423)	vector *HIS3* 2μ	Christianson et al. 1992
pLP956 (pGBD-C1)	GBD *TRP1* 2μ	James et al. 1996
pLP1073	GBD-core *SIR2 TRP1* 2μ	Garcia and Pillus 2002
pLP1074	GBD-*SIR2 TRP1* 2μ	Garcia and Pillus 2002
pLP1205	GAD-*GAS1 LEU2* 2μ	Garcia 2003
pLP1275 (pDM111a)	GST-*SIR2*	Tanny et al. 1999
pLP1276 (pDM360)	GST-*sir2-H364Y*	Tanny et al. 1999
pLP1302 (pGEX-4T-1)	GST	Kaelin et al. 1992
pLP1623 (pRS425)	vector *LEU2* 2μ	Christianson et al. 1992
pLP1777	*HHF2 hht2-K14A TRP1* CEN	
pLP1823 (YEpBS6)	*GAS1 URA3* 2μ	Vai et al. 1991
pLP1951	*GAS1 LEU2* 2μ	
pLP1990	*hhf2-K16A HHT2 TRP1* CEN	
pLP2001	*gas1-E161Q LEU2* 2μ	
pLP2002	*gas1-E262Q LEU2* 2μ	
pLP2057 (pGEX-4T-2)	GST	Kaelin et al. 1992
pLP2087	GST-*GAS1*	
pLP2091	*GAS1 HIS3* 2μ	
pLP2093	*gas1-E161Q HIS3* 2μ	
pLP2094	*gas1-E262Q HIS3* 2μ	
pLP2099	GST-*gas1-E262Q*	
pLP2114	*gas1-E161Q, E262Q LEU2* 2μ	
pLP2117	*gas1-E161Q, E262Q HIS3* 2μ	
pLP2119	GST-*gas1-E161Q, E262Q*	
pLP2181	*hhf2-K5A HHT2 TRP1* CEN	
pLP2282 (pFX05)	*HHF2 hht2-K56Q TRP1* CEN	Xu et al. 2007

[a]Unless otherwise noted, plasmids were constructed during the course of this study and are described in Materials and Methods, or are part of the standard lab collection.

using oLP820 and oLP821, with *gas1-E262Q* mutation verified by sequencing with oLP823. pLP2119 was obtained by PCR mutagenesis of pLP2099 using oLP818 and oLP819, with *gas1-E161Q* mutation verified by sequencing with oLP823. Oligonucleotides used for PCR mutagenesis and sequencing are listed in Table 2-2.

mRNA quantification. RNA was prepared using an RNeasy kit (Qiagen, Valencia, CA). Reverse transcription was performed with a TaqMan kit (ABI, Foster City, CA), with random hexamer priming. cDNA was diluted 125 to 500-fold prior to real-time PCR on a DNA Engine Opticon 2 (MJ Research, Waltham, MA), with primers in Table 2-2.

Immunoblot analysis. Levels of Sir2, Sir3, tubulin, acetylated histone H3K9,K14, acetylated histone H4K5, acetylated H4K16, and histone H3 were evaluated by immunoblot analysis as described (Stone and Pillus 1996). Cell extracts from 0.5 A_{600} cell equivalents were separated on 18% (histones), 10% (tubulin), 9% (Sir2), or 8% (Sir3) SDS-polyacrylamide gels. Sir2 was detected using a 1:5000 dilution of anti-Sir2 (Rusche et al. 2002). Sir3 was detected using a 1:5000 dilution of anti-Sir3 (Stone and Pillus 1996). Tubulin was detected using a 1:10,000 dilution of anti-β-tubulin (Bond et al. 1986). Acetylated H3K9,K14 (AcH3K9,K14) was detected using a 1:2000 dilution of a polyclonal antiserum to acetylated H3K9,K14 (Millipore Corp., Billerica, MA). Acetylated H4K5 (AcH4K5) was detected using a 1:2000 dilution of a polyclonal antiserum to acetylated H4K5 (Serotec, Raleigh, NC). Acetylated H4K16 (AcH4K16) was detected using a 1:2000 dilution of a polyclonal antiserum to acetylated H4K16 (Millipore Corp., Billerica, MA). Histone H3 was detected using a 1:10,000 dilution of a polyclonal antiserum to the C-terminus of

histone H3 (Millipore Corp., Billerica, MA). Horseradish peroxidase-coupled anti-rabbit secondary antibody (Promega Corp., Madison, WI) was used at 1:10,000 and immunoblots were developed using ECL-Plus (GE Healthcare, Piscataway, NJ). Images of blots developed with ECL-Plus were captured on the Typhoon Trio Variable Mode Imager (GE Healthcare, Piscataway, NJ) and analyzed using ImageQuant TL software.

Chromatin immunoprecipitation. Experiments were performed as described (Darst et al. 2008). Immunoprecipitation (IP) mixtures were incubated overnight at 4˚C with anti-Sir2 (Smith et al. 1998), anti-Sir3 (Stone and Pillus 1996), anti-AcH4K16 (Upstate, Charlottesville, VA), or anti-AcH3K56 (Active Motif, Carlsbad, CA). DNA in input and IP samples was quantified by real-time PCR. Primers used are in Table 2-2. For Sir2, values are IP/input normalized to *ACT1* IP/input. For AcH4K16, values are IP/input normalized to the intergenic region IP/input. For AcH3K56, values are IP/input normalized to the intergenic region IP/input.

Fluorescence microscopy. Cells were grown in YPD to log phase (A_{600} of 0.5-0.8) and DAPI was then added to a concentration of 2 μg/ml for one hour at 30˚C. Cells were washed twice with PBS prior to imaging. Cells were visualized using an Axiovert 200M microscope (Carl Zeiss MicroImaging) with a 100x 1.3 NA objective. Images were captured using a monochrome digital camera (Axiocam; Carl Zeiss MicroImaging). GFP images were deconvolved from three original stacks using Axiovision software (Carl Zeiss MicroImaging).

NAD^+ hydrolysis assays. Glutathione S-transferase (GST; pLP1302), GST-Sir2 (pLP1275), GST-Gas1 (pLP2087), and GST-gas1-E161Q E262Q (pLP2119)

fusion proteins were expressed in *E. coli* BL21 (DE3) during a 4- to 5-hr induction with 0.5 mM IPTG at room temperature (for GST and Sir2) or 18˚C (for Gas1). Proteins were purified on glutathione Sepharose beads as directed (GE Healthcare, Piscataway, NJ). Purified proteins were dialyzed against 50 mM sodium phosphate (pH 7.2) and stored at 4°C in 50 mM sodium phosphate (pH 7.2), 0.5 mM dithiothreitol (DTT), and 10% glycerol (Landry et al. 2000b). Protein concentration was established by comparison of Coomassie brilliant blue (CBB) staining of purified GST-protein samples and a concentration series of the BSA protein standard. NAD^+-hydrolysis assays to measure histone deacetylation were performed as described (Landry et al. 2000a). Reactions were carried out in 1 ml with 50 mM sodium acetate (pH 5.5), 0.5 mM DTT, 5 mM tetrasodium pyrophosphate ($Na_4P_2O_7$), 0.1 mg/ml BSA, 1 mg calf thymus histones (Sigma, St. Louis, MO) that were chemically acetylated (Parsons et al. 2003), with 2 μCi [4-^{3}H] NAD^+ (GE Healthcare, Piscataway, NJ, TRA298; 4.3 Ci/mmol, 1 mCi/ml), and 1.85 μg of purified proteins. The reactions were performed in duplicate and incubated at room temperature. Time points at 10 min, 45 min, 2 hr, 3 hr, and 5 hr were taken by transfer of 185 μl of the reaction to tubes containing 135 μl 0.5 M boric acid (pH 8.0) to quench the reaction. 1 ml of ethyl acetate was added and vortexed for 5 min and 700 μl of the ethyl acetate phase was transferred to 3 ml Ecoscint fluid (National Diagnostics, Atlanta, GA) and analyzed by scintillation counting. Radioactivity released from Sir2 wild-type control reactions lacking histones was subtracted to establish values in Figure 2-7*C*.

Two-hybrid and GST-affinity studies. The Sir2 two-hybrid screen (Garcia 2003; Darst et al. 2008) used the reporter strain PJ69-4A (LPY3374) (James et al.

1996). It was co-transformed with pLP1205 (GAD-Gas1) and pLP956 (pGBD-C1), pLP1073 (GBD-core Sir2), or pLP1074 (GBD-Sir2). The GST-affinity binding assays were described previously (Darst et al. 2008). Samples were probed with a 1:10,000 dilution of anti-Gas1 (Nuoffer et al. 1991) (gift from C. Sütterlin). Horseradish peroxidase-coupled anti-rabbit secondary (Promega, Madison, WI) was used at 1:10,000 and detected using enhanced chemiluminescence reagents (PerkinElmer, Waltham, MA).

Anti-β-1,3-glucan immunoprecipitation. Cultures were grown to an A_{600} of 0.8 were lysed with glass beads in Sir2 IP lysis buffer (Darst et al. 2008). 4 μg anti-β-1,3-glucan (Meikle et al. 1991) (Biosupplies Australia) was added to cell extract and incubated at 4˚C for 3 hr. 100 microliters of a 50% slurry of Protein G Sepharose (GE Healthcare, Piscataway, NJ) was then added and incubated for one hour at 4˚C. Beads were washed once with Sir2 IP buffer, and twice with wash buffer (50 mM HEPES pH7.5; 150 mM NaCl; 1 mM EDTA). Immunoblotting was as above, with a 1:5000 dilution of anti-Sir2.

The material in this Chapter has been accepted for publication, in Koch, M. R. and Pillus, L. 2009. The glucanosyltransferase Gas1 functions in transcriptional silencing. *Proceedings of the National Academy of Sciences USA*, in press.

Chapter 3

Genetic analyses in the characterization of *GAS1* functions

INTRODUCTION

Similar to *SIR2*, and its four homologous sirtuin genes in budding yeast, *GAS1* is the founding member of a family of glucanosyltransferase genes, which includes four additional *GAS* genes. Although *SIR2* is conserved from yeast through humans (Brachmann et al. 1995), *GAS1* conservation is limited to yeast and other fungi (Popolo and Vai 1999). *GAS1* is the most well characterized member of the *GAS* gene family, which includes *GAS1*-*GAS5*. *GAS1* encodes Gas1, a GPI anchored protein required for cell wall assembly during vegetative growth that exhibits β-1,3-glucanosyltransferase activity. As described in Chapter 2, the protein also has a recently demonstrated nuclear role in transcriptional silencing.

Functions for Gas2 and Gas4 have been reported. Both proteins encode β-1,3-glucanosyltransferases and show activity as recombinant proteins (Ragni et al. 2007b). *GAS2* and *GAS4* are expressed exclusively during sporulation and their protein products function in the formation of the spore wall (Ragni et al. 2007a). Given their expression profiles and function during meiosis, it is unlikely that *GAS2* and *GAS4* have a function similar to Gas1's function in transcriptional silencing. Roles for *GAS3* and *GAS5* have yet to be identified, but the genes both encode β-1,3-glucanosyltransferases, although in assays of the purified proteins, glucanosyltransferase activity for recombinant Gas3 was undetectable and its

recombinant protein expression was reduced compared to the other Gas proteins (Ragni et al. 2007b). *GAS5* has been identified as both a multi-copy suppressor (Tomishige et al. 2005) and, when mutated, is a phenotypic enhancer of *gas1*Δ (Schuldiner et al. 2005), suggesting that Gas5 can fulfill Gas1's role in its absence, and that it may have at least partially overlapping functions with Gas1.

To further evaluate *GAS1*'s cellular functions beyond cell wall biosynthesis, a large-scale synthetic genetic array (SGA) analysis of *gas1*Δ was completed (Tong et al. 2004; Lesage et al. 2004). The genome-wide screen identified a number of expected interactors with known functions in cell wall biosynthesis. However, several genes whose protein products function in nuclear processes were also identified. These include *RSC2*, which encodes a component of the RSC chromatin remodeling complex, *NEM1*, required for the organization of the nuclear envelope, *DOT1*, which encodes a histone methyltransferase, *SWI4*, which encodes a component of the SBF complex functioning in G1-specific transcription, and *CDC2*/*POL3*, the catalytic component of DNA polymerase delta (Tong et al. 2004; Lesage et al. 2004).

GAS1 has also been uncovered in several SGA screens completed on nuclear protein genes. Reduced fitness is observed when *gas1*Δ is combined with *esa1-L254P* and *eaf1*Δ (Mitchell et al. 2008), two genes that encode components of the NuA4 complex that functions in cell cycle progression, DNA double-strand break repair, transcriptional activation, and transcriptional silencing (reviewed in Lafon et al. 2007). Growth defects have also been seen between *gas1*Δ and *orc2-1* (Suter et al. 2004), a conditional allele of the essential *ORC2* gene that encodes a subunit of the origin recognition complex (ORC). ORC is required for DNA replication and transcriptional

silencing of *HM* loci (reviewed in Loo and Rine 1995; Toone et al. 1997). *GAS1* was also identified as synthetically lethal with deletion of *RAD27* (Loeillet et al. 2005), which encodes an exo/endonuclease functioning in DNA replication and repair, and with deletion of *NPL6* (Wilson et al. 2006a), which encodes a component of the RSC chromatin remodeling complex. Together, multiple genetic interactions have been reported between *GAS1* and genes encoding nuclear proteins. These examples strengthen the idea that Gas1 has nuclear functions, including transcriptional silencing.

This chapter includes a genetic analysis of *GAS1* that extends the initial characterization presented in Chapter 2. This analysis has uncovered cell type specific suppression of the temperature sensitivity of *gas1*Δ mutants, in that simultaneous expression of *MAT***a** and *MAT*α reduces the temperature sensitivity of *gas1*Δ strains. Also, telomeric silencing can be restored in *gas1*Δ through various genetic manipulations, including Sir1 and Sir2 DNA tethering to a telomeric reporter gene, *SIR2* and *SIR3* overexpression, *SIR1* deletion, and *GAS5* overexpression. Analysis of double and triple mutant combinations of deletions of *GAS1*, *GAS3*, and *GAS5* revealed that the *gas1*Δ telomeric silencing defect is enhanced by *GAS5* deletion, in a telomere-specific manner. The synthetic growth defects observed in large-scale studies between *gas1*Δ and *orc2-1*, and *gas1*Δ and *eaf1*Δ, were verified in this study, whereas others were not confirmed. In addition, a novel genetic interaction was discovered between *gas1*Δ and *rpd3*Δ, another synthetic growth defect between two genes with roles in transcriptional silencing. Since this genetic interaction had not been reported in two previous genome-wide screens, there may be other significant genetic interactions waiting for future discovery.

RESULTS

Simultaneous expression of *MAT*a and *MAT*α suppresses *gas1*Δ temperature sensitivity. A major phenotype of *gas1*Δ strains is their slow growth, especially on rich medium, yeast extract-peptone-dextrose (YPD). In addition, they are sensitive to elevated temperature, resulting in a significant defect in growth. During construction of double mutants it was observed that combining *gas1*Δ with deletions of any of the four *SIR* genes resulted in strains that were healthier and more resistant to high temperature, both on YPD and synthetic complete (SC) medium (Figure 3-1). Combining multiple deletions of *SIR* genes in the same *gas1*Δ strain resulted in slightly less suppression of *gas1*Δ temperature sensitivity. This was seen on SC at 37˚C (Figure 3-2) and YPD at 34˚C and 37˚C (Figure 3-3). Because deletion of *SIR* genes rescued *gas1*Δ temperature sensitivity, overexpression of *SIR* genes might be expected to enhance *gas1*Δ temperature sensitivity. However, overexpression of any one of the four *SIR* genes had little effect on *gas1*Δ temperature sensitivity (Figure 3-4, bottom panel). The four *SIR* genes function in silencing of the cryptic mating-type loci, resulting in the expression of the normally silent cryptic copies of the mating type genes, *HMR* and *HML*. The expression of these cryptic copies of mating type genes in *sir* mutants results in a pseudo-diploid state that results in the non-mating phenotype of *sir* mutants (Rine and Herskowitz 1987).

To determine whether simultaneous expression of *MAT***a** and *MAT*α in the same cell suppressed *gas1*Δ temperature sensitivity, strains were transformed with

Figure 3-1. The temperature sensitivity of *gas1*Δ is suppressed by deletion of any of the four *SIR* genes. Wild-type (WT) (LPY5), *sir2*Δ (LPY11), *sir3*Δ (LPY10), *gas1*Δ (LPY10129), *gas1*Δ *sir1*Δ (LPY10665), *gas1*Δ *sir2*Δ (LPY10663), *gas1*Δ *sir3*Δ (LPY10667), and *gas1*Δ *sir4*Δ (LPY10159) strains were plated on synthetic complete (SC) medium at 30˚C to monitor growth, and 37˚C to monitor growth at elevated temperature, and on yeast extract-peptone-dextrose (YPD) medium at 30˚C to monitor growth and 34˚C to monitor growth at elevated temperature.

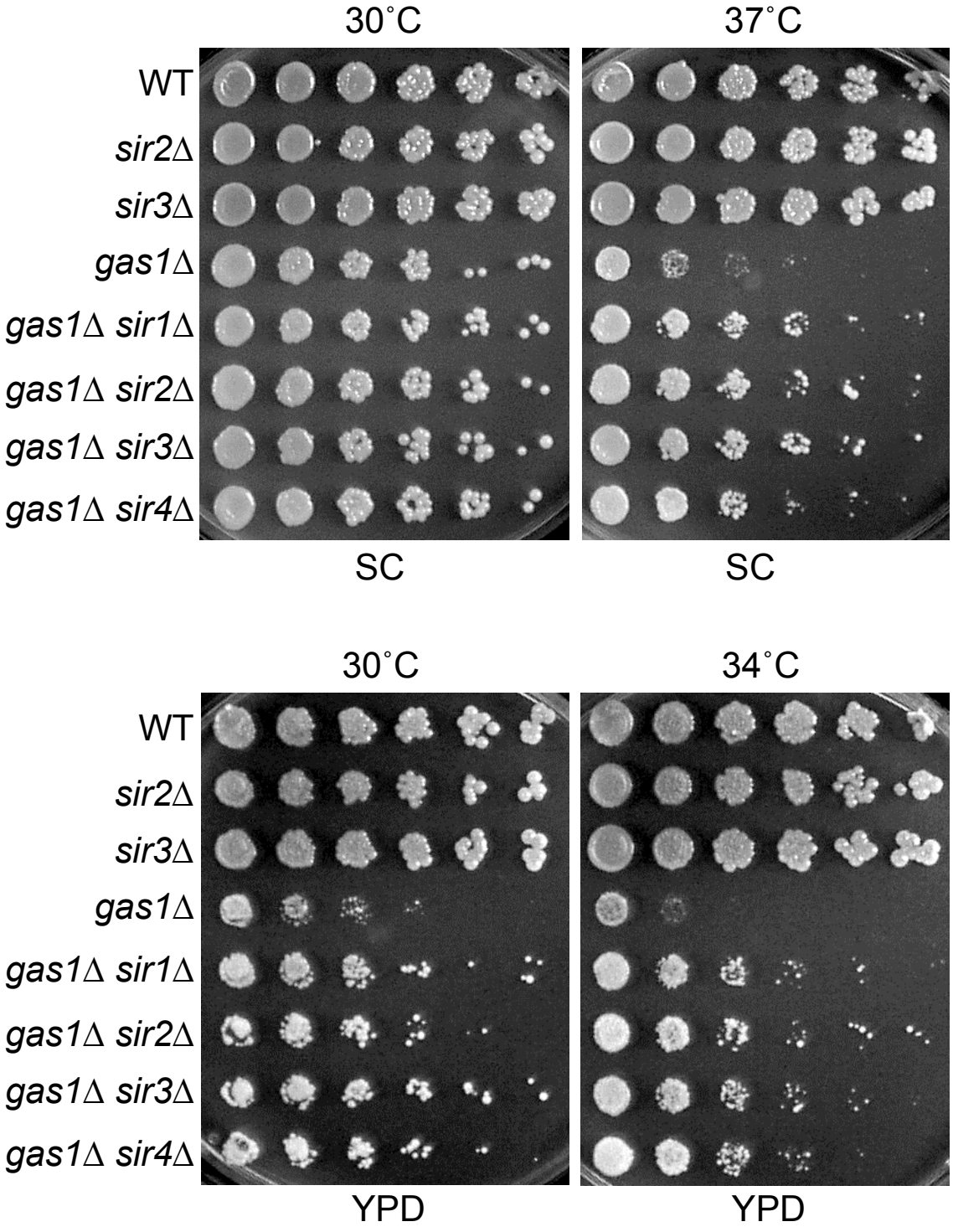
30˚C
37˚C
WT
sir2Δ
sir3Δ
gas1Δ
gas1Δ sir1Δ
gas1Δ sir2Δ
gas1Δ sir3Δ
gas1Δ sir4Δ
SC
SC
30˚C
34˚C
WT
sir2Δ
sir3Δ
gas1Δ
gas1Δ sir1Δ
gas1Δ sir2Δ
gas1Δ sir3Δ
gas1Δ sir4Δ
YPD
YPD

Figure 3-2. The temperature sensitivity of *gas1*Δ on synthetic medium is only partially suppressed by combined deletion of multiple *SIR* genes in the same strain. In the top panels, WT (LPY5), *sir2*Δ (LPY11), *sir3*Δ (LPY10), *sir4*Δ (LPY9), *sir2*Δ *sir3*Δ (LPY13887), *sir2*Δ *sir4*Δ (LPY13889), *sir3*Δ *sir4*Δ (LPY13891), and *sir2*Δ *sir3*Δ *sir4*Δ (LPY13893) were plated. In the bottom panels, *gas1*Δ (LPY10129), *gas1*Δ *sir2*Δ (LPY10663), *gas1*Δ *sir3*Δ (LPY10667), *gas1*Δ *sir4*Δ (LPY12068), *gas1*Δ *sir2*Δ *sir3*Δ (LPY13895), *gas1*Δ *sir2*Δ *sir4*Δ (LPY13896), *gas1*Δ *sir3*Δ *sir4*Δ (LPY13674), and *gas1*Δ *sir2*Δ *sir3*Δ *sir4*Δ (LPY13900) were plated. Strains were plated on SC at 30˚C to monitor growth and 37˚C to monitor growth at elevated temperature.

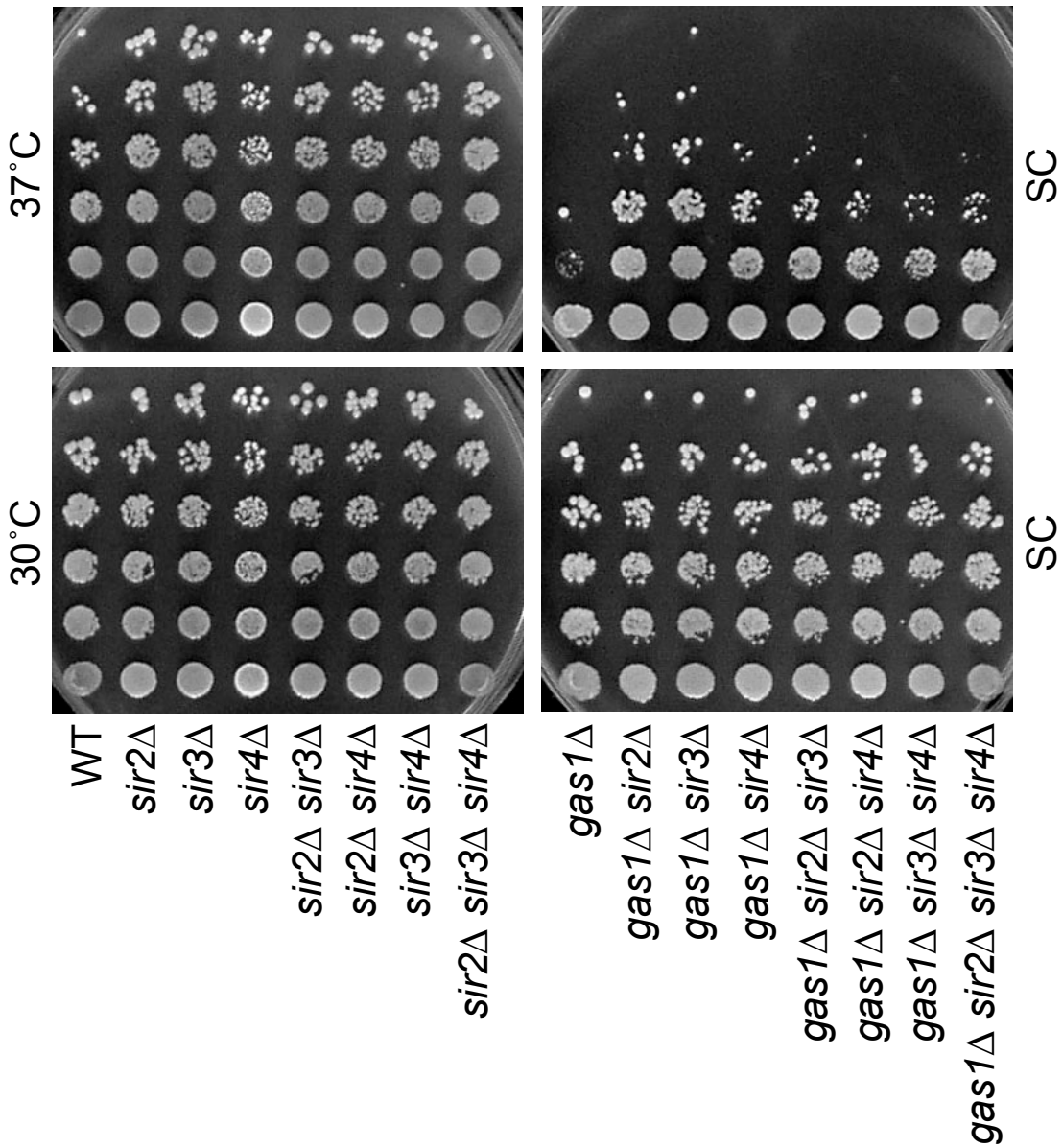
30˚C
37˚C
SC
SC
WT
sir2Δ
sir3Δ
sir4Δ
sir2Δ sir3Δ
sir2Δ sir4Δ
sir3Δ sir4Δ
sir2Δ sir3Δ sir4Δ
gas1Δ
gas1Δ sir2Δ
gas1Δ sir3Δ
gas1Δ sir4Δ
gas1Δ sir2Δ sir3Δ
gas1Δ sir2Δ sir4Δ
gas1Δ sir3Δ sir4Δ
gas1Δ sir2Δ sir3Δ sir4Δ

Figure 3-3. The temperature sensitivity of *gas1*Δ on rich medium is only partially suppressed by combined deletion of multiple *SIR* genes in the same strain. In the top panels, WT (LPY5), *sir2*Δ (LPY11), *sir3*Δ (LPY10), *sir4*Δ (LPY9), *sir2*Δ *sir3*Δ (LPY13887), *sir2*Δ *sir4*Δ (LPY13889), *sir3*Δ *sir4*Δ (LPY13891), and *sir2*Δ *sir3*Δ *sir4*Δ (LPY13893) were plated. In the bottom panels, *gas1*Δ (LPY10129), *gas1*Δ *sir2*Δ (LPY10663), *gas1*Δ *sir3*Δ (LPY10667), *gas1*Δ *sir4*Δ (LPY12068), *gas1*Δ *sir2*Δ *sir3*Δ (LPY13895), *gas1*Δ *sir2*Δ *sir4*Δ (LPY13896), *gas1*Δ *sir3*Δ *sir4*Δ (LPY13674), and *gas1*Δ *sir2*Δ *sir3*Δ *sir4*Δ (LPY13900) were plated. Strains were plated on YPD at 30˚C to monitor growth, and 34˚C and 37˚C to monitor growth at elevated temperature.

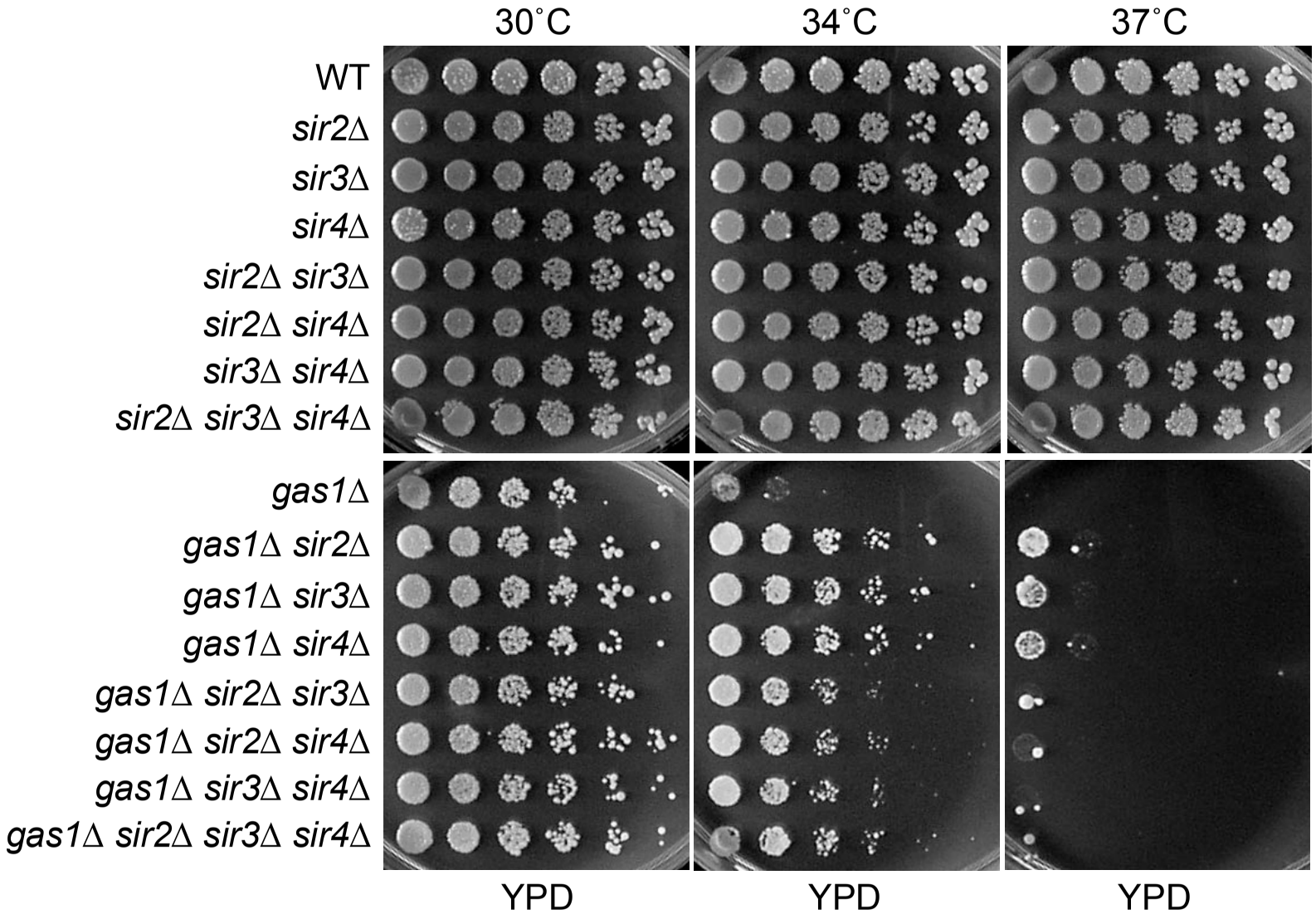
30˚C
34˚C
37˚C
WT
sir2Δ
sir3Δ
sir4Δ
sir2Δ sir3Δ
sir2Δ sir4Δ
sir3Δ sir4Δ
sir2Δ sir3Δ sir4Δ
gas1Δ
gas1Δ sir2Δ
gas1Δ sir3Δ
gas1Δ sir4Δ
gas1Δ sir2Δ sir3Δ
gas1Δ sir2Δ sir4Δ
gas1Δ sir3Δ sir4Δ
gas1Δ sir2Δ sir3Δ sir4Δ
YPD
YPD
YPD

Figure 3-4. Overexpression of *SIR* genes does not affect *gas1*Δ temperature sensitivity. In the top panels, a WT strain (LPY4916) transformed with the 2μ *HIS3* vector plasmid (pLP359), *SIR1* (pLP2192), *SIR2* (pLP891), *SIR3* (pLP1047), *SIR4* (pLP2206), or *GAS1* (pLP2091) plasmids were plated. Transformed strains are LPY13554-LPY13559. In the bottom panels, a *gas1*Δ strain (LPY10362) transformed with the same plasmids were plated. Transformed strains are LPY13563-LPY13568. Strains were plated on SC-histidine (SC-his) at 30˚C to monitor growth, and at 37˚C to monitor growth at elevated temperature.

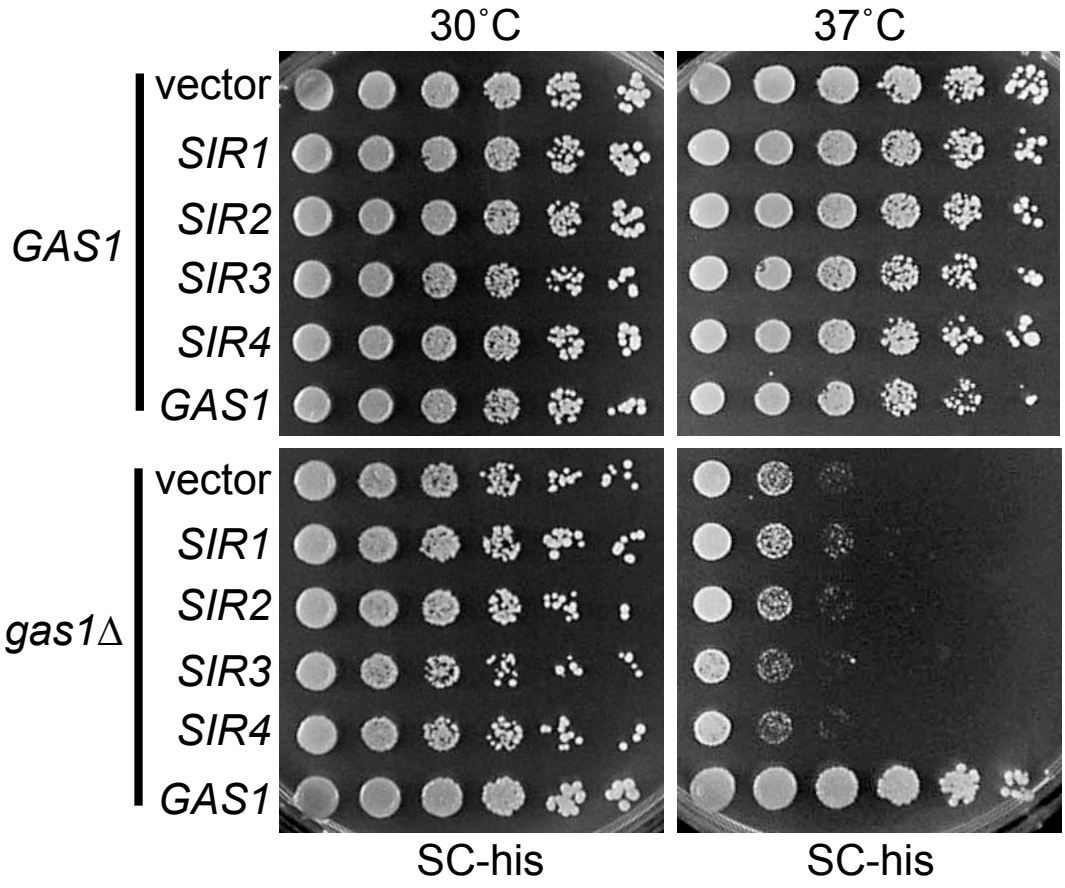
30˚C
37˚C
GAS1
vector
SIR1
SIR2
SIR3
SIR4
GAS1
gas1Δ
vector
SIR1
SIR2
SIR3
SIR4
GAS1
SC-his
SC-his

plasmid-borne copies of the mating type genes. The temperature sensitivity of a *MAT***a** *gas1*Δ strain was suppressed by plasmid-borne *MAT*α (Figure 3-5, top panel). Likewise, the temperature sensitivity of a *MAT*α *gas1*Δ strain was also suppressed by plasmid borne *MAT***a** (Figure 3-5, bottom panel). In control experiments, the growth of wild-type strains was unaffected by extra copies of the mating type genes, and *gas1*Δ strains transformed with vector and the mating type gene matching the mating type of the strain remained sensitive to high temperature.

The *gas1*Δ telomeric silencing defect is suppressed by DNA tethering of Sir1 and Sir2, *SIR2* and *SIR3* overexpression, and *SIR1* deletion. In Chapter 2, the telomeric silencing defect of *gas1*Δ strains was presented (Figure 2-1*D*, 2-1*E*, 2-3). It was important to determine whether alteration of Sir proteins could rescue *gas1*Δ telomeric silencing. Although Sir1 is not required for telomeric silencing, tethering a Gal4-binding domain (GBD) Sir1 fusion protein to a telomere VII-L *URA3* reporter gene enhances silencing in a wild-type strain (Chien et al. 1993). Tethering Sir1 to a telomeric reporter gene in *gas1*Δ also improves silencing, bypassing the requirement for Gas1 in telomeric silencing (Figure 3-6*A*). Also, tethering GBD-Sir2 to a telomeric reporter gene rescues the telomeric silencing defect of *sir2*Δ strains (Garcia and Pillus 2002; Garcia 2003). To test whether GBD-Sir2 tethering restores telomeric silencing in *gas1*Δ mutants, strains were transformed with GBD empty vector, GBD-core Sir2, and a GBD-Sir2 construct containing almost full-length Sir2. The *gas1*Δ telomeric silencing defect was specifically rescued by tethering GBD-Sir2 (Figure 3-6*B*). To test whether overexpression of *SIR* genes alone, without tethering, affects the *gas1*Δ telomeric silencing defect, *gas1*Δ strains were transformed with 2μ plasmids carrying

Figure 3-5. Simultaneous expression of *MAT***a** and *MAT*α in the same strain suppresses *gas1*Δ temperature sensitivity. In the top panels, WT *MAT*α strain (LPY6283), WT *MAT***a** strain (LPY6284), *gas1*Δ *MAT*α strain (LPY10363), and a *gas1*Δ *MAT***a** strain (LPY10362) are transformed with CEN *TRP1* vector plasmid (pLP61), or *MAT*α plasmid (pLP1167). Transformed strains are LPY10653, LPY10654, LPY10650, LPY10651, LPY10659, LPY10660, LPY10656, and LPY10657, respectively. In the bottom panels, the same four strains are transformed with vector or *MAT***a** (pLP1185). Transformed strains are LPY10653, LPY10655, LPY10650, LPY10652, LPY10659, LPY10661, LPY10656, and LPY10658, respectively. Strains were plated on SC-tryptophan (SC-trp) at 30˚C to monitor growth, and at 37˚C to monitor growth at elevated temperature. Arrows indicate strain/plasmid combinations where *gas1*Δ temperature sensitivity suppression is seen.

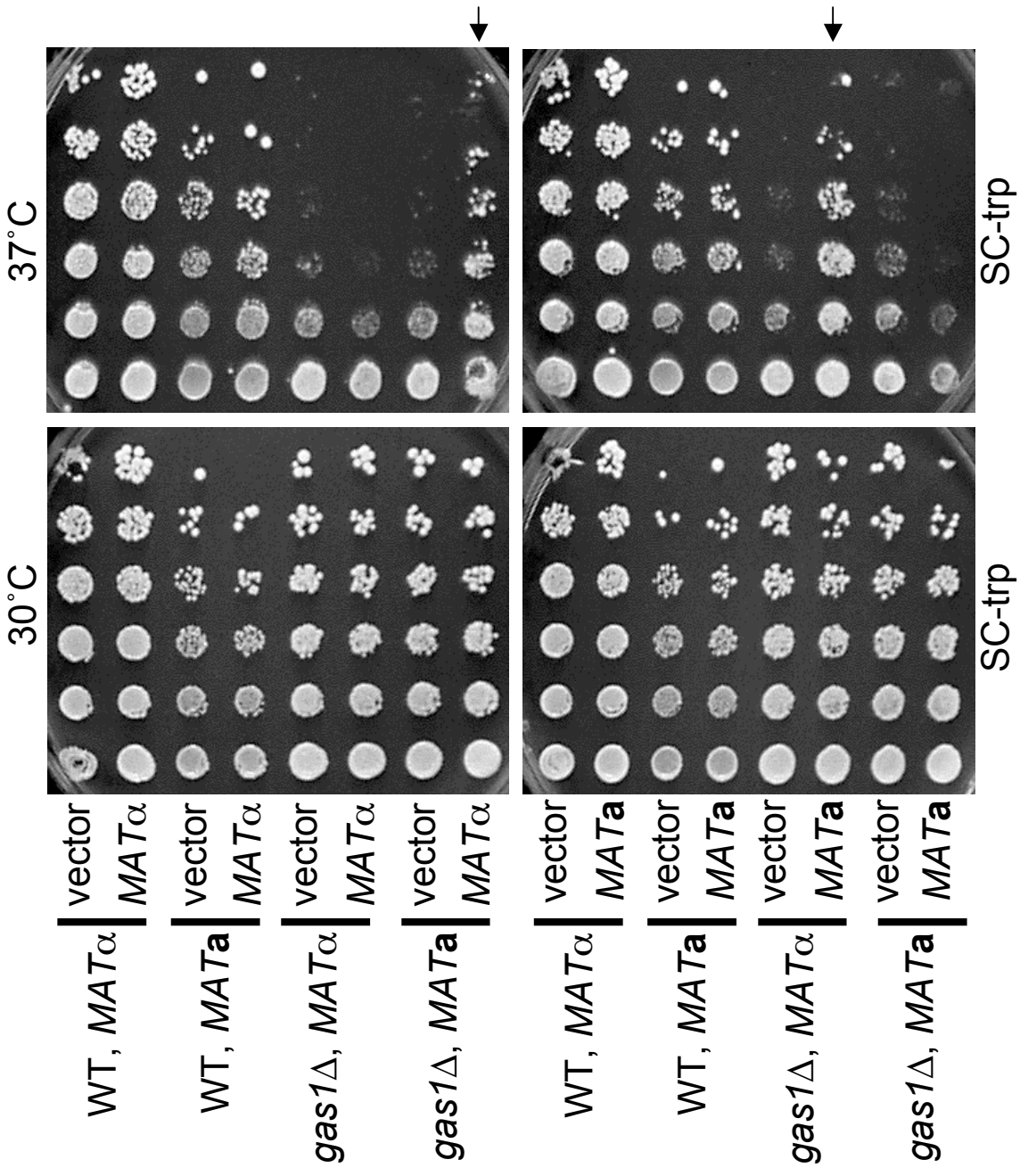
37˚C
30˚C
SC-trp
SC-trp
WT, MATα
vector
MATα
WT, MATa
vector
MATα
gas1Δ, MATα
vector
MATα
gas1Δ, MATa
vector
MATα
WT, MATα
vector
MATa
WT, MATa
vector
MATa
gas1Δ, MATα
vector
MATa
gas1Δ, MATa
vector
MATa

Figure 3-6. DNA tethering of Sir1 or Sir2 to a telomeric reporter gene rescues the *gas1*Δ telomeric silencing defect. *(A)* Sir1 tethering restores telomeric silencing in the *gas1*Δ strain. WT (LPY1030), *sir2*Δ (LPY4624), *sir3*Δ (LPY4417), and *gas1*Δ (LPY10360) strains with the upstream activation sequence (UASg) downstream of the *URA3* reporter at TELVII-L (Chien et al. 1993) was transformed with the 2μ *HIS3* GBD vector plasmid (pLP5 or pLP493, both are pMA424 vector) or GBD-Sir1 (pLP409). Transformed strains are LPY2846, LPY2854, LPY7884, LPY7886, LPY7892, LPY7894, LPY14535, and LPY14536, respectively. Strains were plated at 30˚C on SC-his to monitor growth and SC-his 5-FOA to monitor telomeric silencing. *(B)* Sir2 tethering to the reporter gene promotes telomeric silencing in the *gas1*Δ strain. A *sir2*Δ strain (LPY5611) with the same reporter used in *(A)* was transformed with the 2μ *TRP1* GBD vector plasmid (pLP956) or GBD-Sir2 (pLP1074). Transformed strains are LPY5777 and LPY5779. A *gas1*Δ strain with the same telomeric reporter gene (LPY10360) was transformed with GBD vector, GBD-core Sir2 (pLP1073), or GBD-Sir2. Transformed strains are LPY10498-LPY10500. Strains were plated at 30˚C on SC-trp to monitor growth and SC-trp 5-FOA to monitor telomeric silencing.

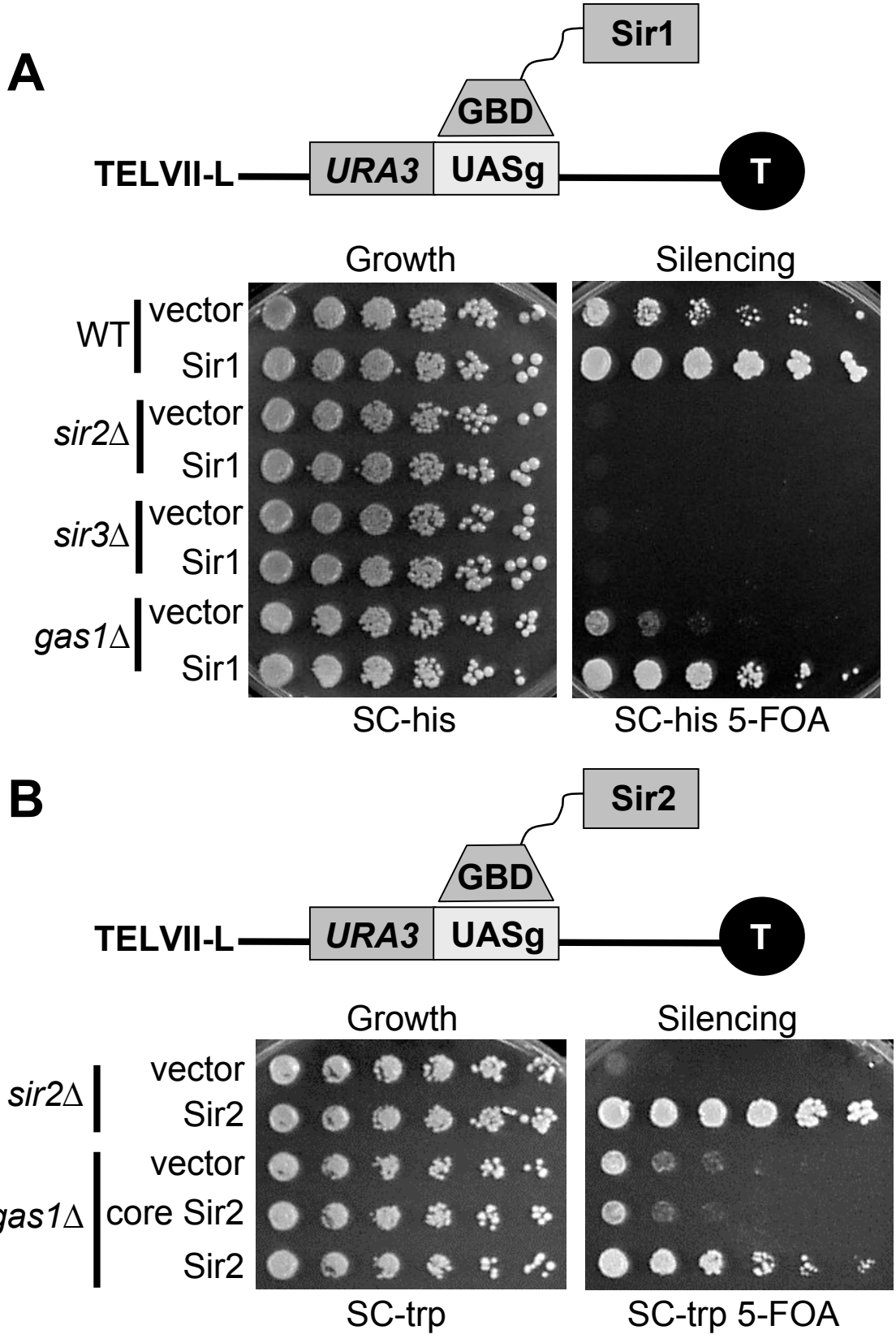
A
Sir1
GBD
TELVII-L
URA3
UASg
T
Growth
Silencing
WT
vector
Sir1
sir2Δ
vector
Sir1
sir3Δ
vector
Sir1
gas1Δ
vector
Sir1
SC-his
SC-his 5-FOA
B
Sir2
GBD
TELVII-L
URA3
UASg
T
Growth
Silencing
sir2Δ
vector
Sir2
gas1Δ
vector
core Sir2
Sir2
SC-trp
SC-trp 5-FOA

SIR1, *SIR2*, *SIR3*, or *SIR4*. The 2μ plasmid expression can vary from cell to cell but is typically expressed at 50-100 copies per cell (Armstrong et al. 1989). Overexpression of *SIR2* and *SIR3* partially suppress *gas1*Δ telomeric silencing defects, compared to the slightly more robust suppression seen in the complementation of *gas1*Δ by *GAS1* overexpression (Figure 3-7, bottom panel). Overexpression of *SIR4* only modestly suppresses the *gas1*Δ telomeric silencing defect (Figure 3-7, bottom panel). Although *SIR1* overexpression enhances the *gas1*Δ telomeric silencing defect (Figure 3-7, bottom panel), it also creates a silencing defect in the wild-type strain (Figure 3-7, top panel) (Chien et al. 1993), suggesting that the effect is not specific to the *gas1*Δ telomeric silencing defect.

Deletion of *SIR2*, *SIR3*, or *SIR4* leads to a complete defect in telomeric silencing. Additional deletion of *GAS1* in these strains did not suppress the telomeric silencing defects (Figure 3-8). Finally, although *SIR1* is not required for silencing at the telomeres, telomeric silencing was restored significantly in a *gas1*Δ *sir1*Δ strain (Figure 3-8).

Reciprocal effects of *GAS5* on *gas1*Δ temperature sensitivity and telomeric silencing defects. Because *GAS1* has four homologous genes in *S. cerevisiae*, it was important to investigate whether there were contributions of the other *GAS* genes to Gas1 functions, especially to determine whether any of the other *GAS* genes functionally substitute for *GAS1* in its absence. Because *GAS2* and *GAS4* have previously been characterized for their role in spore wall formation and are expressed meiotically (Ragni et al. 2007a), these experiments have focused on the remaining homologs, *GAS3* and *GAS5*. *GAS5* was identified in a screen for multi-copy

Figure 3-7. Overexpression of *SIR2* and *SIR3* partially suppresses the *gas1*Δ telomeric silencing defect. In the top panels, a WT strain (LPY4916) containing TELV-R::*URA3* was transformed with the 2μ *HIS3* vector plasmid (pLP359), *SIR1* (pLP2192), *SIR2* (pLP891), *SIR3* (pLP1047), *SIR4* (pLP2206), or *GAS1* (pLP2091). Transformed strains are LPY13554-LPY13559. In the bottom panels, a *gas1*Δ strain (LPY10362) with TELV-R::*URA3* was transformed with the same plasmids. Transformed strains are LPY13563-LPY13568. Strains were plated at 30˚C on SC-his to monitor growth and SC-his 5-FOA to monitor telomeric silencing.

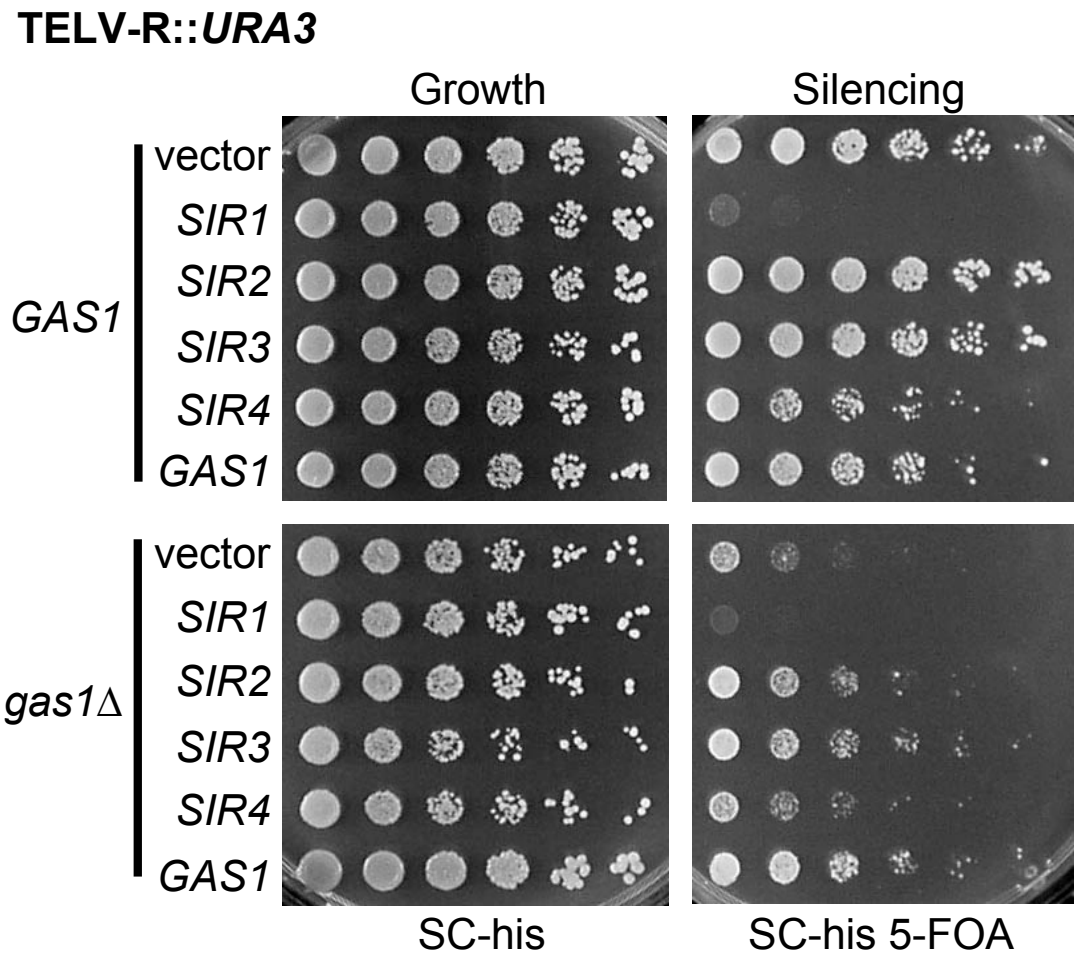
TELV-R::URA3
Growth
Silencing
GAS1
vector
SIR1
SIR2
SIR3
SIR4
GAS1
gas1Δ
vector
SIR1
SIR2
SIR3
SIR4
GAS1
SC-his
SC-his 5-FOA

Figure 3-8. Deletion of *SIR1* suppresses the *gas1*Δ telomeric silencing defect. WT (LPY4916), *sir1*Δ (LPY12045), *sir2*Δ (LPY10397), *gas1*Δ (LPY10362), *gas1*Δ *sir1*Δ (LPY12053), *gas1*Δ *sir2*Δ (LPY9822), *gas1*Δ *sir3*Δ (LPY9818), and *gas1*Δ *sir4*Δ (LPY12065), all containing TELV-R::*URA3* were plated on SC to monitor growth and SC containing 5-FOA to monitor telomeric silencing. Note that the *gas1*Δ *sir3*Δ strain (LPY9818) is genetically *ADE*+ because this strain also contains an additional silencing reporter, rDNA::*ADE2*-*CAN1*.

TELV-R::*URA3*

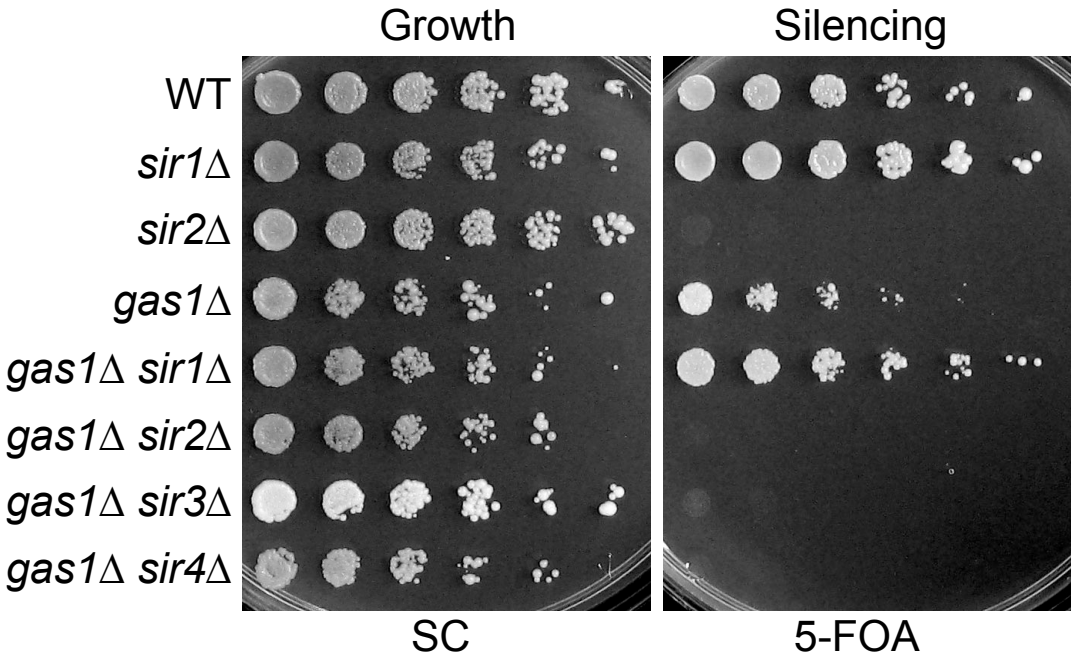
Growth
Silencing
WT
sir1Δ
sir2Δ
gas1Δ
gas1Δ sir1Δ
gas1Δ sir2Δ
gas1Δ sir3Δ
gas1Δ sir4Δ
SC
5-FOA

suppressors of the synthetic lethality of *gas1*Δ *kex2*Δ and was also found to suppress *gas1*Δ sensitivity to Congo red when overexpressed (Tomishige et al. 2005). *KEX2* encodes a processing protease in the late Golgi, which results in cell wall defects when deleted. Multi-copy *GAS5* expression rescued *gas1*Δ temperature sensitivity (Figure 3-9) and its defect in telomeric silencing (Figure 3-10).

To determine whether *gas3*Δ or *gas5*Δ have an additive effect on *gas1*Δ phenotypes, double and triple mutant combinations were constructed. Deletion of *GAS5* was previously identified as a phenotypic enhancer of *gas1*Δ slow growth (Schuldiner et al. 2005). Although *gas5*Δ itself has no defect in growth on rich media or at high temperature, the *gas1*Δ *gas5*Δ strain is dead on rich media (YPD) and at high temperature (Figure 3-11).

Telomeric silencing was also evaluated in the double and triple *gas* mutants. With the TELV-R::*URA3* silencing reporter, no enhancement of the *gas1*Δ telomeric silencing defect was observed in the *gas1*Δ *gas5*Δ strain (Figure 3-12). However, silencing in the *gas1*Δ *gas3*Δ strains was variable (Figure 3-12, compare top and bottom panels). Nonetheless, silencing in multiple *gas1*Δ *gas3*Δ *gas5*Δ strains was similar to the *gas1*Δ mutant, suggesting that overall *gas3*Δ does not enhance *gas1*Δ's telomeric silencing defect. To further investigate the effect of additional *gas* mutations on the *gas1*Δ telomeric silencing defect, double and triple mutant strains were constructed with the TELVII-L::*URA3* reporter. In these assays, *gas5*Δ enhanced the *gas1*Δ telomeric silencing defect whereas *gas3*Δ had no effect (Figure 3-13).

***GAS1* deletion displays synthetic growth defects with *eaf1*Δ, *orc2-1*, and *rpd3*Δ strains**. Several genomewide SGA screens uncovered interactions between

Figure 3-9. *GAS5* overexpression rescues *gas1*Δ temperature sensitivity. A WT strain (LPY5) and *gas1*Δ strain (LPY10129) were transformed with the 2μ *LEU2* vector plasmid (pLP1623), *GAS1* (pLP1951), or two clones of *GAS5* (pLP2012, pLP2013). Transformed strains are LPY14537-LPY14544. Strains were plated on SC-leucine (SC-leu) at 30˚C to monitor growth, and at 34˚C and 37˚C to monitor growth at elevated temperature.

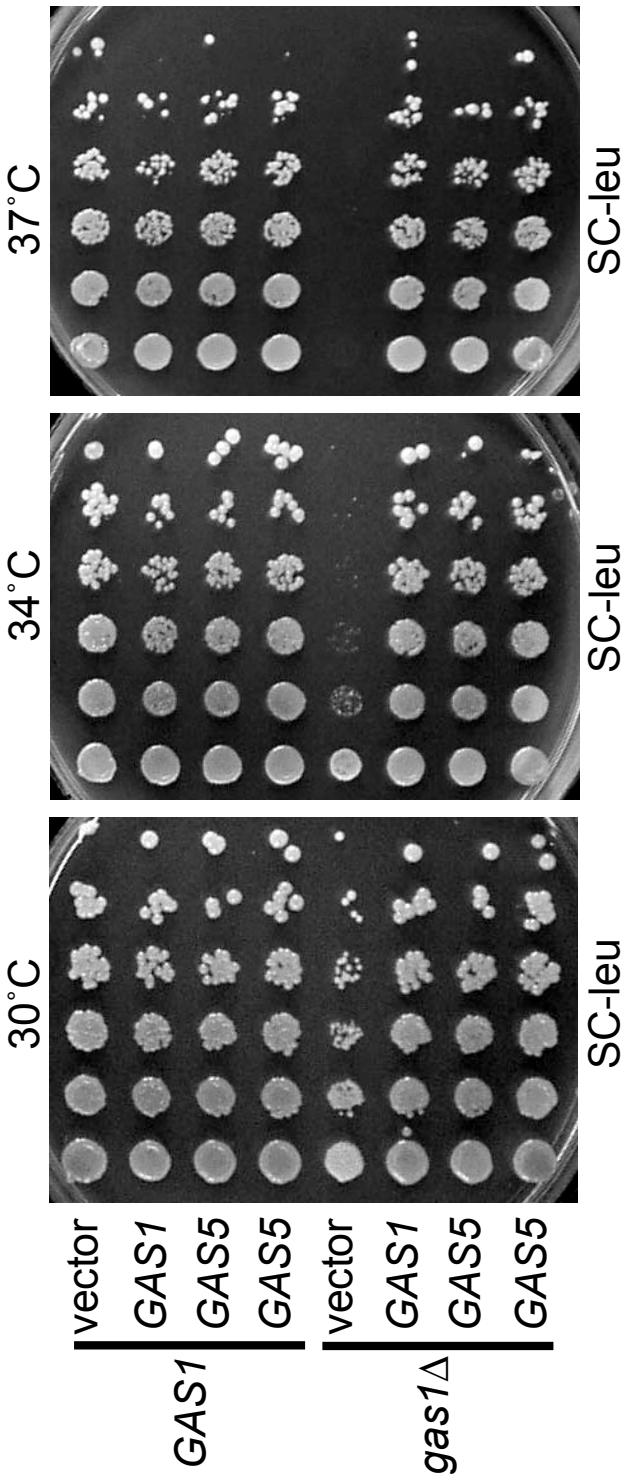
30˚C
34˚C
37˚C
SC-leu
SC-leu
SC-leu
vector
GAS1
GAS5
GAS5
vector
GAS1
GAS5
GAS5
GAS1
gas1Δ

Figure 3-10. *GAS5* overexpression rescues the *gas1*Δ telomeric silencing defect. A WT strain with TELV-R::*URA3* (LPY4916) was transformed with the 2μ *LEU2* vector plasmid (pLP1623) or *GAS5* (pLP2012). Transformed strains are LPY14545 and LPY14549. A *gas1*Δ strain with TELV-R::*URA3* (LPY10362) was transformed with vector (pLP1623), *GAS1* (pLP1951), *gas1-E161Q* (pLP2001), *gas1-E262Q* (pLP2002), or two clones of *GAS5* (pLP2012, pLP2013). Transformed strains are LPY14552-LPY14557. Strains were plated at 30˚C on SC-leu to monitor growth and on SC-leu 5-FOA to monitor telomeric silencing.

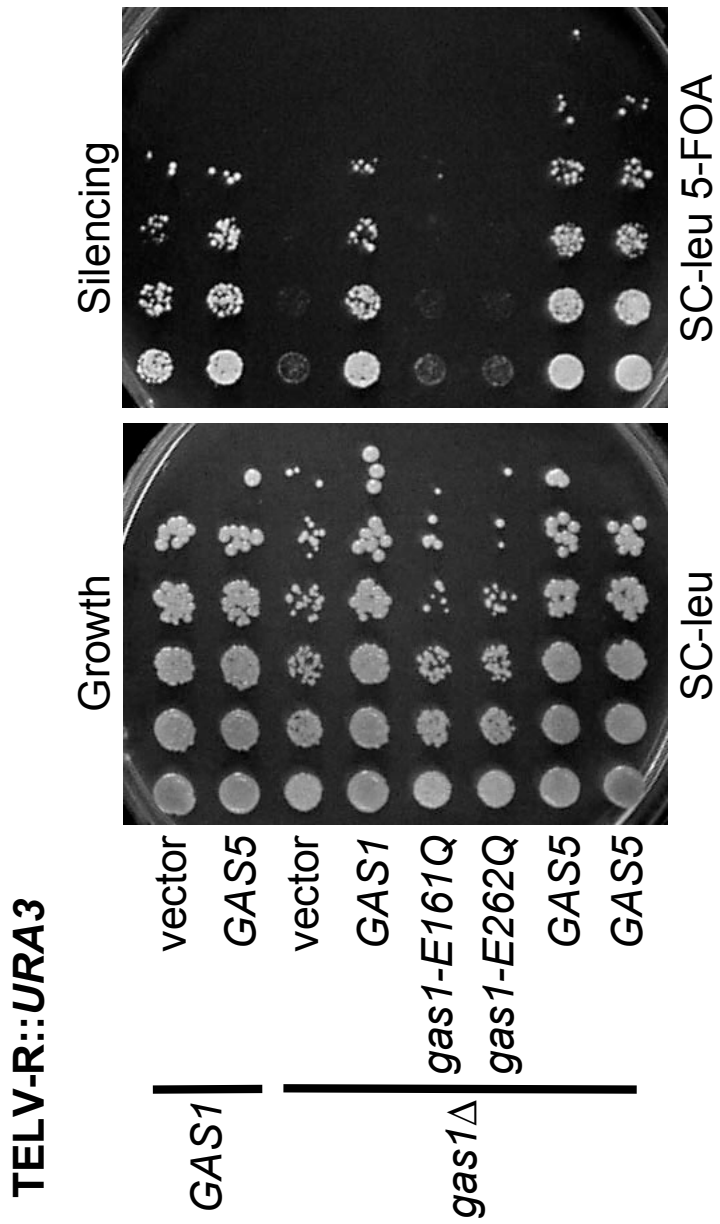
TELV-R::URA3
GAS1
gas1Δ
vector
GAS5
vector
GAS1
gas1-E161Q
gas1-E262Q
GAS5
GAS5
Growth
Silencing
SC-leu
SC-leu 5-FOA

Figure 3-11. Deletion of *GAS5* exacerbates *gas1*Δ slow growth on rich media and sensitivity to elevated temperature. WT (LPY4916), *sir2*Δ (LPY10397), *gas1*Δ (LPY10362), *gas3*Δ (LPY12337), *gas5*Δ (LPY12348), *gas1*Δ *gas3*Δ (LPY14433), *gas1*Δ *gas5*Δ (LPY14429), *gas1*Δ *gas3*Δ *gas5*Δ (LPY14434) strains were plated on SC and YPD at 30˚C to monitor growth, and at 37˚C to monitor growth at elevated temperature.

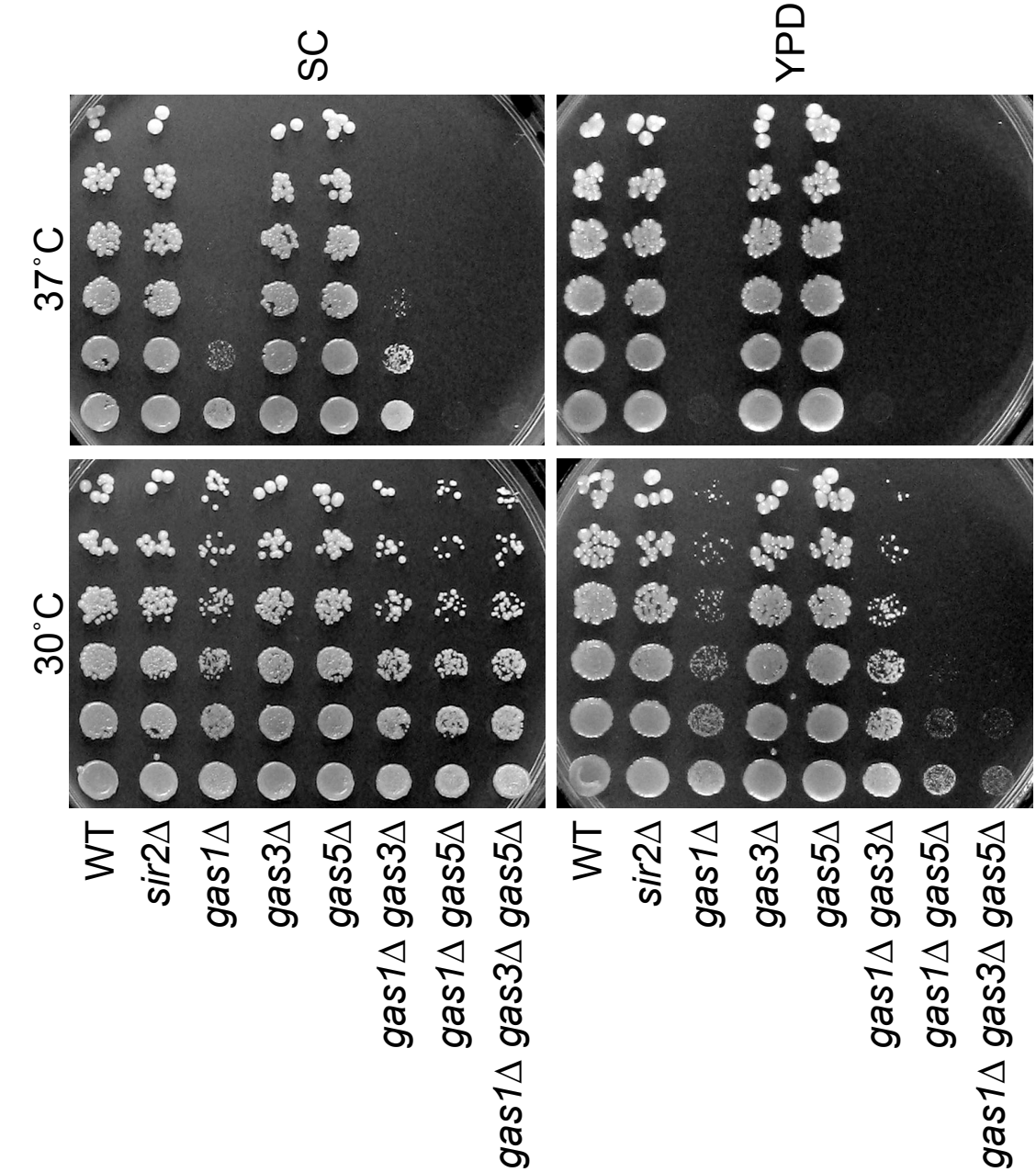
30˚C
37˚C
SC
YPD
WT
sir2Δ
gas1Δ
gas3Δ
gas5Δ
gas1Δ gas3Δ
gas1Δ gas5Δ
gas1Δ gas3Δ gas5Δ

Figure 3-12. Deletion of *GAS3* and/or *GAS5* does not alter the *gas1*Δ silencing defect at telomere V-R. In the top panels, WT (LPY4916), *sir2*Δ (LPY10397), *gas1*Δ (LPY10362), *gas3*Δ (LPY12337), *gas5*Δ (LPY12348), *gas1*Δ *gas3*Δ (LPY14433), *gas1*Δ *gas5*Δ (LPY14429), *gas1*Δ *gas3*Δ *gas5*Δ (LPY14434), all with TELV-R::*URA3* were plated. In the bottom panels, WT (LPY4916), *gas1*Δ (LPY10362), *gas1*Δ *gas3*Δ (LPY14431), *gas1*Δ *gas3*Δ *gas5*Δ (LPY14436), all with TELV-R::*URA3*, and *gas1*Δ *gas3*Δ (LPY14428), *gas1*Δ *gas3*Δ (LPY14435), *gas1*Δ *gas5*Δ (LPY14430), and *gas1*Δ *gas5*Δ (LPY14432), all without the telomeric reporter, were plated. Strains were plated at 30˚C on SC to monitor growth and on SC containing 5-FOA to monitor telomeric silencing.

TELV-R::*URA3*

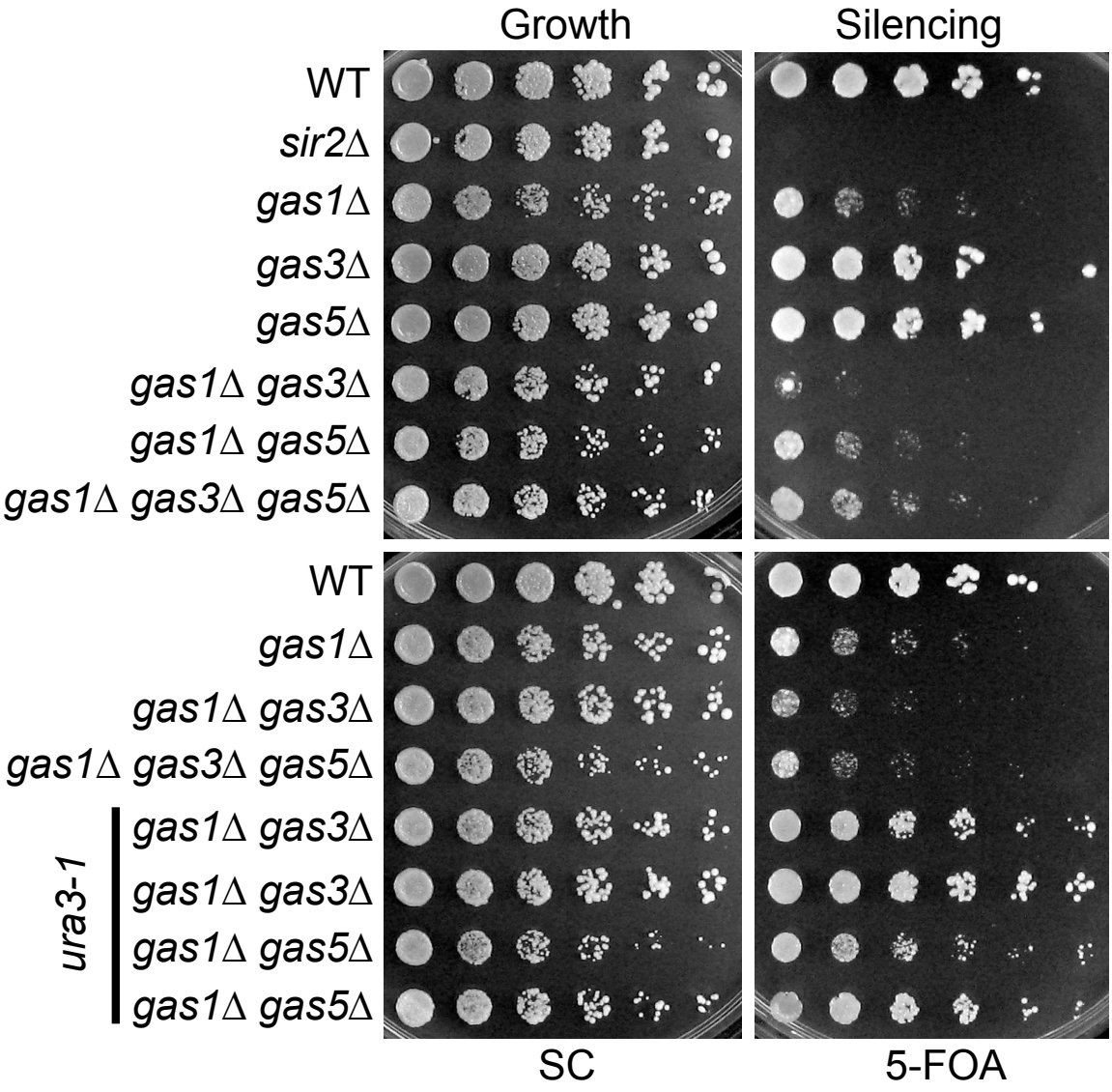
Growth
Silencing
WT
sir2Δ
gas1Δ
gas3Δ
gas5Δ
gas1Δ gas3Δ
gas1Δ gas5Δ
gas1Δ gas3Δ gas5Δ
WT
gas1Δ
gas1Δ gas3Δ
gas1Δ gas3Δ gas5Δ
ura3-1
gas1Δ gas3Δ
gas1Δ gas3Δ
gas1Δ gas5Δ
gas1Δ gas5Δ
SC
5-FOA

Figure 3-13. Deletion of *GAS5* exacerbates the *gas1*Δ telomeric silencing defect at telomere VII-L. In the top panels, WT (LPY1029), *sir2*Δ (LPY12660), *gas1*Δ (LPY10358), *gas3*Δ (LPY14440), *gas5*Δ (LPY14444), *gas1*Δ *gas3*Δ (LPY14420), *gas1*Δ *gas5*Δ (LPY14423), *gas1*Δ *gas3*Δ *gas5*Δ (LPY14424), all with TELVII-L::*URA3* were plated. In the bottom panels, WT (LPY1029), *gas1*Δ (LPY10358), *gas1*Δ *gas5*Δ (LPY14427), *gas1*Δ *gas3*Δ *gas5*Δ (LPY14421), *gas1*Δ *gas3*Δ *gas5*Δ (LPY14425), all with TELVII-L::*URA3*, and *gas1*Δ *gas5*Δ (LPY14419), *gas1*Δ *gas3*Δ (LPY14422), and *gas1*Δ *gas3*Δ (LPY14426), all without the telomeric reporter, were plated. Strains were plated at 30˚C on SC to monitor growth and on SC containing 5-FOA to monitor telomeric silencing.

TELVII-L::*URA3*

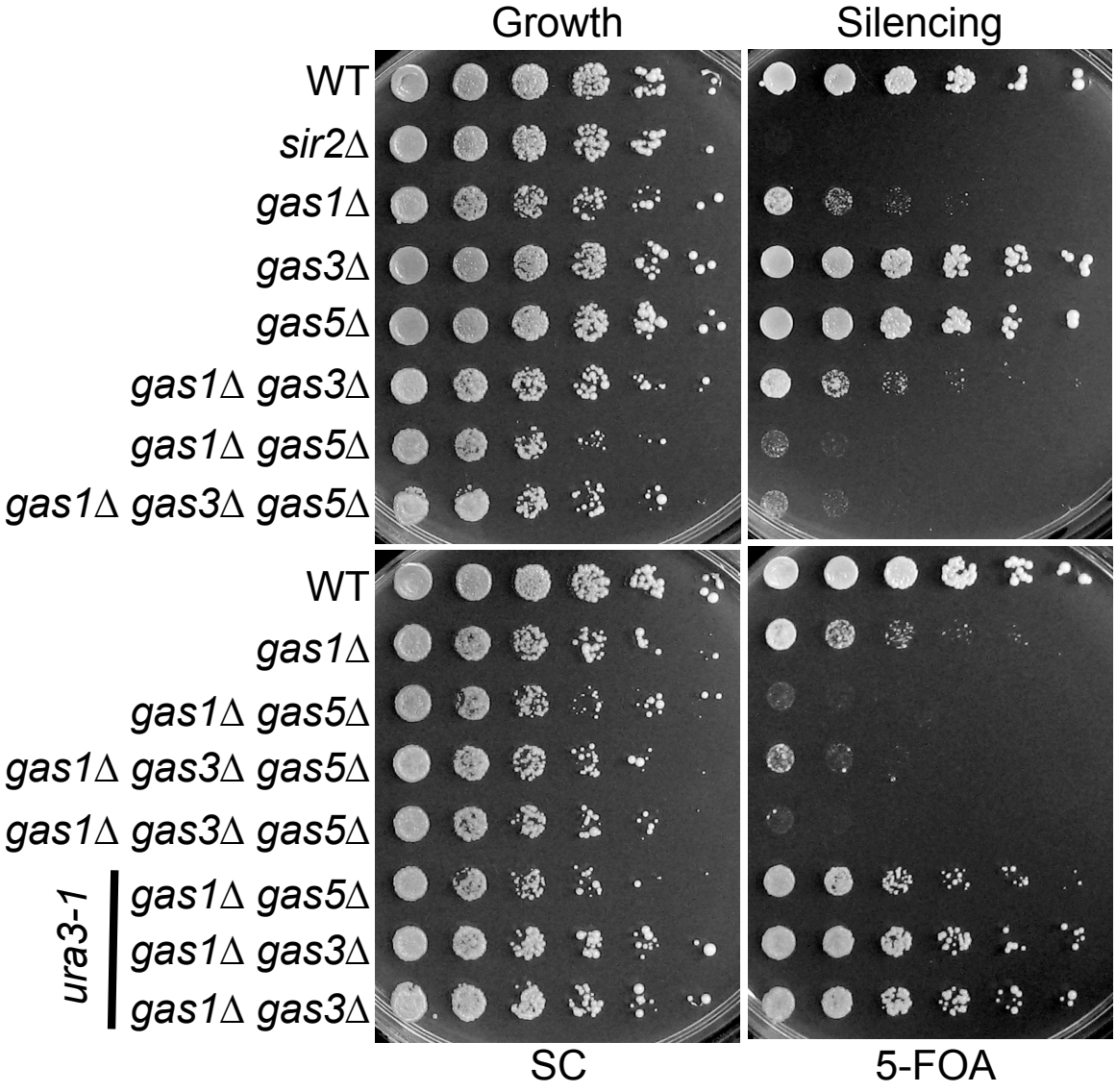

*gas1*Δ and deletion of other silencing-related genes. It is critical to independently validate these findings since high-throughput screens frequently identify false positive genetic interactions. An SGA screen completed for *gas1*Δ revealed synthetic sickness with *dot1*Δ in the BY4741 background (Tong et al. 2004; Lesage et al. 2004). To verify this genetic interaction, *gas1*Δ *dot1*Δ strains were constructed by crossing single mutant strains, covering *gas1*Δ with wild-type *GAS1* on a plasmid. No synthetic sickness was observed in the W303 genetic background (Figure 3-14) or BY4741 genetic background (Figure 3-15), suggesting that the SGA result was spurious.

An SGA screen to identify genetic interactors of *orc2-1* found a synthetic sick interaction with *gas1*Δ in the BY4741 genetic background that was confirmed by random spore analysis and tetrad dissection (Suter et al. 2004). In contrast to the *dot1*Δ *gas1*Δ analysis, this result was independently validated in the W303 genetic background and showed a synthetic lethal interaction in multiple *gas1*Δ *orc2-1* isolates from a cross of the single mutant strains (Figure 3-16).

Another SGA screen showed a synthetic growth defect between *eaf1*Δ and *gas1*Δ in BY4741 that was also confirmed by tetrad dissection (Mitchell et al. 2008). However, this interaction was not reported in an independent study utilizing a similar screening technique, diploid-based synthetic lethality analysis on microarray (dSLAM), also in BY4741 (Lin et al. 2008). To further investigate this genetic interaction, *eaf1*Δ *gas1*Δ strains were constructed. A synthetic lethal interaction was observed in W303 (Figure 3-17). This strain construction was also attempted in BY4741, but multiple attempts at crosses, using several independent parental strains for both *eaf1*Δ and *gas1*Δ, resulted in triploidy, which may point to genomic

Figure 3-14. Deletion of *GAS1* is not synthetically sick in combination with *dot1*Δ in the W303 genetic background. Clockwise starting with WT, the following strains, containing a 2μ *URA3 GAS1* plasmid (pLP1823) were plated, WT (LPY10306), *dot1*Δ (LPY10307), *gas1*Δ (LPY10308), *dot1*Δ *gas1*Δ (LPY10311), *dot1*Δ *gas1*Δ (LPY10312), *dot1*Δ *gas1*Δ (LPY10313). Strains were plated at 30˚C on SC-uracil (SC-ura) to assay growth and on 5-FOA for plasmid counter-selection. A synthetic growth defect was not observed in *dot1*Δ *gas1*Δ, although it was reported in SGA analysis in the BY4741 background (Tong et al. 2004; Lesage et al. 2004).

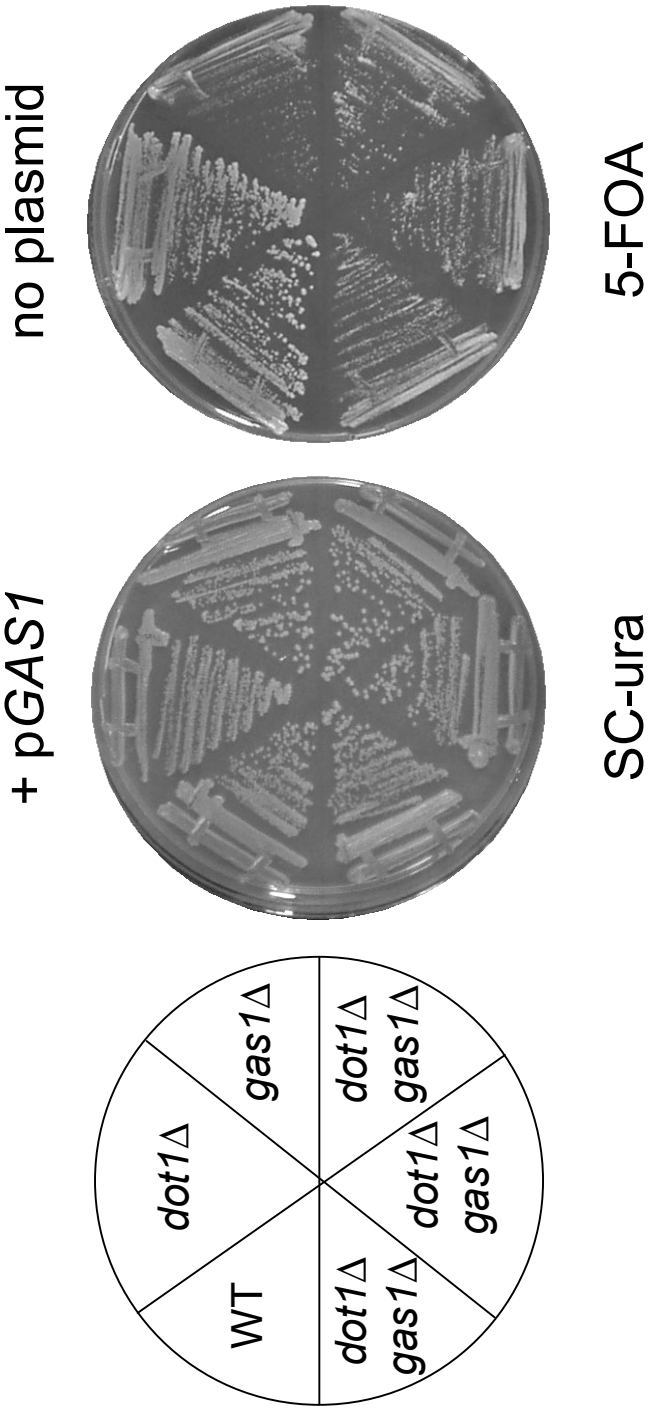
no plasmid
+ pGAS1
5-FOA
SC-ura
WT
dot1Δ
gas1Δ
dot1Δ gas1Δ
dot1Δ gas1Δ
dot1Δ gas1Δ

Figure 3-15. Deletion of *GAS1* is not synthetically sick in combination with *dot1*Δ in the BY4741 genetic background. Clockwise starting with WT, the following strains, containing a 2μ *URA3 GAS1* plasmid (pLP1823) were plated, WT (LPY14490), *dot1*Δ (LPY14491), *gas1*Δ (LPY14492), *dot1*Δ *gas1*Δ (LPY14493), *dot1*Δ *gas1*Δ (LPY14494), and *dot1*Δ *gas1*Δ (LPY14495). Strains were plated at 30˚C and 37˚C on SC-ura to assay growth and on 5-FOA for plasmid counter-selection. A synthetic growth defect was not observed in *dot1*Δ *gas1*Δ, although it was reported in SGA analysis in the same genetic background used here (Tong et al. 2004; Lesage et al. 2004).

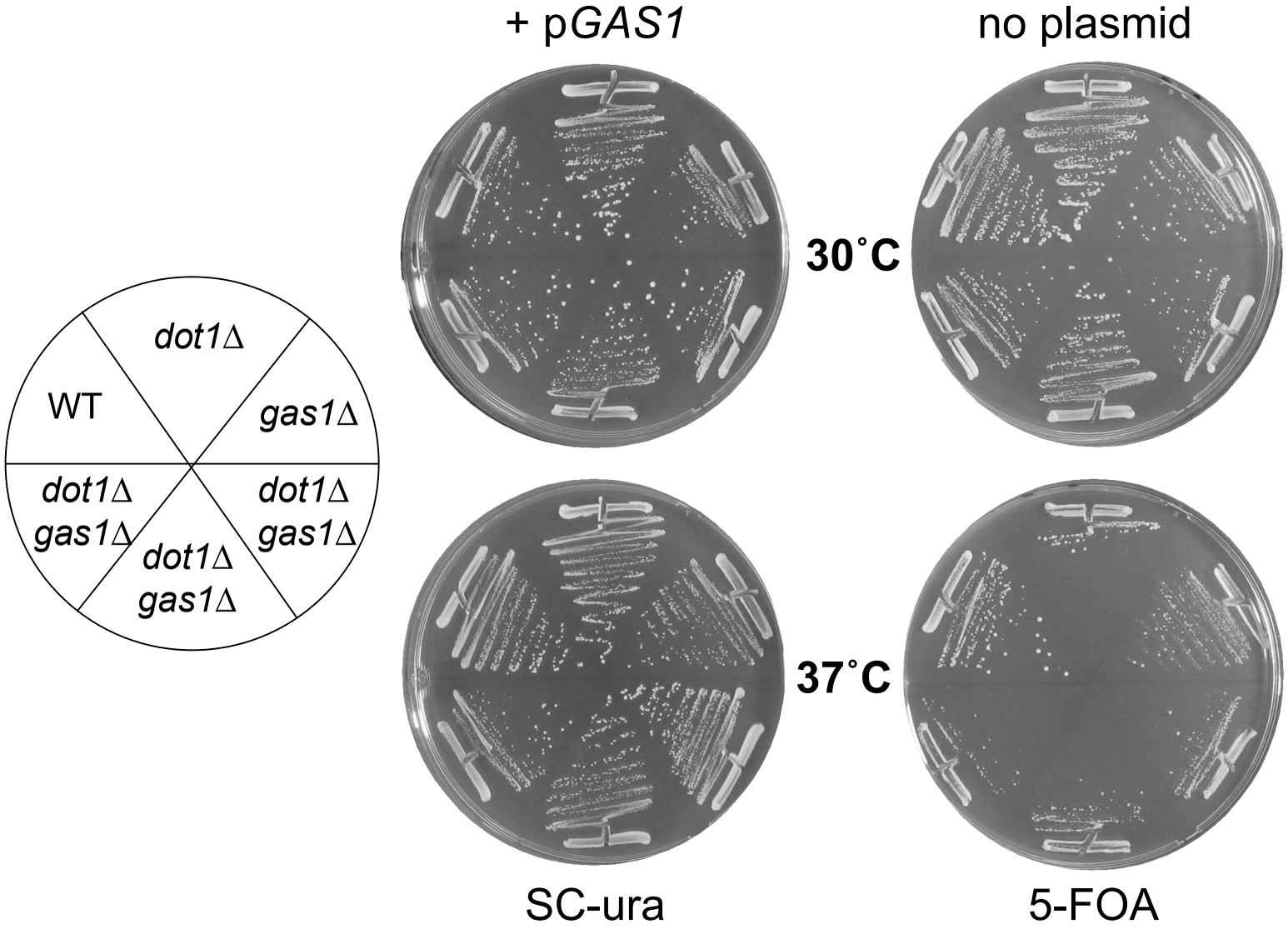
+ p*GAS1*
no plasmid
*dot1*Δ
WT
*gas1*Δ
*dot1*Δ *gas1*Δ
*dot1*Δ *gas1*Δ
*dot1*Δ *gas1*Δ
30˚C
37˚C
SC-ura
5-FOA

Figure 3-16. Deletion of *GAS1* is synthetically lethal in combination with *orc2-1* in the W303 genetic background. Counter-clockwise starting with WT, the following strains, containing a *GAS1* plasmid (pLP1823) were plated, WT (LPY10266), *orc2-1* (LPY10267), *gas1*Δ (LPY10268), *gas1*Δ (LPY10269), *gas1*Δ *orc2-1* (LPY10270), and *gas1*Δ *orc2-1* (LPY10271). Strains were plated at 25˚C (room temperature) on SC-ura to assay growth and on 5-FOA for plasmid counter-selection. The synthetic lethality of *gas1*Δ *orc2-1* independently validates the SGA screen result seen in the BY4741 genetic background (Suter et al. 2004).

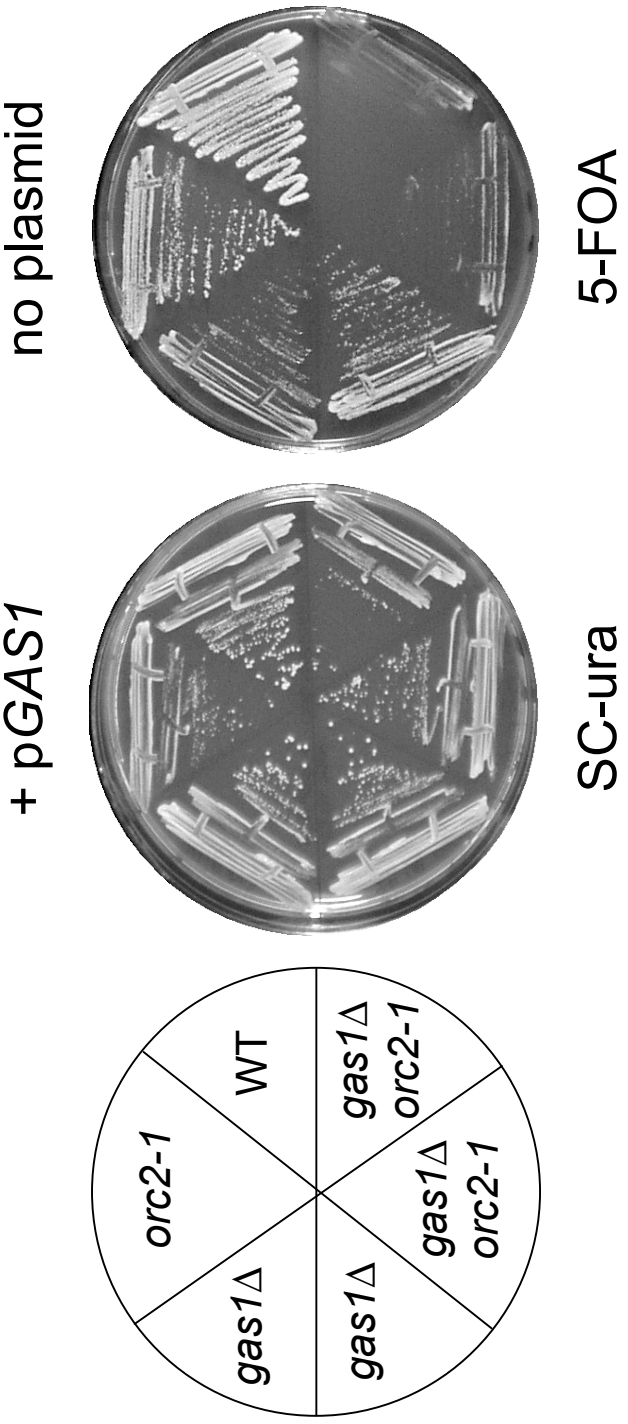
no plasmid
+ pGAS1
5-FOA
SC-ura
orc2-1
WT
gas1Δ orc2-1
gas1Δ
gas1Δ
gas1Δ orc2-1

Figure 3-17. Deletion of *GAS1* is synthetically lethal in combination with *eaf1*Δ in the W303 genetic background. Clockwise starting with WT, the following strains, containing a 2μ *URA3 GAS1* plasmid (pLP1823) were plated, WT (LPY14074), WT (LPY14075), *eaf1*Δ (LPY14076), *eaf1*Δ (LPY14077), *gas1*Δ (LPY14078), *gas1*Δ (LPY14079), *eaf1*Δ *gas1*Δ (LPY14080), and *eaf1*Δ *gas1*Δ (LPY14081). Strains were plated at 25˚C (room temperature) on SC-ura to assay growth and on 5-FOA for plasmid counter-selection. The synthetic lethality of *eaf1*Δ *gas1*Δ independently validates the SGA result seen in the BY4741 genetic background (Mitchell et al. 2008).

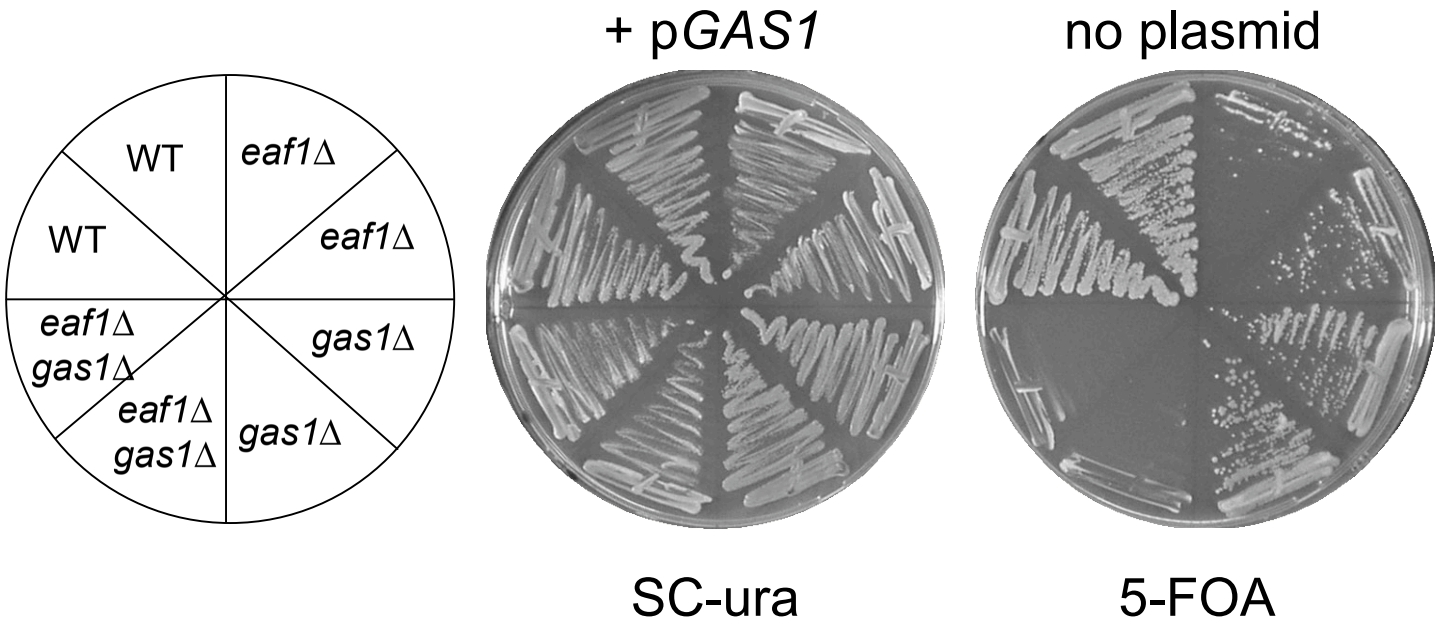
WT
eaf1Δ
WT
eaf1Δ
eaf1Δ
gas1Δ
gas1Δ
eaf1Δ
gas1Δ
gas1Δ
+ pGAS1
no plasmid
SC-ura
5-FOA

instability of the *eaf1*Δ strain, therefore this strain construction effort was abandoned. The *gas1*Δ strain was not suspect because it had been used in previous crosses and did not show evidence of triploidy.

During strain construction to create *gas1*Δ *rpd3*Δ strains to test for telomeric silencing, a synthetic genetic interaction was uncovered. In the W303 genetic background, a synthetic lethal interaction was observed in the *gas1*Δ *rpd3*Δ double mutant when the *GAS1* covering plasmid was counterselected on 5-FOA (Figure 3-18). This genetic interaction had not been observed in the *gas1*Δ SGA analysis in the BY4741 background (Tong et al. 2004; Lesage et al. 2004), or in the *rpd3*Δ dSLAM analysis in the BY4741 background (Lin et al. 2008), suggesting that the genetic interaction might be specific to the W303 genetic background. To test whether the interaction was genetic background-specific, *gas1*Δ *rpd3*Δ strains were constructed in BY4741. Although synthetic lethality was not observed, a synthetic sick interaction was observed in BY4741 upon challenging the *gas1*Δ *rpd3*Δ strains by exposure to high temperature, 37˚C (Figure 3-19). Comparisons have been done for different genetic backgrounds in yeast that revealed numerous gene deletions and polymorphisms (Primig et al. 2000). These genetic background differences may contribute to the magnitude of the synthetic genetic interactions seen here.

DISCUSSION

The genetic analysis of *GAS1* presented above strengthens understanding of *gas1*Δ phenotypes, specifically regarding its temperature sensitivity and telomeric

Figure 3-18. Deletion of *GAS1* is synthetically lethal in combination with *rpd3*Δ in the W303 genetic background. Clockwise starting with WT, the following strains, containing a 2μ *URA3 GAS1* plasmid (pLP1823) were plated, WT (LPY13677), *gas1*Δ (LPY13681), *gas1*Δ (LPY13682), *rpd3*Δ (LPY13683), *gas1*Δ *rpd3*Δ (LPY13678), and *gas1*Δ *rpd3*Δ (LPY13679). Strains were plated at 30˚C on SC-ura to assay growth and on 5-FOA for plasmid counter-selection. The synthetic lethality of *gas1*Δ *rpd3*Δ was not reported in *gas1*Δ SGA analysis (Tong et al. 2004; Lesage et al. 2004), or in *rpd3*Δ dSLAM analysis (Lin et al. 2008). Both of these genome-wide screens were done in the BY4741 genetic background.

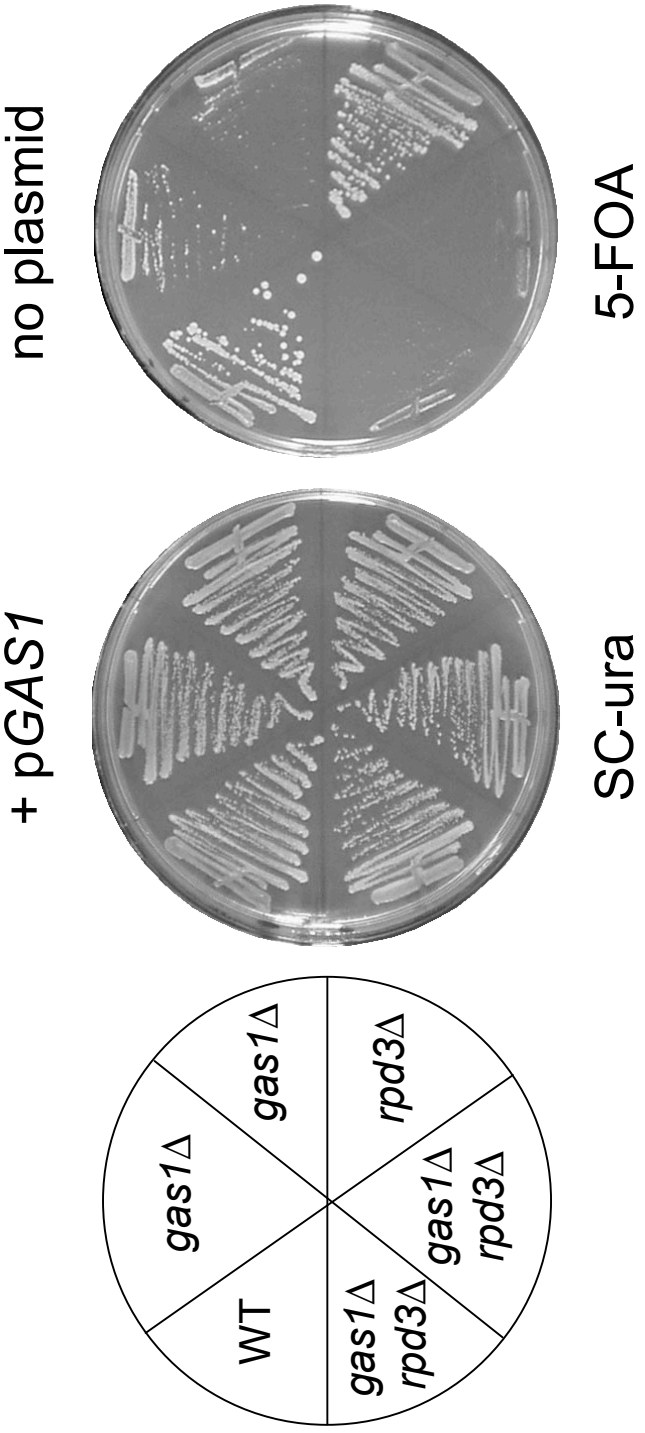
no plasmid
+ pGAS1
5-FOA
SC-ura
WT
gas1Δ
gas1Δ
rpd3Δ
gas1Δ rpd3Δ
gas1Δ rpd3Δ

Figure 3-19. Deletion of *GAS1* is synthetically sick in combination with *rpd3*Δ at high temperature in the BY4741 genetic background. Clockwise starting with WT, the following strains, containing a 2μ *URA3 GAS1* plasmid (pLP1823) were plated, WT (LPY14483), *rpd3*Δ (LPY14484), *gas1*Δ (LPY14485), *gas1*Δ *rpd3*Δ (LPY14486), *gas1*Δ *rpd3*Δ (LPY14487), and *gas1*Δ *rpd3*Δ (LPY14488). Strains were plated at 30˚C and 37˚C on SC-ura to assay growth and on 5-FOA for plasmid counter-selection. The synthetic sickness of *gas1*Δ *rpd3*Δ was not reported in *gas1*Δ SGA analysis (Tong et al. 2004; Lesage et al. 2004), or in *rpd3*Δ dSLAM analysis (Lin et al. 2008). Both of these genome-wide screens were done with the same genetic background (BY4741) used here.

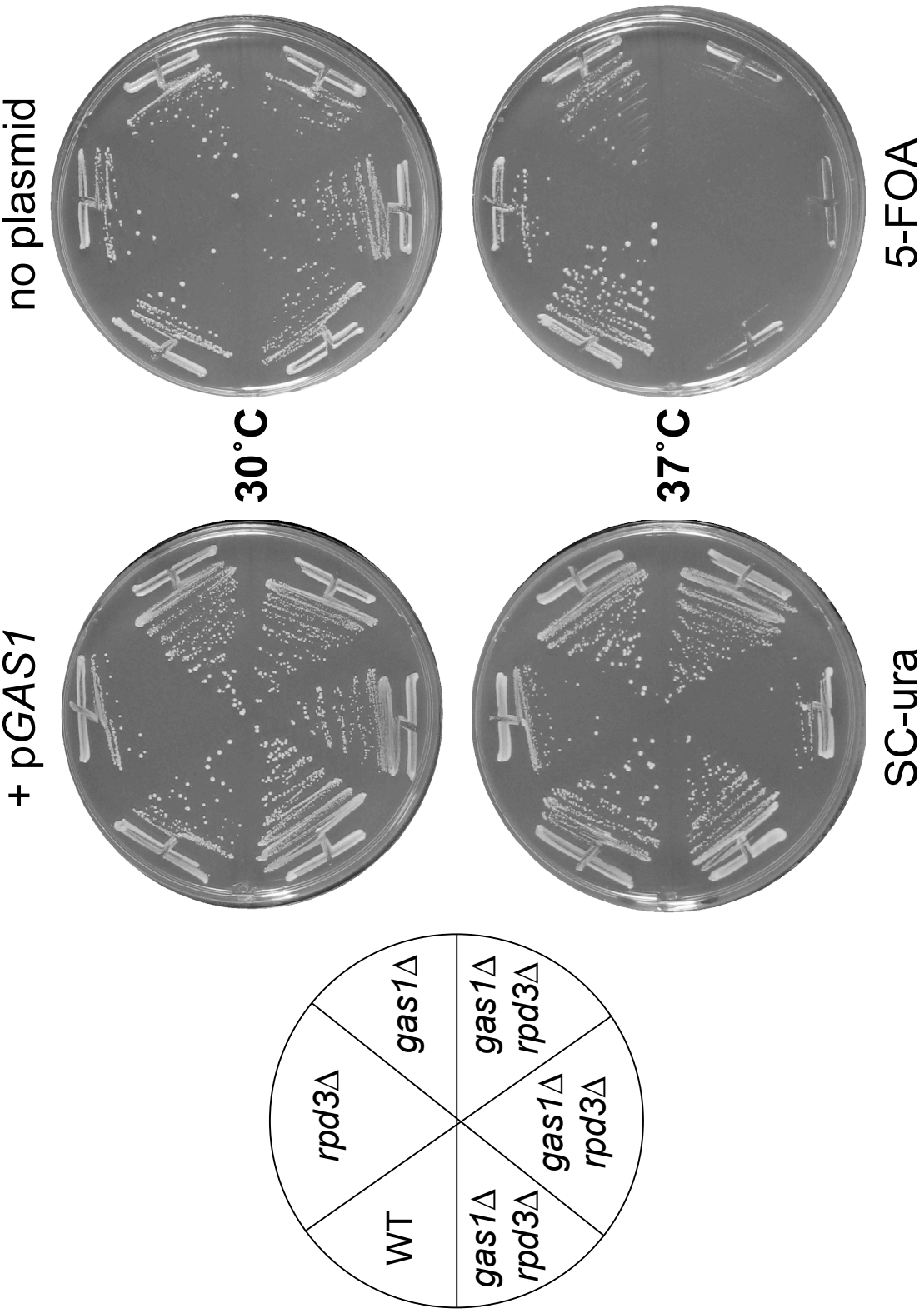
no plasmid
+ pGAS1
30˚C
37˚C
5-FOA
SC-ura
WT
rpd3Δ
gas1Δ
gas1Δ rpd3Δ
gas1Δ rpd3Δ
gas1Δ rpd3Δ

silencing defect. This investigation extends knowledge of interactions between *GAS1*, *SIR* genes, and other *GAS* genes. It also further analyzes growth defects caused by combined deletion of *GAS1* and other genes encoding proteins with silent chromatin-related functions, underscoring an important relationship between *GAS1* and other genes involved in transcriptional silencing. This analysis also raises additional questions as described below.

Cell type-specific suppression of *gas1*Δ temperature sensitivity. The suppression of *gas1*Δ temperature sensitivity that was observed in cases where *MAT***a** and *MAT*α information were expressed simultaneously in the same haploid cell (Figure 3-1 and Figure 3-5) may result from the expression of diploid-specific genes or the repression of haploid-specific genes, the most likely consequence of the pseudodiploid state. Cell-type specific suppression of phenotypes has been observed previously. For example, simultaneous expression in haploid cells of both *MAT***a** and *MAT*α information suppresses the senescent phenotype of telomerase deficient mutants (Lowell et al. 2003). Other examples of suppression by *MAT* heterozygosity exist in relation to mutants with DNA repair and recombination phenotypes. For instance, *MAT* heterozygosity suppresses the double-strand break repair defect of a *rad57* mutant (Fung et al. 2009). Mating-type heterozygosity also suppresses *rad52*, a gene functioning in recombinational repair of DNA damage and in mitotic and meiotic recombination (Schild 1995). The transcriptional circuit for cell-type specification has been characterized (Galgoczy et al. 2004), and may point to haploid-specific genes that are repressed in *gas1*Δ *sir* mutants, which may be responsible for the suppression

of *gas1*Δ temperature sensitivity. The expression of diploid-specific genes in this situation may provide a mechanism for this suppression.

***SIR*-specific effects on the *gas1*Δ telomeric silencing defect**. Transcriptional silencing is sensitive to dosage of Sir proteins. It has previously been observed that the silent chromatin present at telomeres and ribosomal DNA compete for a limited pool of Sir2 (Cockell et al. 1995; Smith et al. 1998). The *gas1*Δ mutants have a defect in silencing at the telomeres (Figure 2-1*D*, 2-1*E*, 2-3), and it was important to establish whether changes in the Sir proteins could influence this silencing defect, or even bypass the requirement for Gas1.

Gene expression effects have been observed upon targeting proteins to a DNA sequence where they would normally not bind. When some histone acetyltransferases are tethered to a telomeric reporter gene, expression of an otherwise silenced gene is observed (Jacobson and Pillus 2004). The same protein targeting system was used in this study to address the possibility that silent chromatin structure or stability was disrupted in *gas1*Δ mutants. Although Sir1 is not required for telomeric silencing, tethering Sir1 to the telomere via an engineered Gal4 DNA binding site was shown to establish silencing when SIR complex members were present, and improved silencing in wild-type cells (Chien et al. 1993) (Figure 3-6*A*). This tethering event is thought to stabilize telomeric silencing through enhanced recruitment of SIR complex members at the telomeres. When Sir1 is tethered at the telomeres, the requirement for Gas1 is completely bypassed (Figure 3-6*A*). Similar to the Sir1 tethering result, Sir2 tethering to a telomeric reporter gene restored silencing to a *gas1*Δ strain (Figure 3-6*B*). This also bypassed the requirement for Gas1 activity in telomeric silencing. Therefore,

silencing can be restored through artificial stabilization of silent chromatin components in *gas1*Δ mutants.

Simply overexpressing certain *SIR* genes also had a positive effect on telomeric silencing of *gas1*Δ strains. Although a reduction in Sir2 and Sir3 proteins levels was not observed in *gas1*Δ strains (Figure 2-5), *SIR2* and *SIR3* overexpression partially restored telomeric silencing in *gas1*Δ strains (Figure 3-7), suggesting that the defect is quite sensitive to Sir protein levels. However, overexpression did not completely bypass the requirement for Gas1 since silencing was not restored to the levels of the wild-type strain or the *gas1*Δ strain complemented by expression of plasmid-borne *GAS1*. The partial rescue of the *gas1*Δ telomeric silencing defect upon *SIR2* and *SIR3* overexpression suggests that Gas1 function is necessary for full telomeric silencing.

Parallel results were observed in the evaluation of *SIR1*'s contribution to *gas1*Δ's telomeric silencing defect. *SIR1* overexpression exacerbated the telomeric silencing defect (Figure 3-7) whereas *SIR1* deletion suppressed the telomeric silencing defect (Figure 3-8). The most likely explanation for these changes in the amount of telomeric silencing observed in the *gas1*Δ strain is a shift in the balance of Sir proteins available for silencing at telomeres and the cryptic mating-type loci. In this hypothesis, when *SIR1* is overexpressed, Sir proteins lose their interaction with the telomeres and associate with the extra Sir1 in the cell, at the cryptic mating-type loci. When *SIR1* is deleted in *gas1*Δ, perhaps Sir proteins are no longer recruited to the cryptic mating-type loci, and more Sir proteins are available for telomeric silencing,

leading to the strengthened telomeric silencing observed in *gas1*Δ *sir1*Δ strains. A summary of the contributions of *SIR* genes to *gas1*Δ phenotypes, including its telomeric silencing defect and temperature sensitivity is presented in Table 3-1.

Effects of other *GAS* genes on *gas1*Δ phenotypes. *GAS1* is the most well-characterized of the duplicated *GAS* genes. Because these genes are all proposed to encode β-1,3-glucanosyltransferases, it is possible that they have overlapping or divergent functions. *GAS2* and *GAS4* are meiotically-expressed genes that function in spore wall formation (Ragni et al. 2007a). Distinct functions for *GAS3* and *GAS5* have yet to be identified. Notably, *GAS5* is a multi-copy suppressor (Tomishige et al. 2005) and phenotypic enhancer (Schuldiner et al. 2005) of *gas1*Δ mutants. This was also observed in independent studies as reported in the Results presented above and summarized in Table 3-2. *GAS5* overexpression complemented *gas1*Δ's temperature sensitivity (Figure 3-9) and telomeric silencing defect (Figure 3-10). Conversely, deletion of *GAS5* exacerbated *gas1*Δ slow growth, especially on rich media (YPD), and worsened *gas1*Δ sensitivity to high temperature (Figure 3-11). These observations suggest that Gas5 can partially fulfill Gas1's role in cell wall biogenesis in the absence of Gas1. When *GAS5* is deleted, cell wall defects are exaggerated, as seen in the severe growth defect at high temperature in *gas1*Δ *gas5*Δ strains.

The effect of deletion of *GAS5* on *gas1*Δ's telomeric silencing defect was also analyzed. At the telomere V-R *URA3* reporter gene, no change in silencing was observed in *gas1*Δ *gas5*Δ strains (Figure 3-12). Although the same reporter gene was assayed at the telomere VII-L *URA3* reporter gene, telomeric silencing was modestly more defective in the *gas1*Δ *gas5*Δ double mutant (Figure 3-13). Therefore, the

Table 3-1. Effects of *SIR* gene dosage on *gas1*Δ telomeric silencing defect and temperature sensitivity.[a]

	SIR1	*SIR2*	*SIR3*	*SIR4*
Telomeric silencing defect				
Deletion	+++	-	-	-
Overexpression	-	++	++	+
DNA tethering	+++	+++	ND	ND
Temperature sensitivity				
Deletion	++	++	++	++
Overexpression	NC	NC	NC	NC

[a]- = worsens phenotype; ++ = phenotype partially rescued; +++ = phenotype fully rescued; ND = not done; NC = no change

Table 3-2. Effects of *GAS* gene dosage on *gas1*Δ telomeric silencing defect and temperature sensitivity.[a]

	GAS3	*GAS5*
Telomeric silencing defect		
Overexpression	ND	+++
Deletion, telomere V-R	NC	NC
Deletion, telomere VII-L	NC	-
Temperature sensitivity		
Overexpression	ND	+++
Deletion	NC	-

[a]- = worsens phenotype; +++ = phenotype rescued; ND = not done; NC = no change

exacerbation of *gas1*Δ's telomeric silencing defect by *GAS5* deletion appears to be telomere-specific. Also, the telomere structure at V-R compared to VII-L may also contribute to the observed difference. *GAS1* encodes the only β-1,3-glucanosyltransferase required for telomeric silencing, but is assisted by Gas5 in silencing of a subset of telomeres. Since Gas5 also localizes to the nucleus (Huh et al. 2003), it may have redundant functions in transcriptional silencing, overlapping Gas1 nuclear function.

Synthetic genetic interactions between *GAS1* and other silencing genes. Results from several genome-wide screens have suggested genetic interactions between *GAS1* and genes encoding silencing factors. A major caveat when considering these screens is that genetic interactions can be missed, leading to false negatives, or can be scored incorrectly, leading to false positives. An example of a false positive interaction is the synthetic sickness reported for *dot1*Δ *gas1*Δ (Tong et al. 2004; Lesage et al. 2004). In two genetic backgrounds, *dot1*Δ *gas1*Δ strains appeared as healthy as either single mutant strain (Figure 3-14, 3-15). This reinforces the importance of independent validation of screen results.

Two different *GAS1* genetic interactions found here were not reported in the SGA/dSLAM screens. The *eaf1*Δ *gas1*Δ synthetic growth defect was observed in one study (Mitchell et al. 2008) but not another (Lin et al. 2008). Construction of the *eaf1*Δ *gas1*Δ strain in a different genetic background (W303) than was used in these screens reproduced the synthetic lethal interaction of this combination of gene deletions (Figure 3-17). When attempting to construct this same double mutant strain in the BY4741 background used in the SGA and dSLAM screens, triploidy was observed on

multiple occasions during the attempt at diploid construction by crosses of several independent *eaf1*Δ and *gas1*Δ strains. The triploidy is likely contributed by the BY4741 *eaf1*Δ strains since a number of successful crosses have been done with the BY4741 *gas1*Δ strains.

The *gas1*Δ *rpd3*Δ synthetic growth defect was not reported in multiple genome-wide screens (Tong et al. 2004; Lesage et al. 2004; Lin et al. 2008). This genetic interaction was first observed in the W303 genetic background (Figure 3-18), which at first glance may point to the interaction being specific to the genetic background, especially since the interaction was not observed in the screens for synthetic genetic interactors of *gas1*Δ or *rpd3*Δ in the BY4741 genetic background. However, in the independent construction of *gas1*Δ *rpd3*Δ reported here, the synthetic growth defect was observed at high temperature in the BY4741 background (Figure 3-19), and is therefore an example of a false negative SGA/dSLAM result. Typically, the BY4741 background strains are healthier than strains of other genetic backgrounds, such as W303, stressing the importance of challenging strains as was done for *gas1*Δ *rpd3*Δ by exposure to high temperature.

The molecular underpinnings of the genetic interactions confirmed and reported here have not yet been defined. Further study is necessary to comprehend the complicated nature of these genetic interactions, however speculation of the significance of each of the genetic interactions as presented here may lead to ideas for future experimentation.

EAF1 encodes an integral component of the NuA4 histone acetyltransferase complex. NuA4 also contains a catalytic subunit, the histone acetyltransferase Esa1.

Notably, *gas1*Δ has synthetic growth defects with both *eaf1*Δ and *esa1-L254P* in genomewide SGA analysis (Mitchell et al. 2008). Synthetic growth defects are also observed between *eaf1*Δ or *esa1-L254P* and deletion of *CDA2*, *PUB1* and *SLX5*/*HEX3* (Mitchell et al. 2008). Gas1, Cda2, Pub1, and Slx5 were all identified as two-hybrid interactors of the histone deacetylase Sir2 (Garcia 2003; Darst et al. 2008). Another significant relationship exists between *SIR2* and *ESA1*, as overexpressing *ESA1* and *SIR2* reciprocally suppresses the rDNA silencing defects of *sir2*Δ and *esa1* mutants (Clarke et al. 2006). The synthetic growth defect observed by the combined deletion of *GAS1* with *eaf1*Δ and *esa1-L254P* shows that these genes contribute to a function that is important for cell viability. One shared function is in telomeric silencing given that *esa1* mutants are defective in silencing telomeres (Clarke et al. 2006), and *GAS1* is also required for telomeric silencing (Figure 2-1*D*, 2-1*E*, 2-3). Although there is no reported role for telomeric silencing in cell fitness, it is conceivable that the separate contributions of *ESA1* and *GAS1* to transcriptional silencing at telomeres are vital to cell survival. In addition to transcriptional silencing, Esa1 is required for cell cycle progression, DNA double-strand break repair, and transcriptional activation (reviewed in Lafon et al. 2007; Pillus 2008). Since both Gas1 and Esa1 have other functions beyond transcriptional silencing, it is possible that the combined loss of other functions of these proteins lead to the observed synthetic growth defect.

ORC2 encodes a component of ORC. ORC's primary function is in DNA replication (reviewed in Toone et al. 1997; Sasaki and Gilbert 2007). ORC also functions in silencing of the *HM* cryptic mating-type locus (Micklem et al. 1993; Bell et al. 1993; Foss et al. 1993), a function that is separable from its function in DNA

replication (Ehrenhofer-Murray et al. 1995). The synthetic lethality of *gas1*Δ *orc2-1* strains is an additional noteworthy genetic interaction between two genes with transcriptional silencing functions. Although *GAS1* does not contribute to *HM* silencing, the combined loss of *HM* and telomeric silencing in *gas1*Δ *orc2-1* may result in the observed growth defect. However, deletions of *SIR* genes also exhibit the combined loss of *HM* and telomeric silencing and result in viable healthy cells. To determine whether the *gas1*Δ *orc2-1* genetic interaction is specific to ORC function, it will be important to determine whether *gas1*Δ shows a growth defect in combination with conditional alleles of other *ORC* genes. ORC contains five other essential subunits. The SGA screen was also done for *orc5-1*, although *GAS1* was not identified (Suter et al. 2004), however *gas1*Δ may exhibit synthetic sick interactions with one or more of the other four *ORC* genes. ORC's function in DNA replication is likely to contribute significantly to the synthetic lethality of *gas1*Δ *orc2-1* since DNA replication is a vital cellular function.

RPD3 encodes a histone deacetylase, the catalytic component of the Rpd3S and Rpd3L complexes. *RPD3* negatively regulates transcriptional silencing, as its deletion enhances telomeric, *HM*, and rDNA silencing (De Rubertis et al. 1996; Rundlett et al. 1996; Vannier et al. 1996; Sun and Hampsey 1999). The mechanism for these effects on silencing is currently unknown. The basis of the synthetic growth defect observed in *gas1*Δ *rpd3*Δ strains may be related to their shared contributions to silent chromatin function. Both *gas1*Δ and *rpd3*Δ enhance rDNA silencing when deleted (Figure 2-1*C*) (Sun and Hampsey 1999), but there is no evidence that a robust rDNA silencing phenotype reduces cellular fitness. The effects of *GAS1* and *RPD3* in

telomeric silencing compensate for each other since *gas1*Δ reduces telomeric silencing and *rpd3*Δ enhances telomeric silencing, therefore effects on telomeric silencing cannot be the explanation for the *gas1*Δ *rpd3*Δ synthetic lethality.

In future experiments, it will be important to dissect the cause of the *gas1*Δ *rpd3*Δ lethality by determining whether point mutants disrupting the catalytic activity of the proteins recapitulate the genetic interaction of the null mutants. In addition, since Rpd3 is found in two distinct complexes, it will be important to determine whether the *gas1*Δ *rpd3*Δ lethality is specific to one of the two complexes by combining *gas1*Δ with mutants encoding Rpd3L or Rpd3S subunits. This would help to further define the basis of the *gas1*Δ *rpd3*Δ genetic interaction. *RPD3* also contributes to non-homologous end joining (Jazayeri et al. 2004) and transcriptional regulation (Bernstein et al. 2000), two other crucial cellular functions. Interestingly, Rpd3 has been implicated in controlling the activation of genes required for cell wall biosynthesis, a link to Gas1's cell wall function (Vannier et al. 2001). The synthetic lethality of *gas1*Δ *rpd3*Δ is most likely a consequence of loss of these Rpd3 functions, combined with the loss of Gas1's function in transcriptional silencing, cell wall biogenesis, or an undiscovered Gas1 function. Since the function of Gas1 in silencing is only recently realized, despite the gene being discovered almost twenty years ago, additional Gas1 functions remain to be uncovered. These other roles for Gas1 may involve other nuclear functions besides its proposed action in transcriptional silencing described in Chapter 2.

MATERIALS AND METHODS

Yeast strains and methods. Yeast strains are listed in Table 3-3. Strains were constructed during this study unless otherwise noted and grown at 30˚C with standard manipulations (Amberg et al. 2005). Lithium acetate transformation was used (Ito et al. 1983). Yeast extract-peptone-dextrose (YPD) and synthetic selective media were prepared as described (Sherman 1991). 5-fluoroorotic acid (5-FOA; United States Biological, Inc., Swampscott, MA) was added at 0.1% to test for *URA3* reporter gene expression. Telomeric silencing assays were performed as described previously (van Leeuwen and Gottschling 2002). For serial-dilution assays, five-fold dilutions were plated from cultures grown at 30˚C, starting at an A_{600} of 1.0. Plates were incubated at 30˚C unless otherwise indicated for 3 days prior to digital image capture.

Plasmids. Plasmids used are part of the standard lab collection, or were constructed during the course of this work, and are listed in Table 3-4. pLP2192 contains the *SIR1 Eag*I-*Sal*I fragment from pLP17 (pJR910) inserted at *Eag*I-*Sal*I digested pLP359 (pRS423, 2μ *HIS3* vector). pLP2206 contains the *Eco*RI-*Sac*II insert from pLP1609 (pGM300) (Murphy et al. 2003) in *Eco*RI-*Sac*II digested pLP359. The *GAS5* clones (pLP2012, pLP2013) were obtained by amplification of *GAS5* from wild-type (LPY5) genomic DNA using oligonucleotides oLP815 and oLP816. The *Eag*I-*Bam*HI digested *GAS5* product was ligated to *Eag*I-*Bam*HI digested pLP1623 (pRS425, 2μ *LEU2* vector). The sequence of the entire *GAS5* ORF was confirmed using T3, T7, and oLP833 oligonucleotides. Oligonucleotides are listed in Table 3-5.

Table 3-3. Yeast strains used in Chapter 3.[a]

Strain	Genotype	Source/Reference
LPY5	W303-1a *MAT***a** *ade2-1 can1-100 his3-11,15 leu2-3,112 trp1-1 ura3-1*	R. Rothstein
LPY9	W303-1a *sir4::HIS3*	
LPY10	W303-1a *sir3::TRP1*	
LPY11	W303-1a *sir2::HIS3*	
LPY79	W303-1b *MAT*α *ade2-1 can1-100 his3-11,15 leu2-3,112 trp1-1 ura3-1*	R. Rothstein
LPY1029	YDS631 W303-1b *adh4::URA3-*$(C_{1\text{-}3}A)_n$	Chien et al. 1993
LPY1030	YDS634 W303-1b *adh4::URA3-4XUAS*$_G$*-*$(C_{1\text{-}3}A)_n$	Chien et al. 1993
LPY2846	LPY1030 + pLP493	
LPY2854	LPY1030 + pLP409	
LPY4417	W303-1b *sir3::TRP1 adh4::URA3-4XUAS*$_G$*-*$(C_{1\text{-}3}A)_n$	
LPY4624	W303-1a *sir2::TRP1 adh4::URA3-4XUAS*$_G$*-*$(C_{1\text{-}3}A)_n$	
LPY4916	W303-1a TELVR*::URA3*	
LPY5611	W303-1a *sir2::HIS3 adh4::URA3-4XUAS*$_G$*-*$(C_{1\text{-}3}A)_n$	
LPY5777	LPY5611 + pLP956	
LPY5779	LPY5611 + pLP1074	
LPY6283	W303-1b *trp1Δ0* TELVR::*URA3*	
LPY6284	W303-1a *trp1Δ0* TELVR::*URA3*	
LPY7884	LPY4624 + pLP493	
LPY7886	LPY4624 + pLP409	
LPY7892	LPY4417 + pLP493	
LPY7894	LPY4417 + pLP409	
LPY9818	W303-1b *gas1Δ::kanMX sir3::TRP1* rDNA::*ADE2-CAN1* TELVR::*URA3*	
LPY9822	W303-1b *gas1Δ::kanMX sir2::HIS3* TELVR::*URA3*	
LPY10129	W303-1a *gas1Δ::kanMX*	
LPY10159	W303-1a *gas1Δ::kanMX sir4::HIS3*	
LPY10266	W303-1a rDNA::*ADE2-CAN1* + pLP1823	
LPY10267	W303-1b *orc2-1* rDNA::*ADE2-CAN1* + pLP1823	
LPY10268	W303-1b *gas1Δ::kanMX* rDNA::*ADE2-CAN1* + pLP1823	
LPY10269	W303-1b *gas1Δ::kanMX orc2-1* rDNA::*ADE2-CAN1* + pLP1823	
LPY10270	W303-1b *gas1Δ::kanMX orc2-1* rDNA::*ADE2-CAN1* + pLP1823	
LPY10271	W303-1a *gas1Δ::kanMX orc2-1* rDNA::*ADE2-CAN1* + pLP1823	
LPY10306	W303-1b + pLP1823	
LPY10307	W303-1a *dot1Δ::kanMX* + pLP1823	
LPY10308	W303-1b *gas1Δ::kanMX* + pLP1823	
LPY10311	W303-1b *dot1Δ::kanMX gas1Δ::kanMX* + pLP1823	
LPY10312	W303-1b *dot1Δ::kanMX gas1Δ::kanMX* + pLP1823	
LPY10313	W303-1b *dot1Δ::kanMX gas1Δ::kanMX* + pLP1823	
LPY10358	W303-1a *trp1Δ0 ura3Δ0 gas1Δ::kanMX adh4::URA3-*$(C_{1\text{-}3}A)_n$	
LPY10360	W301-1a *gas1Δ::kanMX adh4::URA3-4XUAS*$_G$*-*$(C_{1\text{-}3}A)_n$	

Table 3-3. Yeast strains used in Chapter 3. (continued)

LPY10362	W303-1a *gas1*Δ*::kanMX* TELVR*::URA3*
LPY10363	W303-1b *gas1*Δ*::kanMX* TELVR::*URA3*
LPY10397	W303-1a *sir2::HIS3* TELVR::*URA3*
LPY10498	LPY10360 + pLP956
LPY10499	LPY10360 + pLP1073
LPY10500	LPY10360 + pLP1074
LPY10650	LPY6284 + pLP61
LPY10651	LPY6284 + pLP1167
LPY10652	LPY6284 + pLP1185
LPY10653	LPY6283 + pLP61
LPY10654	LPY6283 + pLP1167
LPY10655	LPY6283 + pLP1185
LPY10656	LPY10362 + pLP61
LPY10657	LPY10362 + pLP1167
LPY10658	LPY10362 + pLP1185
LPY10659	LPY10363 + pLP61
LPY10660	LPY10363 + pLP1167
LPY10661	LPY10363 + pLP1185
LPY10663	W303-1a *gas1*Δ*::kanMX sir2::HIS3*
LPY10665	W303-1a *gas1*Δ*::kanMX sir1*Δ*::LEU2*
LPY10667	W303-1a *gas1*Δ*::kanMX sir3::TRP1*
LPY12045	W303-1b *sir1*Δ*::LEU2* TELVR::*URA3*
LPY12053	W303-1a *gas1*Δ*::kanMX sir1*Δ*::LEU2* TELVR::*URA3*
LPY12065	W303-1 *gas1*Δ*::kanMX sir4::HIS3* TELVR::*URA3*
LPY12068	W303-1 *gas1*Δ*::kanMX sir4::HIS3*
LPY12337	W303-1a *gas3*Δ*::kanMX* TELVR::*URA3*
LPY12348	W303-1a *gas5*Δ*::kanMX* TELVR::*URA3*
LPY12660	W303-1b *ura3*Δ*0 sir2::HIS3 adh4::URA3-*$(C_{1\text{-}3}A)_n$
LPY13554	LPY4916 + pLP359
LPY13555	LPY4916 + pLP2192
LPY13556	LPY4916 + pLP891
LPY13557	LPY4916 + pLP1047
LPY13558	LPY4916 + pLP2206
LPY13559	LPY4916 + pLP2091
LPY13563	LPY10362 + pLP359
LPY13564	LPY10362 + pLP2192
LPY13565	LPY10362 + pLP891
LPY13566	LPY10362 + pLP1047
LPY13567	LPY10362 + pLP2206
LPY13568	LPY10362 + pLP2091
LPY13674	W303-1b *gas1*Δ*::kanMX sir3::TRP1 sir4::HIS3*
LPY13677	W303-1a + pLP1823
LPY13678	W303-1a *gas1*Δ*::kanMX rpd3*Δ*::kanMX* + pLP1823

Table 3-3. Yeast strains used in Chapter 3. (continued)

LPY13679	W303-1b *gas1*Δ*::kanMX rpd3*Δ*::KanMX* + pLP1823
LPY13681	W303-1a *gas1*Δ*::kanMX* + pLP1823
LPY13682	W303-1b *gas1*Δ*::kanMX* + pLP1823
LPY13683	W303-1a *rpd3*Δ*::kanMX* + pLP1823
LPY13887	W303-1a *sir2::HIS3 sir3::TRP1*
LPY13889	W303-1a *sir2::HIS3 sir4::HIS3*
LPY13891	W303-1a *sir3::TRP1 sir4::HIS3*
LPY13893	W303-1a *sir2::HIS3 sir3::TRP1 sir4::HIS3*
LPY13895	W303-1b *gas1*Δ*::kanMX sir2::HIS3 sir3::TRP1*
LPY13896	W303-1b *gas1*Δ*::kanMX sir2::HIS3 sir4::HIS3*
LPY13900	W303-1b *gas1*Δ*::kanMX sir2::HIS3 sir3::TRP1 sir4::HIS3*
LPY14074	W303-1a + pLP1823
LPY14075	W303-1b *hmr*Δ*E::TRP1* + pLP1823
LPY14076	W303-1a *eaf1*Δ*::kanMX* + pLP1823
LPY14077	W303-1b *eaf1*Δ*::kanMX* + pLP1823
LPY14078	W303-1a *gas1*Δ*::kanMX hmr*Δ*E::TRP1* + pLP1823
LPY14079	W303-1b *gas1*Δ*::kanMX hmr*Δ*E::TRP1* + pLP1823
LPY14080	W303-1a *eaf1*Δ*::kanMX gas1*Δ*::kanMX hmr*Δ*E::TRP1* + pLP1823
LPY14081	W303-1b *eaf1*Δ*::kanMX gas1*Δ*::kanMX hmr*Δ*E::TRP1* + pLP1823
LPY14419	W303-1b *gas1*Δ*::kanMX gas5*Δ*::kanMX*
LPY14420	W303-1a *gas1*Δ*::kanMX gas3*Δ*::kanMX adh4::URA3-*$(C_{1\text{-}3}A)_n$
LPY14421	W303-1b *gas1*Δ*::kanMX gas3*Δ*::kanMX gas5*Δ*::kanMX adh4::URA3-*$(C_{1\text{-}3}A)_n$
LPY14422	W303-1b *gas1*Δ*::kanMX gas3*Δ*::kanMX*
LPY14423	W303-1a *gas1*Δ*::kanMX gas5*Δ*::kanMX adh4::URA3-*$(C_{1\text{-}3}A)_n$
LPY14424	W303-1a *gas1*Δ*::kanMX gas3*Δ*::kanMX gas5*Δ*::kanMX adh4::URA3-*$(C_{1\text{-}3}A)_n$
LPY14425	W303-1b *gas1*Δ*::kanMX gas3*Δ*::kanMX gas5*Δ*::kanMX adh4::URA3-*$(C_{1\text{-}3}A)_n$
LPY14426	W303-1a *gas1*Δ*::kanMX gas3*Δ*::kanMX*
LPY14427	W303-1a *gas1*Δ*::kanMX gas5*Δ*::kanMX adh4::URA3-*$(C_{1\text{-}3}A)_n$
LPY14428	W303-1a *gas1*Δ*::kanMX gas3*Δ*::kanMX*
LPY14429	W303-1a *gas1*Δ*::kanMX gas5*Δ*::kanMX* TELVR::*URA3*
LPY14430	W303-1b *gas1*Δ*::kanMX gas5*Δ*::kanMX*
LPY14431	W303-1b *gas1*Δ*::kanMX gas3*Δ*::kanMX* TELVR::*URA3*
LPY14432	W303-1b *gas1*Δ*::kanMX gas5*Δ*::kanMX*
LPY14433	W303-1a *gas1*Δ*::kanMX gas3*Δ*::kanMX* TELVR::*URA3*
LPY14434	W303-1a *gas1*Δ*::kanMX gas3*Δ*::kanMX gas5*Δ*::kanMX* TELVR::*URA3*
LPY14435	W303-1a *gas1*Δ*::kanMX gas3*Δ*::kanMX*
LPY14436	W303-1b *gas1*Δ*::kanMX gas3*Δ*::kanMX gas5*Δ*::kanMX* TELVR::*URA3*
LPY14440	W303-1a *gas3*Δ*::kanMX adh4::URA3-*$(C_{1\text{-}3}A)_n$

Table 3-3. Yeast strains used in Chapter 3. (continued)

LPY14444	W303-1a *gas5*Δ*::kanMX adh4::URA3-*$(C_{1\text{-}3}A)_n$
LPY14483	*MAT***a** *his3*Δ*1 leu2*Δ*0 lys2*Δ*0 ura3*Δ*0* + pLP1823
LPY14484	*MAT***a** *his3*Δ*1 leu2*Δ*0 lys2*Δ*0 ura3*Δ*0 rpd3*Δ*::kanMX* + pLP1823
LPY14485	*MAT***a** *his3*Δ*1 leu2*Δ*0 lys2*Δ*0 met15*Δ*0 ura3*Δ*0 gas1*Δ*::kanMX* + pLP1823
LPY14486	*MAT***a** *his3*Δ*1 leu2*Δ*0 lys2*Δ*0 met15*Δ*0 ura3*Δ*0 gas1*Δ*::kanMX rpd3*Δ*::kanMX* + pLP1823
LPY14487	*MAT***a** *his3*Δ*1 leu2*Δ*0 lys2*Δ*0 ura3*Δ*0 gas1*Δ*::kanMX rpd3*Δ*::kanMX* + pLP1823
LPY14488	*MAT*α *his3*Δ*1 leu2*Δ*0 met15*Δ*0 ura3*Δ*0 gas1*Δ*::kanMX rpd3*Δ*::kanMX* + pLP1823
LPY14490	*MAT***a** *his3*Δ*1 leu2*Δ*0 lys2*Δ*0 met15*Δ*0 ura3*Δ*0* + pLP1823
LPY14491	*MAT***a** *his3*Δ*1 leu2*Δ*0 met15*Δ*0 ura3*Δ*0 dot1*Δ*::kanMX* + pLP1823
LPY14492	*MAT***a** *his3*Δ*1 leu2*Δ*0 lys2*Δ*0 met15*Δ*0 ura3*Δ*0 gas1*Δ*::kanMX* + pLP1823
LPY14493	*MAT***a** *his3*Δ*1 leu2*Δ*0 ura3*Δ*0 dot1*Δ*::kanMX gas1*Δ*::kanMX* + pLP1823
LPY14494	*MAT***a** *his3*Δ*1 leu2*Δ*0 lys2*Δ*0 ura3*Δ*0 dot1*Δ*::kanMX gas1*Δ*::kanMX* + pLP1823
LPY14495	*MAT*α *his3*Δ*1 leu2*Δ*0 ura3*Δ*0 dot1*Δ*::kanMX gas1*Δ*::kanMX* + pLP1823
LPY14535	LPY10360 + pLP5
LPY14536	LPY10360 + pLP409
LPY14537	LPY5 + pLP1623
LPY14538	LPY5 + pLP1951
LPY14539	LPY5 + pLP2012
LPY14540	LPY5 + pLP2013
LPY14541	LPY10129 + pLP1623
LPY14542	LPY10129 + pLP1951
LPY14543	LPY10129 + pLP2012
LPY14544	LPY10129 + pLP2013
LPY14545	LPY4916 + pLP1623
LPY14549	LPY4916 + pLP2012
LPY14552	LPY10362 + pLP1623
LPY14553	LPY10362 + pLP1951
LPY14554	LPY10362 + pLP2001
LPY14555	LPY10362 + pLP2002
LPY14556	LPY10362 + pLP2012
LPY14557	LPY10362 + pLP2013

[a]Unless otherwise noted, strains were constructed during the course of this study or are part of the standard lab collection.

Table 3-4. Plasmids used in Chapter 3.[a]

Plasmid (alias)	Description	Source/Reference
pLP5 (pMA424)	GBD vector *HIS3* 2μ	Ma and Ptashne 1987
pLP17 (pJR910)	*SIR1 URA3* CEN	
pLP61 (pRS314)	vector *TRP1* CEN	Sikorski and Hieter 1989
pLP359 (pRS423)	vector *HIS3* 2μ	Christianson et al. 1992
pLP409 (pKL5)	GBD-*SIR1* 2μ	Chien et al. 1991
pLP493 (pMA424)	GBD vector *HIS3* 2μ	Ma and Ptashne 1987
pLP891	*SIR2 HIS3* 2μ	
pLP956	GBD vector *TRP1* 2μ	James et al. 1996
pLP1047	*SIR3 HIS3* 2μ	
pLP1073	GBD-core *SIR2 TRP1* 2μ	Garcia and Pillus 2002
pLP1074	GBD-*SIR2 TRP1* 2μ	Garcia and Pillus 2002
pLP1167	*MAT*α *TRP1* CEN	
pLP1185	*MAT***a** *TRP1* CEN	Lowell et al. 2003
pLP1609 (pGM300)	*SIR4 LEU2* 2μ	Murphy et al. 2003
pLP1623	vector *LEU2* 2μ	Christianson et al. 1992
pLP1823 (YEpBS6)	*GAS1 URA3* 2μ	Vai et al. 1991
pLP1951	*GAS1 LEU2* 2μ	
pLP2001	*gas1-E161Q LEU2* 2μ	
pLP2002	*gas1-E262Q LEU2* 2μ	
pLP2012	*GAS5 LEU2* 2μ	
pLP2013	*GAS5 LEU2* 2μ	
pLP2091	*GAS1 HIS3* 2μ	
pLP2192	*SIR1 HIS3* 2μ	
pLP2206	*SIR4 HIS3* 2μ	

[a]Unless otherwise noted plasmids are part of the standard lab collection or were constructed during the course of this study as described in Materials and Methods.

Table 3-5. Oligonucleotides used in Chapter 3.

Oligo	Name	Sequence (5' to 3')[a]
	T7	TAATACGACTCACTATAGGG
	T3	ATTAACCCTCACTAAAGGGA
oLP815	*GAS5*-F *Eag*I	CTTCGATCTGCGG**C**CGTTACTTCTAACG
oLP816	*GAS5*-R *Bam*HI	TGAGGAT**C**CAACTTCGATCTCATCAGCG
oLP833	*GAS5*_seq	CTGTGGATAACTCGCAAGATC

[a]Nucleotides in **bold** in the above sequences are mutagenic, compared to the wild-type sequence.

Chapter 4

Biochemical and cell biological investigation of Gas1 function in transcriptional silencing

INTRODUCTION

The SIR complex functions in transcriptional silencing at the telomeres and *HM* loci. The formation of silent chromatin results from the recruitment of the SIR complex by DNA-bound proteins such as Rap1 (Moretti et al. 1994). Sir2's deacetylase activity removes acetyl groups from lysine residues of histones, leading to hypoacetylated chromatin that promotes the spreading of the SIR complex (Chapter 1 and reviewed in Rusche et al. 2003). Cooperative interactions enable spreading, with Sir3 and Sir4 binding to the deacetylated tails of histone H3 and H4 (Hecht et al. 1995; Hecht et al. 1996; Carmen et al. 2002). Much investigation has concerned the formation of the SIR complex and interactions between SIR complex members. A Sir2-Sir4 complex with no or little Sir3 is present in cell extracts, however independent interactions between all SIR complex members are observed (Moazed et al. 1997).

In *in vitro* assays, Sir2 activity targets histone H3K9, K14, and K56 and histone H4K16 (Imai et al. 2000; Tanny and Moazed 2001; Xu et al. 2007). Analysis of mutants suggest that Sir2's *in vivo* activity is limited to H4K16 and H3K56 because only those sites have increased acetylation when assayed by immunoblot or chromatin immunoprecipitation (Suka et al. 2001, Xu, 2007 #41). However, all the acetylatable

lysine tails of histone H3 and H4 are fully deacetylated at silenced loci (Suka et al. 2001), which implicates other deacetylases in targeting the additional lysine residues that are not substrate of Sir2.

In Chapter 2, a telomeric silencing defect was reported in strains deleted for *GAS1* (Figure 2-1*D*, 2-1*E*, 2-3). The Gas1 glucanosyltransferase activity is directly implicated in silencing function because *gas1* enzymatically inactive mutants remain defective in silencing and an antibody directed against Gas1's substrate, β-1,3-glucan, immunoprecipitates Sir2 from protein extracts (Figure 2-11). Although telomeric silencing was disrupted, the SIR complex components Sir2 and Sir3 were bound to the telomere and *in vivo* Sir2 targets were deacetylated in *gas1*Δ mutants (Figure 2-6, 2-7*A*).

In the analysis presented here, the SIR complex was further investigated in *gas1*Δ mutants. Sir4 was telomere-associated and interacted with Sir2 in *gas1*Δ, demonstrating the wild-type configuration of the SIR complex in mutant strains despite the observed telomeric silencing defect. In Gas1 chromatin immunoprecipitation analysis, no Gas1 was found associated with telomeres. Although Gas1 does not appear stably bound to DNA, this does not eliminate the hypothesis of Gas1 directly promotes transcriptional silencing. Additional analysis showed a higher molecular weight form of Sir3 predominates in *gas1*Δ strains. Although the exact modification of Sir3 has not been deduced, this higher molecular weight Sir3 may be hyperphosphorylated. Sir3 that is hyperphosphorylated may be partially responsible for the reduced telomeric silencing observed in *gas1*Δ mutants. In analysis of the Yku70/Yku80 proteins that are implicated in telomeric silencing

function, altered localization was seen that may partially account for the *gas1*Δ telomeric silencing defect.

In additional analysis of the potential β-1,3-glucan modification of Sir2, or Sir2-interacting factors, first proposed in Chapter 2 (Figure 2-11*B*), no changes to Sir2 were observed upon incubation with zymolyase, an enzyme which hydrolyzes the glycosidic bonds of the β-1,3-glucan polymer. Additionally, no enhancement of Sir2 enzymatic activity was seen in *in vitro* deacetylase assays in the presence of Gas1 and its substrate, β-1,3-glucan. Further protein interaction tests demonstrate that the Sir2-Gas1 interaction may not be stable *in vivo* since it was not observed in co-immunoprecipitation analysis. This supports the model that Gas1 modifies Sir2, or a Sir2-associated factor, through a structurally transient interaction.

RESULTS

Further investigation of silent chromatin and silent chromatin factors in *gas1*Δ mutants. In Chapter 2, Sir2 and Sir3 were found to bind to the telomere in *gas1*Δ mutants (Figure 2-6*B*, 2-7*A*). The SIR complex, which is critical for silent chromatin formation, consists of the histone deacetylase Sir2 and the structural components Sir3 and Sir4. To determine whether the third SIR complex component was bound at the telomere in *gas1*Δ mutants, Sir4 chromatin immunoprecipitation (ChIP) was done. As seen for Sir2 and Sir3, Sir4 was enriched at the telomere in *gas1*Δ mutants, with slightly elevated Sir4 binding compared to wild-type (Figure 4-1). Sir4 transcript levels were unaltered in *gas1*Δ microarray analysis (Lagorce et al.

2003). Since there is no evidence for enhanced steady state levels of Sir4 in *gas1*Δ mutants, the source of this enrichment is not clear at the present time. Because no *HM* silencing defect is seen in *gas1*Δ mutants (Figure 2-1*A*, 2-1*B*), Sir4 is unlikely to have delocalized from the *HM* loci.

To determine whether Gas1 itself is a component of silent chromatin, Gas1 chromatin immunoprecipitations were carried out utilizing anti-Gas1. These experiments were also done in samples pre-cleared with Protein A Sepharose to reduce background. The Gas1 chromatin immunoprecipitation did not show enrichment of Gas1 at the telomere compared to the *gas1*Δ negative control (Figure 4-2). However, no positive control exists for this experiment since genome-wide ChIP-chip experiments have not been performed. Other experiments to establish if Gas1 is chromatin-bound could be explored in the future.

The SIR complex members were bound to the telomere in *gas1*Δ strains, but the chromatin immunoprecipitation experiments do not assess the stability of SIR complex interactions. As one test of this possibility, Sir4 immunoprecipitations were performed to test whether Sir2 co-immunoprecipitation is dependent on Gas1. As expected from the chromatin immunoprecipitation results, Sir2 and Sir4 co-immunoprecipitated in the *gas1*Δ strain (Figure 4-3). Thus, the SIR complex interaction between Sir2 and Sir4 was not disrupted in the *gas1*Δ mutant.

It has previously been shown that phosphorylation of the SIR complex component Sir3 strengthens telomeric silencing (Stone and Pillus 1996). Sir3 phosphorylation has also been associated with reduced lifespan (Ray et al. 2003). Furthermore, hyperphosphorylation of Sir3 leads to a reduction in subtelomeric

Figure 4-1. Sir4 binds to the telomere in *gas1*Δ mutants. Sir4 chromatin immunoprecipitation was carried out in wild-type (WT) (LPY5), *sir4*Δ (LPY9), *sir2*Δ (LPY11), and *gas1*Δ (LPY10129) strains using anti-Sir4 (2913/8) (Palladino et al. 1993). Immunoprecipitated DNA was analyzed by quantitative PCR using primers specific to 0.2 kb and 1 kb from the end of telomere VI-R. IP/input values at the telomere were normalized to the IP/input at the non-specific locus *ACT1*. This figure represents data obtained from a single pilot ChIP experiment.

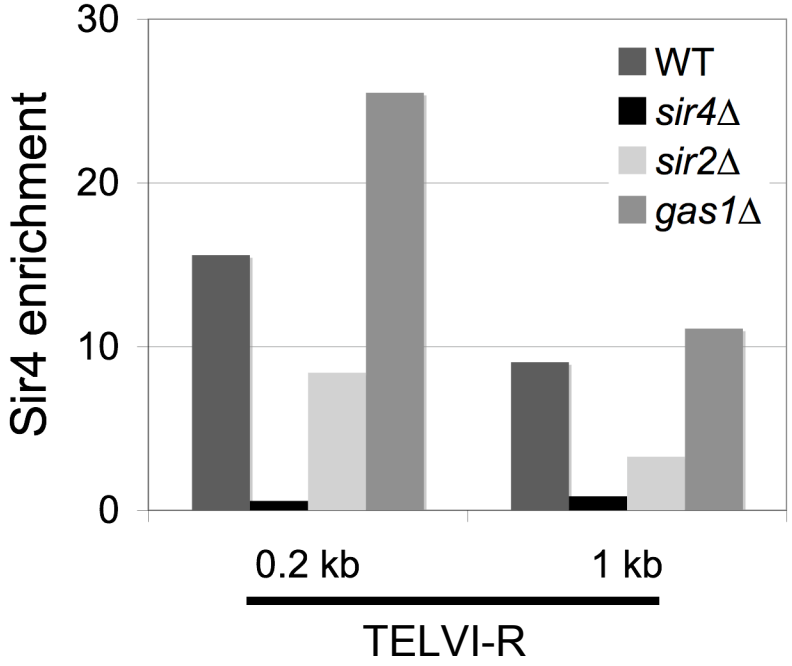
30
20
10
0
Sir4 enrichment
WT
sir4Δ
sir2Δ
gas1Δ
0.2 kb
1 kb
TELVI-R

Figure 4-2. Gas1 does not bind to the telomere. Gas1 chromatin immunoprecipitation was done with WT (LPY5) and *gas1*Δ (LPY10129) strains using anti-Gas1 (Doering and Schekman 1997) (gift from R. Schekman). Indicated samples were pre-cleared for one hour with protein A Sepharose beads prior to immunoprecipitation with anti-Gas1. Immunoprecipitated DNA was analyzed by quantitative PCR using primers specific to 0.2 kb and 1 kb from the end of telomere VI-R. IP/input values at the telomere were normalized to the IP/input at the non-specific locus *ACT1*. This figure is a representative experiment from several independent ChIP experiments, all of which showed no Gas1 enrichment at the telomere.

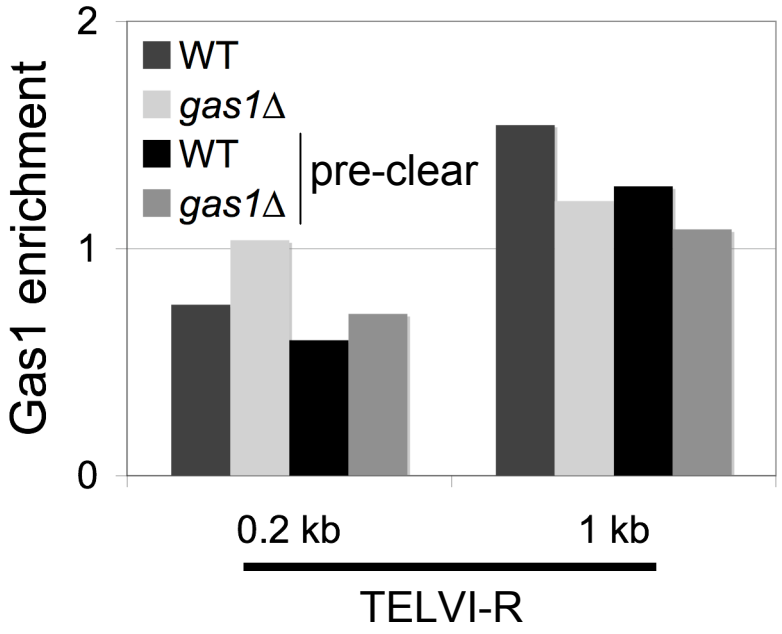
2
1
0
Gas1 enrichment
WT
gas1Δ
WT
gas1Δ
pre-clear
0.2 kb
1 kb
TELVI-R

Figure 4-3. Sir2 and Sir4 co-immunoprecipitate when Sir4 is immunoprecipitated in a *gas1*Δ strain. Sir4 was immunoprecipitated in WT (LPY5), *sir4*Δ (LPY9), *sir3*Δ (LPY10), *sir2*Δ (LPY11), and *gas1*Δ (LPY10129) strains using anti-Sir4 (2913/8) (Palladino et al. 1993). Input and immunoprecipitated (IP) samples were analyzed by immunoblot using anti-Sir2 (2916/8) (Smith et al. 1998). The IgG heavy chain runs near Sir2 and is indicated. Unexpectedly, a faint Sir2 band appeared in the immunoprecipitated material from the *sir4*Δ strain showing that a small amount of Sir2 was non-specifically precipitated by anti-Sir4. Note that Sir2 in input samples is not well-detected on this immunoblot but is readily detected in the IPs.

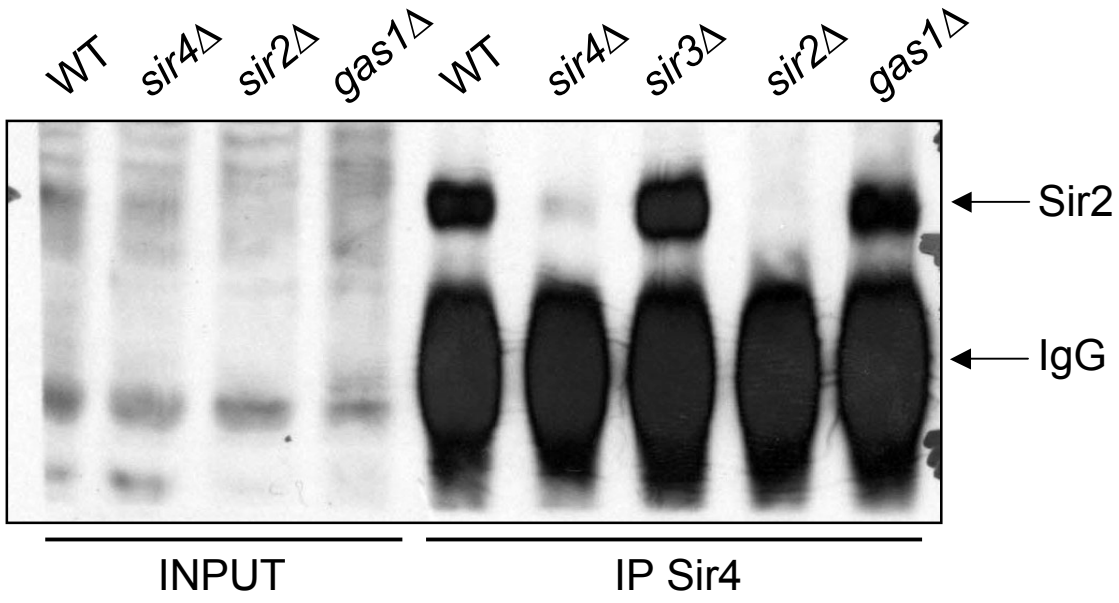
WT
sir4Δ
sir2Δ
gas1Δ
WT
sir4Δ
sir3Δ
sir2Δ
gas1Δ
Sir2
IgG
INPUT
IP Sir4

silencing (Ai et al. 2002). Sir3 levels were previously shown to be unaltered in *gas1*Δ mutants (Figure 2-5*B*). To determine whether Sir3 was modified in *gas1*Δ, protein extracts were examined under conditions to optimize separation of Sir3 species of different mobilities. A higher molecular weight form of Sir3 was present in *gas1*Δ mutants, compared to Sir3 in wild-type cells, suggesting Sir3 was hyperphosphorylated or was somehow differently modified in the mutant (Figure 4-4). If this represents hyperphosphorylated Sir3, this is correlated with the reduced telomeric silencing observed in *gas1*Δ mutants (Figure 2-1*D*, 2-1*E*, 2-3). Whether hyperphosphorylated Sir3 predominates in *gas1*Δ is an area for further investigation.

The Yku70 and Yku80 proteins make up the Ku heterodimer that function in telomeric silencing (Boulton and Jackson 1998; Laroche et al. 1998; Nugent et al. 1998) and in genomic stability, including roles in DNA repair and telomere length maintenance (Milne et al. 1996; Boulton and Jackson 1996a; Boulton and Jackson 1996b). The Ku heterodimer is released from telomeric chromatin in response to DNA strand breaks (Martin et al. 1999). Because the Yku proteins are a critical component of telomeric chromatin, their localization was analyzed in *gas1*Δ mutants. Analysis of GFP-Yku70 showed fainter staining and less localization to telomeric foci in some *gas1*Δ mutant cells (Figure 4-5). GFP-Yku80 analysis was similar and the protein appeared to be dispersed in some cells (Figure 4-6). These observed changes in the Yku proteins are subtle and may represent both quantitative and qualitative differences.

Purified Gas1 did not alter Sir2 activity *in vitro*. Although no change in Sir2 deacetylase histone substrates at telomeres is seen *in vivo* in *gas1*Δ mutants (Figure 2-

Figure 4-4. Sir3 may be hyperphosphorylated in *gas1*Δ mutants. WT (LPY5) and *gas1*Δ (LPY10129) strains were transformed with a 2μ vector (pLP26) and *SIR3* (pLP27). As a negative control, a *sir3*Δ strain was transformed with pLP26. Whole cell extracts were separated on a 10 x 12cm 8% polyacrylamide gel, loading 1 O.D. cell equivalent and ½ O.D. cell equivalent. Protein immunoblotting was done using anti-Sir3 (7796) (Ray et al. 2003). Sir3-specific bands indicate that a higher molecular weight form of Sir3 predominates in the *gas1*Δ mutant.

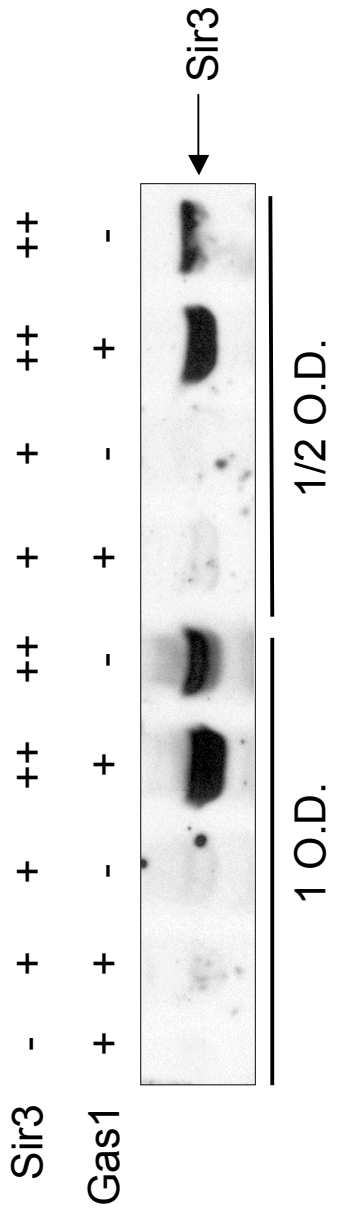
Sir3
Gas1
- + + + ++ ++ + + ++ ++
+ + - + + - + + - +
Sir3
1 O.D.
1/2 O.D.

Figure 4-5. GFP-Yku70 localization may be more diffuse in *gas1*Δ mutants. WT (LPY13993) and *gas1*Δ (LPY13995) diploids with GFP-Yku70 (green) were visualized by live cell confocol microscopy. Cells in log phase growth were stained with DAPI (blue) for one hour prior to visualization. Images shown are representative deconvolved images showing overlap of GFP-Yku70/DAPI (green/blue), GFP-YKu70 alone (green), and DAPI alone (blue). Note the non-optimal staining of live cells by DAPI, mostly mitochondrial DNA staining is observed.

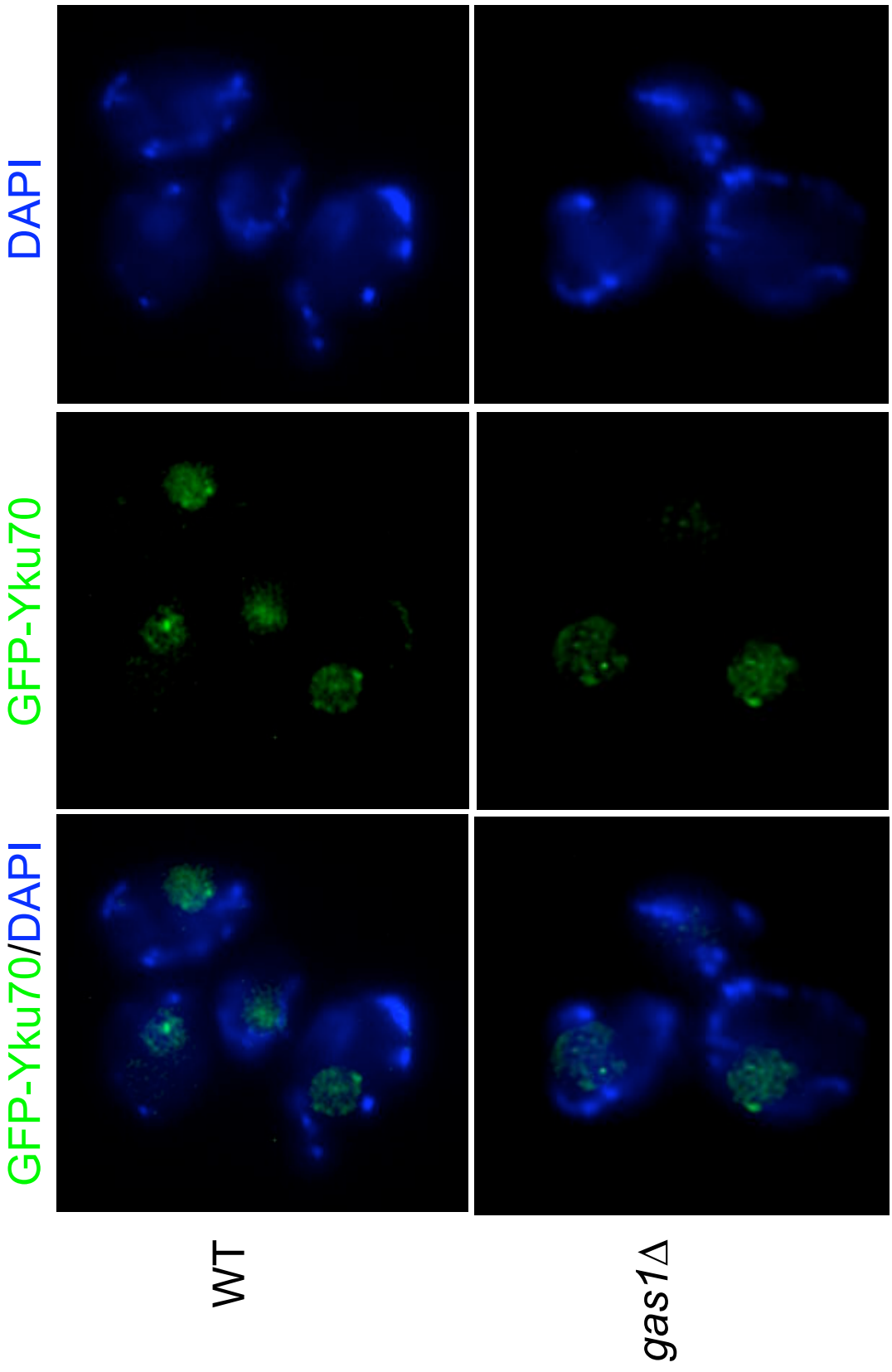
DAPI
GFP-Yku70
GFP-Yku70/DAPI
WT
gas1Δ

Figure 4-6. GFP-Yku80 localization may be more diffuse in *gas1*Δ mutants. WT (LPY13997) and *gas1*Δ (LPY13999) diploids with GFP-Yku80 (green) were visualized by live cell confocol microscopy. Cells in log phase growth were stained with DAPI (blue) for one hour prior to visualization. Images shown are representative deconvolved images showing overlap of GFP-Yku80/DAPI (green/blue), GFP-YKu80 alone (green), and DAPI alone (blue). Note the non-optimal staining of live cells by DAPI, mostly mitochondrial DNA staining is observed.

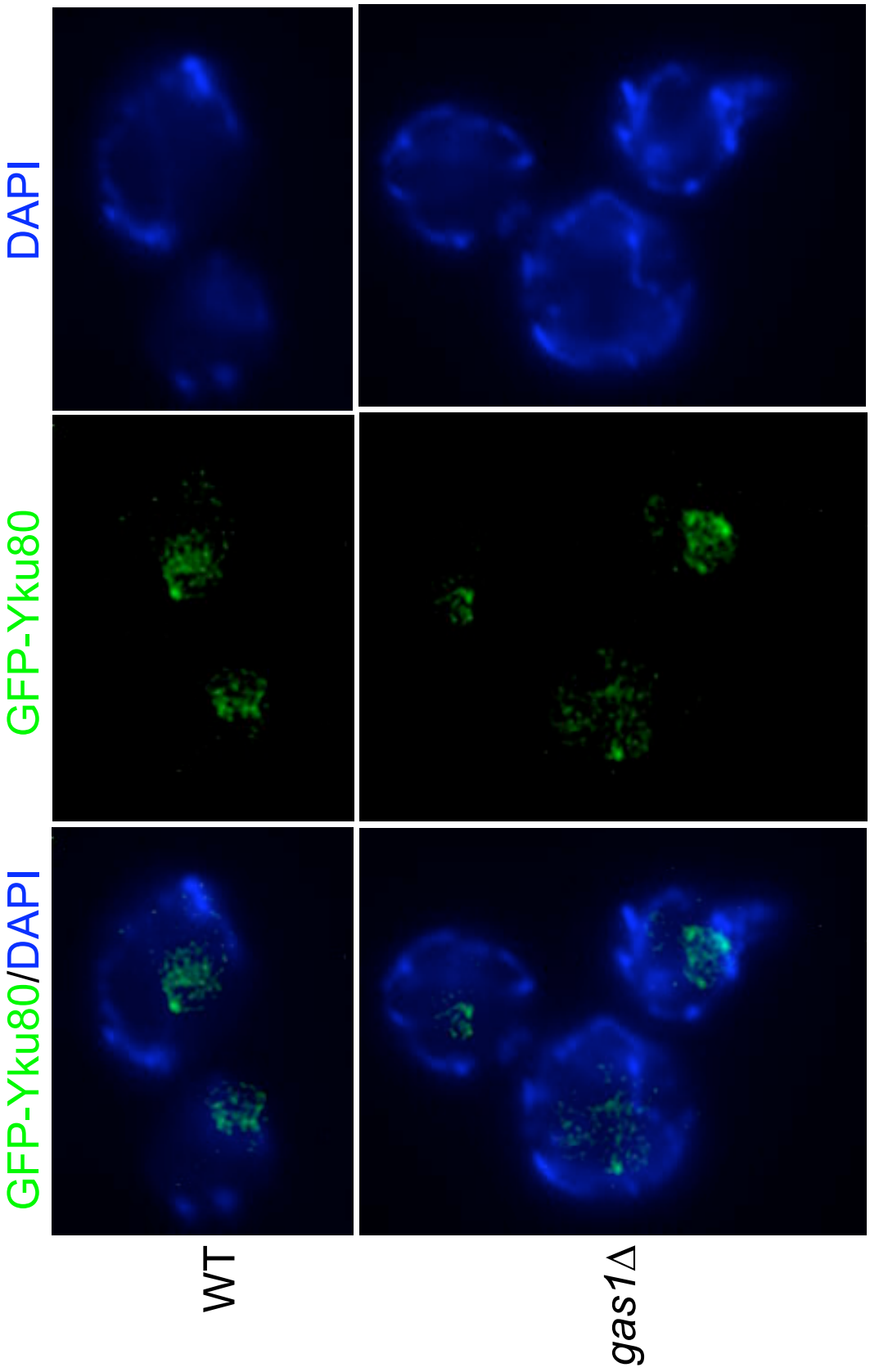
DAPI
GFP-Yku80
GFP-Yku80/DAPI
WT
gas1Δ

6*C*, 2-6*D*), it was hypothesized that Gas1 may influence Sir2's deacetylase activity. The Sir2 *in vitro* assay measures the hydrolysis of NAD^+ to nicotinamide, a byproduct of Sir2 histone deacetylation in the assay. Activity assays have been published for both Sir2 (Landry et al. 2000a) and Gas1 (Carotti et al. 2004), and these vary in multiple components, including pH. In *in vitro* experiments with purified Gas1 added to the Sir2 deacetylase assays, no alteration of Sir2 activity was observed (Figure 2-7*C*).

Additional tests were pursued to determine if Gas1 activity altered Sir2's histone deacetylation under other conditions. It was necessary to closely imitate the conditions where Gas1 glucanosyltranferase activity was most active. This was done by comparison of Sir2 deacetylase activity in Sir2 buffer conditions (pH 9) to its activity under Gas1 buffer conditions (pH 5.5). Sir2 remained active in the more acidic Gas1 buffer conditions, however the activity was reduced by half compared to its activity in the standard deacetylase assay (Figure 4-7*A*). Since Sir2 activity was seen in the Gas1 buffer conditions, the following experiments were also performed with the more acidic buffer to best mimic the environment for maximum Gas1 activity.

In vitro assays for Gas1 activity include laminarin as a substrate (Hartland et al. 1996; Carotti et al. 2004). Laminarin, a polymer of β-1,3-glucan, was added to the Sir2 deacetylase assays to ask whether the addition of Gas1's substrate affected Sir2 activity. With laminarin present in the reaction, Sir2 deacetylase activity was increased slightly with Gas1 present compared to Sir2 alone, however the same effect was observed with the catalytically inactive gas1-E161Q, E262Q protein (Figure 4-7*B*).

Figure 4-7. Sir2 deacetylase activity is not enhanced in the presence of Gas1 or laminarin in NAD^+ hydrolysis assays. *(A)* Sir2 activity decreases in Gas1 buffer conditions. Recombinant GST (pLP1302) and GST-Sir2 (pLP1275) were purified from bacteria and tested for *in vitro* NAD^+ hydrolysis by Sir2 under Sir2 buffer conditions (50 mM glycine, pH 9) and Gas1 buffer conditions (50 mM sodium acetate, pH 5.5). Control reactions with no protein addition were included. *(B)* Sir2 activity increases slightly with Gas1 and laminarin present in the reaction. Recombinant GST, GST-Sir2, GST-Gas1 (pLP2087), GST-gas1-E161Q, E262Q (pLP2119) were purified from bacteria and tested for *in vitro* Sir2 NAD^+ hydrolysis activity in Gas1 buffer conditions in the presence of laminarin, a polymer of β-1,3-glucan added to the reaction to serve as substrate for Gas1 activity. *(C)* Overall Sir2 activity is greater in reactions without laminarin added. The same purified proteins as in *(B)* were isolated and tested for *in vitro* Sir2 activity in Gas1 buffer with and without laminarin added to the reactions. Additional control reactions of only Gas1 addition to the reaction were also performed.

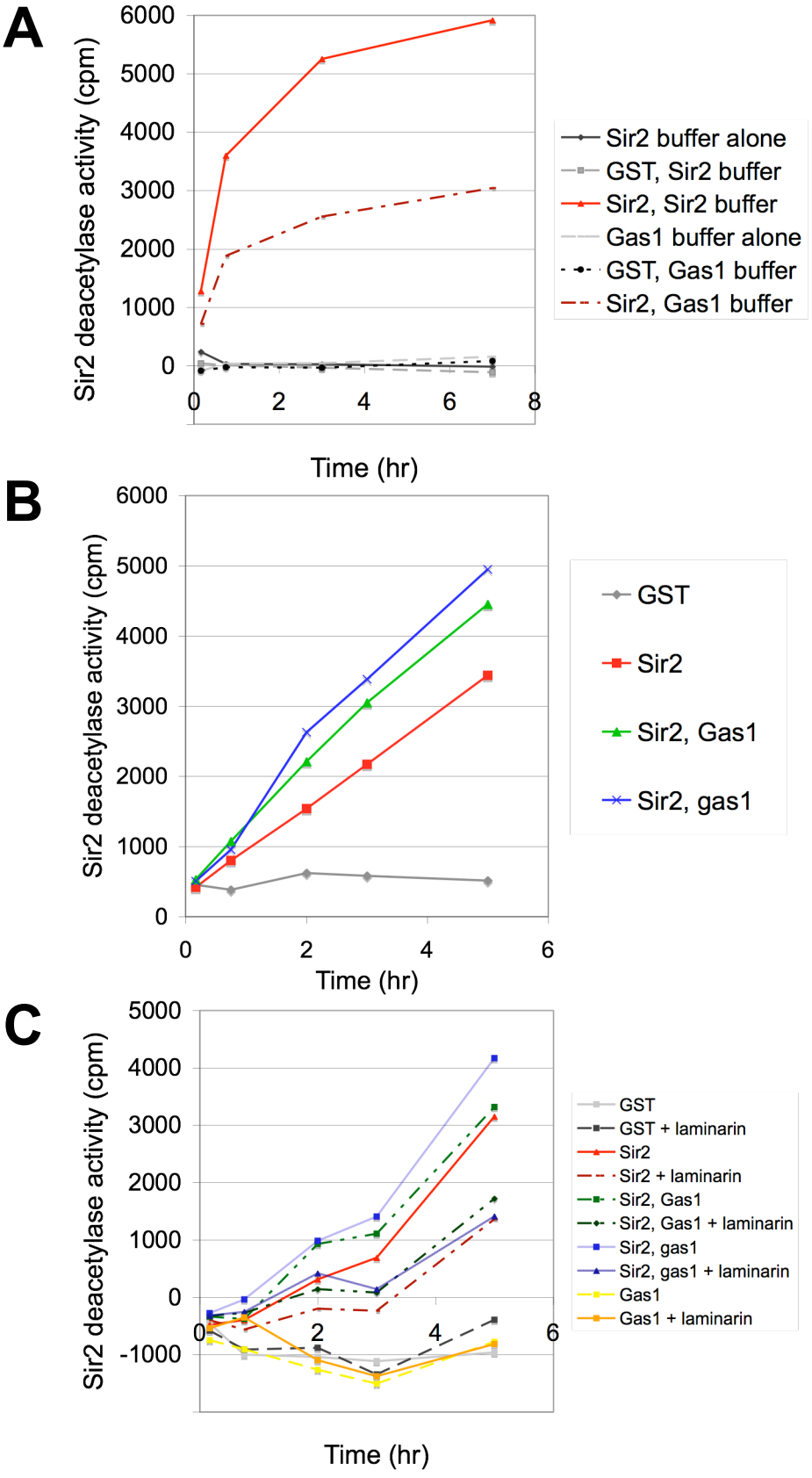
A
Sir2 deacetylase activity (cpm)
6000
5000
4000
3000
2000
1000
0
0
2
4
6
8
Time (hr)
Sir2 buffer alone
GST, Sir2 buffer
Sir2, Sir2 buffer
Gas1 buffer alone
GST, Gas1 buffer
Sir2, Gas1 buffer
B
Sir2 deacetylase activity (cpm)
6000
5000
4000
3000
2000
1000
0
0
2
4
6
Time (hr)
GST
Sir2
Sir2, Gas1
Sir2, gas1
C
Sir2 deacetylase activity (cpm)
5000
4000
3000
2000
1000
0
-1000
0
2
4
6
Time (hr)
GST
GST + laminarin
Sir2
Sir2 + laminarin
Sir2, Gas1
Sir2, Gas1 + laminarin
Sir2, gas1
Sir2, gas1 + laminarin
Gas1
Gas1 + laminarin

To directly compare Sir2 activity with laminarin, several combinations of recombinant proteins with and without laminarin present were analyzed. Overall, addition of laminarin lowered Sir2 deacetylase activity compared to reactions with no laminarin added (Figure 4-7*C*). The slight enhancement of Sir2 activity with Gas1 present was observed with and without laminarin present and was not dependent on Gas1 enzymatic activity since the same effect was seen with gas1-E161Q, E262Q (Figure 4-7*C*).

β-1-3 glucanase treatments of protein extracts for analysis of the potentially β-glucan-modified Sir2. In Chapter 2, Sir2 was shown to be immunoprecipitated by β-1,3-glucan (Figure 2-11*B*). Therefore, β-1,3-glucan was proposed to be a modification of Sir2 or Sir2-interacting factors. To pursue this potential modification, zymolyase digestion of protein extracts from various strains was performed, followed by protein immunoblotting for Sir2. Zymolyase is a mixture of β-1,3-glucanase, mannase, and proteases, purified from *Arthrobacter luteus*, and hydrolyzes β-1,3-glucan, breaking the β-1,3 linkages in the linear glucose polymer (Kitamura and Yamamoto 1972). If Sir2 was β-1,3-glucan modified, treatment of samples with zymolyase may result in differences in apparent molecular weight of Sir2. Protease inhibitors were added to these experiments in an attempt to inactivate proteases known to be present in commercially available zymolyase. Control experiments that contained only the SCE buffer in which zymolyase is dissolved were performed at the same time. Zymolyase digestion resulted in loss of the Sir2-specific band in all strains and the appearance of a band specific to the *gas1*Δ and *gas1*Δ *gas3*Δ *gas5*Δ samples that was absent from the wild-type sample (Figure 4-8, band identified

by *). The identity of this band was unclear, but it seemed possible that in wild-type cells all of Sir2 was proteolyzed but some was protected in the *gas* mutants.

As controls for general proteolysis, phosphoglycerate kinase (Pgk1) and β-tubulin (Tub2) were also examined from the same samples. These showed some proteolysis but not complete loss of either control protein (Figure 4-9).

In an attempt to evaluate only β-1,3-glucanase and minimizing non-specific effects due to proteolysis, recombinant β-1,3-glucanase was purified from bacteria and added to protein extracts. The activity of purified recombinant β-1,3-glucanase was verified. No effect on Sir2-specific bands was observed (Figure 4-10).

To determine whether the band that was present in *gas1*Δ and *gas1*Δ *gas3*Δ *gas5*Δ treated with zymolyase (Figure 4-8, band identified by *) was Sir2-specific, the experiment was repeated with protein extracts from a *gas1*Δ *sir2*Δ strain. The band that appears in the Sir2 immunoblot was *gas1*Δ-specific, but not Sir2-specific, and was enriched in the zymolyase-treated protein extracts (Figure 4-11). Therefore, there is no evidence that Sir2 itself is specifically sensitive to digestion with β-1,3-glucanase. In future studies, further evaluation of Sir2 and its interacting factors should be completed utilizing similar enzyme treatments.

Unresolved tests of protein-protein interactions between Gas1 and the SIR complex members Sir2 and Sir3. In Chapter 2, the physical interaction between Gas1 and Sir2 is shown by both two-hybrid and GST-Sir2 affinity binding (Figure 2-9). To follow up on these results, co-immunoprecipitation studies were pursued. In a Sir2 immunoprecipitation, no Gas1 was recovered (Figure 4-12*A*). In a reciprocal test with anti-Gas1, no Sir2 was found in Gas1 immunoprecipitations (Figure 4-12*B*).

Figure 4-8. Zymolyase treatment of whole cell extracts leads to disappearance of Sir2 and appearance of a novel band in only *gas1*Δ and *gas1*Δ *gas3*Δ *gas5*Δ strains. Whole-cell extracts from WT (LPY5), *gas1*Δ (LPY10129), *gas1*Δ *gas3*Δ *gas5*Δ (LPY13543), and *sir2*Δ (LPY11) strains were incubated with zymolyase (+) or SCE (-) for 1 hour at room temperature. Immunoblotting of samples was performed with anti-Sir2 (2931/4) (Axelrod 1991). Leftmost sample is untreated whole-cell extract from the WT strain. The star (*) indicates a band specific to the *gas1*Δ and *gas1*Δ *gas3*Δ *gas5*Δ samples that is more prominent in the zymolyase-treated samples.

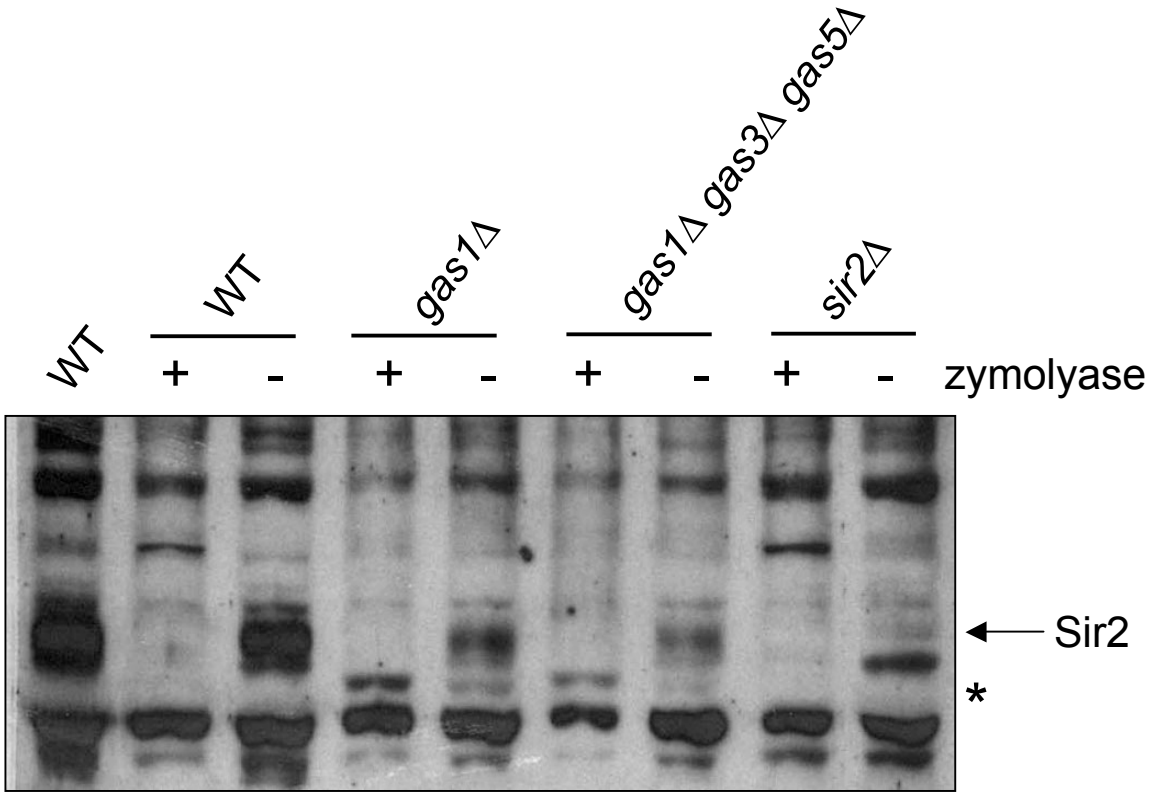
WT
WT
gas1Δ
gas1Δ gas3Δ gas5Δ
sir2Δ
+ - + - + - + -
zymolyase
Sir2
*

Figure 4-9. Zymolyase treatment leads to some degradation of β-tubulin and phosphoglycerate kinase but not complete loss of either protein. Whole-cell extracts from WT (LPY5), *gas1*Δ (LPY10129), *gas1*Δ *gas3*Δ *gas5*Δ (LPY13543), and *sir2*Δ (LPY11) strains were incubated with zymolyase (+) or SCE (-) for 1 hour at room temperature. Immunoblotting of samples was performed with anti-β-tubulin (Tub2) (Bond et al. 1986) and anti-phosphoglycerate kinase (Pgk1) (Baum et al. 1978) (gift from J. Thorner). Leftmost sample is untreated whole-cell extract from the WT strain.

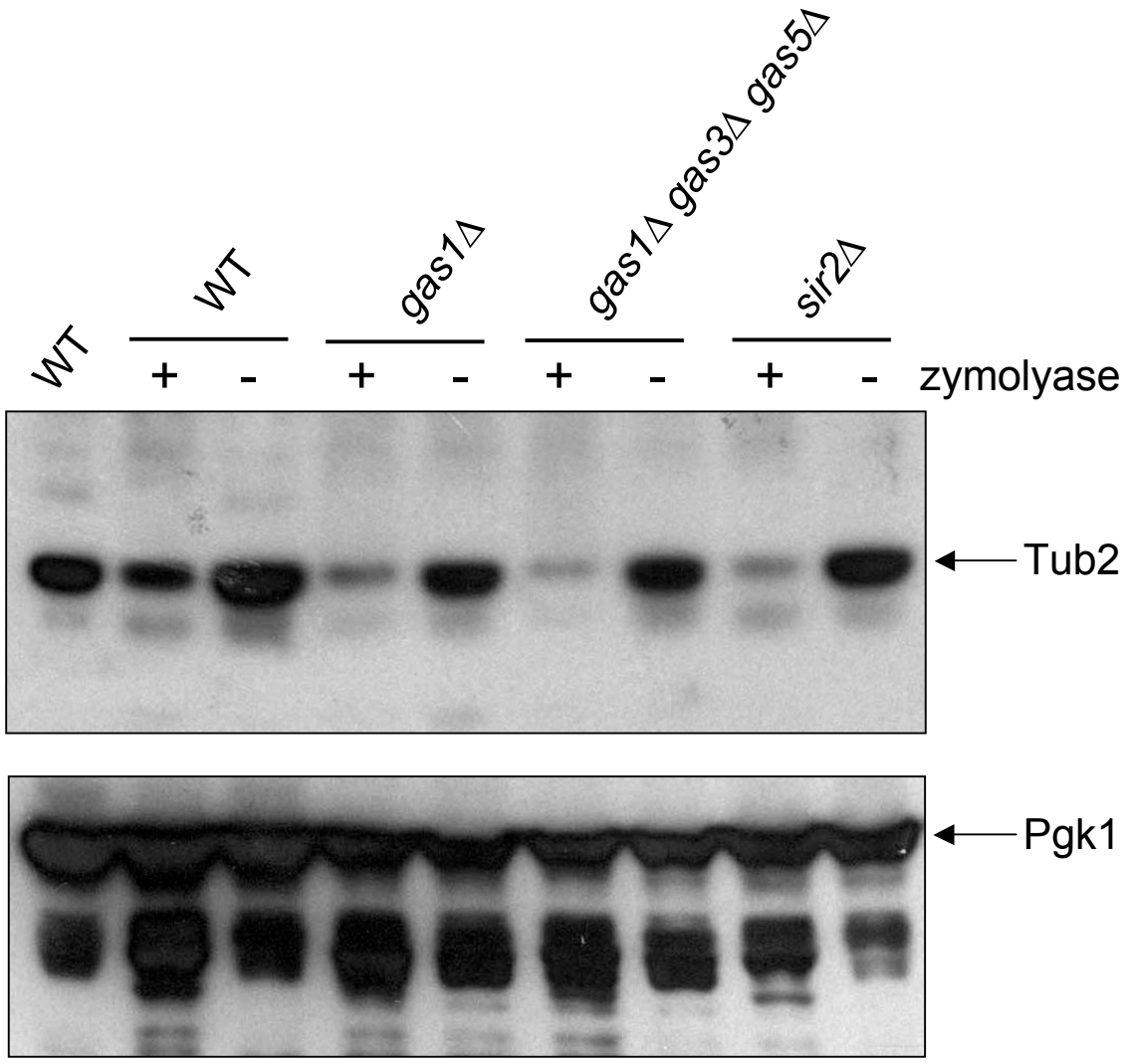
WT
WT
gas1Δ
gas1Δ gas3Δ gas5Δ
sir2Δ
+ - + - + - + -
zymolyase
Tub2
Pgk1

Figure 4-10. Purified glucanase treatment does not degrade or alter Sir2. Whole-cell extracts from WT (LPY5), *gas1*Δ (LPY10129), and *sir2*Δ (LPY11) strains were incubated with SCE, zymolyase, or β-1,3-glucanase for 15 minutes at room temperature. Immunoblotting of samples was performed with anti-Sir2 (2931/4) (Axelrod 1991).

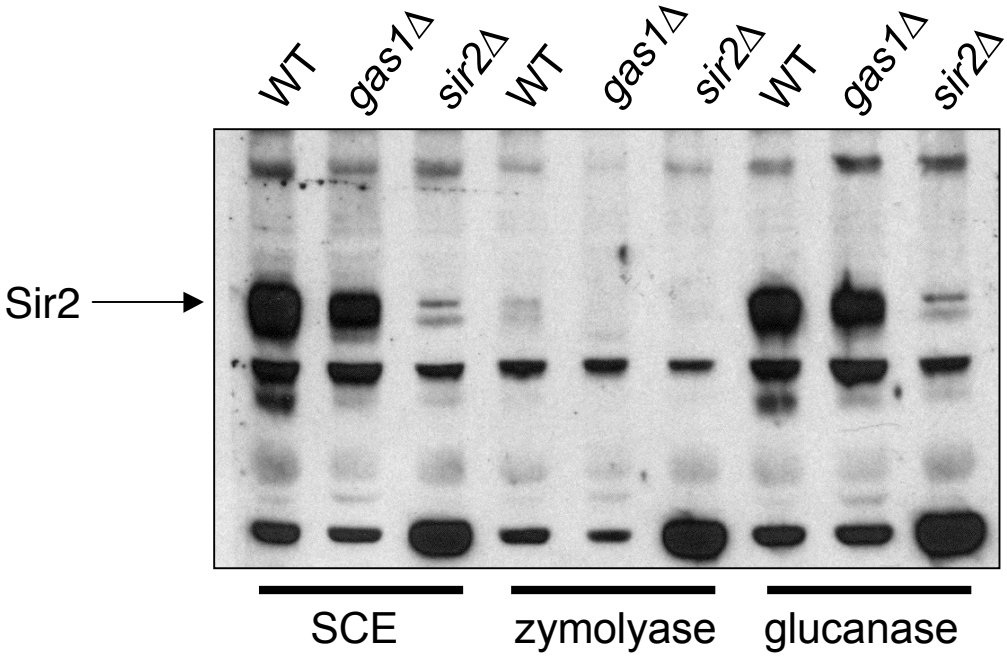
WT
gas1Δ
sir2Δ
WT
gas1Δ
sir2Δ
WT
gas1Δ
sir2Δ
Sir2
SCE
zymolyase
glucanase

Figure 4-11. The band that appears in zymolyase-treated whole-cell extracts from *gas1*Δ strains on the Sir2 immunoblot is not Sir2-specific. Whole-cell extracts from WT (LPY5), *gas1*Δ (LPY10129), *gas1*Δ *sir2*Δ (LPY10663), and *sir2*Δ (LPY11) strains were incubated with SCE or zymolyase for 15 minutes at room temperature. Immunoblotting of samples was performed with anti-Sir2 (2931/4) (Axelrod 1991). The star (*) indicates a Sir2 non-specific band that is specific to the *gas1*Δ and *gas1*Δ *sir2*Δ samples that is more prominent in the zymolyase-treated samples and therefore is likely to represent proteolysis of a distinct protein.

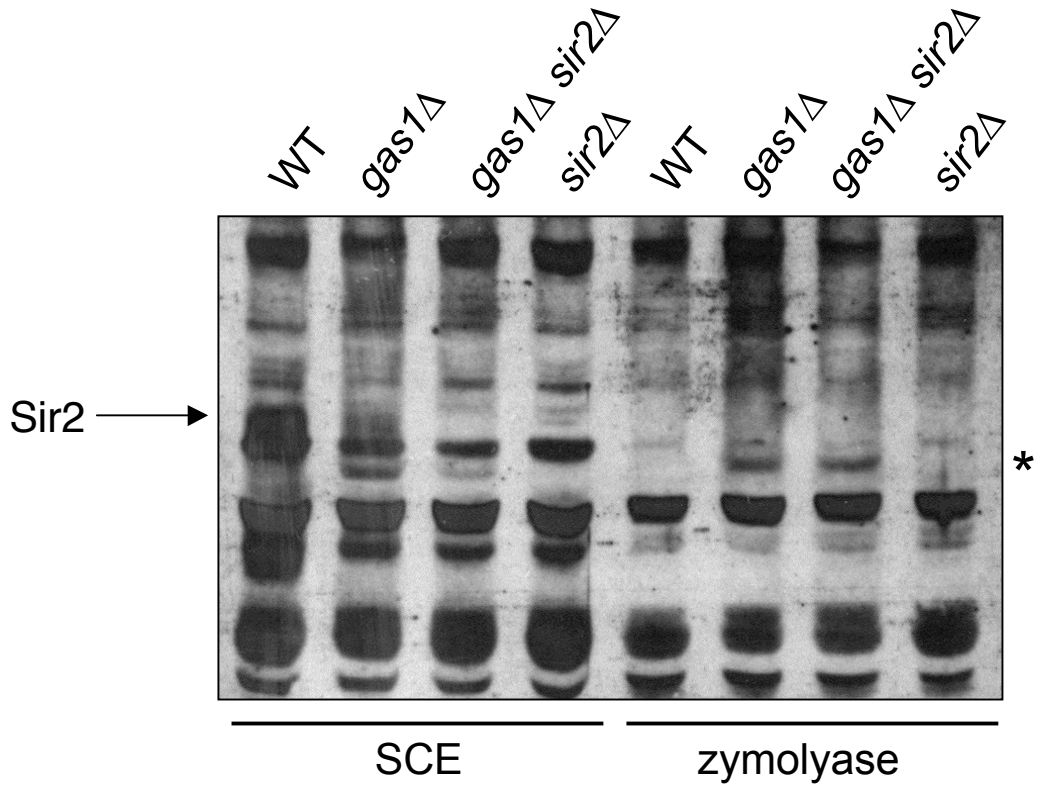
WT
gas1Δ
gas1Δ sir2Δ
sir2Δ
WT
gas1Δ
gas1Δ sir2Δ
sir2Δ
Sir2
*
SCE
zymolyase

Figure 4-12. Sir2 and Gas1 do not co-immunoprecipiate. *(A)* Gas1 is not recovered when Sir2 is immunoprecipitated. Sir2 immunoprecipitations were carried out in whole-cell extracts from WT (LPY5), *gas1*Δ (LPY10129), *sir2*Δ (LPY11), and *sir3*Δ (LPY10) strains with anti-Sir2 (2916/8). Input (IN), immunoprecipitated (IP), and unbound flow-through (FT) samples were analyzed by Gas1 immunoblotting (anti-Gas1 from C. Sütterlin) and Sir2 immunoblotting using the same anti-Sir2 used to IP Sir2. *(B)* Sir2 is not recovered when Gas1 is immunoprecipitated. Gas1 IPs were carried out in whole-cell extracts from WT (LPY6497), *hst2*Δ (LPY6623), *sir2*Δ (LPY6637), and *gas1*Δ (LPY6911) strains with anti-Gas1. Input and IP samples were analyzed by Gas1 immunoblotting to evaluate efficiency of Gas1 IP and by Sir2 immunoblotting.

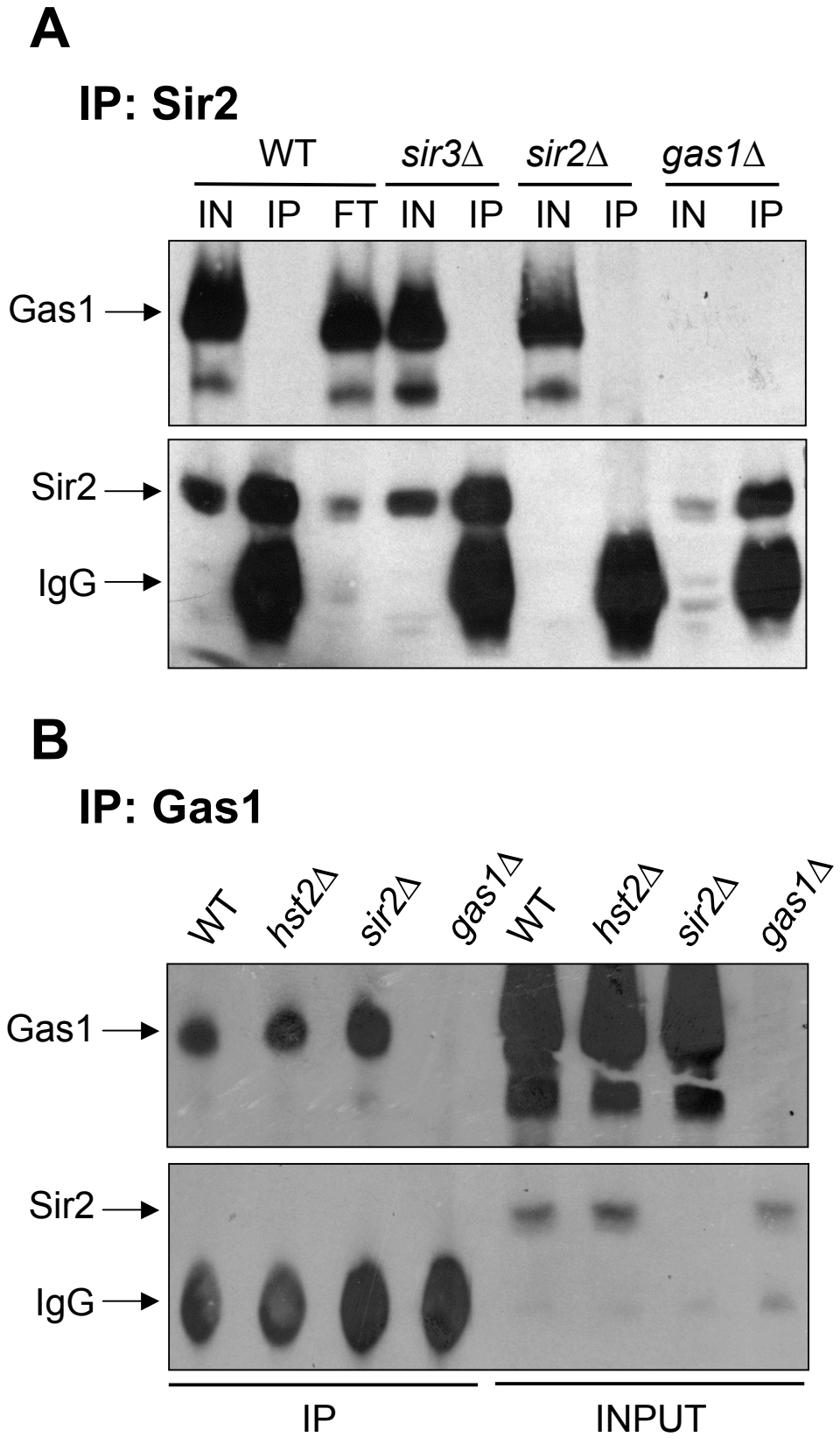
A
IP: Sir2
WT
sir3Δ
sir2Δ
gas1Δ
IN IP FT IN IP IN IP IN IP
Gas1
Sir2
IgG
B
IP: Gas1
WT
hst2Δ
sir2Δ
gas1Δ
WT
hst2Δ
sir2Δ
gas1Δ
Gas1
Sir2
IgG
IP
INPUT

Although these negative co-immunoprecipitation results do not provide independent support for the Sir2-Gas1 physical interaction they point to the likelihood that the interaction between Sir2 and Gas1 may be transient compared to other stable interactions, such as the interactions between dedicated SIR complex members.

Since Gas1 and Sir2 physically associate in GST-Sir2 affinity binding assays (Figure 2-9*A*, 2-10*A*), the reciprocal test was done with GST-Gas1. Initially, GST-Gas1 was observed to cleanly precipitate Sir2 in wild-type cells with endogenous Gas1 present (Figure 4-13*A*). Although this result repeated, follow up experiments were complicated because Sir2 was found to associate with GST alone, despite pre-incubation with BSA and higher salt washes to remove background (Figure 4-13*B*). Because of these conflicting results, the Gas1-Sir2 interaction in GST-Gas1 affinity binding assays cannot be definitively demonstrated.

Gas1 also was reported to associate with the SIR complex member Sir3 in genome-wide analysis of protein-protein interactions by mass spectrometry (Ho et al. 2002). To independently evaluate this finding, Sir3 immunoprecipitations were performed to test association with Gas1. When Sir3 was overexpressed and immunoprecipitated, Gas1 co-precipitated in the sample (Figure 4-14*A*) but not under conditions of endogenous *SIR3* expression. This experiment was repeated. In this case, the Sir3-Gas1 interaction was not clear since higher background was observed in the immunoprecipitated samples and the *gas1*Δ sample was not clean as it had been in the previous experiment (Figure 4-14*B*). It remains unresolved but promising that Gas1 and Sir3 co-immunoprecipitate. In affinity binding assays with recombinant GST-Gas1, Sir3 was not recovered, but faint Sir3 immunoreactive fragments that were

Figure 4-13. Gas1 and Sir2 may interact by GST affinity binding. *(A)* Sir2 is affinity bound to GST-Gas1. GST (pLP1302) and GST-Gas1 (pLP2087) are recombinant proteins purified from bacteria. GST fusion proteins were incubated for 1 hour with whole-cell extracts from WT (LPY5), *gas1*Δ (LPY10129), and *sir2*Δ (LPY11) strains. Input and affinity bound material was analyzed by immunoblotting with anti-Sir2 (2916/8). *(B)* Sir2 is affinity bound to GST alone. Experiment was done as in *(A)* except for the addition of pre-incubation with BSA and higher salt washes after incubation of purified GST proteins with yeast whole-cell protein extracts. Input and affinity bound material was analyzed by immunoblotting with anti-Sir2 (2916/8).

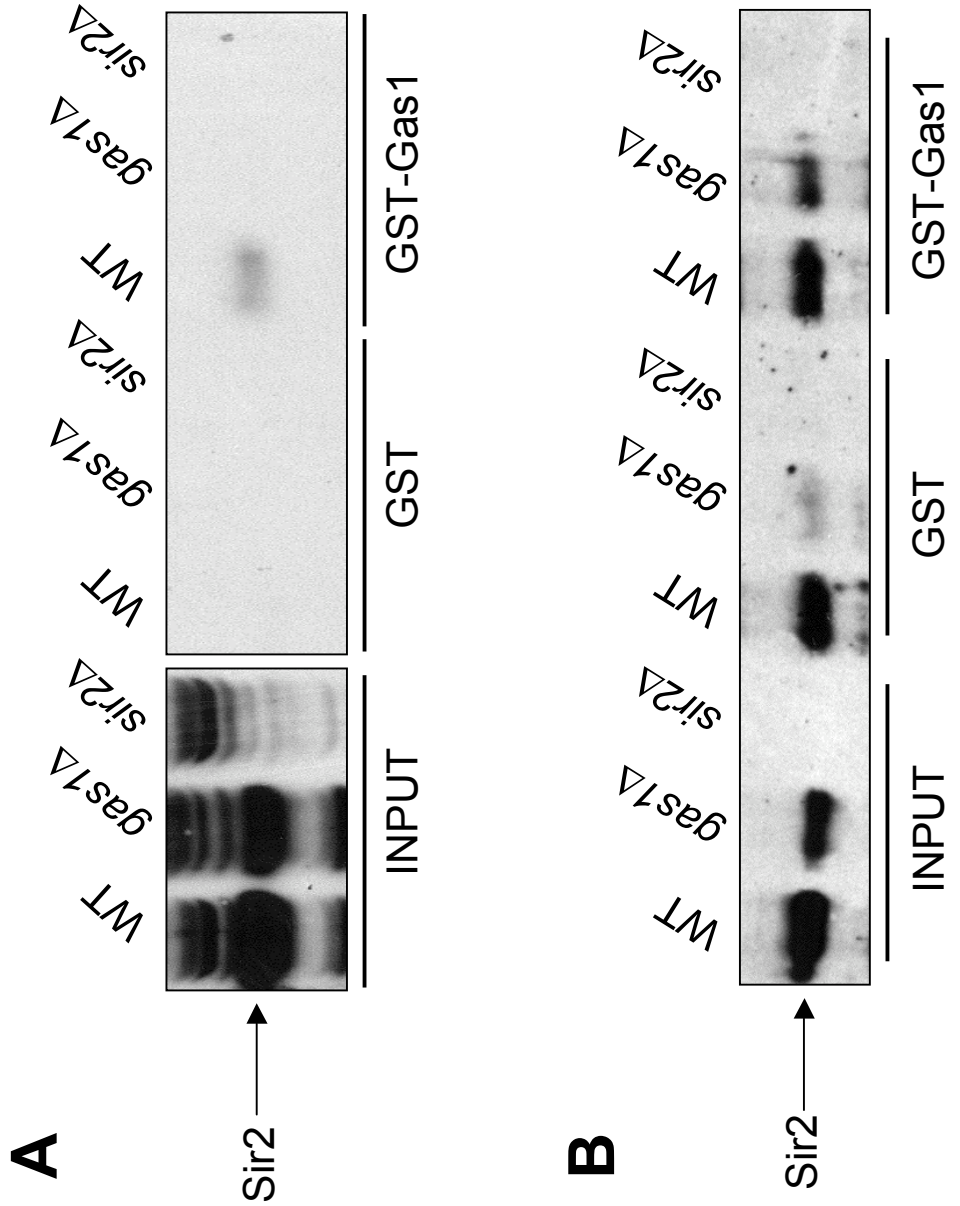
A
Sir2
INPUT
GST
GST-Gas1
WT
gas1Δ
sir2Δ
WT
gas1Δ
sir2Δ
WT
gas1Δ
sir2Δ
B
Sir2
INPUT
GST
GST-Gas1
WT
gas1Δ
sir2Δ
WT
gas1Δ
sir2Δ
WT
gas1Δ
sir2Δ

Figure 4-14. Sir3 and Gas1 may co-immunoprecipitate. *(A)* Gas1 is recovered when Sir3 is immunoprecipitated from cells overexpressing *SIR3*. Sir3 immunoprecipitations were carried out in whole-cell extracts from WT (LPY5), WT transformed with 2μ *SIR3* (LPY1857), *sir3*Δ (LPY10), and *gas1*Δ (LPY10129) strains with anti-Sir3 (2936/4) (Stone and Pillus 1996). Input (IN), immunoprecipitated (IP), and unbound flow-through (FT) samples were analyzed by Gas1 immunoblotting (anti-Gas1 from C. Sütterlin) and Sir3 immunoblotting using the same anti-Sir3 used to IP Sir3. *(B)* Gas1 and Sir3 may co-immunoprecipitate when *SIR3* is overexpressed. Experiment was done as in *(A)*, with the same strains.

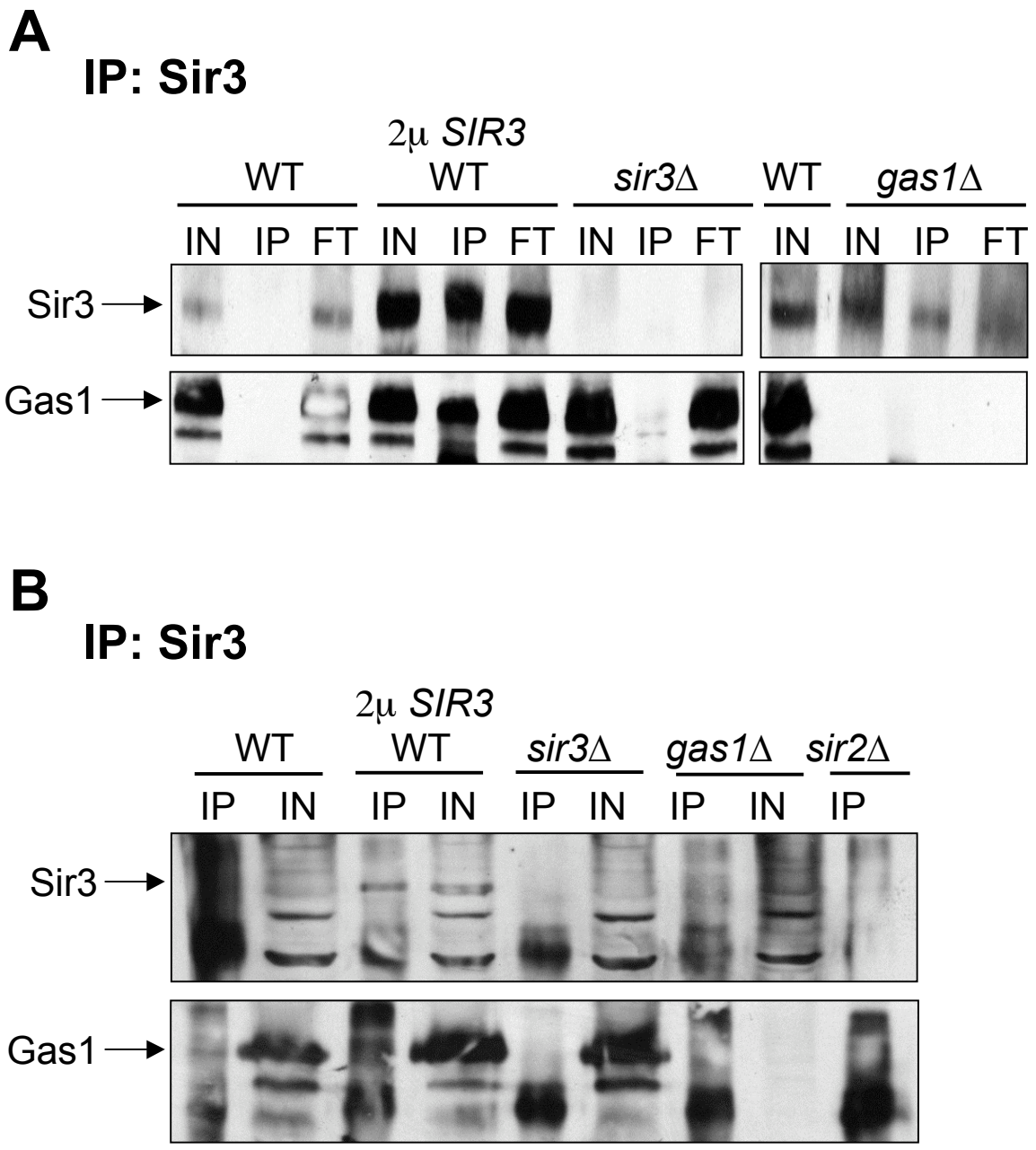
A
IP: Sir3
2μ SIR3
WT
WT
sir3Δ
WT
gas1Δ
IN IP FT IN IP FT IN IP FT IN IN IP FT
Sir3
Gas1
B
IP: Sir3
2μ SIR3
WT
WT
sir3Δ
gas1Δ
sir2Δ
IP IN IP IN IP IN IP IN IP
Sir3
Gas1

Figure 4-15. Gas1 may interact with Sir3 fragments by GST affinity binding. GST (pLP1302) and GST-Gas1 (pLP2087) are recombinant proteins purified from bacteria. GST fusion proteins were incubated for 1 hour with protein extracts from WT (LPY5), *gas1*Δ (LPY10129), and *sir3*Δ (LPY10) strains. Input and affinity bound material were analyzed by immunoblot with anti-Sir3 (2936/4) (Stone and Pillus 1996). Sir3 immunoreactive bands recognized in the GST-Gas1 affinity binding assay are identified on the figure with light gray arrows.

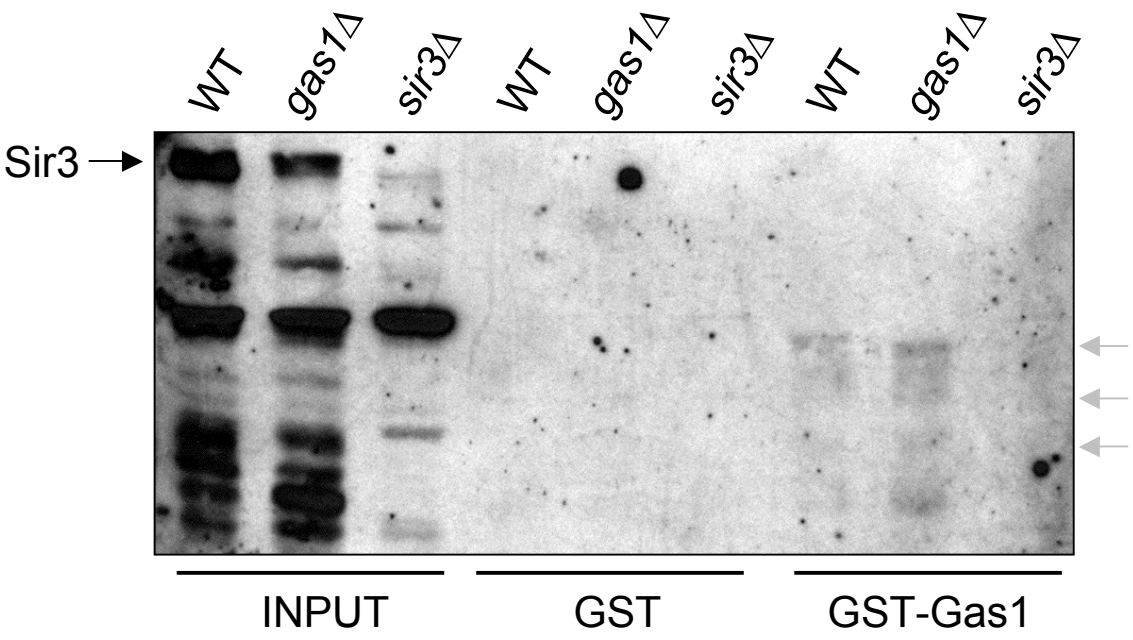
WT
gas1Δ
sir3Δ
WT
gas1Δ
sir3Δ
WT
gas1Δ
sir3Δ
Sir3
INPUT
GST
GST-Gas1

absent in the *sir3*Δ samples appeared to associate specifically with GST-Gas1 and not GST alone (Figure 4-15). Sir3 may be susceptible to cleavage by proteases during protein extract preparation and incubation with the recombinant GST proteins, producing proteolytically cleaved forms of Sir3 that are bound by GST-Gas1.

DISCUSSION

In this study, additional analyses were completed in an attempt to further characterize Gas1's function in transcriptional silencing. Although *gas1*Δ mutants are defective in telomeric silencing (Figure 2-1*D*, 2-1*E*), the SIR complex is telomere-bound (Figure 2-6*B*, 2-7*A*, 4-1). An increase in Sir4 binding is seen in *gas1*Δ mutants (Figure 4-1). Previously, moderate overexpression of *SIR4* was shown to interfere with silencing (Cockell et al. 1995), so the additional Sir4 bound in *gas1*Δ may have a negative effect on telomeric silencing. The SIR complex was not disrupted, since the Sir2-Sir4 interaction was observed in the absence of *GAS1* (Figure 4-3). Gas1 itself was not a component of silent chromatin seen in Gas1 chromatin immunoprecipitation studies that showed no Gas1 enrichment at a telomere (Figure 4-2). Gas1 glucanosyltransferase activity may contribute to silent chromatin prior to SIR complex binding, or may associate with silent chromatin components in a non-stable manner that cannot be observed by chromatin immunoprecipitation analysis.

Two observations in *gas1*Δ mutants may help explain the telomeric silencing defect in *gas1*Δ mutants. First, Sir3 is differentially modified in *gas1*Δ (Figure 4-4). Whether this difference represents hyperphosphorylated Sir3 has not been verified.

Although phosphorylation of Sir3 strengthens telomeric silencing (Stone and Pillus 1996), overly phosphorylated Sir3 hinders subtelomeric silencing (Ai et al. 2002). The Ku complex consists of Yku70 and Yku80 and is required for telomeric silencing. The localization of these proteins was altered slightly in *gas1*Δ mutants (Figure 4-5, 4-6). The potential change in the distribution of the Ku complex, which are critical telomeric silencing factors, may point to a mechanism to explain the defect in telomeric silencing observed in *gas1*Δ mutants.

To pursue the potential action of Gas1 glucanosyltransferase activity in telomeric silencing, two lines of investigation were employed. First, Sir2 NAD^+ hydrolysis activity assays were completed with addition of purified Gas1. These experiments were also tested with addition of laminarin as substrate for Gas1 activity. β-1,3-glucan and Sir2 co-immunoprecipitate (Figure 2-11*B*), therefore the proposed β-1,3-glucan modification of Sir2 may affect its deacetylase activity. Sir2 activity increased slightly with Gas1 and laminarin present, but the slight enhancement was not dependent of Gas1 enzymatic activity since the Gas1 catalytic mutant exhibited the same effect (Figure 4-7*B*). Overall, laminarin addition reduced Sir2's deacetylase activity compared to control reactions without laminarin (Figure 4-7*C*). Whether the glucanosyltransferase activity of the recombinant Gas1 used in these experiments was active under the conditions of the assay has not been confirmed, but remain to be important to establish. Thus, the assays completed so far may not yet be a fair and complete evaluation of whether Gas1 enzymatic activity affects Sir2 deacetylase activity since additional enzymes that are required for linking β-1,3-glucan to their substrate are absent from the *in vitro* assay. Further, if the co-immunoprecipitation of

Sir2 with β-1,3-glucan is linked through bridging factors, these are also absent from the assay. In the future, similar experiments should be pursued measuring Sir2 deacetylation with the addition of yeast protein extract to include the other possible proteins that may factor in the interaction between β-1,3-glucan and Sir2.

To attempt to detect the β-1,3-glucan modification of Sir2, zymolyase and purified β-1,3-glucanase treatment of protein extracts was completed. In the zymolyase treated extracts, a shift in Sir2 upon removal of β-1,3-glucan might be expected, however complete disappearance of Sir2 was observed in all instances (Figure 4-8). The disappearance of Sir2 may result from the proteases present in the commercially available zymolyase and incomplete action of protease inhibitors included in the reactions. Recombinant β-1,3-glucanase treatment did not degrade Sir2 but also did not change Sir2, as analyzed by Sir2 immunoblot (Figure 4-10). Overall this set of experiments did not succeed in furthering our understanding of the interaction between β-1,3-glucan and Sir2. Future experiments should address the proteolysis observed in the zymolyase treatments, or utilize other commercially available enzymes to cleave the β-1,3-glucan linked directly, or indirectly, to Sir2. Alternatively, other potential substrates of β-1,3-glucan modification, such as histones could be analyzed through similar experimentation.

In a high-throughput screen to detect protein complexes, an interaction between Sir3 and Gas1 was uncovered (Ho et al. 2002). To independently evaluate the screen result, two protein interaction tests were completed. First, Sir3 immunoprecipitations bound Gas1 (Figure 4-14*A*), however the immunoblots from a repeated test did not clearly show the *in vivo* Sir3-Gas1 interaction (Figure 4-14*B*).

Then, GST-Gas1 affinity binding assays were analyzed for Sir3 protein. Although full-length Sir3 was not observed, smaller proteins that were absent in the *sir3*Δ control were interacted specifically with GST-Gas1 (Figure 4-15). Although these results were not completely satisfactory in verifying the Sir3-Gas1 interaction, are supportive of the high-throughput result.

In addition to the potential physical interaction between Sir3 and Gas1, Gas1 also associates with Sir2 by two-hybrid and GST-Sir2 affinity binding (Figure 2-9). To follow up on the Sir2-Gas1 physical interaction, the reciprocal test was pursued, utilizing GST-Gas1 affinity binding assays. Although in initial experiments GST-Gas1 cleanly pulled down Sir2 (Figure 4-13*A*), later experiments showed Sir2 associated with GST alone (Figure 4-13*B*), despite attempts to reduce background. To verify the interaction *in vivo*, reciprocal co-immunoprecipitation experiments were also done. The immunoprecpitation of Sir2 and Gas1 did not co-precipitate Gas1 or Sir2, respectively (Figure 4-12). Although this physical interaction test was negative it supports the model that the Sir2-Gas1 interaction is not structurally stable and that the proteins may be only briefly associated at the moment when Gas1 modifies Sir2 or its interacting partners.

Many of the experiments reported in this chapter represent pilot of incompletely resolved experimental approaches that probe for deeper molecular insight into the nature of *GAS1*'s function in transcriptional silencing. These experiments will require further modification or optimization to produce definitive answers to the questions they address, but provide valuable first steps in guiding future studies.

MATERIALS AND METHODS

Yeast methods and strains, and plasmids. Yeast strains used are listed in Table 4-1. Plasmids used are listed in Table 4-2. Standard yeast methods were used (Amberg et al. 2005), including lithium acetate transformation of plasmids (Ito et al. 1983).

Chromatin immunoprecipitation. Experiments were performed as described (Darst et al. 2008) with 100 A_{600} cell equivalents of the indicated strains. Immunoprecipitation (IP) mixtures were incubated overnight at 4˚C with 4 microliters anti-Sir4 (Palladino et al. 1993) or 1 microliter anti-Gas1 (Doering and Schekman 1997) (gift from R. Schekman). DNA in input and IP samples was quantified by real-time PCR. Primers used are in Table 4-3. Values are IP/input normalized to *ACT1* IP/input.

Co-immunoprecipitation studies. From each of the indicated strains, 40 A_{600} cell equivalents were used per immunoprecipitation (IP). Sir2 and Sir4 IPs were performed as described (Garcia and Pillus 2002) with anti-Sir2 (2916/8) (Smith et al. 1998) or anti-Sir4 (2913/8) (Palladino et al. 1993). Sir3 IP was performed as described, with anti-Sir3 (2936/4) (Stone and Pillus 1996). Gas1 IP was performed as described (Sutterlin et al. 1997), with anti-Gas1 (Nuoffer et al. 1991) (gift from C. Sütterlin). Input and immunoprecipitated samples were separated on 10 x 12 cm 8-9% SDS-polyacrylamide gels. Sir2 was analyzed by immunoblot using a 1:5000 dilution of anti-Sir2 (2916/8). Sir3 was analyzed by immunoblot using a 1:5000 dilution of

anti-Sir3 (2936/4). Gas1 was analyzed by immunoblot using a 1:10,000 dilution of anti-Gas1. Secondary antibody, horseradish peroxidase (HRP)-coupled anti-rabbit (Promega, Madison, WI) was used at 1:10,000 and detected using enhanced chemiluminescence reagents (PerkinElmer, Waltham, MA).

Protein immunoblotting. Protein extracts were harvested as described (Stone and Pillus 1996) and separated on 10 x 12 cm 8% SDS-polyacrylamide gels to separate phosphorylated forms of Sir3. Immunoblotting was performed with a 1:5000 dilution of anti-Sir3 (7796) (Ray et al. 2003) followed by a 1:10,000 dilution of secondary antibody anti-rabbit HRP (Promega, Madison, WI). Sir3 was detected using enhanced chemiluminescence reagents (PerkinElmer, Waltham, MA).

Fluorescence microscopy. Cells were grown in YPD to log phase (A_{600} of 0.5-0.8) and DAPI was added to a concentration of 2 μg/ml for one hour at 30˚C. Cells were washed twice with PBS prior to imaging. Cells were visualized using an Axiovert 200M microscope (Carl Zeiss MicroImaging) with a 100x 1.3 NA objective. Images were captured using a monochrome digital camera (Axiocam; Carl Zeiss MicroImaging). GFP images were deconvolved from three original stacks using Axiovision software (Carl Zeiss MicroImaging). In future studies, further optimization of DAPI staining will be necessary since primarily mitochondrial DNA was detected in these images.

NAD^+ hydrolysis assays. Glutathione S-transferase (GST; pLP1302), GST-Sir2 (pLP1275), GST-Gas1 (pLP2087), and GST-gas1-E161Q, E262Q (pLP2119) fusion proteins were expressed in *E. coli* BL21 (DE3) during a 4- to 5-hr induction with 0.5 mM IPTG at room temperature (for GST and Sir2) or 18˚C (for Gas1).

Table 4-1. Yeast strains used in Chapter 4.[a]

Strain	Genotype	Source/Reference
LPY5	W303-1a *MAT***a** *ade2-1 can1-100 his3-11,15 leu2-3,112 trp1-1 ura3-1*	R. Rothstein
LPY9	W303-1a *sir4::HIS3*	
LPY10	W303-1a *sir3::TRP1*	
LPY11	W303-1a *sir2::HIS3*	
LPY79	W303-1b *MAT*α *ade2-1 can1-100 his3-11,15 leu2-3,112 trp1-1 ura3-1*	R. Rothstein
LPY1857	LPY5 + pLP27	
LPY6497	*MAT***a** *his3Δ1 leu2Δ0 lys2Δ0 ura3Δ0*	
LPY6623	*MAT***a** *his3Δ1 leu2Δ0 lys2Δ0 ura3Δ0 hst2Δ::kanMX*	
LPY6637	*MAT***a** *his3Δ1 leu2Δ0 lys2Δ0 ura3Δ0 sir2Δ::kanMX*	
LPY6911	*MAT***a** *his3Δ1 leu2Δ0 lys2Δ0 met15Δ0 ura3Δ0 gas1Δ::kanMX*	
LPY10129	W303-1a *gas1Δ::kanMX*	
LPY10663	W303-1a *gas1Δ::kanMX sir2::HIS3*	
LPY13543	W303-1b *gas1Δ::kanMX gas3Δ::kanMX gas5Δ::kanMX*	
LPY13993	*MAT***a**/*MAT*α *his3Δ1/his3Δ1 leu2Δ0/leu2Δ0 LYS2/lys2Δ0 met15Δ0/MET15 ura3Δ0/ura3Δ0 GFP-YKU70-HIS3MX6/GFP-YKU70-HIS3MX6*	
LPY13995	*MAT***a**/*MAT*α *his3Δ1/his3Δ1 leu2Δ0/leu2Δ0 LYS2/lys2Δ0 ura3Δ0/ura3Δ0 GFP-YKU70-HIS3MX6/GFP-YKU70-HIS3MX6 gas1Δ::kanMX/gas1Δ::kanMX*	
LPY13997	*MAT***a**/*MAT*α *his3Δ1/his3Δ1 leu2Δ0/leu2Δ0 LYS2/lys2Δ0 met15Δ0/MET15 ura3Δ0/ura3Δ0 GFP-YKU80-HIS3MX6/GFP-YKU80-HIS3MX6*	
LPY13999	*MAT***a**/*MAT*α *his3Δ1/his3Δ1 leu2Δ0/leu2Δ0 LYS2/lys2Δ0 MET15/met15Δ0 ura3Δ0/ura3Δ0 GFP-YKU80-HIS3MX6/GFP-YKU80-HIS3MX6 gas1Δ::kanMX/gas1Δ::kanMX*	

[a]Unless otherwise noted strains were constructed during the course of this study or are part of the standard lab collection.

Table 4-2. Plasmids used in Chapter 4.[a]

Plasmid (alias)	Description	Source/Reference
pLP26 (YEp24)	vector *URA3* 2μ	Botstein et al. 1979
pLP27	*SIR3 URA3* 2μ	Kimmerly and Rine 1987
pLP1275	GST-*SIR2*	Tanny et al. 1999
pLP1302	GST	Kaelin et al. 1992
pLP2087	GST-*GAS1*	
pLP2119	GST-*gas1-E161Q, E262Q*	
pLP2288 (pUV5-G1S)	β-1,3-glucanase	Shen et al. 1991

[a]Unless otherwise noted, plasmids were constructed during the course of this study and are described in Materials and Methods, or are part of the standard lab collection.

Proteins were purified on glutathione Sepharose beads as directed (GE Healthcare, Piscataway, NJ). Purified proteins were dialyzed against 50 mM sodium phosphate (pH 7.2) and stored at 4°C in 50 mM sodium phosphate (pH 7.2), 0.5 mM dithiothreitol (DTT), and 10% glycerol (Landry et al. 2000b). Protein concentration was established by comparison of Coomassie brilliant blue (CBB) staining of purified GST-protein samples and a concentration series of the BSA protein standard. NAD^+-hydrolysis assays to measure histone deacetylation were performed as described (Landry et al. 2000a). Reactions were carried out in 1 ml with 50 mM glycine (pH 9) (Sir2 buffer conditions) or 50 mM sodium acetate (pH 5.5) (Gas1 buffer conditions), 0.5 mM DTT, 5 mM tetrasodium pyrophosphate ($Na_4P_2O_7$), 0.1 mg/ml BSA, 1 mg calf thymus histones (Sigma, St. Louis, MO) that were chemically acetylated (Parsons et al. 2003), with 2 μCi [4-^{3}H] NAD^+ (GE Healthcare, Piscataway, NJ, TRA298; 4.3 Ci/mmol, 1 mCi/ml), and 1.85 μg of purified proteins. Laminarin (Sigma, St. Louis, MO) was added to the indicated reactions to a final concentration of 2 μg/ml. The reactions were performed in duplicate and incubated at room temperature. Time points at 10 min, 45 min, 2 hr, 3 hr, and 5 hr were taken by transfer of 185 μl of the reaction to tubes containing 135 μl 0.5 M boric acid (pH 8) to quench the reaction. 1 ml of ethyl acetate was added and vortexed for 5 min and 700 μl of the ethyl acetate phase was transferred to 3 ml Ecoscint fluid (National Diagnostics, Atlanta, GA) and analyzed by scintillation counting. Radioactivity released from Sir2 wild-type control reactions lacking histones was subtracted to establish values in Figure 4-7.

Zymolyase and purified β-1,3-glucanase treatment of protein extracts. Protein extracts were made as described (Stone and Pillus 1996). To 2 A_{600} cell

equivalents of protein extract, 1 unit of zymolyase (United States Biological Inc., Swampscott, MA) or the same volume of SCE buffer (0.9 M sorbitol, 100 mM sodium citrate, 60 mM EDTA, pH 8), and protease inhibitors (leupeptin, pepstatin, PMSF, TPCK, benzamidine) were added to 1x final concentration. Recombinant *O. xanthineolytica* β-1,3-glucanase was purified as described (Wongwisansri and Laybourn 2004) from DH5α *E. coli* cells expressing the β-1,3-glucanase gene in the expression vector pLP2288 (pUV5-G1S) (Shen et al. 1991) (gift from P. Laybourn) and its activity was compared to zymolyase in cell clearing assays (Wongwisansri and Laybourn 2004). β-1,3-glucanase was added to extracts using an approximation of the activity compared to zymolyase. Reactions were incubated at room temperature for 15-60 min. Then, sample-loading buffer (SLB) was added to 1x and samples were boiled. For Sir2, samples were separated on 9% polyacrylamide. For Tub2 and Pgk1, samples were separated on 10% polyacrylamide. Sir2 was analyzed by immunoblot using a 1:5000 dilution of anti-Sir2 (2931/4) (Axelrod 1991). Tubulin (Tub2) was analyzed by immunoblot using a 1:10,000 dilution of anti-β-tubulin (Bond et al. 1986). Phosphoglucerate kinase (Pgk1) was analyzed by immunoblot using a 1:20,000 dilution of anti-Pgk1 (Baum et al. 1978) (gift from J. Thorner). Secondary antibody, HRP-coupled anti-rabbit (Promega, Madison, WI) was used at 1:10,000 and detected using enhanced chemiluminescence reagents (Pierce, Rockford, IL).

GST-affinity binding studies. The GST-affinity binding assays were described previously (Darst et al. 2008). Glutathione S-transferase (GST; pLP1302) and GST-Gas1 (pLP2087) fusion proteins were expressed in *E. coli* BL21 (DE3) during a 4- to 5-hr induction with 0.5 mM IPTG at 18˚C. Proteins were purified on

glutathione Sepharose beads as directed (GE Healthcare, Piscataway, NJ). Purified GST-fusion proteins were incubated with 20 A_{600} cell equivalents of whole cell extracts from the indicated yeast strains for 1 hour at 4˚C. In the indicated experiments, yeast whole-cell extracts were pre-incubated with 10 μg/ml BSA for 1 hour at 4˚C and washes were done with higher salt wash buffer containing 500 mM NaCl. Samples were probed with a 1:5000 dilution of anti-Sir2 (2916/8) (Smith et al. 1998) or a 1:5000 dilution of anti-Sir3 (2936/4) (Stone and Pillus 1996). HRP-coupled anti-rabbit secondary (Promega, Madison, WI) was used at 1:10,000 and detected using enhanced chemiluminescence reagents (Pierce, Rockford, IL).

Chapter 5

The Sir2-interacting protein Kre6 functions in transcriptional silencing

INTRODUCTION

The analysis of *gas1*Δ mutants presented in Chapter 2 provides a link between an enzyme involved in cell wall biogenesis and transcriptional silencing. In this analysis, it was determined that not all genes encoding proteins with functions in cell wall biogenesis act in silencing by demonstrating that deletion of *BGL2*, *GAS3*, or *GAS5* leads to normal silencing of telomeres (Figure 2-4). Gas1's functions in cell wall biogenesis and transcriptional silencing are also separable (Figure 2-10*B*).

It is possible that other proteins with known roles in cell wall biogenesis also function in silencing. Indeed, in addition to Gas1, other cell wall proteins were recovered in the same Sir2 two-hybrid screen (Garcia 2003). Sir2 is a central factor responsible for transcriptional silencing at the telomeres, *HM* loci, and rDNA through its histone deacetylase activity and interactions with other silencing factors. Kre6 also interacted with the core domain Sir2 two-hybrid construct containing its deacetylase domain (Garcia 2003). *KRE6* was first identified in a screen for killer toxin resistant mutants (Al-Aidroos and Bussey 1978). *KRE6* is necessary for synthesis of β-1,6-glucan and is a putative β-glucan synthase that appears to be functionally redundant with the β-glucan synthase gene *SKN1* (Roemer and Bussey 1991; Roemer et al. 1993). Of note is the observation that *gas1*Δ *kre6*Δ mutants are synthetically lethal

(Popolo et al. 1997), which is attributed to their important dual roles in cell wall biogenesis.

Kre6's two-hybrid interaction with the protein deacetylase Sir2 points to the possibility that Kre6 may function in the nucleus in silencing along with Gas1. Additional evidence supporting a nuclear function for Kre6 are synthetic sick genetic interactions between *kre6*Δ and deletion of nuclear protein genes, including *SWI3*, that encodes a subunit of the SWI/SNF chromatin remodeling complex, *RTF1*, encoding a subunit of the Paf1 complex acting in transcription elongation, and *ACE2*, a transcription factor that activates G1-specific genes (Tong et al. 2004).

In this analysis, *kre6*Δ mutants were found to be defective in telomeric silencing. In contrast to *gas1*Δ mutants, *kre6*Δ strains did not exhibit increased silencing of the rDNA. Although *gas1*Δ and *kre6*Δ mutants are distinct in their rDNA silencing phenotypes, their telomeric silencing defects were similar and suggest that the two genes may function together in telomeric silencing. In the initial examination of hallmarks of silent chromatin in *kre6*Δ strains, Sir2 was bound to the telomere despite the observed defect in telomeric silencing. Similar to this observation in *kre6*Δ, in *gas1*Δ mutants, Sir2 is also telomere-bound and in histones are deacetylated at the telomere (Figure 2-6). In the analysis of *kre6*Δ *sir2*Δ mutants, a growth defect at high temperature was seen. This result points to *KRE6* and *SIR2* functioning in a pathway required for optimal cell viability. This may involve multiple functions, including transcriptional silencing, Kre6's involvement in cell wall biogenesis, or other critical Sir2 functions, such as rDNA recombination and aging.

RESULTS

Deletion of *KRE6* results in a defect in telomeric silencing. *KRE6* and *GAS1* both encode enzymes that function in cell wall biogenesis, however *GAS1* also functions in transcriptional silencing (Chapter 2). Kre6 and Gas1 were both identified in the same Sir2 two-hybrid screen (Garcia 2003). Given that *gas1*Δ mutants are defective in telomeric silencing, *kre6*Δ mutants were evaluated to determine if transcriptional silencing was also altered. Mutants of *kre6*Δ were constructed in a reporter strain with *URA3* on telomere V-R. A significant telomeric silencing defect was observed in both the original *kre6*Δ knockout and backcrossed strains (Figure 5-1*A*). Importantly, *kre6*Δ strains without the reporter (*kre6*Δ *ura3-1*) were not sensitive to 5-FOA. To determine whether the telomeric silencing defect was independent of the reporter gene assayed, *kre6*Δ strains were constructed with a different reporter gene, *ADE2* also on telomere V-R. In this assay, *kre6*Δ strains displayed a phenotype similar to *sir2*Δ, the white colony color indicative of elevated *ADE2* expression. In contrast, the wild-type strain silenced *ADE2* and displayed a combination of white and pink colony color (Figure 5-1*B*).

To verify that the *kre6*Δ gene deletion was responsible for the observed telomeric silencing defect wild-type *KRE6* was tested for the ability to complement the defect. *KRE6* was cloned and when overexpressed *KRE6* restored telomeric silencing to *kre6*Δ strains (Figure 5-2). Additionally, *KRE6* overexpression interfered with silencing in wild-type cells (Figure 5-2), showing that telomeric silencing may be sensitive to *KRE6* levels. Although *GAS1* and *KRE6* did not reciprocally complement

Figure 5-1. Deletion of *KRE6* causes defects in transcriptional silencing at telomeres. *(A) kre6*Δ strains are defective in silencing *URA3* reporter at TELV-R. Wild-type (WT) (LPY4916), *sir2*Δ (LPY10397), *gas1*Δ (LPY10362), *kre6*Δ (LPY11255), *kre6*Δ (LPY11269), and *kre6*Δ (LPY11265), all containing TELV-R::*URA3*, and two *kre6*Δ without the reporter (*kre6*Δ *ura3-1*) (LPY11267, LPY11263) were plated on synthetic complete (SC) to monitor growth, and on SC containing 5-FOA to monitor telomeric silencing at 30˚C. LPY11255 is an original *kre6*Δ deletion transformant strain, LPY11263, LPY11265, LPY11267, and LPY11269 are from a backcross of *kre6*Δ deletions to wild-type. Decreased growth on 5-FOA indicates defective silencing *(B) kre6*Δ is defective in silencing *ADE2* at TELV-R. WT (LPY9911), *sir2*Δ (LPY9961), and *kre6*Δ (LPY11548) strains with TELV-R::*ADE2* were plated for single colonies on yeast extract-peptone-dextrose (YPD) plates. Plates with WT and *sir2*Δ colonies were incubated at 30˚C for 3 days prior to shifting plates to 4˚C for color development. Plates with *kre6*Δ colonies were incubated at 30˚C for 5 days prior to shifting plates to 4˚C for color development. Plates were at 4˚C approximately 1 week prior to digital image capture. *ADE2* expression (white colonies) indicates defective silencing.

A

TELV-R::*URA3*

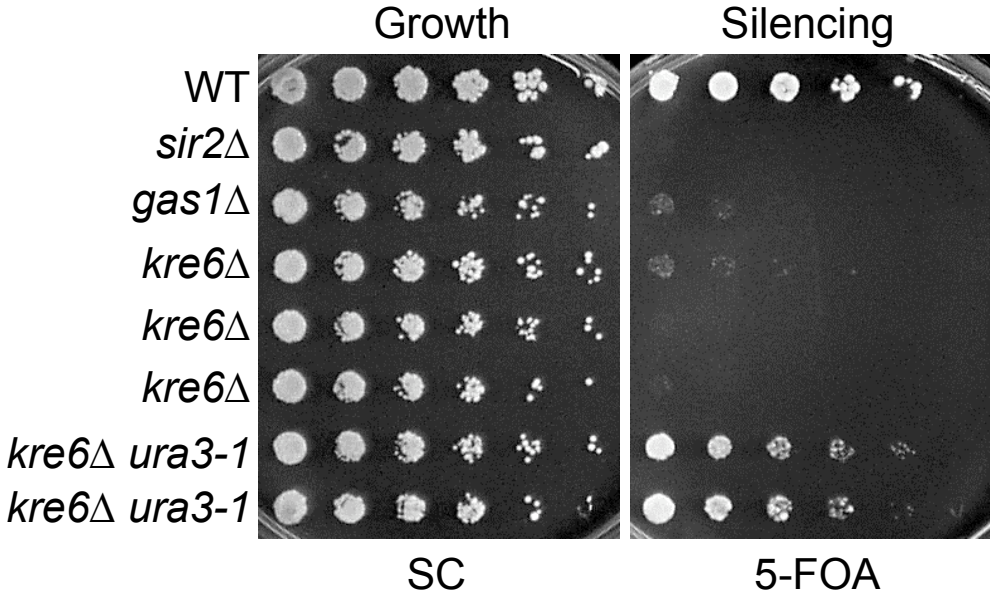

B

TELV-R::*ADE2*

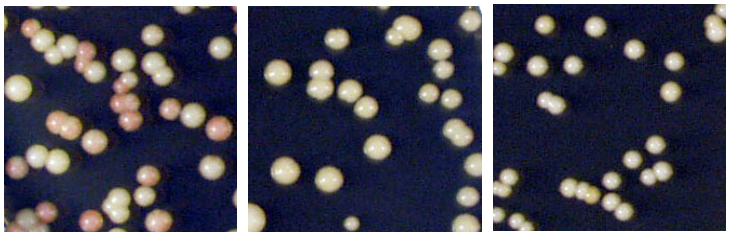

Figure 5-2. The *kre6*Δ telomeric silencing defect is partially complemented by *KRE6*, and *KRE6* overexpression interferes with telomeric silencing in wild-type cells. WT (LPY4916) was transformed with 2μ *LEU2* vector (pLP1623) and *KRE6* (pLP2014), *gas1*Δ (LPY10362) and *kre6*Δ strains (LPY11269) were transformed with pLP1623, *GAS1* (pLP1951), and pLP2014. Transformed strains are LPY14545, LPY14551, LPY14552, LPY14553, and LPY14558-LPY14561. Transformed strains were plated on SC-leucine (SC-leu) to monitor growth at 30˚C and 37˚C and on SC-leu containing 5-FOA at 30˚C to monitor telomeric silencing. Decreased growth on SC-leu 5-FOA indicates defective silencing.

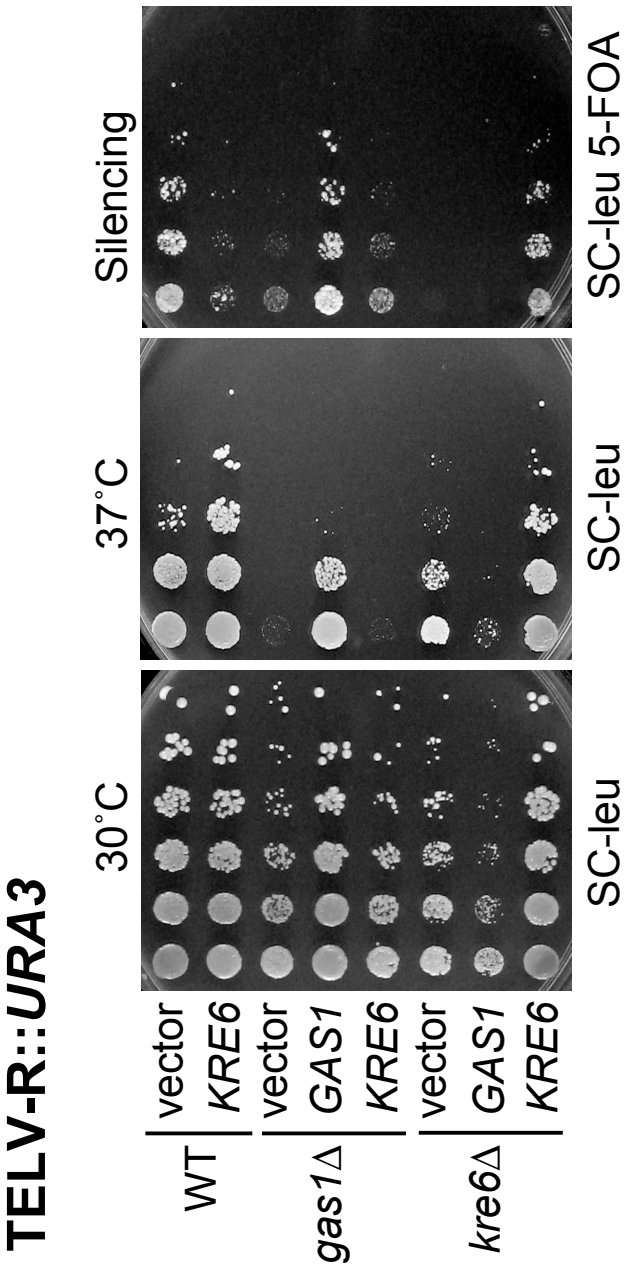
TELV-R::URA3
30˚C
37˚C
Silencing
WT
vector
KRE6
gas1Δ
vector
GAS1
KRE6
kre6Δ
vector
GAS1
KRE6
SC-leu
SC-leu
SC-leu 5-FOA

the *kre6*Δ and *gas1*Δ telomeric silencing defects, respectively, *GAS1* overexpression in *kre6*Δ resulted in slow growth and temperature sensitivity at high temperature (Figure 5-2). The *kre6*Δ mutant is sensitive to levels of *GAS1* since *kre6*Δ *gas1*Δ is synthetically lethal (Popolo et al. 1997), an observation that was independently validated in the W303 and BY4741 genetic backgrounds (data not shown).

Since telomeric silencing was altered in *kre6*Δ, silent chromatin was examined by Sir2 chromatin immunoprecipitation to determine whether Sir2 was bound at telomeres in *kre6*Δ. Although there was slightly less Sir2 bound at the telomeres in the *kre6*Δ strain compared to wild-type, Sir2 was not lost from the telomeres in *kre6*Δ (Figure 5-3), despite the loss of telomeric silencing in the mutant (Figure 5-1).

Because *gas1*Δ strains display increased silencing at the rDNA (Figure 2-1*C*), rDNA silencing in *kre6*Δ was examined. Using the same reporter gene where increased silencing was observed in *gas1*Δ, no change in 5S rDNA silencing was seen in the *kre6*Δ mutant (Figure 5-4).

Slow growth and temperature sensitivity was observed in *kre6*Δ *sir2*Δ mutants. The genetic analyses of *kre6*Δ strains support a new role for *KRE6* in transcriptional silencing. Because of the proposed role for Kre6 in silencing and its two-hybrid physical interaction with the silencing protein Sir2 (Garcia 2003), *kre6*Δ *sir2*Δ mutants were constructed. Surprisingly, a synthetic growth defect was observed in *kre6*Δ *sir2*Δ strains, which was most apparent when the strains were grown at high temperature, 37˚C (Figure 5-5). To determine whether this synthetic growth defect could be rescued when wild-type *KRE6* or *SIR2* was added back to the *kre6*Δ *sir2*Δ strains, the mutant was transformed with a single copy CEN *SIR2* plasmid or an

Figure 5-3. Sir2 remains enriched at telomeres in *kre6*Δ mutants. Chromatin immunoprecipitation of Sir2 was done in WT (LPY5), *kre6*Δ (LPY11263), and *sir2*Δ (LPY11) strains. Immunoprecipitated DNA was analyzed by qPCR with primers specific to 0.2 kb and 1 kb from the end of telomere VI-R. IP/input at the telomere was normalized to IP/input at the non-specific locus *ACT1*.

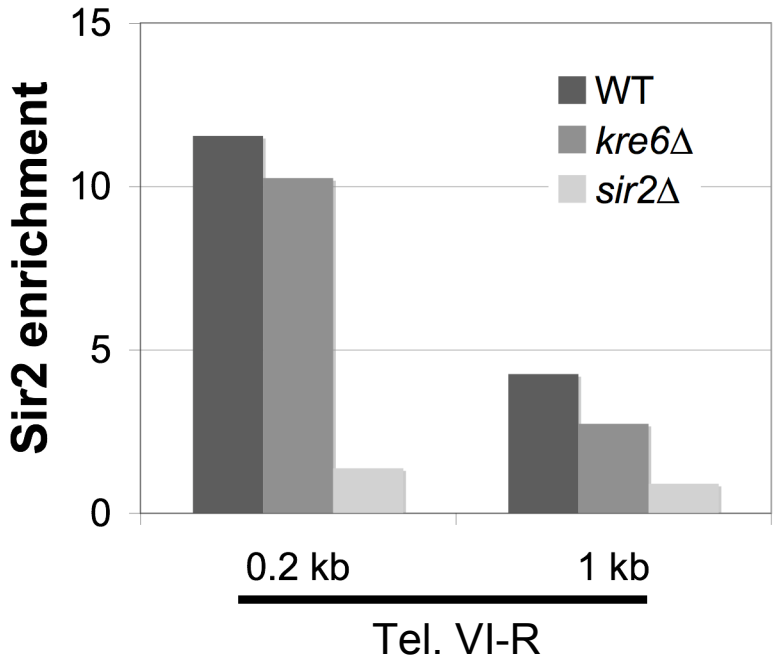
15
10
5
0
Sir2 enrichment
WT
kre6Δ
sir2Δ
0.2 kb
1 kb
Tel. VI-R

Figure 5-4. Deletion of *KRE6* does not affect silencing in the ribosomal DNA near the 5S rRNA gene. WT (LPY2446), *sir2*Δ (LPY2447), *gas1*Δ (LPY10074), *gas1*Δ *sir2*Δ (LPY10078), and *kre6*Δ (LPY11545) strains with *RDN::mURA3* were plated on SC to monitor growth and SC-uracil (SC-ura) to monitor rDNA silencing. Increased growth on SC-ura indicates defective silencing.

RDN::mURA3

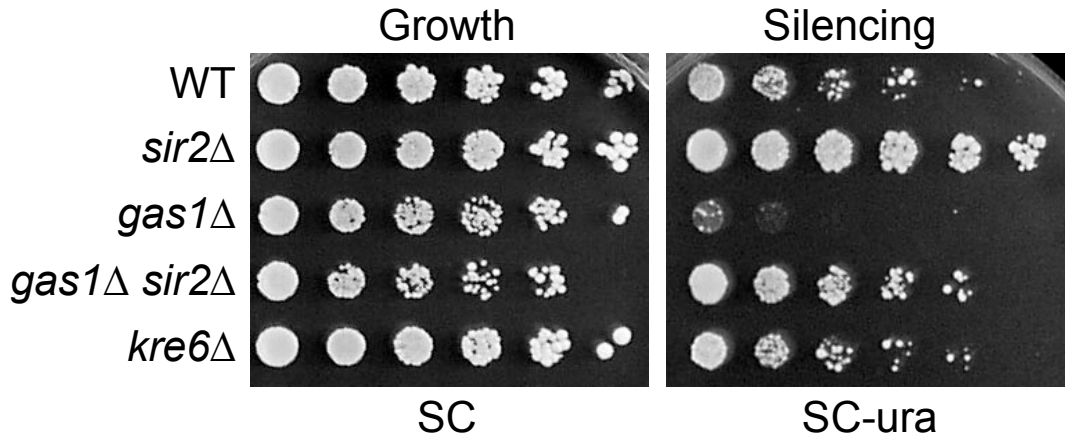

Figure 5-5. Multiple isolates of *kre6*Δ *sir2*Δ strains are temperature sensitive. WT (LPY5), *sir2*Δ (LPY11), *kre6*Δ (LPY11263), *kre6*Δ (LPY11264), *kre6*Δ *sir2*Δ (LPY11326), *kre6*Δ *sir2*Δ (LPY11324), *kre6*Δ *sir2*Δ (LPY11325), and *kre6*Δ *sir2*Δ (LPY11327) were plated on SC at 30˚C to monitor growth and at 37˚C to monitor growth at elevated temperature.

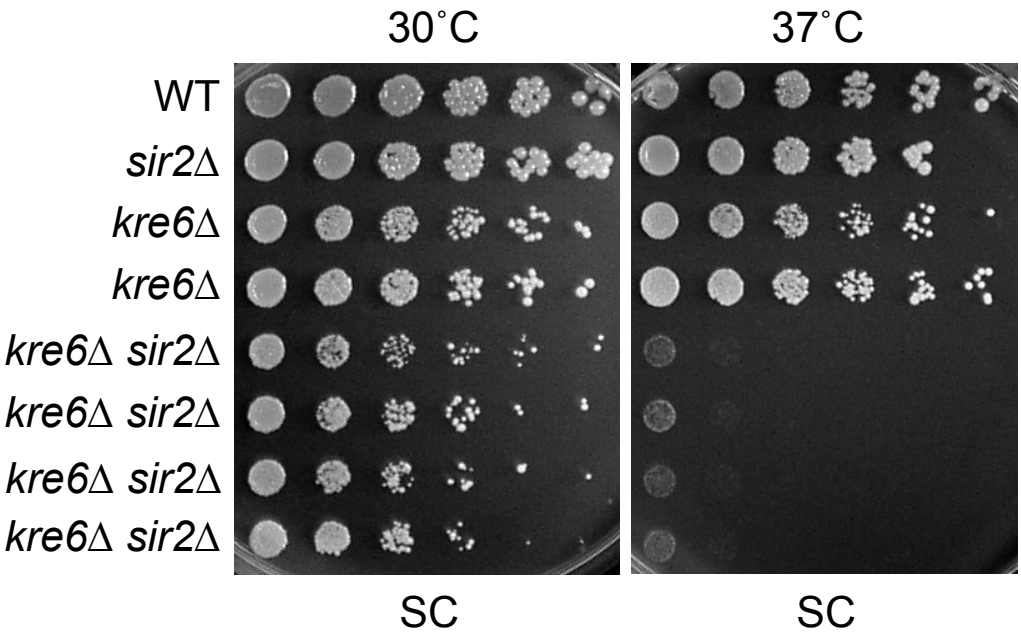
30˚C
37˚C
WT
sir2Δ
kre6Δ
kre6Δ
kre6Δ sir2Δ
kre6Δ sir2Δ
kre6Δ sir2Δ
kre6Δ sir2Δ
SC
SC

overexpression 2μ *KRE6* plasmid. When *kre6*Δ *sir2*Δ expressed CEN *SIR2*, no restoration of growth was observed in the strain, and *SIR2* expression exacerbated growth of the strain at high temperature (Figure 5-6*A*). Although *kre6*Δ *sir2*Δ was synthetically sick, adding back *SIR2* to the strain exacerbated the synthetic sickness in a situation were it would be expected to rescue the synthetic growth defect. However, when *KRE6* was overexpressed in *kre6*Δ *sir2*Δ strains, the growth defect at high temperature was partially suppressed (Figure 5-6*B*). The nature of these surprising effects of *SIR2*-mediated exacerbation has not been resolved, but is reminiscent of some classic modifiers of epigenetic position effects.

DISCUSSION

The analysis presented here of *KRE6* in chromatin functions is not yet as complete as that for *GAS1*. However, even the preliminary studies presented here point to the possibility that multiple enzymes with carbohydrate substrates may share chromatin functions. The transcriptional silencing defect observed at telomeres in *kre6*Δ strains mirrors the defects seen in *gas1*Δ mutants (Figure 5-1). Although *KRE6* complements the *kre6*Δ telomeric silencing defect, it also interfered with silencing in wild-type cells (Figure 5-2). Telomeric silencing is quite sensitive to *KRE6* levels since a defect is observed both when the gene is deleted and overexpressed. *KRE6*'s crucial function in telomeric silencing must be adversely affected when too much Kre6 is present, pointing to a regulatory role for Kre6 in silencing.

Figure 5-6. The temperature sensitivity of *kre6*Δ *sir2*Δ is not complemented by *SIR2* and is partially complemented by *KRE6* overexpression. *(A)* The temperature sensitivity of *kre6*Δ *sir2*Δ strains is not rescued by expression of plasmid-borne *SIR2*. WT (LPY5), *sir2*Δ (LPY11), *kre6*Δ (LPY11263), and *kre6*Δ *sir2*Δ (LPY11326) strains were transformed with CEN *LEU2* vector (pLP62) and CEN *SIR2* (pLP1237). Transformed strains were plated on SC-leu at 30˚C to monitor growth, and at 34˚C and 37˚C to monitor growth at elevated temperature. Instead of rescuing *kre6*Δ *sir2*Δ, *SIR2* expression exacerbated growth at 37˚C. The nature of the exacerbation remains unknown but will be the subject of future studies. *(B)* The *kre6*Δ *sir2*Δ strains are more resistant to high temperature when *KRE6* is overexpressed. WT (LPY5) and *sir2*Δ (LPY11) were transformed with 2μ *LEU2 KRE6* (pLP2014) and *kre6*Δ (LPY11263), and two *kre6*Δ *sir2*Δ strains (LPY11324, LPY11326) were transformed with 2μ *LEU2* vector (pLP1623) and pLP2014. Transformed strains were plated on SC-leu at 30˚C to monitor growth, and at 34˚C and 37˚C to monitor growth at elevated temperature.

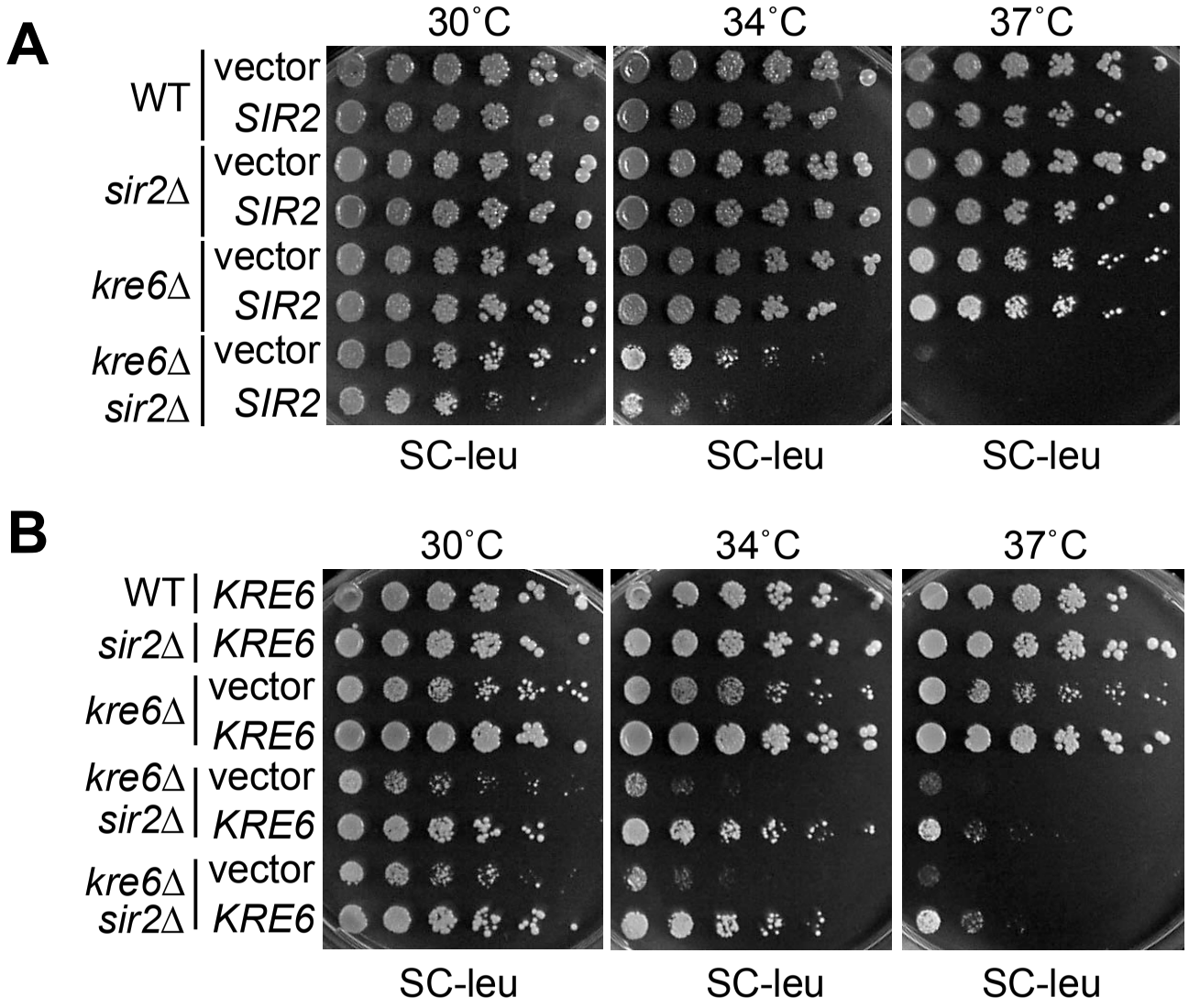
A
30˚C
34˚C
37˚C
WT
vector
SIR2
sir2Δ
vector
SIR2
kre6Δ
vector
SIR2
kre6Δ sir2Δ
vector
SIR2
SC-leu
SC-leu
SC-leu
B
30˚C
34˚C
37˚C
WT
KRE6
sir2Δ
KRE6
kre6Δ
vector
KRE6
kre6Δ sir2Δ
vector
KRE6
kre6Δ sir2Δ
vector
KRE6
SC-leu
SC-leu
SC-leu

Although the telomeric silencing defects of *kre6*Δ and *gas1*Δ was similar, wild-type levels of rDNA silencing were observed in *kre6*Δ mutants, whereas *gas1*Δ strains showed increased rDNA silencing (Figure 5-4). Silencing of *HM* loci remains to be evaluated in *kre6*Δ strains. Additional future analysis, such as telomere VII-L reporter assays and transcript analysis of the telomere VI-R proximal *YFR057W*, will be necessary to validate the conclusion that *kre6*Δ is necessary for silencing at telomeres. Although the silencing phenotypes of *gas1*Δ and *kre6*Δ do not overlap completely, it is possible that *GAS1* and *KRE6* act in the same pathway to promote telomeric silencing. The genes do not functionally substitute for each other in telomeric silencing (Figure 5-2). In fact, *GAS1* levels negatively affect *kre6*Δ growth, observed in the slow growth and temperature sensitivity of *kre6*Δ transformed with multi-copy *GAS1* (Figure 5-2) and the synthetic lethal phenotype of the *gas1*Δ *kre6*Δ combination (Popolo et al. 1997). The genes both encode activities that are required for cell wall biogenesis. Gas1's enzymatic activity was also required for telomeric silencing (Figure 2-11*A*) and it will be important in the future to establish whether *kre6* enzymatically inactive mutants are also defective in telomeric silencing.

Although further analysis remains to be completed, one of the major hallmarks of silent chromatin, Sir2 binding at the telomeres, is intact in *kre6*Δ mutants (Figure 5-3). This is similar to *gas1*Δ mutants, that also had Sir2 and Sir3 bound at the telomeres (Figure 2-6*B*, 2-7*A*). Sir2's histone deacetylase activity targets histone H3K56 and H4K16. Deacetylation of H3K56 and H4K16 at the telomeres was observed in *gas1*Δ mutants (Figure 2-6*C*, 2-6*D*), and it will be necessary to establish whether *kre6*Δ mutants also maintain deacetylation of histones at telomeres.

Gas1's β-1,3-glucanosyltransferase activity is directly implicated in silencing, through modification of Sir2 or Sir2-associated factors (Figure 2-11). An important line of investigation will be determining whether Sir2 is immunoprecipitated by β-1,3-glucan in *kre6*Δ strains, since Sir2 is immunoprecipitated in wild-type cells (Figure 2-11*B*). Kre6 is one of several glucan synthases, including the functionally redundant Skn1 (Roemer et al. 1993). Since at least ten other enzymes with similar enzymatic activity exist in budding yeast, at least some β-glucan remains in the cell in *kre6*Δ mutants. If Sir2 is not pulled down by the anti-glucan antibody in *kre6*Δ strains this will further implicate Kre6 in Gas1's transcriptional silencing function (Figure 5-7). Kre6 and Sir2 exhibit genetic and physical interactions so Kre6 may directly act in this potential modification of Sir2. The physical interaction of Kre6 with Sir2 remains to be evaluated by co-immunoprecipitation studies, or experiments utilizing recombinant proteins in *in vitro* pull-down assays.

The contribution of *KRE6* and *SIR2* to optimal cellular growth was apparent in the growth defect of *kre6*Δ *sir2*Δ mutants at high temperature (Figure 5-5). Curiously, *SIR2* expression did not restore growth at high temperature to the *kre6*Δ *sir2*Δ mutants, although *KRE6* overexpression partially rescued the defect (Figure 5-6). In fact, single-copy (CEN) *SIR2* expression appeared to slightly exacerbate growth of *kre6*Δ *sir2*Δ at high temperature (Figure 5-6*A*). This is a surprising finding for single-copy *SIR2* expression although highly expressed *SIR2* is toxic to cells (Holmes et al. 1997), so there is a previously reported link between *SIR2* expression and cell viability.

Figure 5-7. A model for Gas1 and Kre6 contributions to telomeric silencing through Sir2, or a Sir2-interacting factor. The glucan synthase Kre6 produces β-glucan (hexagon), a potential modification of Sir2, or other chromatin proteins (light gray circles surrounding Sir2). The Kre6-Sir2 interaction may be bridged through the unknown protein linking the β-glucan to Sir2. Gas1 interacts with Sir2, elongating and re-arranging the β-1,3-glucan side chains. The telomeric silencing function of Sir2 is enhanced by this carbohydrate modification.

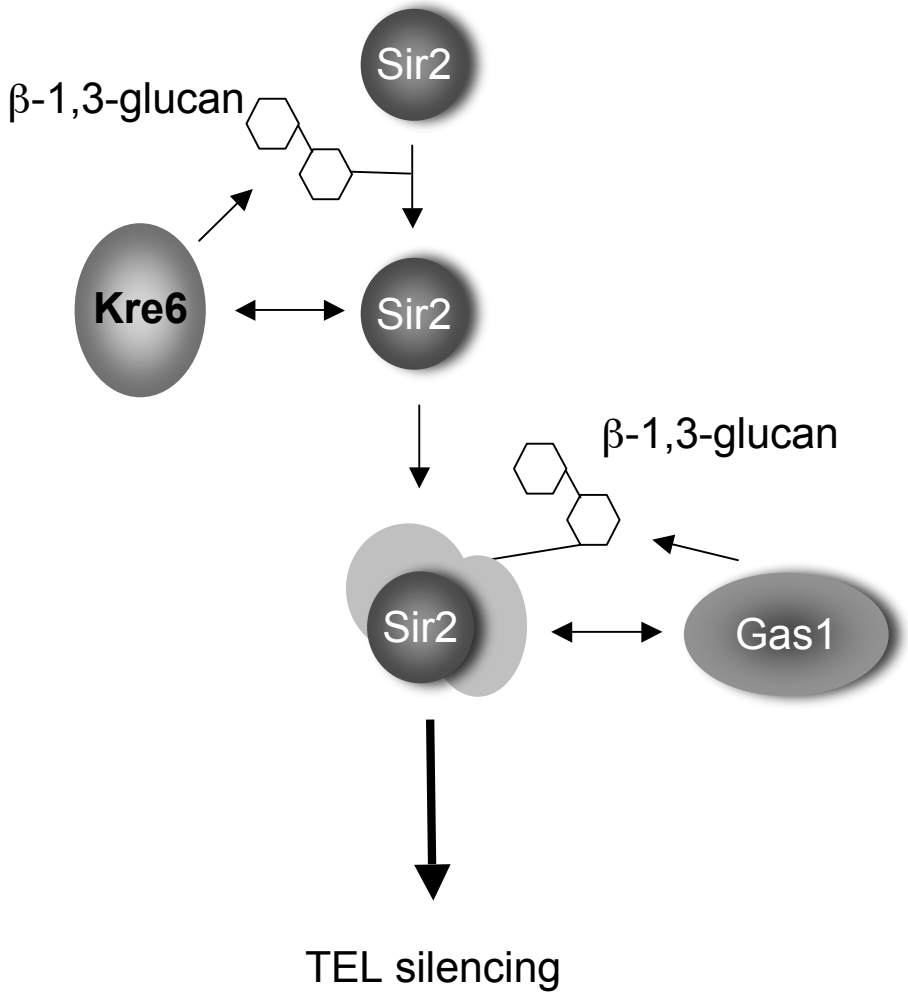
Sir2
β-1,3-glucan
Kre6
Sir2
β-1,3-glucan
Sir2
Gas1
TEL silencing

In future experiments, it will be important to determine whether the *kre6*Δ *sir2*Δ sickness is rescued by *SIR2* in a cross with *kre6*Δ *sir2*Δ covered by plasmid-borne *SIR2*. Also, the *kre6*Δ *sir2*Δ growth defect and temperature sensitivity should be evaluated with sorbitol added to plates since sorbitol suppresses *gas1*Δ temperature sensitivity but not its telomeric silencing defect (Figure 2-10*B*). In addition, preliminary analyses suggest that the genetic interaction between *KRE6* and *SIR2* is specific. The genetic interaction is not common to *SIR* genes, because no sickness was observed in *kre6*Δ *sir1*Δ or *kre6*Δ *sir4*Δ strains (data not shown). In addition, the interaction is also not shared with all budding yeast sirtuin genes, since no synthetic sickness was seen in *kre6*Δ *hst1*Δ or *kre6*Δ *hst2*Δ strains (data not shown). This analysis should be extended to include combinations of all *SIR* (*SIR1-SIR4*) and sirtuin genes (*HST1-HST4*) in budding yeast to determine the specificity of the genetic interaction between *KRE6* and *SIR2*. The *kre6*Δ *sir2*Δ genetic interaction should also be evaluated in the BY4741 genetic background since the interaction was observed in the W303 genetic background and was not reported in the diploid-based synthetic lethality analysis on microarray (dSLAM) screen completed for *sir2*Δ, a genome-wide screen carried out in the BY4741 background (Lin et al. 2008).

Recently, a limited number of synthetic sick or lethal genetic interactions have been reported for *sir2*Δ. Synthetic growth defects have been observed between *sir2*Δ and deletion or mutation of genes encoding NuA4 components including *EAF1*, *ESA1*, *EPL1*, and *YNG2* in the genome-wide dSLAM analysis of genes contributing to histone (de)acetylation (Lin et al. 2008). The dSLAM analysis also uncovered a synthetic growth defect between *sir2*Δ and deletion of *ACS2*, which encodes one of

two acetyl CoA synthetases. Synthetic genetic interactions have also been observed between *sir2*Δ and deletion of *SLX5*, encoding a ubiquitin E3 ligase, and deletion of *ULP2*, encoding a SUMO isopeptidase (Darst et al. 2008). Deletion of *SIR2* also compromises viability in strains with mutation of *CDC13*, which encodes an essential single-stranded DNA binding protein that binds to telomeres and is necessary for telomerase activity (Greenall et al. 2008).

The synthetic sickness of *kre6*Δ *sir2*Δ strains at high temperature supports the hypothesis that *KRE6* and *SIR2* contribute to functions that are necessary for cell survival. Both genes have now been shown to contribute to transcriptional silencing. However there is no existing evidence that silencing is essential for growth since *sir* mutants are viable. *KRE6*'s established role in cell wall biogenesis may also contribute to the temperature sensitive phenotype of *kre6*Δ *sir2*Δ. Important functions of Sir2 besides its silencing function include roles in controlling rDNA recombination and regulating lifespan (reviewed in Buck et al. 2004), both of which are closely linked to cellular survival. The *kre6*Δ mutants are impaired for growth, and the additional deletion of *SIR2* and loss of critical Sir2-regulated processes further impairs growth when cells are stressed by exposure to high temperature. Understanding the molecular reason for the *kre6*Δ *sir2*Δ synthetic growth defect may lead to a model for the interplay between *KRE6* and *SIR2* in transcriptional silencing.

MATERIALS AND METHODS

Yeast strains and methods. Yeast strains are listed in Table 5-1. Strains were constructed during this study unless otherwise noted and grown at 30˚C with standard manipulations (Amberg et al. 2005). Deletion mutants were created with standard methods and oligonucleotide sequences of primers used are in Table 5-2. Synthetic selective media were prepared as described (Sherman 1991). 5-fluoroorotic acid (5-FOA; United States Biological, Inc., Swampscott, MA) was added at 0.1% to test for *URA3* reporter gene expression. Silencing assays were performed as described (van Leeuwen and Gottschling 2002). For serial-dilution assays, five-fold dilutions were plated from cultures grown at 30˚C, starting at an A_{600} of 1.0. Plates were incubated at 30˚C unless otherwise indicated for 3 days prior to digital image capture.

Plasmids. Plasmids used are listed in Table 5-3. The *KRE6* clone (pLP2014) was obtained by PCR amplification of *KRE6* from wild-type (LPY5) genomic DNA using oLP733 and oLP734. The *Hind*III-*Bam*HI digested *KRE6* PCR product was ligated to *Hind*III-*Bam*HI digested pLP1623 (pRS425, 2μ *LEU2* vector). The entire *KRE6* clone, including the entire ORF and additional 5' and 3' sequence was verified by sequencing using T3, T7, oLP834, and oLP835 oligonucleotides.

Chromatin Immunoprecipitation. Experiments were performed as described (Darst et al. 2008). Immunoprecipitation (IP) mixtures were incubated overnight at 4˚C with anti-Sir2 (Smith et al. 1998). DNA in input and IP samples was quantified by real-time PCR. Primers used are in Table 5-2. Values are IP/input normalized to *ACT1* IP/input.

Table 5-1. Yeast strains used in Chapter 5.[a]

Strain	Genotype	Source/Reference
LPY5	W303-1a *MAT***a** *ade2-1 can1-100 his3-11,15 leu2-3,112 trp1-1 ura3-1*	R. Rothstein
LPY11	W303-1a *sir2::HIS3*	
LPY79	W303-1b *MAT*α *ade2-1 can1-100 his3-11,15 leu2-3,112 trp1-1 ura3-1*	R. Rothstein
LPY2446	JS128 *MAT*α *his3*Δ*200 leu2*Δ*1 ura3-167 RDN::Ty1-mURA3*	Smith and Boeke 1997
LPY2447	JS163 *MAT*α *his3*Δ*200 leu2*Δ*1 ura3-167 sir2*Δ*2::HIS3 RDN::Ty1-mURA3*	
LPY4916	W303-1a TELVR*::URA3*	
LPY9911	W303-1a TELVR::*ADE2*	
LPY9961	W303-1b *sir2::HIS3* TELVR::*ADE2*	
LPY10074	*MAT*α *his3*Δ*200 leu2*Δ*1 ura3-167 gas1*Δ*::kanMX RDN::Ty-1-mURA3*	
LPY10078	*MAT*α *his3*Δ*200 leu2*Δ*1 ura3-167 gas1*Δ*::kanMX sir2*Δ*2::HIS3 RDN::Ty-1-mURA3*	
LPY10362	W303-1a *gas1*Δ*::kanMX* TELVR*::URA3*	
LPY10397	W303-1a *sir2::HIS3* TELVR::*URA3*	
LPY11255	W303-1a *kre6*Δ*::kanMX* TELVR::*URA3*	
LPY11263	W303-1a *kre6*Δ*::kanMX*	
LPY11264	W303-1b *kre6*Δ*::kanMX*	
LPY11265	W303-1a *kre6*Δ*::kanMX* TELVR::*URA3*	
LPY11267	W303-1a *kre6*Δ*::kanMX*	
LPY11269	W303-1a *kre6*Δ*::kanMX* TELVR::*URA3*	
LPY11324	W303-1a *kre6*Δ*::kanMX sir2::HIS3*	
LPY11325	W303-1a *kre6*Δ*::kanMX sir2::HIS3*	
LPY11326	W303-1b *kre6*Δ*::kanMX sir2::HIS3*	
LPY11327	W303-1b *kre6*Δ*::kanMX sir2::HIS3*	
LPY11545	*MAT*α *his3*Δ*200 leu2*Δ*1 ura3-167 kre6*Δ*::kanMX RDN::Ty-1-mURA3*	
LPY11548	W303-1a *kre6*Δ*::kanMX* TELVR::*ADE2*	
LPY14545	LPY4916 + pLP1623	
LPY14551	LPY4916 + pLP2014	
LPY14552	LPY10362 + pLP1623	
LPY14553	LPY10362 + pLP1951	
LPY14558	LPY10362 + pLP2014	
LPY14559	LPY11269 + pLP1623	
LPY14560	LPY11269 + pLP1951	
LPY14561	LPY11269 + pLP2014	

[a]Unless otherwise noted, strains are part of the standard lab collection or were constructed during the course of this study.

Table 5-2. Oligonucleotides used in Chapter 5.

Oligo	Name	Sequence (5' to 3')[a]	Source/Reference
	T7	TAATACGACTCACTATAGGG	
	T3	ATTAACCCTCACTAAAGGGA	
oLP733	*KRE6*-F	AACGCCAAAGAATCATCCTGAAGCGG	
oLP734	*KRE6*-R (*Bam*HI)	TAAGCATAGATTAGAGG**G**GATCCTGG	
oLP766	TEL6R-1 kb-F	GGACCTACTAGTGTCTATAGTAAGTG	Darst et al. 2008
oLP767	TEL6R-1 kb-R	CTCTAACATAACTTTGATCCTTACTCG	Darst et al. 2008
oLP778	TEL6R-0.2 kb-F	AAATGGCAAGGGTAAAAACCG	Emre et al. 2005
oLP779	TEL6R-0.2 kb-R	TCGGATCACTACACACGGAAAT	Emre et al. 2005
oLP798	*ACT1*-F1	GGTGGTTCTATCTTGGCTTC	Darst et al. 2008
oLP799	*ACT1*-R1	ATGGACCACTTTCGTCGTAT	Darst et al. 2008
oLP834	*KRE6*_seq_1	GGTATCCTGCTTCATCGTTC	
oLP835	*KRE6*_seq_2	GCTAGTACCCAAGGTGTCTG	

[a]Nucleotides in **bold** in the above sequences are mutagenic, compared to the wild-type sequence.

Table 5-3. Plasmids used in Chapter 5.[a]

Plasmid (alias)	Description	Source/Reference
pLP62 (pRS315)	vector *LEU2* CEN	Sikorski and Hieter 1989
pLP1237	SIR2 *LEU2* CEN	Garcia and Pillus 2002
pLP1623 (pRS425)	vector *LEU2* 2μ	Christianson et al. 1992
pLP1951	*GAS1 LEU2* 2μ	
pLP2014	*KRE6 LEU2* 2μ	

[a]Unless otherwise noted, plasmids are part of the standard lab collection or were constructed during the course of this study as described in Materials and Methods.

Chapter 6

Initial dissection of carbohydrate modification pathways in transcriptional silencing

INTRODUCTION

The β-1,3-glucanosyltransferase activity of Gas1 is required for transcriptional silencing at telomeres (Figure 2-11). Upstream of glucanosyltransferase activity are enzymes that synthesize β-1,3-glucan (Figure 6-1), the functionally redundant β-1,3-glucan synthases Fks1 and Gsc2/Fks2 (Douglas et al. 1994; Inoue et al. 1995; Mazur et al. 1995). Of note is the synthetic lethal phenotype of the *fks1*Δ *gsc2*Δ mutant, suggesting that the redundant function of the enzymes is essential for cell survival (Lesage et al. 2004). These enzymes are of interest because of their role in the production of Gas1's carbohydrate substrate.

Several clues in the literature from genome-wide analyses point to a link between *FKS1* and nuclear functions. Deletion of *FKS1* shows a synthetic growth defect with deletion of several genes encoding proteins with nuclear functions, including *SWI4*, which encodes a component of the SBF complex acting in G1-specific transcription, *TOP1*, which encodes a DNA topoisomerase, *SNF2*, which is required for transcription of glucose-repressed genes, and *SLT2*, involved in MAP kinase signaling and phosphorylation of the SIR complex component Sir3 (Lesage et al. 2004). In addition *fks1*Δ exhibits a synthetic growth defect with deletion or mutation of *RTT109*, a histone H3K56 acetyltransferase also implicated in the DNA

Figure 6-1. Fks1 and Pmt1 function in the same pathway as Gas1 to modify cell wall proteins. The mannosyltransferase Pmt1 attaches a mannose residue (black hexagon) to the target cell wall protein through a serine or threonine residue. The glucan synthase Fks1 produces β-1,3-glucan (white hexagon), which is attached to the previously attached mannose residue of the cell wall protein. Gas1 further modifies the β-1,3-glucan linkages of the cell wall protein through chain elongation and branching.

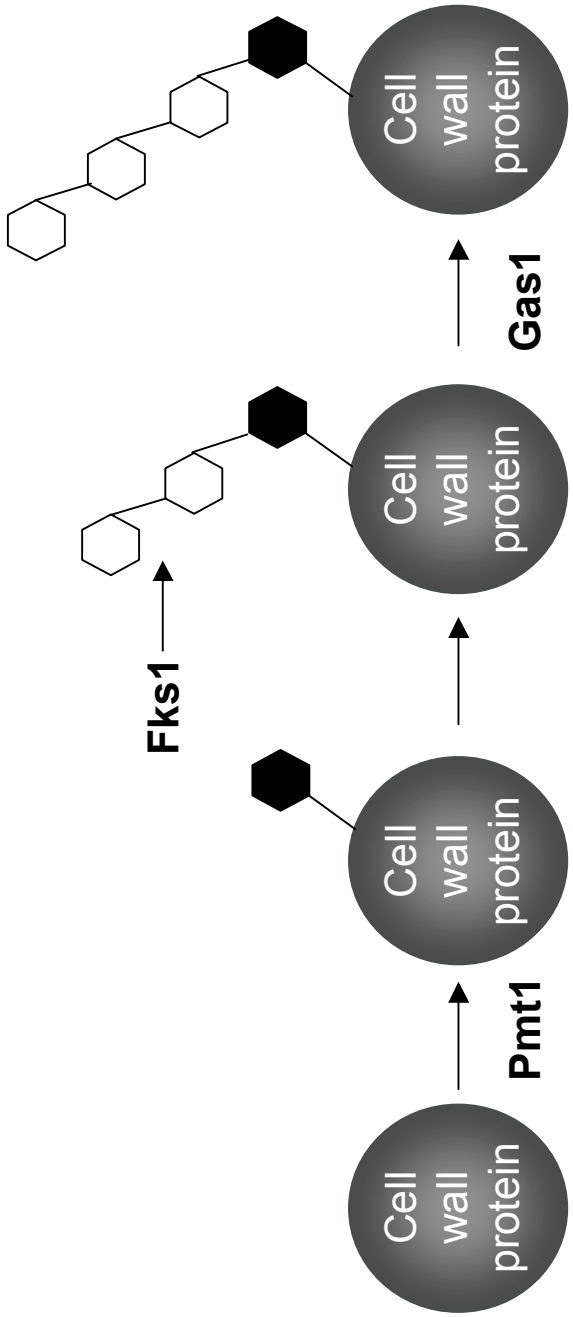
Cell wall protein
Gas1
Cell wall protein
Fks1
Cell wall protein
Pmt1
Cell wall protein

damage response (Fillingham et al. 2008), and *CDC13*, a single-stranded DNA binding protein that binds to telomeres and is necessary for telomerase activity (Addinall et al. 2008). *ZDS1* is a multicopy suppressor of an *fks1* catalytically inactive mutant (Sekiya-Kawasaki et al. 2002) that has also been linked to transcriptional silencing by negatively regulating silencing of the rDNA and cryptic mating-type loci, and positively regulating telomeric silencing (Roy and Runge 2000). In addition, the silencing protein Sir3 exhibits a decrease in phosphorylation when *ZDS1* is deleted (Roy and Runge 2000).

Whereas the synthases are responsible for β-1,3-glucan production, there are also classes of enzymes involved in the attachment of β-1,3-glucan to their protein substrates. This first requires the attachment of a mannose residue to a serine or threonine residue of the target protein (Figure 6-1). Protein-O-mannosyltransferases are the enzymes responsible for this activity. The mannosyltransferase Pmt1 is one of seven related proteins that include Pmt1-Pmt7 (Strahl-Bolsinger et al. 1993). Pmt1 acts in a complex with Pmt2 and less frequently is found in complex with Pmt3 (Girrbach and Strahl 2003). Synthetic growth defects have been reported between *pmt1*Δ and deletion of *PMT2*, *PMT3*, or *PMT4* (Gentzsch and Tanner 1996). Although the functions of the *PMT* genes appear redundant, the observation that double mutant combinations are lethal suggests that distinct combinations of mannosyltransferase activity are vital for cellular function.

A key link between the functions of *GAS1* and *PMT1* is the discovery that *pmt1*Δ is a phenotypic enhancer of *gas1*Δ (Schuldiner et al. 2005). Pmt1 was also identified as a two-hybrid interactor with histone H4, histone H2A, and histone H2B

(Krogan et al. 2006). The interaction of Pmt1 with core histones suggests that a pool of Pmt1 may reside in the nucleus or contribute to histone function after synthesis in the cytoplasm. Pmt1 also interacts by two-hybrid with the nuclear proteins Hmo1, a chromatin-associated HMG protein, and Stm1, a DNA-binding protein that may function with Cdc13 in maintenance of telomere structure (Krogan et al. 2006). Few interactions with nuclear protein genes have been uncovered for *PMT1*, but interestingly, *pmt1*Δ was identified as a suppressor of the temperature sensitive *cdc13* mutant (Addinall et al. 2008). The *gas1*Δ mutant was also identified in this screen, although it is noteworthy that almost 300 *cdc13* suppressors were found in the screen that have not been individually validated. The suppression found with *pmt1*Δ is in contrast to the synthetic growth defect noted above for *cdc13 fks1*Δ mutants.

In this analysis, for the first time, *FKS1* and *PMT1* are linked to telomeric transcriptional silencing, specifically at the telomeres. No change in silencing was observed at the rDNA locus, which is similar to *kre6*Δ (Figure 5-4) and in contrast to *gas1*Δ strains (Figure 2-1*C*). In addition, an *fks1*Δ *gas1*Δ mutant's telomeric silencing defect paralleled either single mutant, suggesting that the genes function in the same pathway in telomeric silencing. In line with the observation that *pmt1*Δ is a phenotypic enhancer of *gas1*Δ (Schuldiner et al. 2005), *gas1*Δ *pmt1*Δ strains were slower growing, more sensitive to high temperature, and were more defective in telomeric silencing than *gas1*Δ strains. These observations suggest that *FKS1* and *PMT1* may have nuclear functions with *GAS1* in transcriptional silencing, specifically at the telomeres.

RESULTS

Deletion of *FKS1* leads to a defect in silencing telomeres. The enzymatic activity of the β-1,3-glucanosyltransferase Gas1 catalyzes elongation and re-arrangement of the side chains of β-1,3-glucan. To determine whether enzymes that synthesize β-1,3-glucan also had phenotypes similar to *gas1*Δ, gene deletions were constructed for analysis of silencing phenotypes. *FKS1* encodes a β-1,3-glucan synthase. If Sir2, or another silencing factor, is modified by β-1,3-glucan, and is necessary for telomeric silencing, then *fks1*Δ deletion may result in a telomeric silencing defect similar to *gas1*Δ. *FKS1* was deleted in a strain with the *URA3* telomeric reporter on telomere V-R. The original *fks1*Δ and backcrossed *fks1*Δ strains are defective in telomeric silencing, and the defect mirrors the magnitude of the *gas1*Δ silencing defect (Figure 6-2). Unlike *gas1*Δ mutants, *fks1*Δ strains were neither slow growing nor sensitive to high temperature (Figure 6-2).

To determine whether *FKS1* and *GAS1* had additive effects on telomeric silencing, *fks1*Δ *gas1*Δ strains were constructed. The defect in telomeric silencing observed in the *fks1*Δ *gas1*Δ strains paralleled either single mutant strain (Figure 6-3). Unexpectedly, *fks1*Δ *gas1*Δ strains were slightly less sensitive to high temperature than the *gas1*Δ mutant (Figure 6-3).

The *gas1*Δ strains also demonstrate an increase in rDNA silencing (Figure 2-1*C*). Because *fks1*Δ and *gas1*Δ strains exhibited a similar defect in telomeric silencing, rDNA silencing levels were assessed in *fks1*Δ. The *fks1*Δ strains did not have

Figure 6-2. Deletion of *FKS1* leads to defects in transcriptional silencing at telomeres. Wild-type (WT) (LPY4916), *sir2*Δ (LPY10397), *gas1*Δ (LPY10362), *fks1*Δ (LPY14004), *fks1*Δ (LPY14005), WT (LPY14002), WT (LPY14003), and *fks1*Δ (LPY13927), with TELV-R::*URA3*, were plated on synthetic complete (SC) to monitor growth at 30˚C and 37˚C, and on SC containing 5-FOA to monitor telomeric silencing at 30˚C. LPY14002-LPY14005 are a complete tetrad from a backcross of the original *fks1*Δ deletion transformant strain (LPY13927).

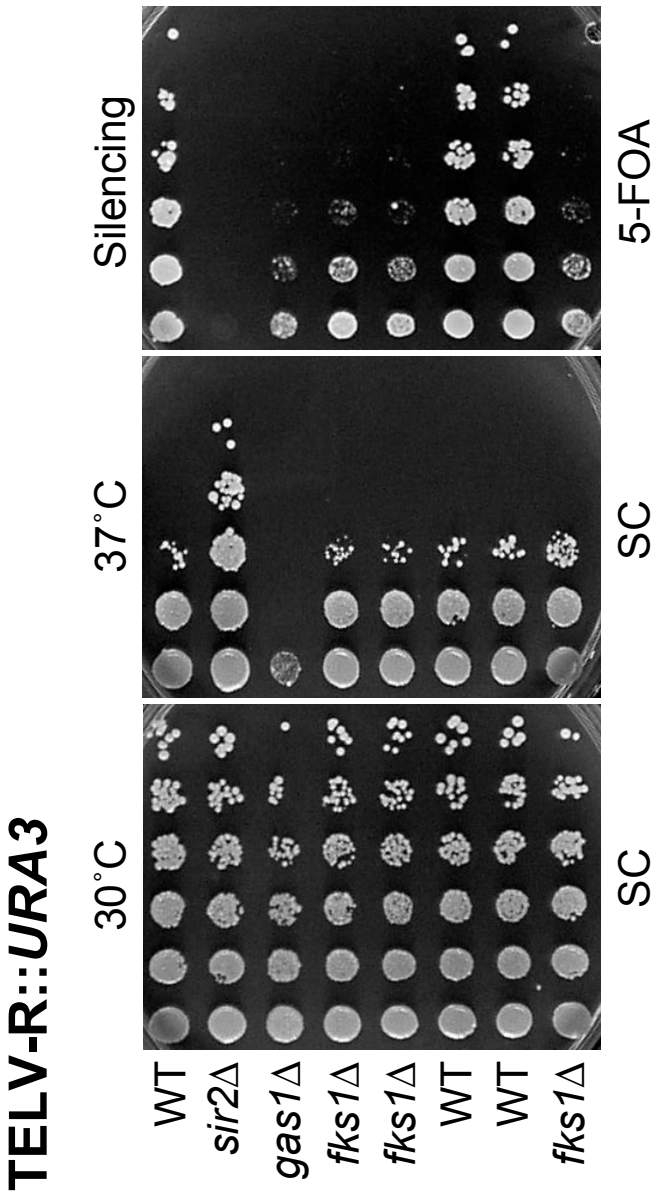
TELV-R::URA3
30˚C
37˚C
Silencing
WT
sir2Δ
gas1Δ
fks1Δ
fks1Δ
WT
WT
fks1Δ
SC
SC
5-FOA

Figure 6-3. Deletion of *FKS1* partially suppresses *gas1*Δ temperature sensitivity but does not alter *gas1*Δ's telomeric silencing defect. WT (LPY4916), *sir2*Δ (LPY10397), *gas1*Δ (LPY10362), *fks1*Δ (LPY14004), *fks1*Δ *gas1*Δ (LPY14451), *fks1*Δ *gas1*Δ (LPY14450), *fks1*Δ *gas1*Δ (LPY14446), all containing TELV-R::*URA3*, and *fks1*Δ *gas1*Δ without the reporter (*fks1*Δ *gas1*Δ *ura3-1*) (LPY14447) were plated on SC to monitor growth at 30˚C and 37˚C and on SC containing 5-FOA to monitor silencing at 30˚C.

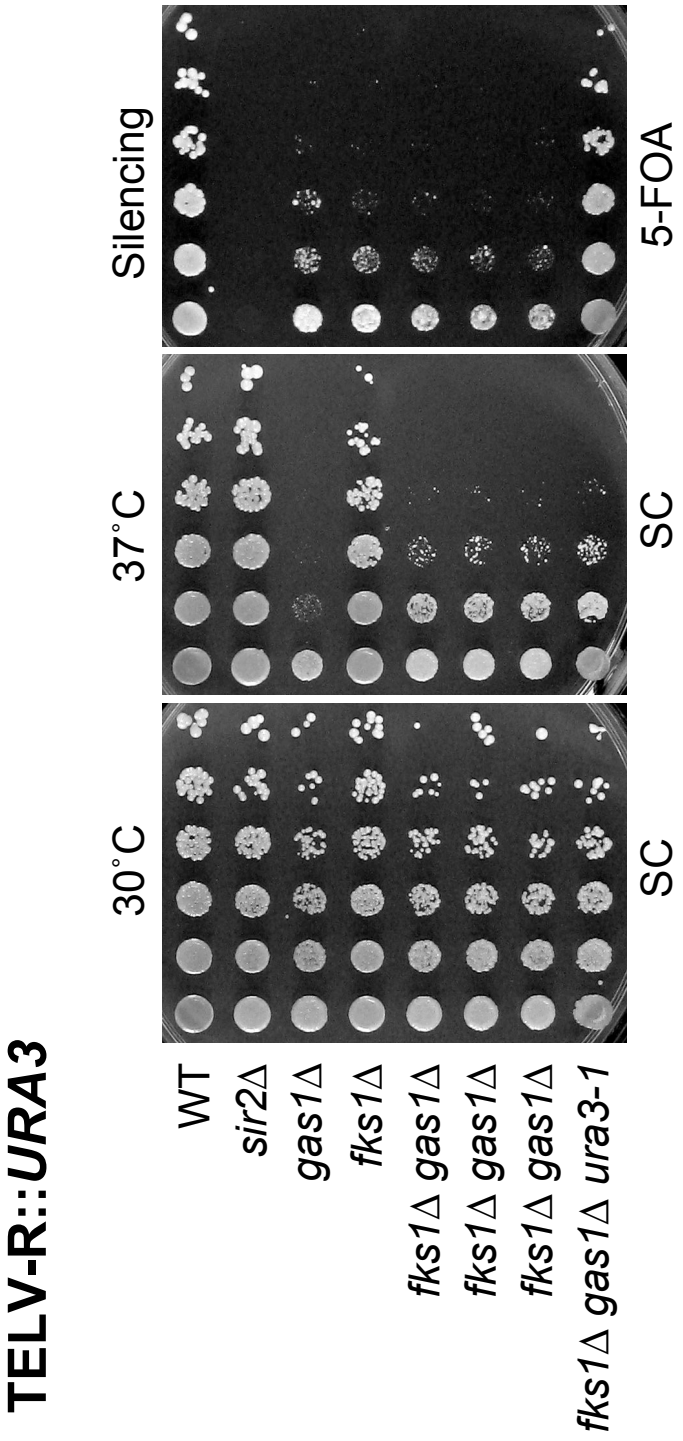
TELV-R::URA3
30˚C
37˚C
Silencing
WT
sir2Δ
gas1Δ
fks1Δ
fks1Δ gas1Δ
fks1Δ gas1Δ
fks1Δ gas1Δ
fks1Δ gas1Δ ura3-1
SC
SC
5-FOA

enhanced rDNA silencing. Instead the level of silencing was decreased slightly compared to wild-type (Figure 6-4).

Deletion of *PMT1* decreases telomeric silencing and enhances *gas1*Δ phenotypes, including its defect in telomeric silencing. The β-1,3-glucan modification is not attached directly to a protein substrate, but is instead joined to a previously attached mannose residue. It is likely that a similar sequence of modification is required for the potential modification of nuclear proteins if they occur. Pmt1 is one of several mannosyltransferases in yeast. To test for telomeric silencing defects, *PMT1* was deleted in a strain with the *URA3* telomeric reporter on telomere V-R. The original *pmt1*Δ and backcrossed *pmt1*Δ strains displayed a variable small decrease in telomeric silencing (Figure 6-5). Unlike *gas1*Δ mutants, *pmt1*Δ strains were not slow growing and not sensitive to high temperature (Figure 6-5). Similar to *fks1*Δ, *pmt1*Δ strains did not exhibit increased rDNA silencing, instead silencing was slightly decreased relative to levels observed in the wild-type strain (Figure 6-4).

To determine whether *PMT1* and *GAS1* had additive effects on telomeric silencing, *gas1*Δ *pmt1*Δ strains were constructed. Deletion of *PMT1* enhanced the telomeric silencing defect of *gas1*Δ (Figure 6-6). In line with this observation, *pmt1*Δ also enhanced the slow growth and temperature sensitivity of *gas1*Δ strains (Figure 6-6).

Figure 6-4. Deletion of *FKS1* or *PMT1* does not increase silencing in the rDNA. WT (LPY2446), *sir2*Δ (LPY2447), *gas1*Δ (LPY10074), *gas1*Δ *sir2*Δ (LPY10078), *fks1*Δ (LPY13938), *fks1*Δ (LPY13939), *pmt1*Δ (LPY13940), and *pmt1*Δ (LPY13941), all containing *RDN::URA3* were plated at 30˚C on SC to monitor growth and on SC-uracil (SC-ura) to monitor rDNA silencing.

RDN::mURA3

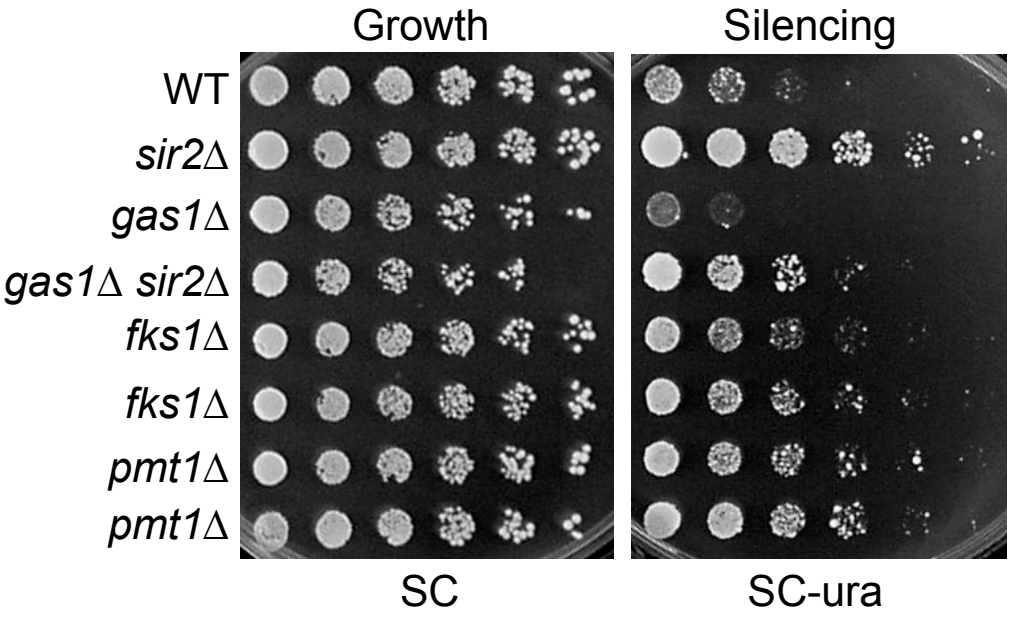
Growth
Silencing
WT
sir2Δ
gas1Δ
gas1Δ sir2Δ
fks1Δ
fks1Δ
pmt1Δ
pmt1Δ
SC
SC-ura

Figure 6-5. Deletion of *PMT1* leads to slight, variable, telomeric silencing defects. Wild-type (WT) (LPY4916), *sir2*Δ (LPY10397), *gas1*Δ (LPY10362), *pmt1*Δ (LPY14011), *pmt1*Δ (LPY14013), WT (LPY14012), WT (LPY14014), and *pmt1*Δ (LPY13929), all containing TELV-R::*URA3* were plated on SC to monitor growth at 30˚C and 37˚C, and on SC containing 5-FOA to monitor telomeric silencing at 30˚C. LPY14011-LPY14014 are a complete tetrad from a backcross of the original *pmt1*Δ deletion transformant strain (LPY13929).

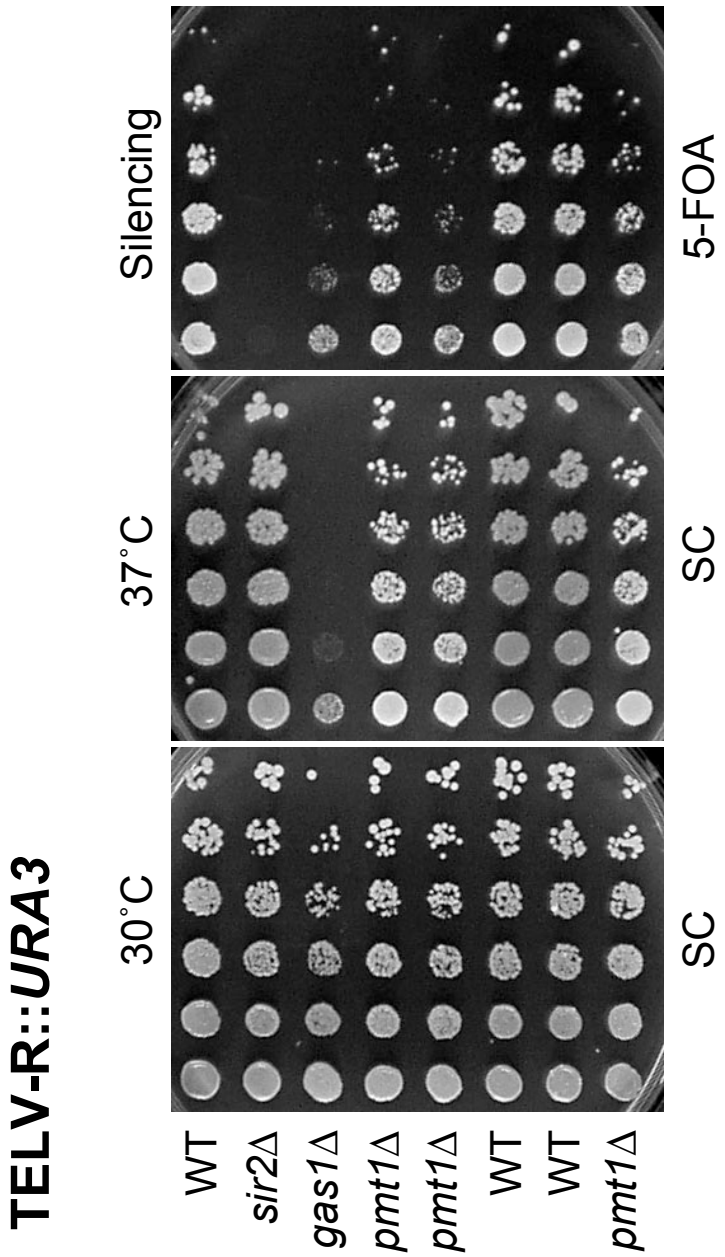
TELV-R::URA3
30˚C
37˚C
Silencing
WT
sir2Δ
gas1Δ
pmt1Δ
pmt1Δ
WT
WT
pmt1Δ
SC
SC
5-FOA

Figure 6-6. Deletion of *PMT1* exacerbates *gas1*Δ slow growth, temperature sensitivity, and telomeric silencing defects. WT (LPY4916), *sir2*Δ (LPY10397), *gas1*Δ (LPY10362), *pmt1*Δ (LPY14011), *pmt1*Δ (LPY14454), *gas1*Δ *pmt1*Δ (LPY14455), *gas1*Δ *pmt1*Δ (LPY14456), all containing TELV-R::*URA3*, and *pmt1*Δ without the reporter (*pmt1*Δ *ura3-1*) (LPY14458) were plated on SC to monitor growth at 30˚C and 37˚C and on SC containing 5-FOA to monitor silencing at 30˚C.

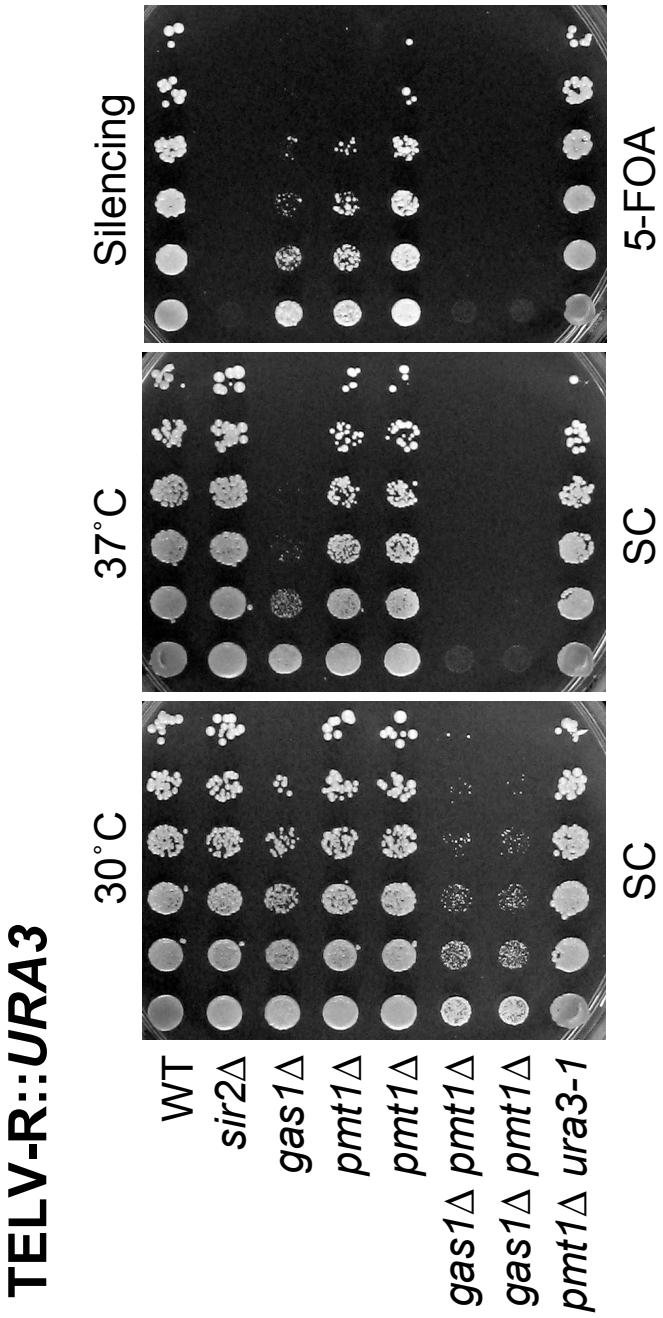
TELV-R::URA3
30˚C
37˚C
Silencing
WT
sir2Δ
gas1Δ
pmt1Δ
pmt1Δ
gas1Δ pmt1Δ
gas1Δ pmt1Δ
pmt1Δ ura3-1
SC
SC
5-FOA

DISCUSSION

The telomeric silencing defects observed upon deletion of *FKS1* and *PMT1* point to a role for their encoded proteins in transcriptional silencing. *FKS1* encodes a β-1,3-glucan synthase and is redundant with the alternate catalytic subunit Gsc2/Fks2. This enzymatic activity is required for the production of the carbohydrate substrate of Gas1's catalytic activity. If the β-1,3-glucan modification of Sir2, or other silencing proteins, is important for silencing, then loss of the enzyme producing the substrate, Fks1 or Gsc2/Fks2, may result in defective silencing (Figure 6-7). It will be necessary to examine *gsc2*Δ mutants in the future to establish whether these mutants also exhibit telomeric silencing defects, or if the defect is specific to *fks1*Δ strains.

PMT1 is a member of a family of mannosyltransferases that include six other *PMT* genes. In addition, at least twenty other proteins in budding yeast have annotated mannosyltransferase activity. When *PMT1* was deleted, a variable telomeric silencing defect was observed (Figure 6-5). Deletion of *PMT1* also enhanced the *gas1*Δ telomeric silencing defect, however this effect was not specific to telomeric silencing since enhancement of *gas1*Δ slow growth and temperature sensitivity was also observed (Figure 6-6). This observation shows that Pmt1 function is protective for slow growth and telomeric silencing in the absence of *GAS1*. The enhancement of telomeric silencing seen in *gas1*Δ *pmt1*Δ mutants indicates that Gas1 and Pmt1 may function in parallel pathways to promote telomeric silencing. This leads to the hypothesis that Pmt1 functions in the modification of not only cell wall proteins, but also of nuclear target proteins, such as Sir2 or other silencing proteins, by attachment

Figure 6-7. A model for how Fks1 and Pmt1 function with Gas1 to strengthen telomeric silencing through modification of Sir2 or a Sir2-interacting factor. The mannosyltransferase Pmt1 attaches a mannose residue (black hexagon) to Sir2 (or Sir2-interacting factor, shown as light gray circles surrounding Sir2). The glucan synthase Fks1 produces β-1,3-glucan (white hexagon) which becomes attached to the previously attached mannose residue. The glucanosyltransferase Gas1 then further alters the β-1,3-glucan modification of Sir2 (or Sir2-interacting factor). This carbohydrate modification of Sir2 enhances the protein's function in telomeric silencing. Likewise, loss of Pmt1 leads to exacerbated growth and silencing defects in *gas1*Δ mutants. This may reflect a partially protective effect of mannose modification, even in the absence of Gas1's glucanosyltranferase activity in this pathway.

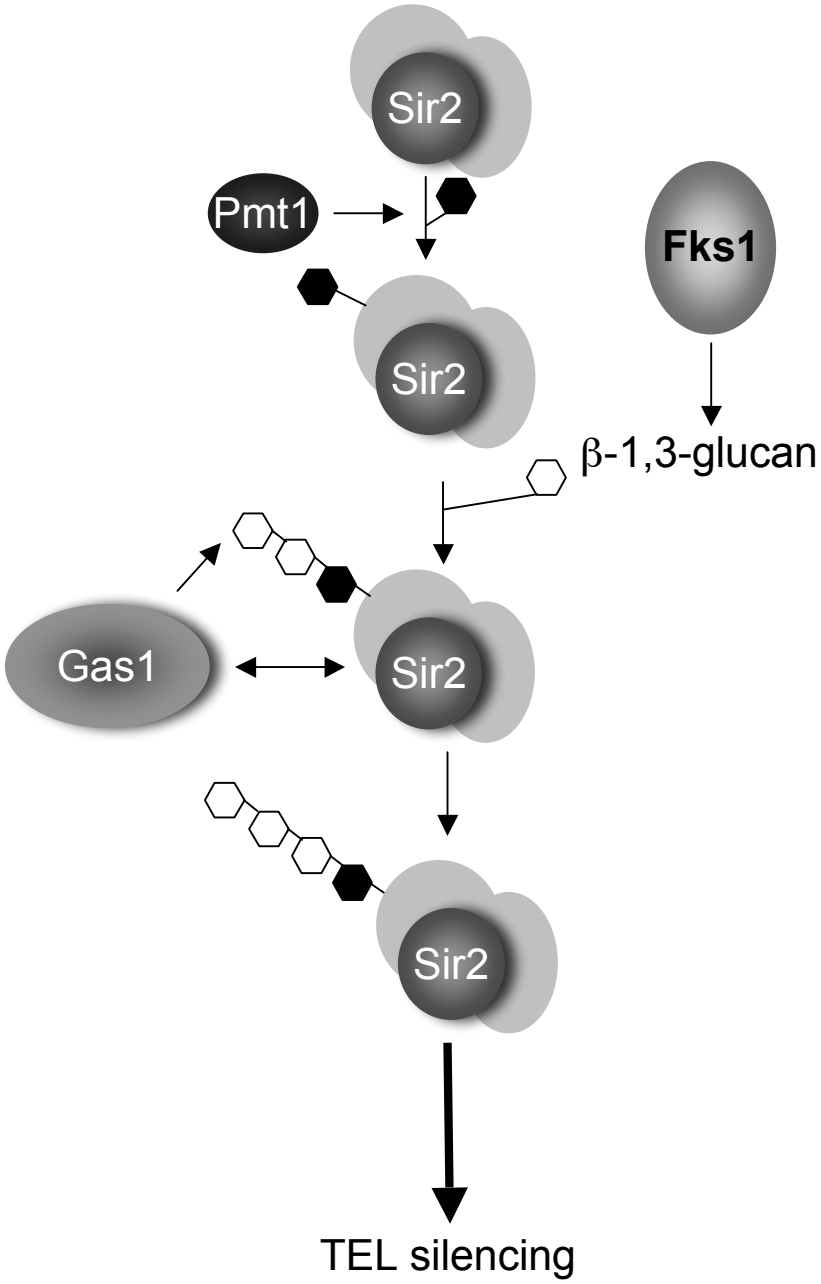
Sir2
Pmt1
Fks1
Sir2
β-1,3-glucan
Gas1
Sir2
Sir2
TEL silencing

of a mannose residue (Figure 6-7). This attachment is necessary for the sequential attachment of β-glucan. Future experiments could utilize antibodies that recognize mannose to determine if this is a modification of chromatin, Sir2, or Sir2 interacting factors. If this modification of a nuclear target protein were required for telomeric silencing, than the absence of mannosyltransferase activity would be expected to result in a defect in telomeric silencing. Since *PMT1* has multiple closely related homologs, it will be crucial to examine telomeric silencing in other *pmt* mutants and in strains with deletion of the many additional genes encoding mannosyltransferase activity. This analysis will determine whether telomeric silencing function is specific to Pmt1 or is common to all mannosyltransferases.

Deletion of *FKS1* or *PMT1* led to transcriptional silencing defects at telomeres, and no change in silencing of the rDNA. *HM* loci silencing has not been assessed in these mutants, but they do not have gross mating defects since spores recovered from crosses are mating-competent. To follow up on this initial characterization of *FKS1* and *PMT1* in transcriptional silencing at telomeres, analyses similar to that completed for *GAS1* should be pursued. This includes determining whether SIR complex proteins, Sir2, Sir3, and Sir4, are bound to telomeres in *fks1*Δ and *pmt1*Δ strains. Analysis of H4K16 acetylation levels at telomeres in these mutants should also be evaluated since defective telomeric silencing is normally associated with an increase in H4K16 acetylation. To determine whether *FKS1* and *PMT1* contribute to the interaction between β-glucan and Sir2 in the β-1,3-glucan immunoprecipitation, the experiment should be repeated in *fks1*Δ and *pmt1*Δ mutant strains. If Sir2 is not immunoprecipitated in the mutants, this will further support the conclusion that *FKS1*

and *PMT1* function in transcriptional silencing at the telomeres with *GAS1*. Another potential line of future investigation is analysis of *fks1*Δ *pmt1*Δ mutants and combinations of *fks1*Δ and *pmt1*Δ mutants with deletion of *SIR* genes to determine whether additional phenotypes or genetic interactions are uncovered. Discovery of telomeric silencing phenotypes for glucan producing and linking enzymes points to direct involvement of these protein families in transcriptional silencing. Further genetic analysis of these gene families with other silencing genes will more precisely define their role in silencing and relation to other silencing factors that may be modified by carbohydrate residues.

MATERIALS AND METHODS

Yeast strains and methods. Yeast strains are listed in Table 6-1. Strains were constructed during this study unless otherwise noted and grown at 30˚C with standard manipulations (Amberg et al. 2005). Deletion mutants were created with standard methods and oligonucleotide sequences of primers used are in Table 6-2. Synthetic selective media were prepared as described (Sherman 1991). 5-fluoroorotic acid (5-FOA; United States Biological, Inc., Swampscott, MA) was added at 0.1% to test for *URA3* reporter gene expression. Telomeric silencing assays were performed as described previously (van Leeuwen and Gottschling 2002). For serial-dilution assays, five-fold dilutions were plated from cultures grown at 30˚C, starting at an A_{600} of 1.0. Plates were incubated at 30˚C unless otherwise indicated for 3 days prior to digital image capture.

Table 6-1. Yeast strains used in Chapter 6.[a]

Strain	Genotype	Source/Reference
LPY5	W303-1a *MAT***a** *ade2-1 can1-100 his3-11,15 leu2-3,112 trp1-1 ura3-1*	R. Rothstein
LPY79	W303-1b *MAT*α *ade2-1 can1-100 his3-11,15 leu2,3,112 trp1-1 ura3-1*	R. Rothstein
LPY2446	JS128 *MAT*α *his3*Δ*200 leu2*Δ*1 ura3-167 RDN::Ty1-mURA3*	Smith and Boeke 1997
LPY2447	JS163 *MAT*α *his3*Δ*200 leu2*Δ*1 ura3-167 sir2*Δ*2::HIS3 RDN::Ty1-mURA3*	
LPY4916	W303-1a TELVR*::URA3*	
LPY10074	*MAT*α *his3*Δ*200 leu2*Δ*1 ura3-167 gas1*Δ*::kanMX RDN::Ty-1-mURA3*	
LPY10078	*MAT*α *his3*Δ*200 leu2*Δ*1 ura3-167 gas1*Δ*::kanMX sir2*Δ*2::HIS3 RDN::Ty-1-mURA3*	
LPY10362	W303-1a *gas1*Δ*::kanMX* TELVR*::URA3*	
LPY10397	W303-1a *sir2::HIS3* TELVR::*URA3*	
LPY13927	W303-1a *fks1*Δ*::kanMX* TELVR::*URA3*	
LPY13929	W303-1a *pmt1*Δ*::kanMX* TELVR::*URA3*	
LPY13938	*MAT*α *his3*Δ*200 leu2*Δ*1 ura3-167 fks1*Δ*::kanMX RDN::Ty1-mURA3*	
LPY13939	*MAT*α *his3*Δ*200 leu2*Δ*1 ura3-167 fks1*Δ*::kanMX RDN::Ty1-mURA3*	
LPY13940	*MAT*α *his3*Δ*200 leu2*Δ*1 ura3-167 pmt1*Δ*::kanMX RDN::Ty1-mURA3*	
LPY13941	*MAT*α *his3*Δ*200 leu2*Δ*1 ura3-167 pmt1*Δ*::kanMX RDN::Ty1-mURA3*	
LPY14002	W303-1a TELVR::*URA3*	
LPY14003	W303-1b TELVR::*URA3*	
LPY14004	W303-1a *fks1*Δ*::kanMX* TELVR::*URA3*	
LPY14005	W303-1b *fks1*Δ*::kanMX* TELVR::*URA3*	
LPY14011	W303-1a *pmt1*Δ*::kanMX* TELVR::*URA3*	
LPY14012	W303-1b TELVR::*URA3*	
LPY14013	W303-1b *pmt1*Δ*::kanMX* TELVR::*URA3*	
LPY14014	W303-1a TELVR::*URA3*	
LPY14446	W303-1b *fks1*Δ*::kanMX gas1*Δ*::kanMX* TELVR::*URA3*	
LPY14447	W303-1a *fks1*Δ*::kanMX gas1*Δ*::kanMX*	
LPY14450	W303-1b *fks1*Δ*::kanMX gas1*Δ*::kanMX* TELVR::*URA3*	
LPY14451	W303-1a *fks1*Δ*::kanMX gas1*Δ*::kanMX* TELVR::*URA3*	
LPY14454	W303-1a *pmt1*Δ*::kanMX* TELVR::*URA3*	
LPY14455	W303-1a *gas1*Δ*::kanMX pmt1*Δ*::kanMX* TELVR::*URA3*	
LPY14456	W303-1b *gas1*Δ*::kanMX pmt1*Δ*::kanMX* TELVR::*URA3*	
LPY14458	W303-1a *pmt1*Δ*::kanMX*	

[a]Unless referenced, strains are from the lab collection or were created for this study.

Table 6-2. Oligonucleotides used in Chapter 6.

Oligo	Name	Sequence (5’ to 3’)
oLP1111	*FKS1*-F	CGCGTCCTTGTACTGCGTCTAACG
oLP1112	*FKS1*-R	CGTTGGGGCTCGCAACTATCTAGC
oLP1113	*PMT1*-F	CTCGCGCAATTTGTCCTTTGC
oLP1114	*PMT1*-R	CGGTTGCATATAGCATTGCC

Chapter 7

Future Directions

The goal of this thesis was to further understand chromatin and the regulation of transcriptional silencing through the analysis of novel silencing factors. This analysis led to a proposed role for carbohydrate modification in the regulation of silencing. Carbohydrate modification, particularly β-glucan, has been studied at two levels. The first well-studied role is its function as a structural component of fungi cell walls (Lesage and Bussey 2006). β-glucans have also been studied as stimulants of the immune system in humans (Mantovani et al. 2008).

The research in this thesis points to a new nuclear role for β-glucans and other carbohydrate modifications in influencing chromatin and transcription. The genes encoding the enzymes under study are all members of gene families with multiple members. Thus, much remains to be done to understand the affect of carbohydrate modifications on nuclear functions. Some specific possibilities and high priorities for studies to extend the findings reported here are noted below.

The function of *GAS1* in transcriptional silencing. In Chapter 2, the characterization of *GAS1*'s role in silencing is described. In analysis of *gas1*Δ mutant phenotypes, disrupted telomeric silencing and enhanced rDNA silencing is seen (Figure 2-1). Although telomeric silencing is disrupted, the SIR complex is telomere-bound (Figure 2-6*B*, 2-7*A*, 4-1) and targets of Sir2-mediated deacetylation, histone H3K56 and H4K16, are deacetylated (Figure 2-6*C*, 2-6*D*). This leads to the hypothesis that some other component crucial for silent chromatin is disrupted in *gas1*Δ mutants.

Additional Sir2 histone targets may remain to be uncovered since all acetylatable histone lysines are deacetylated in silent chromatin (Suka et al. 2001) and Sir2 also targets histone H3K9 and H3K14 *in vitro* (Imai et al. 2000; Tanny and Moazed 2001). H3K56 is a recently identified substrate for Sir2 activity (Xu et al. 2007), so there may be additional acetylated histone lysines modified by Sir2 that are not yet known. The loss of deacetylation of one of these potential Sir2 histone substrates may explain the telomeric silencing defect in *gas1*Δ mutants. There are also a number of other critical histone modifications not regulated by Sir2 that are implicated in silent chromatin, such as histone methylation and ubiquitination (reviewed in Shilatifard 2006). It is possible that other histone modifications that remain to be pursued are altered in *gas1*Δ mutants.

Sir2 is the founding member of a family of sirtuin genes that is conserved from archaea and eubacteria through vertebrates (Brachmann et al. 1995). Non-histone substrates, such as p53 and tubulin, have been identified for the human homologs of Sir2 (reviewed in Buck et al. 2004). Non-histone substrates of yeast Sir2 have been more elusive until recently, when Sir2 was shown to deacetylate the phosphoenolpyruvate carboxykinase Pck1, both *in vivo* and *in vitro* (Lin et al. 2009). Although Pck1 has not been previously implicated in transcriptional silencing, it is possible that it, or other another yet unidentified Sir2 non-histone substrate, is required for silencing. If the acetylation of these Sir2 substrates is lost in *gas1*Δ mutants, this will augment the model for *GAS1*'s function in telomeric silencing.

Instead of affecting Sir2 deacetylase function, Gas1 may function in telomeric silencing through its own catalytic activity. Gas1 β-1,3-glucanosyltransferase activity

is required for cell wall biogenesis, and also for telomeric silencing (Figure 2-11*A*). These two distinct functions are separable (Figure 2-10*B*), so *gas1*Δ telomeric silencing defects are not a consequence of loss of cell wall biogenesis. Additionally, an antibody directed against the carbohydrate substrate of Gas1 activity, β-1,3-glucan, immunoprecipitates Sir2 (Figure 2-11*B*). Determining whether β-1,3-glucan is directly linked to Sir2 or if the interaction is bridged through another protein is a high priority for future exploration. The interaction remains in *sir3*Δ *sir4*Δ mutants, therefore it is not bridged through the SIR complex (Figure 2-10*C*). It will be necessary to assess whether the interaction exists when other Sir2-interacting proteins, such as Kre6 and Ktr4, are eliminated (Garcia 2003).

The potential β-1,3-glucan modification of Sir2 was further analyzed by zymolyase or β-1,3-glucanase treatment of protein extracts to determine if an electrophoretic shift of Sir2 is observed. The experiments completed did not uncover a shift for Sir2, instead most of Sir2 disappeared under zymolyase treatment, caused by presence of proteases in the commercially available zymolyase (Figure 4-8 – Figure 4-11). This line of experimentation remains a possibility for the analysis of Sir2 modification. In future experiments, purified enzymes should be tested for hydrolysis of β-1,3-glucan from Sir2, or a Sir2 interacting protein. This could be done by enzyme treatments of material from Sir2 purifications from yeast, for example using a TAP tagged Sir2. Treating the purified Sir2, which should also contain interacting proteins, with β-1,3-glucanase to catalyze the breakdown of β-1,3-glucan should allow for detection of electrophoretic differences under enzyme treatment, for Sir2 and other interacting proteins.

Histones remain a potential target of modification with β-1,3-glucan. Early studies showed glycosylation of histones (Levy-Wilson 1983), so other carbohydrate modifications of histones may be possible. Immunoprecipitations with β-1,3-glucan should be analyzed for presence of histone proteins in the immunoprecipitated material. Additionally, chromatin immunoprecipitation with the β-1,3-glucan antibody has been considered but not attempted because of the lack of necessary positive and negative controls for the experiment. However, β-1,3-glucan may be associated with silent chromatin. Optimistically, future advances in techniques could be used to investigate whether β-1,3-glucan is chromatin-bound through genome-wide analysis.

Other carbohydrate modification enzymes are involved in transcriptional silencing. The initial characterization of the roles of three other enzymes, Kre6, Fks1, and Pmt1, in transcriptional silencing has been accomplished. Kre6, a Sir2 two-hybrid interacting protein, is a β-1,6-glucan synthase. Since Kre6's enzymatic activity functions in synthesizing a glucose polymer similar to Gas1's carbohydrate substrate, it was hypothesized that Kre6 also functions in silencing. In the evaluation of *kre6*Δ mutants, a telomeric silencing defect is seen (Figure 5-1). This observation leads to the hypothesis that Kre6 function is important for silencing, but whether the enzyme acts directly in silencing is not currently known. Kre6's silencing function may be in the same pathway as Gas1 since Sir2 remains telomere-bound in both *gas1*Δ and *kre6*Δ mutants despite their loss of telomeric silencing (Figure 2-6*B*, 5-3). In addition, a synthetic sick interaction is seen in *kre6*Δ *sir2*Δ mutants (Figure 5-5), which points to Kre6 fulfilling a critical role in the cell in the absence of Sir2. Since silencing is lost in *sir2*Δ mutants, it is realistic to predict that this critical Kre6 role is in a function other

than silencing, such as in cell wall biogenesis, or other yet unidentified Kre6 cellular roles.

Fks1 synthesizes the β-1,3-glucan carbohydrate substrate for Gas1 enzymatic activity. Since β-1,3-glucan modification is required for silencing and may be linked to Sir2 or other chromatin proteins (Figure 2-11), it was hypothesized that loss of the enzyme producing β-1,3-glucan would result in defective silencing. Indeed, *fks1*Δ mutants are defective (Figure 6-1). No exacerbation of the telomeric silencing defect is seen in *fks1*Δ *gas1*Δ mutants (Figure 6-2), reinforcing the model that the proteins function in the same pathway, with Fks1 activity upstream of Gas1. Since a homolog of Fks1, Gsc2/Fks2, functions redundantly with Fks1, *gsc2*Δ mutants should be analyzed in future studies to determine whether the telomeric silencing defect observed in *fks1*Δ is shared when another β-1,3-glucan synthase is absent.

The activity of mannosyltranferases is also upstream of Gas1 enzymatic activity. Mannosyltransferases transfer a mannose residue to a target protein through a serine or threonine residue. Then, glucose polymer, such as β-1,3-glucan, can be added to the target protein (Figure 6-1). If the same series of events is required for β-1,3-glucan modification of nuclear target proteins, such as Sir2, then there may be a mannosyltransferase fulfilling this role in the nucleus. Although not yet characterized, a putative mannosyltransferase, Ktr4, was identified as an interacting protein of the Sir2 core domain two-hybrid construct (Garcia 2003). Interestingly, the Ktr4-Sir2 two-hybrid interaction is lost in a construct expressing catalytically inactive *sir2-H364Y* (Table A-3, Figure A-5). The observation that the interaction disappears when Sir2 deacetylase activity is absent suggests that the interaction may be mediated through

Sir2's catalytic core domain, and that Ktr4 may be a substrate of Sir2's catalytic activity, and/or involved in the regulation of Sir2 deacetylase activity. Analysis of *KTR4* in transcriptional silencing and additional experiments addressing Ktr4's physical association with Sir2 is a relevant subject for future research.

Another mannosyltransferase, Pmt1, was reported to interact with nuclear proteins, such as histones, in a high-throughput mass spectrometric study to identify protein complexes (Krogan et al. 2006). Because of its interaction with multiple core histone proteins, Pmt1 was analyzed for a nuclear role in transcriptional silencing. The *pmt1*Δ mutants had a variable, modest, decrease in telomeric silencing (Figure 6-5). The deletion of *PMT1* also exacerbated the *gas1*Δ telomeric silencing defect, as well as its slow growth and temperature sensitivity (Figure 6-6). This suggests that *GAS1* and *PMT1* function in separate pathways to promote telomeric silencing. Therefore the pathway in which mannosyltransferase activity functions in telomeric silencing may be protective for telomeric silencing in *GAS1*'s absence. However, with the loss of both Gas1 and Pmt1 proteins, telomeric silencing is completely lost. It will be crucial to determine whether other mannosyltranferases, such as other Pmt proteins, also function in transcriptional silencing, or if silencing function is Pmt1-specific.

To further address the role of *KRE6*, *FKS1*, and *PMT1* in transcriptional silencing, the same analysis completed for *GAS1* should be pursued. First, complete chromatin immunoprecipitation analysis of SIR complex binding and telomeric histone modifications should address whether silent chromatin is disrupted at the level of SIR complex recruitment to telomeres, or deacetylation of histones by Sir2 in *kre6*Δ, *fks1*Δ, and *pmt1*Δ mutants. If these chromatin marks appear normal, it will be

important to establish whether any of the three genes are required for anti-β-1,3-glucan immunoprecipitation of Sir2. If this co-precipitation interaction were lost in one of the mutants, it would suggest that the gene in question encodes a protein that is required for the β-1,3-glucan modification of Sir2, or of a Sir2-interacting factor.

If supporting evidence is obtained from the additional analysis suggested here, this will further illustrate a direct role for carbohydrate modifying enzymes in transcriptional silencing and open a new line of investigation into the function of carbohydrate modification in transcriptional regulation. O-linked beta-N-acetylglucosamine (O-GlcNAc) modification of nuclear proteins in mammalian cells has a critical transcriptional role (reviewed in Hart et al. 2007; Bouwman and Philipsen 2002). Although O-GlcNAc modification has not been observed in yeast, it is possible that β-1,3-glucan or related modifications may serve as its replacement in yeast, fulfilling a similar role in regulation of transcription and other nuclear functions.

Appendix A

Two-hybrid analysis of Sir2-interacting proteins with Sir2 family members and catalytically inactive sir2-H364Y

Two-hybrid analysis of Hst2 with Sir2-interacting proteins: Gas1 and Dps1 interact with full-length Hst2. To further understand the function and regulation of the protein deacetylase Sir2 in functions beyond transcriptional silencing, a Sir2 two-hybrid screen was previously completed (Garcia 2003). Twenty unique Sir2 interacting proteins were found, of which one only interacted with a nearly full-length Sir2 construct, eighteen only interacted with a core domain Sir2 construct, and one interacted with both Sir2 constructs (Garcia 2003). Sir2 is the founding member of a family of sirtuin genes, conserved through humans (Brachmann et al. 1995). Four other sirtuin genes are found in budding yeast.

To determine the specificity of the interactions between Sir2 and these interacting proteins, directed two-hybrid analysis was done to detect interactions of these proteins with the Sir2 homolog Hst2. A normally cytoplasmic protein, Hst2 is actively transported from the nucleus (Wilson et al. 2006b). Substrates of Hst2 deacetylase activity are not currently identified. Hst2 two-hybrid analysis of Sir2-interacting proteins revealed a subset of proteins that also interact with Hst2 (Table A-1). Two proteins exhibited strong interactions with full-length Hst2, Gas1 (Figure A-1*A*) and Dps1 (Figure A-1*B*). Weak interactions were also observed with Ade6, Adh4, Gln1, Luc7, Pub1, and Slx5. Gas1's interaction with Sir2 and role in transcriptional silencing is presented in Chapter 2-4.

Table A-1. Two-hybrid analysis of Sir2 family members with full-length Hst2[a]

Plasmid	Protein	SC-his-leu-ura + 3-AT[b]	SC-ade-his-leu-ura
pLP1203	Pub1	-	+
pLP1204	Kre6	-	-
pLP1205	Gas1	++	++
pLP1206	Cda2	-	-
pLP1207	Pph22	-	-
pLP1208	Luc7	+	-
pLP1209	Tfp1	-	-
pLP1210	Pat1	-	-
pLP1211	Vma2	-	-
pLP1212	Slx5	++	-
pLP1213	Ktr4	-	-
pLP1214	Adh4	-	+
pLP1217	Ade6	-	+
pLP1218	Gln1	++	-
pLP1220	Arg4	-	-
pLP1221	Dps1	++	++
pLP1222	Tkl1	-	-
pLP1223	Plb1	-	-
pLP1224	Pho11	-	-
pLP1228	Aim25	-	-

[a]++ = strong interaction, + = weak interaction, - = no interaction
[b]SC-leu-ura-his + 3-AT plates measure interactions that activate a single reporter, *HIS3*. 3-AT addition reduces background on these plates.

Figure A-1. Full-length Hst2 interacts with Gas1 and Dps1 by two-hybrid. *(A)* Gas1 interacts with Hst2 by two-hybrid. The two-hybrid strain LPY3374 (PJ69-4A) (James et al. 1996) was transformed with the following sets of plasmids, starting with the top left strain on the plate: pLP1205 (GAD-*GAS1*), pLP1161 (GBD-*HST2*); pLP1204 (GAD-*KRE6*), pLP1161; pLP1203 (GAD-*PUB1*), pLP1161; pLP1206 (GAD-*CDA2*), pLP959 (pGBDU-C1); pLP1207 (GAD-*PPH22*), pLP1161; and pLP1206, pLP1161. Plate shown is the two-hybrid interaction specific to Gas1 and Hst2, assayed on SC plates lacking adenine, histidine, leucine, and uracil (SC-ade-his-leu-ura). Growth control selected for growth of both plasmids on SC-leu-ura (not shown). Positive controls of Sir2 interactions were completed simultaneously on SC lacking adenine, histidine, leucine, and tryptophan (SC-ade-his-leu-trp). *(B)* Dps1 interacts with Hst2 by two-hybrid. LPY3374 was transformed with the following sets of plasmids, starting with the top left strain on the plate: pLP1218 (GAD-*GLN1*), pLP1161 (GBD-*HST2*); pLP1217 (GAD-*ADE6*), pLP1161; pLP1214 (GAD-*ADH4*), pLP1161; pLP1220 (GAD-*ARG4*), pLP959 (pGBDU-C1); pLP1221 (GAD-*DPS1*), pLP1161; and pLP1220, pLP1161. Plate shown is the two-hybrid interaction specific to Gas1 and Hst2, assayed as in *(A)* on SC-ade-his-leu-ura.

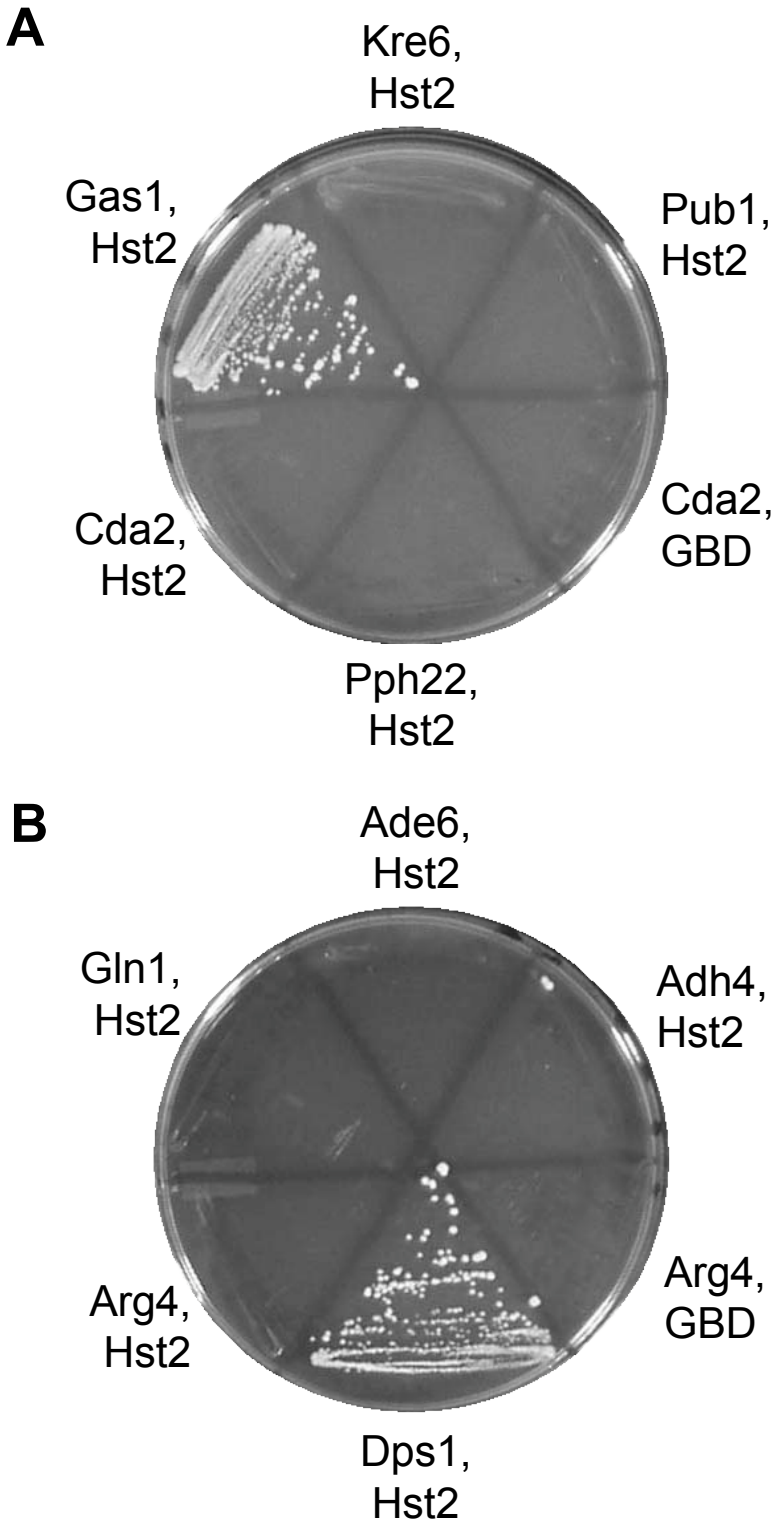
A
Kre6,
Hst2
Gas1,
Hst2
Pub1,
Hst2
Cda2,
Hst2
Cda2,
GBD
Pph22,
Hst2
B
Ade6,
Hst2
Gln1,
Hst2
Adh4,
Hst2
Arg4,
Hst2
Arg4,
GBD
Dps1,
Hst2

Two-hybrid analysis of Sir2 family members with Sir2-interacting proteins: Luc7 interacts specifically with the core domain of Sir2. To address the specificity of the physical interaction between Sir2 and the Sir2-interacting proteins, two-hybrid constructs containing the catalytic core domains of other Sir2 family members were made. These include constructs with the core domains of Hst2, Hst3, Hst4, a human homolog, SIRT2 (closely related to yeast Hst2), and a bacterial homolog, *Thermatoga* Sir2 (TmSir2). Mutant Hst2 and Hst3 constructs were obtained in the process of plasmid construction and were also included in the analysis.

Several interesting observations were drawn from these two-hybrid analyses, summarized in Table A-2. Overall, less interaction was seen with the human and bacterial homologs, compared to Hst proteins. Also, some specificity among interactions with Hst proteins was observed. For example, Gas1 interacted with the core domains of Sir2, Hst2, Hst4, and SIRT2, but did not interact with Hst3, or the bacterial TmSir2 (Figure A-2). Some interactions were less specific, for example Pat1 interacts with the core domains of every construct tested (Figure A-3). Interestingly, one interacting protein, Ktr4, only weakly interacts with Sir2 and the human homolog SIRT2, but none of the other Sir2 family members (Table A-2). Also of note is the specific interaction observed between Luc7 and Sir2 (Figure A-4), which is the only Sir2-interacting protein that interacts with the conserved core domain of Sir2 but not the core domains of other Sir2 family members. *LUC7* encodes an essential gene that is involved in splicing, specifically in splice site recognition (Fortes et al. 1999). This physical interaction points to a connection between splicing and silencing, although

Table A-2. Two-hybrid analysis of Sir2 interactors with Sir2 family members[a]

Protein (pLP)	Sir2 WT (1073)	Hst2 WT (1771)	Hst2 H53Y[b] (1772)	Hst3 Q151L[b] (1773)	Hst3 WT (1774)	Hst4 WT (1819)	SIRT2 WT (1791)	TmSir2 WT (1826)
Pub1 (1203)	+	-	++	-	+	++	+	++
Kre6 (1204)	+	++	+++	++	++	++	-	-
Gas1 (1205)	++	+++	++	-	-	+++	+++	-
Cda2 (1206)	++	++	++	+	++	++	+	-
Pph22 (1207)	++	+	+	++	+	+++	+	-
Luc7 (1208)	++	-	-	-	-	-	-	-
Tfp1 (1209)	++	++	++	+	++	++	+	-
Pat1 (1210)	+++	+++	++	++	+++	+++	+++	+++
Vma2 (1211)	+	++	++	++	++	++	+	-
Slx5 (1212)	-	-	-	-	-	-	-	-
Ktr4 (1213)	+	-	-	-	-	-	+	-
Adh4 (1214)	+	++	++	++	++	+	++	-
Ade6 (1217)	++	++	++	++	++	++	+	-
Gln1 (1218)	+	-	+	-	++	-	-	-
Arg4 (1220)	+++	++	++	-	+++	+++	-	+
Dps1 (1221)	+++	++	++	+	+	-	+	-
Tkl1 (1222)	+	++	++	+	+	+	+	-
Plb1 (1223)	++	++	++	-	++	+	-	-
Pho11 (1224)	-	+	+	-	+	+	+	-
Aim25 (1228)	+	+	++	-	+	+	-	-

[a]+++ = strong interaction, ++ = medium interaction, + = weak interaction, - = no interaction, as assayed on SC-ade-his-leu-trp
[b]*HST2-H53Y* and *HST3-Q151L* mutations occurred in PCR amplification during construct creation

Figure A-2. Gas1 interacts with specific Sir2 family members. LPY3374 was transformed with GAD-*GAS1* (pLP1205) and the following GBD fusion constructs, starting with GBD, pLP956 (pGBD-C1), pLP1073 (GBD-core *SIR2*), pLP1771 (GBD-core *HST2*), pLP1772 (GBD-core *HST2-H53Y*), pLP1773 (GBD-core *HST3-Q151L*), pLP1774 (GBD-core *HST3*), pLP1819 (GBD-*HST4*), pLP1791 (GBD-SIRT2), or pLP1826 (GBD-core TmSIR2). Plate template, growth control (SC-leu-trp), and interaction (SC-ade-his-leu-trp) plates are shown, demonstrating a two-hybrid interaction between Gas1 and Sir2, Hst2, Hst4, and SIRT2.

GAD-Gas1

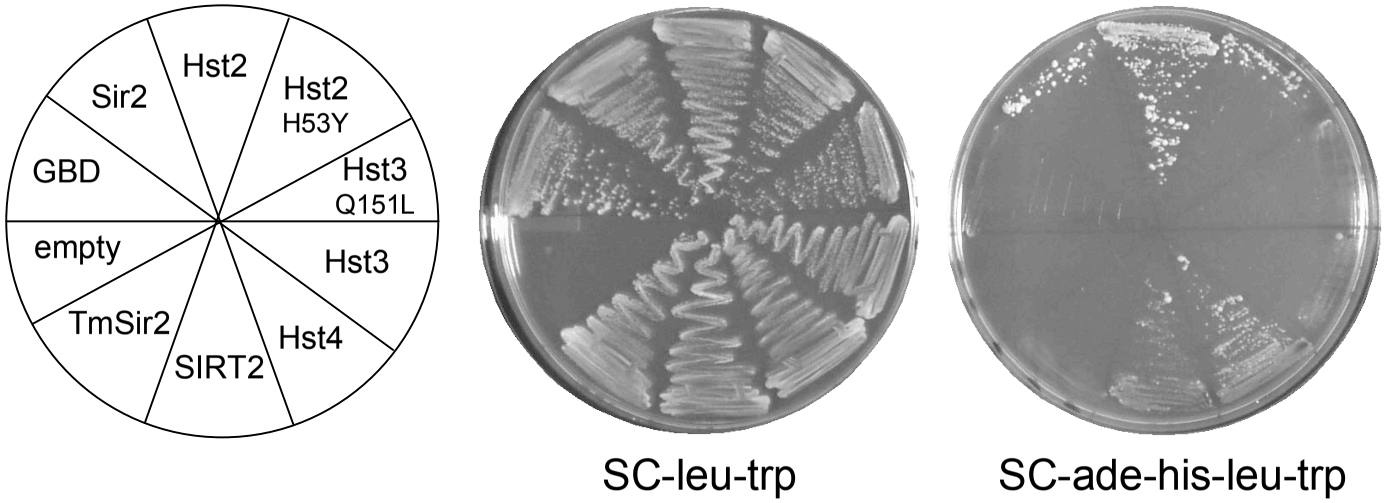
Growth
Interaction
Hst2
Hst2
H53Y
Sir2
GBD
Hst3
Q151L
empty
Hst3
TmSir2
Hst4
SIRT2
SC-leu-trp
SC-ade-his-leu-trp

Figure A-3. Pat1 interacts with all Sir2 family members. LPY3374 was transformed with GAD-*PAT1* (pLP1210) and the following GBD fusion constructs, starting with GBD, pLP956 (pGBD-C1), pLP1073 (GBD-core *SIR2*), pLP1771 (GBD-core *HST2*), pLP1772 (GBD-core *HST2-H53Y*), pLP1773 (GBD-core *HST3-Q151L*), pLP1774 (GBD-core *HST3*), pLP1819 (GBD-*HST4*), pLP1791 (GBD-SIRT2), or pLP1826 (GBD-core TmSIR2). Plate template, growth control (SC-leu-trp), and interaction (SC-ade-his-leu-trp) plates are shown, demonstrating a two-hybrid interaction between Pat1 and the core domains of all Sir2 family members.

GAD-Pat1

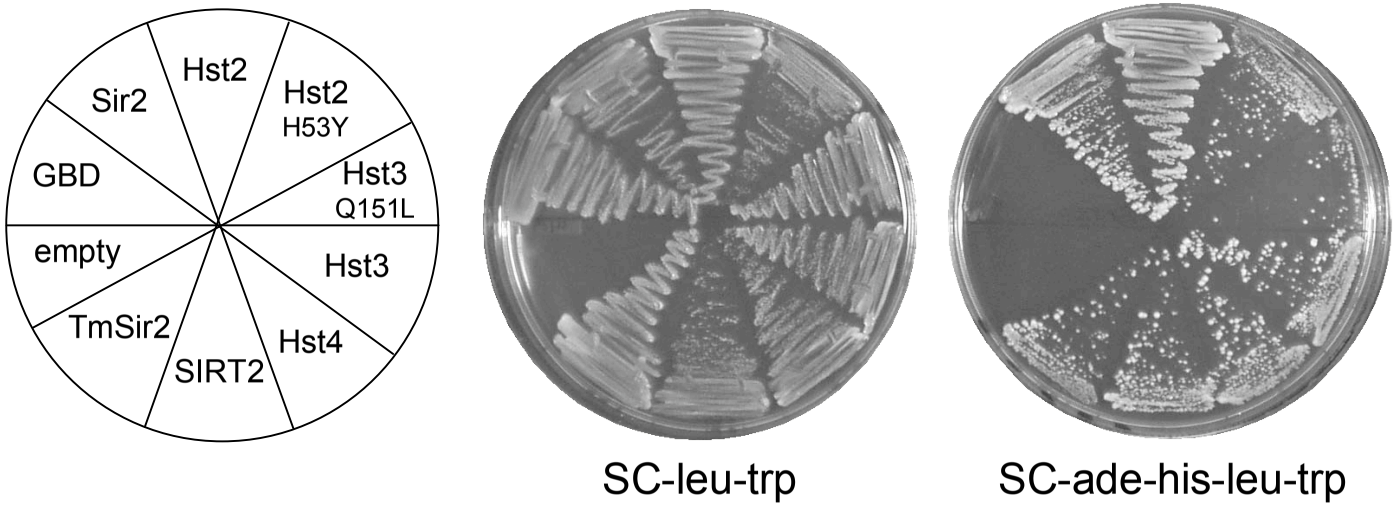
Growth
Interaction
Hst2
Hst2
H53Y
Sir2
GBD
Hst3
Q151L
empty
Hst3
TmSir2
Hst4
SIRT2
SC-leu-trp
SC-ade-his-leu-trp

Figure A-4. Luc7 interacts specifically with Sir2. LPY3374 was transformed with GAD-*LUC7* (pLP1208) and the following GBD fusion constructs, starting with GBD, pLP956 (pGBD-C1), pLP1073 (GBD-core *SIR2*), pLP1771 (GBD-core *HST2*), pLP1772 (GBD-core *HST2-H53Y*), pLP1773 (GBD-core *HST3-Q151L*), pLP1774 (GBD-core *HST3*), pLP1819 (GBD-*HST4*), pLP1791 (GBD-SIRT2), or pLP1826 (GBD-core TmSIR2). Plate template, growth control (SC-leu-trp), and interaction (SC-ade-his-leu-trp) plates are shown, demonstrating a specific two-hybrid interaction between Luc7 and the core domain of Sir2.

GAD-Luc7


Growth
Interaction
Hst2
Hst2
H53Y
Sir2
GBD
Hst3
Q151L
empty
Hst3
TmSir2
Hst4
SIRT2
SC-leu-trp
SC-ade-his-leu-trp

silencing functions are not reported for *LUC7* and there are no previous connections to splicing for *SIR2*.

Two-hybrid analysis of catalytically inactive sir2-H364Y with Sir2-interacting proteins: Ktr4's interaction with Sir2 is dependent on Sir2's deacetylase activity. In an observed physical interaction, identification of a factor that disrupts the interaction could help in the formation of hypotheses to understand why the proteins interact in the cell. A core domain Sir2 construct was made with mutation of a previously identified Sir2 residue, H364, which is critical for its deacetylase activity.

The two-hybrid analysis of sir2-H364Y resulted in mostly positive physical interactions with all of the Sir2-interacting proteins (Table A-3). However, three interactions were affected. The interaction between Sir2 and Ktr4 was weak, but was completely absent with sir2-H364Y, except for one colony on the interaction plate, compared to the several colonies seen with wild-type Sir2 (Figure A-5). *KTR4* encodes a putative mannosyltransferase and its potential function in transcriptional silencing is proposed in Chapter 7. The interactions were weaker with sir2-H364Y, but were not lost for two other Sir2-interacting proteins, Pph22 (Figure A-6) and Pho11 (Figure A-7). *PPH22* encodes a PP2A-like phosphatase. The simplest explanation for its recovery in the Sir2 two-hybrid screen is that it dephosphorylates histones, although there is no evidence currently for Pph22 to function in histone dephosphorylation. Pph22 is implicated in Ty1 transcriptional silencing (Jiang 2008), therefore it is possible that it also contributes to silent chromatin through its interaction with Sir2.

Table A-3. Two-hybrid analysis of Sir2-interacting proteins with sir2-H364Y[a]

Plasmid	Protein	GBD-core Sir2 (pLP1073)	GBD-core sir2-H364Y (pLP2352)
pLP1203	Pub1	++	++
pLP1204	Kre6	+++	+++
pLP1205	Gas1	++	++
pLP2101	gas1-E262Q	++	++
pLP1206	Cda2	++++	++++
pLP1207	Pph22	++	+
pLP1208	Luc7	+	+
pLP1209	Tfp1	+++	+++
pLP1210	Pat1	++++	++++
pLP1211	Vma2	+	+
pLP1213	Ktr4	+	-
pLP1214	Adh4	++	++
pLP1217	Ade6	++	++
pLP1218	Gln1	++	++
pLP1220	Arg4	++++	++++
pLP1221	Dps1	++	++
pLP1222	Tkl1	+	+
pLP1223	Plb1	++	+++
pLP1224	Pho11	++	+
pLP1228	Aim25	++	++

[a]++++ = very strong interaction, +++ = strong interaction, ++ = medium interaction, + = weak interaction, - = no interaction, as assayed on SC-ade-his-leu-trp

Figure A-5. Ktr4 fails to interact with catalytically inactive sir2-H364Y. LPY3374 was transformed with pLP1213 (GAD-*KTR4*) and pLP956 (pGBD-C1), pLP1073 (GBD-core *SIR2*), or pLP2352 (GBD-core *sir2-H364Y*). Growth control (SC-leu-trp) and interaction (SC-ade-his-leu-trp) plates are shown, which shows a weak interaction between Ktr4 and Sir2 that is lost in the absence of Sir2 deacetylase activity.

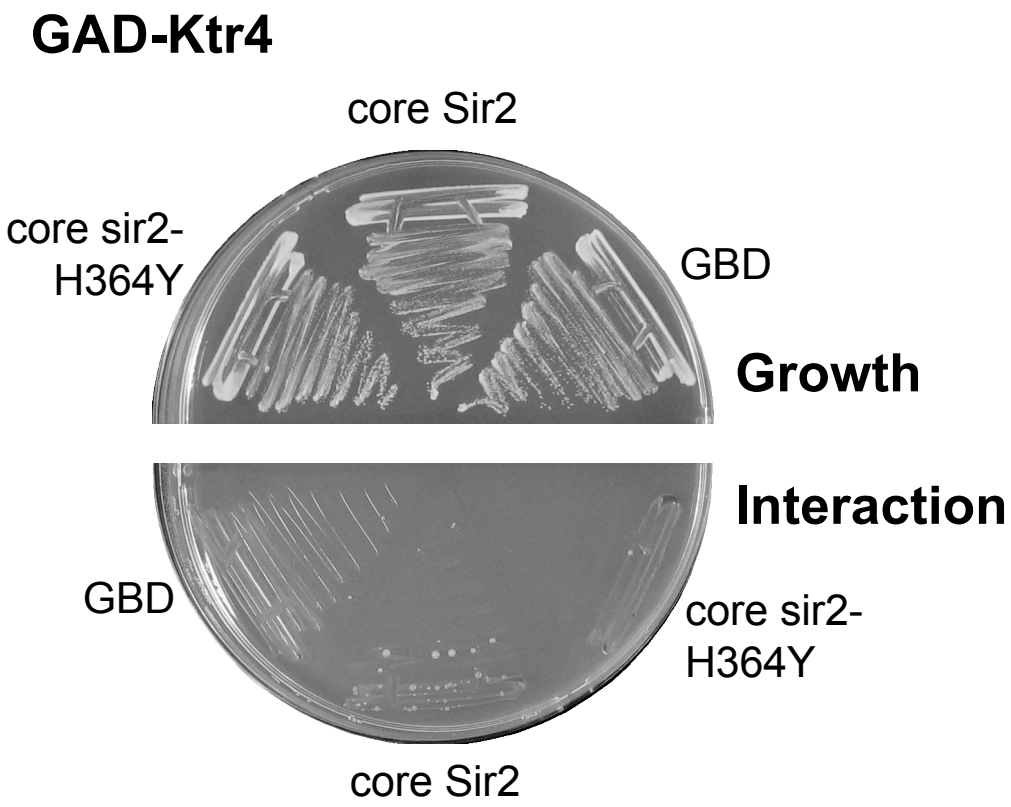
GAD-Ktr4
core Sir2
core sir2-
H364Y
GBD
Growth
Interaction
GBD
core sir2-
H364Y
core Sir2

Figure A-6. Pph22 interacts weakly with catalytically inactive sir2-H364Y. LPY3374 was transformed with pLP1207 (GAD-*PPH22*) and pLP956 (pGBD-C1), pLP1073 (GBD-core *SIR2*), or pLP2352 (GBD-core *sir2-H364Y*). Growth control (SC-leu-trp) and interaction (SC-ade-his-leu-trp) plates are shown, which shows a weak interaction between Pph22 and catalytically inactive Sir2.

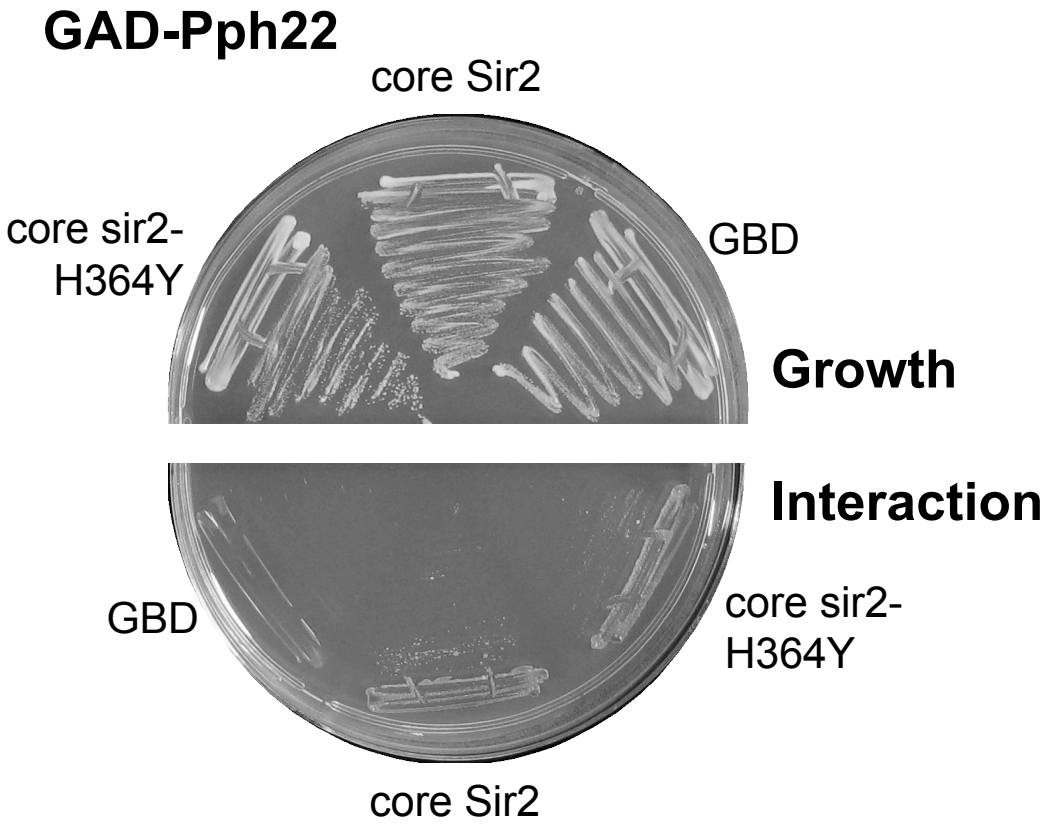
GAD-Pph22
core Sir2
core sir2-
H364Y
GBD
Growth
Interaction
GBD
core sir2-
H364Y
core Sir2

Figure A-7. Pho11 interacts weakly with catalytically inactive sir2-H364Y. LPY3374 was transformed with pLP1224 (GAD-*PHO11*) and pLP956 (pGBD-C1), pLP1073 (GBD-core *SIR2*), or pLP2352 (GBD-core *sir2-H364Y*). Growth control (SC-leu-trp) and interaction (SC-ade-his-leu-trp) plates are shown, which shows a weak interaction between Pho11 and catalytically inactive Sir2.

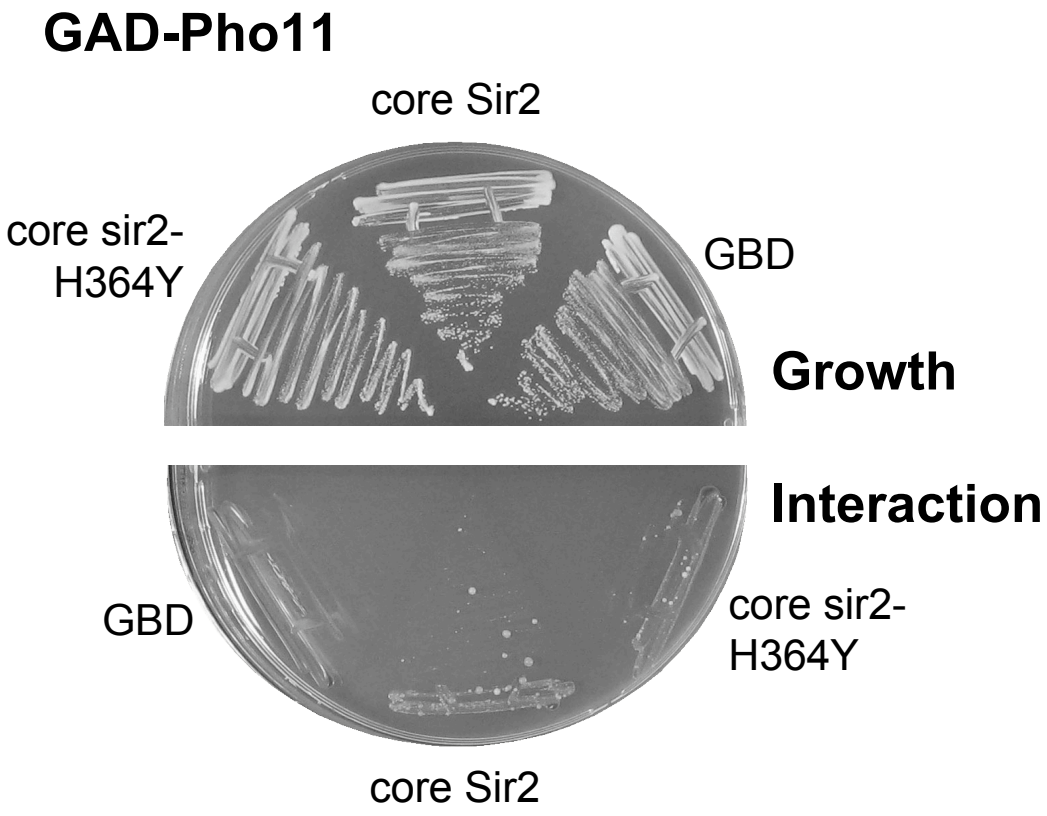
GAD-Pho11
core Sir2
core sir2-
H364Y
GBD
Growth
Interaction
GBD
core sir2-
H364Y
core Sir2

MATERIALS AND METHODS

Yeast two-hybrid strain and methods. The two-hybrid yeast strain LPY3374 (PJ69-4A; *MAT***a** *gal4*Δ *gal80*Δ *his3-200 leu2-3,112 trp1-901 ura3-52 GAL2-ADE2 LYS2::GAL1-HIS3 met2::GAL7-lacZ*) (James et al. 1996) was used for all experiments. Lithium acetate transformation (Ito et al. 1983) of two plasmids (GBD fusion and GAD fusion) was done simultaneously, selecting for transformed yeast on synthetic complete (SC) lacking leucine and tryptophan (SC-leu-trp) or SC lacking leucine and uracil (SC-leu-ura). Plates were incubated for 3 days at 30˚C. Transformed yeast were selected from these plates and struck heavily onto SC-leu-trp or SC-leu-ura for 3 days at 30˚C. This process was repeated three additional times. After these successive platings, two-hybrid interactions were assayed on SC also lacking histidine, or lacking histidine and adenine. Plates were incubated for 6 days at 30˚C prior to digital image capture. 3-aminotriazole (3-AT) was added to the indicated plates lacking histidine to a final concentration of 1 mM to lower background of the *HIS3* reporter.

Plasmid construction. Two-hybrid plasmids used are in Table A-4. The GBD vectors pGBD-C1 (pLP956), pGBD-C2 (pLP957), and pGBD-C3 (pLP958) were used for cloning (James et al. 1996). The sequences of oligonucleotides used in plasmid construction and sequencing are listed in Table A-5. *HST2* was amplified from pLP1393 using oLP508 and oLP294, then digested with *Bgl*II, and cloned into *Bgl*II-digested pLP957 to create pLP1771. pLP1772 is a similar construct made in the same manner, with an *HST2-H53Y* mutation that occurred during amplification. *HST3* was

Table A-4. Plasmids used in Appendix A.[a]

Plasmid (alias)	Description	Reference
pLP660	*H. sapiens* SIRT2 *LEU2* 2μ	Sherman et al. 1999
pLP956 (pGBD-C1)	GBD vector *TRP1* 2μ	James et al. 1996
pLP957 (pGBD-C2)	GBD vector *TRP1* 2μ	James et al. 1996
pLP958 (pGBD-C3)	GBD vector *TRP1* 2μ	James et al. 1996
pLP959 (pGBDU-C1)	GBD vector *URA3* 2μ	James et al. 1996
pLP1073	GBD-core *SIR2 TRP1* 2μ	Garcia and Pillus 2002
pLP1074	GBD-*SIR2 TRP1* 2μ	Garcia and Pillus 2002
pLP1161	GBD-*HST2 URA3* 2μ	
pLP1203	GAD-*PUB1 LEU2* 2μ	Garcia 2003
pLP1204	GAD-*KRE6 LEU2* 2μ	Garcia 2003
pLP1205	GAD-*GAS1 LEU2* 2μ	Garcia 2003
pLP1206	GAD-*CDA2 LEU2* 2μ	Garcia 2003
pLP1207	GAD-*PPH22 LEU2* 2μ	Garcia 2003
pLP1208	GAD-*LUC7 LEU2* 2μ	Garcia 2003
pLP1209	GAD-*TFP1 LEU2* 2μ	Garcia 2003
pLP1210	GAD-*PAT1 LEU2* 2μ	Garcia 2003
pLP1211	GAD-*VMA2 LEU2* 2μ	Garcia 2003
pLP1212	GAD-*SLX5 LEU2* 2μ	Garcia 2003
pLP1213	GAD-*KTR4 LEU2* 2μ	Garcia 2003
pLP1214	GAD-*ADH4 LEU2* 2μ	Garcia 2003
pLP1217	GAD-*ADE6 LEU2* 2μ	Garcia 2003
pLP1218	GAD-*GLN1 LEU2* 2μ	Garcia 2003
pLP1220	GAD-*ARG4 LEU2* 2μ	Garcia 2003
pLP1221	GAD-*DPS1 LEU2* 2μ	Garcia 2003
pLP1222	GAD-*TKL1 LEU2* 2μ	Garcia 2003
pLP1223	GAD-*PLB1 LEU2* 2μ	Garcia 2003
pLP1224	GAD-*PHO11 LEU2* 2μ	Garcia 2003
pLP1228	GAD-*AIM25 LEU2* 2μ	Garcia 2003
pLP1393	*HST2* Bluescript SK	
pLP1464	GBD-*HST4 TRP1* CEN	
pLP1705	*HST3 HIS3* CEN	
pLP1743	*T. maritima* Sir2 T7 *HIS6*	R. Dutnall
pLP1771	GBD-core *HST2 TRP1* 2μ	
pLP1772	GBD-core *HST2-H53Y TRP1* 2μ	
pLP1773	GBD-core *HST3-Q151L TRP1* 2μ	
pLP1774	GBD-core *HST3 TRP1* 2μ	
pLP1791	GBD-core SIRT2 *TRP1* 2μ	
pLP1819	GBD-core *HST4 TRP1* 2μ	
pLP1826	GBD-core TmSIR2 *TRP1* 2μ	
pLP2101	GAD-*gas1-E262Q LEU2* 2μ	
pLP2352	GBD-core *sir2-H364Y TRP1* 2μ	

[a]Plasmids are part of the lab collection, or were constructed during this study and are described in Materials and Methods. References for published plasmids are noted.

Table A-5. Oligonucleotides used in Appendix A.

Oligo	Name	Sequence (5' to 3')[a]
oLP229	*HST3* (-400)	GGGATCCTTCAGAGGTAAAATGCGC
oLP294	*HST2*-3'*Eco*RI	CCGAATTCGCTGCATTGACGGTTCGGGAACCCAT
oLP374	PAS BAIT	GCGACATCATCATCGGAAGAGAGTAGTAAC
oLP457	GAD-R THL5	CGATGATGAAGATACCCC
oLP508	*HST2* (5' *Bgl*II)	GATGTCGGTTAGGAAGA**T**CTCTGC
oLP509	*HST3* (3' *Bgl*II)	GCCTTTAATTATGTCAAGAT**C**TAGGCC
oLP523	TmSIR2 (5' *Bam*HI)	GGAATTCCTGGATCCTCTCAATGAATCC
oLP524	TmSIR2 (3' *Pst*I)	ATCGCTTCCCTGCAGGCATCTTGCG
oLP525	SIRT2 (5' *Bam*HI)	ACTTCCTGCGGA**T**C**C**TATTCTCCCAGACG
oLP526	SIRT2 (3' *Pst*I)	AAGTCTGACTGC**C**T**G**CAGGAGAAGAAACGC
oLP820	*GAS1-E262Q*-F	CCTGTTTTCTTCTCT**C**AATACGGTTGTAACG
oLP821	*GAS1-E262Q*-R	CGTTACAACCGTATT**G**AGAGAAGAAAACAGG
oLP1208	*SIR2-H364Y*-F	CTGGTGCAGTGC**T**ATGGCTCTTTTGC
oLP1209	*SIR2-H364Y*-R	GCAAAAGAGCCAT**A**GCACTGCACCAG

[a]Nucleotides in **bold** in the above sequences are mutagenic, compared to the wild-type sequence.

amplified from pLP1705 using oLP509 and oLP229, then digested with *Bgl*II, and cloned into *Bgl*II-digested pLP956 to create pLP1774. pLP1773 is a similar construct made in the same manner with an *HST3-Q151L* mutation that occurred during amplification. SIRT2 was amplified from pLP660 using oLP525 and oLP526, then digested with *Bam*HI and *Pst*I, and cloned into *Bam*HI-*Pst*I-digested pLP957 to create pLP1791. To create pLP1819, pLP1464 was first *Eco*RI-*Pst*I-digested to drop *HST4* from the polylinker. This fragment was further digested by *Ava*II and filled with Klenow, then ligated to *Sma*I-digested pLP956 to create pLP1819. The core domain sequence of the *Thermotoga* homolog of *SIR2* was amplified from pLP1743 (gift from R. Dutnall) with oLP523 and oLP524, then digested with *Bam*HI and *Pst*I, and ligated to *Bam*HI-*Pst*I-digested pLP958 to create pLP1826. All of the GBD fusion constructs were confirmed by sequencing using oLP374, to confirm the junction between GBD and the gene sequence, and to confirm that the sequence was in frame for reading of codons. To create pLP2101, direct PCR mutagenesis was done on pLP1205 with oLP820 and oLP821. The *gas1-E262Q* mutation in pLP2101 was verified by sequencing using oLP457. To create pLP2352, direct PCR mutagenesis was done on pLP1073 with oLP1208 and oLP1209. The *sir2-H364Y* mutation in pLP2352 was verified by sequencing using oLP374.

Appendix B

Slx5 interacts with Sir2 by GST affinity binding

Slx5 interacts with Sir2 by GST affinity binding. Slx5 was identified as a two-hybrid interacting protein with a nearly full-length Sir2 two-hybrid construct (Garcia 2003; Darst et al. 2008). Of note was that the two-hybrid interaction was disrupted with sir2-R139K (Garcia 2003), a Sir2 mutant protein with compromised deacetylase activity compared to wild-type Sir2 (Garcia and Pillus 2002). To independently examine the Slx5-Sir2 physical interaction, GST affinity binding experiments were performed with GST-Sir2, and GST-sir2-R139K. Slx5 was bound in GST-Sir2 affinity precipitation, and did not associate with GST alone (Figure B-1*A*). In addition, Slx5's interaction with sir2-R139K was weaker, but detectable (Figure B-1*A*), which is in contrast to the loss of the interaction between Slx5 and this mutant Sir2 protein in two-hybrid (Garcia 2003; Darst et al. 2008).

Slx5 interacts with Sir2 in the absence of Slx8 and the SIR complex. Slx5 exists in a complex with Slx8, and Sir2 exists in the SIR complex with the Sir3 and Sir4 proteins. To determine whether these complex members contribute to the interaction between Slx5 and Sir2, a series of affinity binding experiments were pursued. If the interacting proteins were not required for the interaction, it was expected that the interaction would become stronger because of the absence of other proteins binding to either Slx5 or Sir2. The interaction between Slx5 and Sir2 was not dependent on Slx8 because binding experiments in an *slx8*Δ strain showed a stronger Slx5-Sir2 interaction (Figure B-2*A*, B-3*A*). This interaction also occurred with the

Figure B-1. Slx5 interacts with Sir2 by GST affinity binding. *(A)* Slx5 interacts with Sir2. Protein extracts were isolated from an untagged wild-type (WT) strain (LPY5) and a WT strain with HA-Slx5 (LPY9187). Extracts from these strains were incubated with purified GST (pLP1302), GST-Sir2 (pLP1275), and GST-sir2-R139K (pLP1335). Input and bound material was analyzed by immunoblotting with anti-HA. *(B)* GST and GST-Sir2 are present at similar levels in the binding experiment. Samples from *(A)* were analyzed by immunoblot with anti-GST.

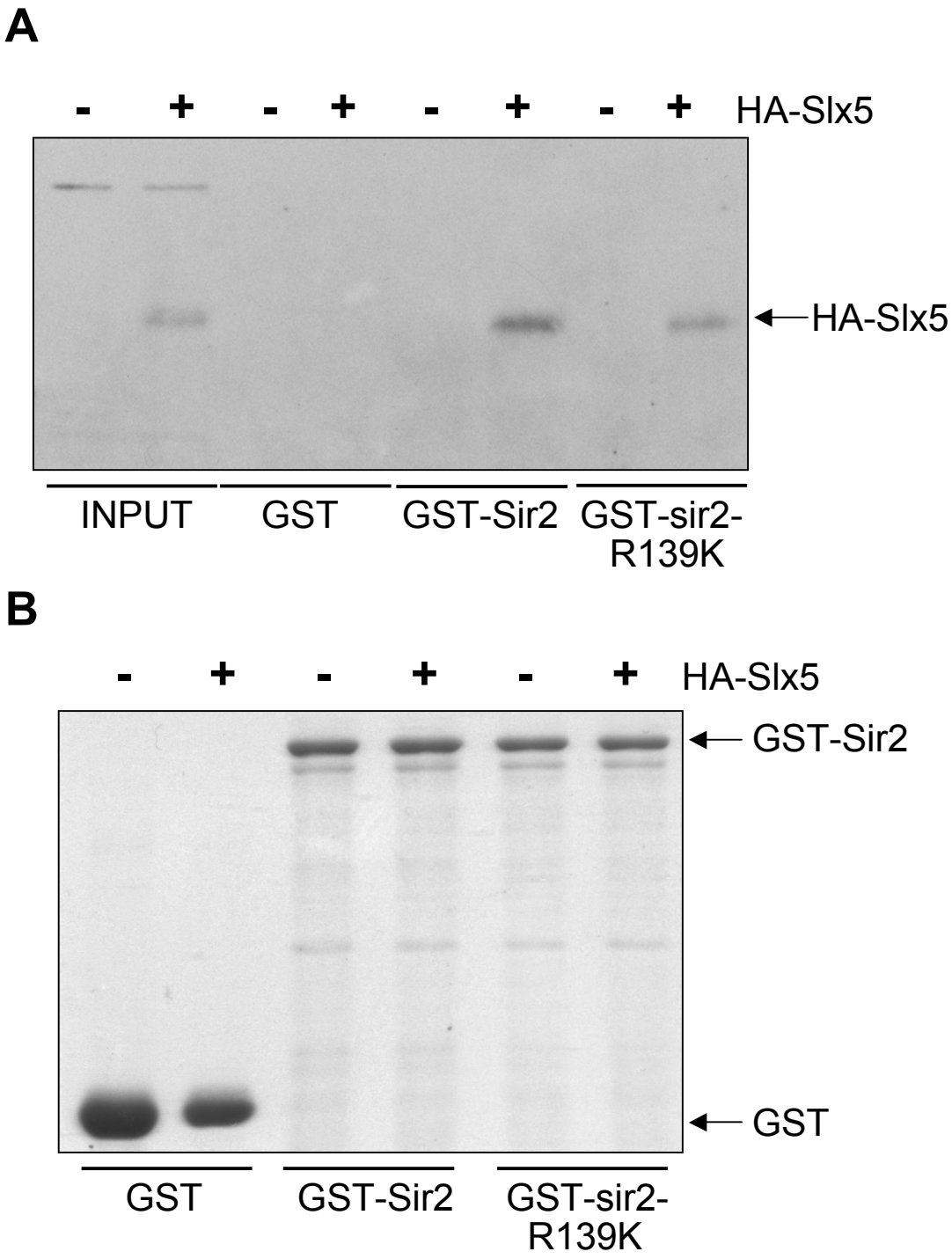
A
- + - + - + - + HA-Slx5
HA-Slx5
INPUT
GST
GST-Sir2
GST-sir2-R139K
B
- + - + - + HA-Slx5
GST-Sir2
GST
GST
GST-Sir2
GST-sir2-R139K

Figure B-2. Slx5 interacts with Sir2 in the absence of Slx8. *(A)* Slx5 interacts with Sir2 in an *slx8*Δ mutant. Protein extracts were isolated from an untagged wild-type strain (LPY5), a WT strain with HA-Slx5 (LPY9187), and an *slx8*Δ strain with HA-Slx5 (LPY12490). Extracts from these strains were incubated with purified GST (pLP1302) and GST-Sir2 (pLP1275). Input and bound material was analyzed by immunoblotting with anti-HA. *(B)* Slx5 interacts with sir2-R139K in an *slx8*Δ mutant. This experiment was done as in *(A)*, with GST-sir2-R139K (pLP1335).

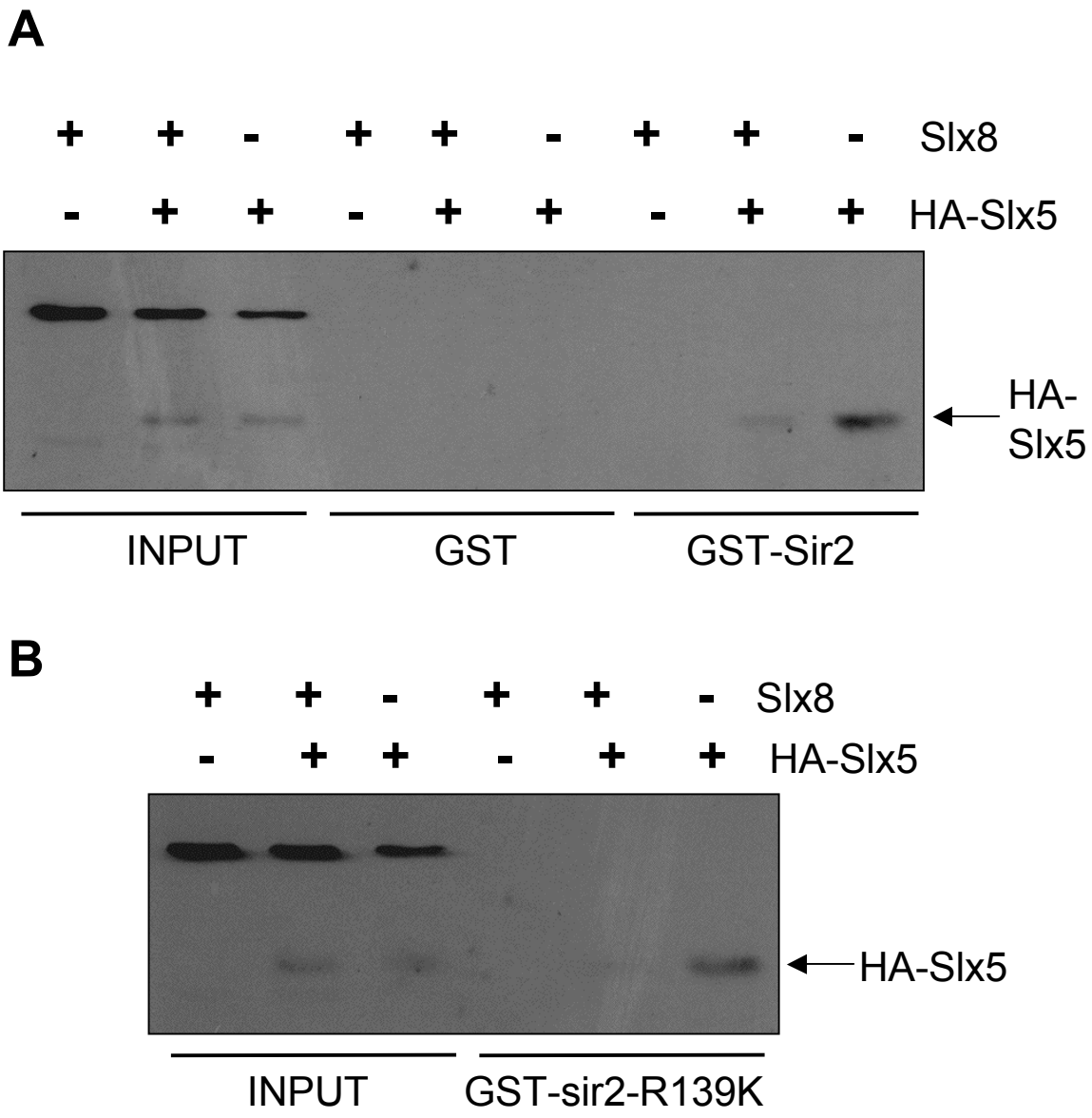
A
+ + - + + - + + - Slx8
- + + - + + - + + HA-Slx5
HA-Slx5
INPUT
GST
GST-Sir2
B
+ + - + + - Slx8
- + + - + + HA-Slx5
HA-Slx5
INPUT
GST-sir2-R139K

Figure B-3. Slx5 interacts with Sir2 in the absence of Slx8 and the SIR complex members Sir3 and Sir4. *(A)* Slx5 interacts with Sir2 in the absence of Slx8. Protein extracts were isolated from an untagged wild-type strain (LPY5), a WT strain with HA-Slx5 (LPY9187), and an *slx8*Δ strain with HA-Slx5 (LPY12490). Extracts from these strains were incubated with purified GST (pLP1302) and GST-Sir2 (pLP1275). In the top panel, input and bound material was analyzed by immunoblotting with anti-HA. In the bottom panel, the same samples were analyzed by immunoblotting with anti-GST. *(B)* Slx5 interacts with Sir2 in the absence of Slx8, Sir3, and Sir4. This experiment was done as in *(A)* with a *sir3*Δ *sir4*Δ (LPY12629), a *sir3*Δ *sir4*Δ *slx8*Δ (LPY12630), and a *sir2*Δ (LPY9189), all with HA-tagged Slx5.

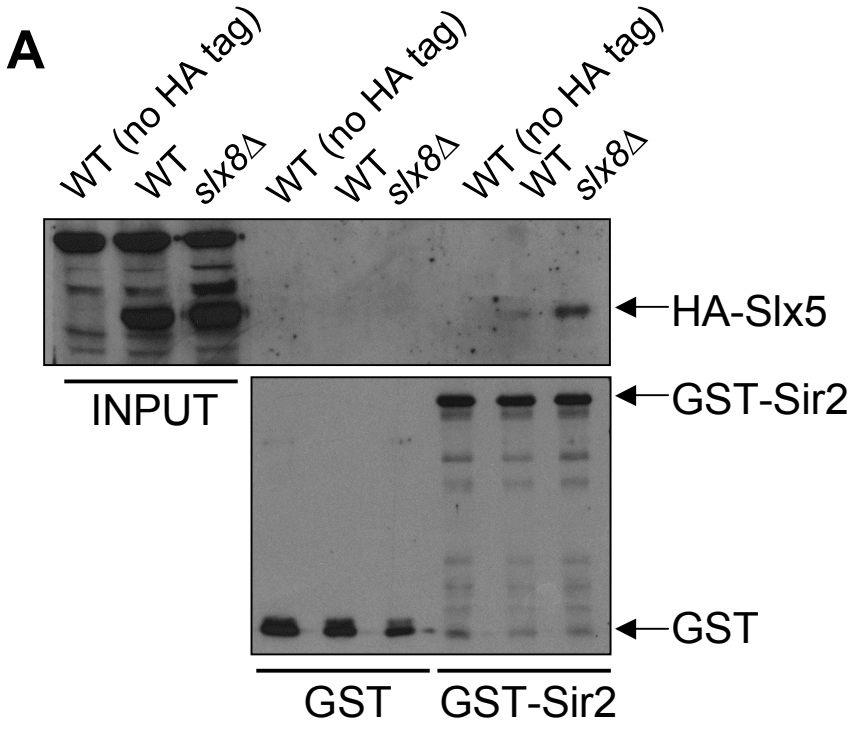
A
WT (no HA tag)
WT
slx8Δ
WT (no HA tag)
WT
slx8Δ
WT (no HA tag)
WT
slx8Δ
HA-Slx5
INPUT
GST-Sir2
GST
GST
GST-Sir2

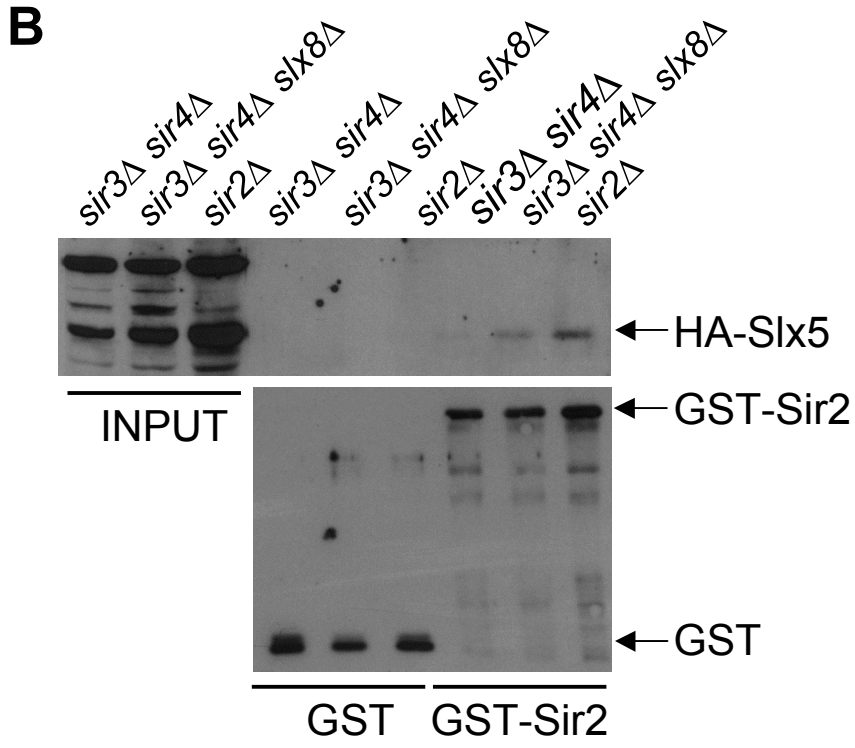
B
sir3Δ sir4Δ
sir3Δ sir4Δ slx8Δ
sir2Δ
sir3Δ sir4Δ
sir3Δ sir4Δ slx8Δ
sir2Δ
sir3Δ sir4Δ
sir3Δ sir4Δ slx8Δ
sir2Δ
HA-Slx5
INPUT
GST-Sir2
GST
GST
GST-Sir2

mutant sir2-R139K protein (Figure B-2*B*). Although a very faint Slx5 band was present in bound material from a *sir3*Δ *sir4*Δ strain, a strong interaction was seen in an *slx8*Δ *sir3*Δ *sir4*Δ triple mutant strain, demonstrating that the SIR complex is not required for the interaction between Sir2 and Slx5. Slx5's physical interaction with Sir2 may be a function of its role in transcriptional silencing, which has been investigated further (Darst et al. 2008).

MATERIALS AND METHODS

Yeast strains and methods. Yeast strains are listed in Table B-1. Strains were constructed during this study unless otherwise noted and grown at 30˚C with standard manipulations (Amberg et al. 2005).

Plasmids. The GST empty vector pLP1302 was used as a control (Kaelin et al. 1992). The GST-Sir2 and GST-sir2-R139K proteins were expressed from plasmids pLP1275 (Tanny et al. 1999) and pLP1335 (Garcia and Pillus 2002), respectively.

GST affinity binding. Glutathione S-transferase (GST; pLP1302), GST-Sir2 (pLP1275), and GST-sir2-R139K (pLP1335) fusion proteins were expressed in *E. coli* BL21 DE3 during a 4 hr induction with 0.5 mM IPTG at room temperature. Cells were resuspended in lysis buffer (20 mM Tris [pH 8]; 1 mM EDTA; 1 mM EGTA; 1x protease inhibitors TPCK, PMSF, benzamidine, leupeptin, and pepstatin; 200 mg/ml lysozyme; 1% NP-40; 350 mM NaCl; 10 mM DTT) and lysed on ice for 30 min, followed by sonication. Proteins were purified from the *E. coli* extracts on glutathione beads as directed by the manufacturer (GE Healthcare, Piscataway, NJ). Whole-cell

extracts were prepared from the indicated yeast strains in Sir2 IP lysis buffer (50 mM HEPES [pH 7.5]; 0.5 M NaCl; 0.5% NP-40; 10% glycerol; 1 mM EDTA; 1x PMSF, TPCK, leupeptin, pepstatin, and benzamidine). Whole-cell extracts (approximately 45 A_{600} cell equivalents) were mixed with ~10 µg GST, GST-Sir2, and GST-sir2-R139K bound to sepahrose beads and incubated at 4°C for 1 hr. The beads were washed once with Sir2 lysis buffer and twice with wash buffer (50 mM HEPES [pH 7.5], 150 mM NaCl, 1 mM EDTA) and then boiled in 50 µl 1x sodium dodecyl sulfate (SDS) sample loading buffer. For hemagglutinin (HA) immunoblot analysis, 40 µl of sample was loaded onto 9% SDS-polyacrylamide gels (10 by 12 cm). Immunoblots were probed with a 1:5,000 dilution of mouse anti-HA monoclonal antiserum (Covance Research Products, Berkeley, CA). An HRP-coupled anti-mouse secondary antibody (Promega, Madison, WI) was used at 1:10,000 and detected with enhanced chemiluminescence reagents (Perkin-Elmer, Waltham, MA). For GST immunoblot analysis, 5 µl of sample was loaded onto a 10% SDS-polyacrylamide gel (8 by 10 cm). Immunoblots were probed with a 1:5,000 dilution of rabbit anti-GST (Sigma-Aldrich, St. Louis, MO). A horseradish peroxidase-coupled anti-rabbit secondary antibody (Promega, Madison, WI) was used at 1:10,000 and detected with enhanced chemiluminescence reagents (Perkin-Elmer, Waltham, MA).

Results reported in this Appendix have been published in Darst, R. P., Garcia, S. N., Koch, M. R., and Pillus, L. 2008. Slx5 promotes transcriptional silencing and is required for robust growth in the absence of Sir2. *Molecular and Cellular Biology* 28(4):1361-1372.

Table B-1. Yeast strains used in Appendix B.[a]

Strain	Genotype	Source/Reference
LPY5	W303-1a *MAT***a** *ade2-1 can1-100 his3-11,15 leu2-3,112 trp1-1 ura3-1*	R. Rothstein
LPY79	W303-1b *MAT*α *ade2-1 can1-100 his3-11,15 leu2-3,112 trp1-1 ura3-1*	R. Rothstein
LPY9187	W303-1a *HA-SLX5::URA3*	
LPY9189	W303-1a *HA-SLX5::URA3 sir2::HIS3*	
LPY12490	W303-1a *HA-SLX5::URA3 slx8*Δ*::kanMX*	
LPY12629	W303-1b *HA-SLX5::URA3 sir3::TRP1 sir4::HIS3*	
LPY12630	W303-1b *HA-SLX5::URA3 sir3::TRP1 sir4::HIS3 slx8*Δ*::kanMX*	

[a]Unless otherwise noted, strains were constructed during the course of this study or are part of the standard lab collection.

Appendix C

Cell type specific defects in telomeric silencing

Wild-type pseudodiploids are defective in telomeric silencing. In Chapter 3, simultaneous expression of *MAT***a** and *MAT*α restored growth at high temperature to *gas1*Δ mutants (Figure 3-5). To further investigate this finding, a similar experiment was completed to ask if simultaneous expression of *MAT***a** and *MAT*α would restore telomeric silencing to *gas1*Δ. Surprisingly, control experiments in wild-type cells exhibited a telomeric silencing defect. A defect in telomeric silencing was observed in a wild-type *MAT***a** strain transformed with plasmid-borne *MAT*α, and likewise, in a wild-type *MAT*α strain transformed with plasmid-borne *MAT***a** (Figure C-1). To determine if this was a consequence of the pseudodiploid state in a haploid cell, diploid strains with a telomeric reporter gene were constructed.

Wild-type diploids are defective in telomeric silencing. Several independent *MAT***a**/*MAT*α diploids with the TELV-R::*URA3* reporter on both chromosome V-R telomeres were defective in telomeric silencing, comparably to the *sir2*Δ control strain (Figure C-2). The defect was seen in diploids created in other genetic backgrounds and with reporter genes located on other telomeres as well (data not shown). To determine if this silencing defect is a consequence of *MAT***a** and *MAT*α expression in the diploid, *MAT*α/*MAT*α and *MAT***a**/*MAT***a** strains were constructed by mitotic recombination of a diploid parent strain. These strains that were homozygous for *MAT* silenced the telomeric reporter slightly better than the *MAT***a**/*MAT*α diploid strain (Figure C-3), showing that heterozygosity of *MAT* creates the observed telomeric silencing defect.

Figure C-1. Simultaneous expression of *MAT***a** and *MAT*α creates a telomeric silencing defect in wild-type cells. A wild-type (WT) *MAT***a** strain (LPY6284) and a WT *MAT*α strain (LPY6283) with TELV-R::*URA3* were transformed with the following plasmids, *TRP1* CEN vector (pLP61), *MAT*α (pLP1167), and *MAT***a** (pLP1185). Transformed strains are LPY10650-LPY10655. The transformed strains were plated on synthetic complete (SC) lacking tryptophan (SC-trp) to assay growth and on SC-trp containing 5-FOA to assay silencing. Decreased growth on SC-trp 5-FOA indicates defective silencing. The telomeric silencing defect observed when both *MAT***a** and *MAT*α are expressed is shown with arrows.

TELV-R::*URA3*

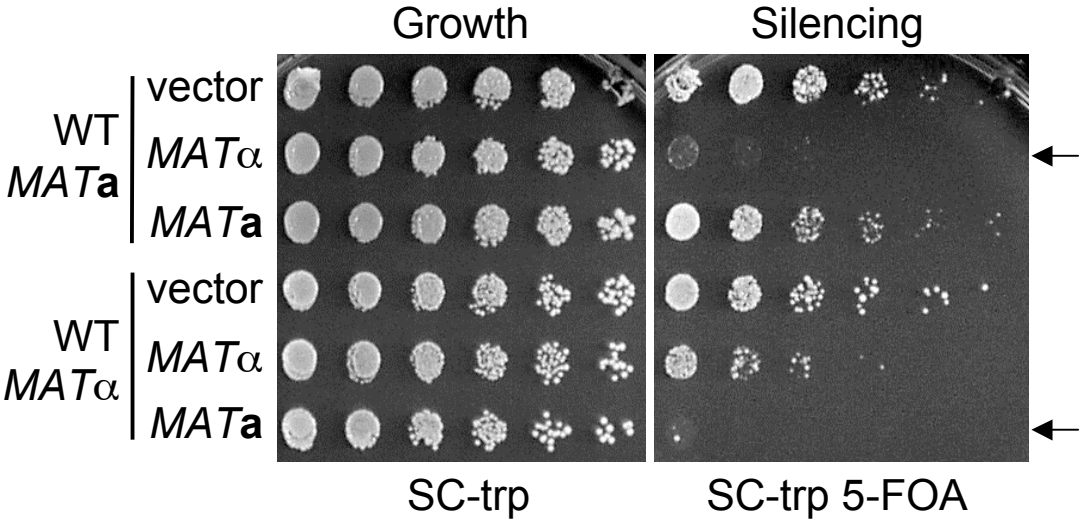
Growth
Silencing
WT
MATa
vector
MATα
MATa
WT
MATα
vector
MATα
MATa
SC-trp
SC-trp 5-FOA

Figure C-2. Wild-type diploids are defective in telomeric silencing. The first three strains are haploids with TELV-R::*URA3* and the last four are diploids with TELV-R::*URA3* on both chromosome V-R telomeres. A *MAT***a** WT (LPY6284), *MAT***a** *sir2*Δ (LPY10397), *MAT***a** *gas1*Δ (LPY10362), and four *MAT***a**/*MAT*α WT (LPY10403-LPY10406) strains were plated on SC to assay growth and on SC containing 5-FOA to assay silencing. Decreased growth on 5-FOA indicates defective silencing.

TELV-R::*URA3*

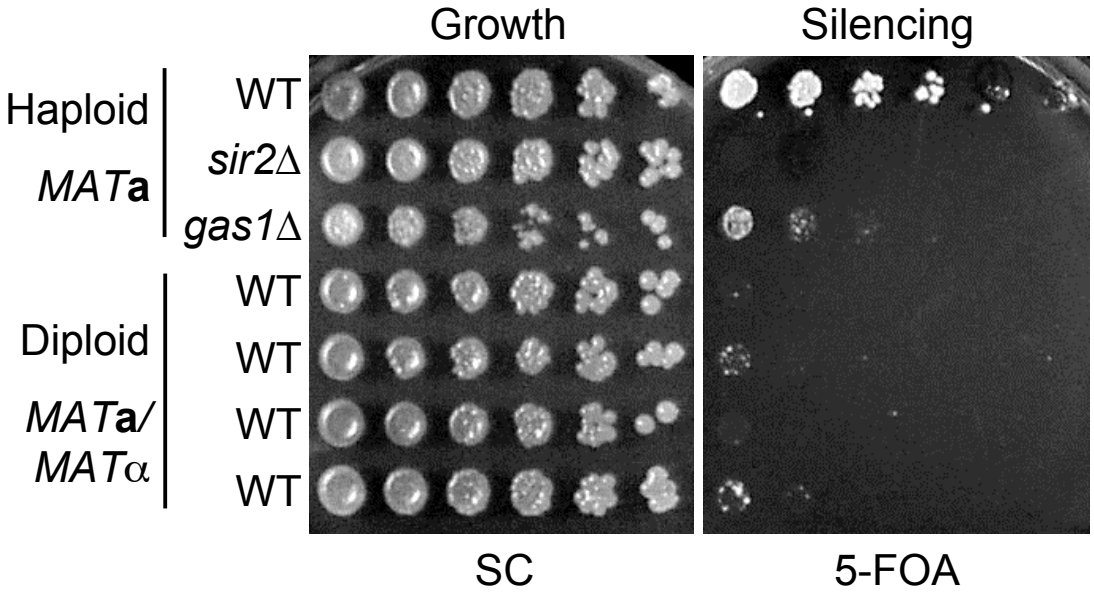
Growth
Silencing
Haploid
MATa
WT
sir2Δ
gas1Δ
Diploid
MATa/
MATα
WT
WT
WT
WT
SC
5-FOA

Figure C-3. *MAT***a**/*MAT***a** and *MAT*α/*MAT*α diploids partially silence telomeres. The first three strains are haploids with TELV-R::*URA3* and the last five strains are diploids with TELV-R::*URA3* on both chromosome V-R telomeres. A *MAT***a** WT (LPY6284), *MAT*α WT (LPY6283), *MAT***a** *sir2*Δ (LPY10397), *MAT***a**/*MAT*α WT (LPY10403), two *MAT***a**/*MAT***a** WT (LPY10669 and LPY10670), and two *MAT*α/*MAT*α WT (LPY10671 and LPY10672) strains were plated on yeast extract-peptone-dextrose (YPD) to assay growth and on synthetic complete containing 5-FOA to assay silencing. Decreased growth on 5-FOA indicates defective silencing. Note the slower growth on the growth control plate for the *MAT***a**/*MAT***a** WT strain LPY10669, which may be indicative of a gene besides *MAT* being affected during mitotic recombination in construction of this strain. Telomeric silencing appears partially restored in the diploids that are homozygous for the *MAT* locus (last four strains on plate).

TELV-R::*URA3*

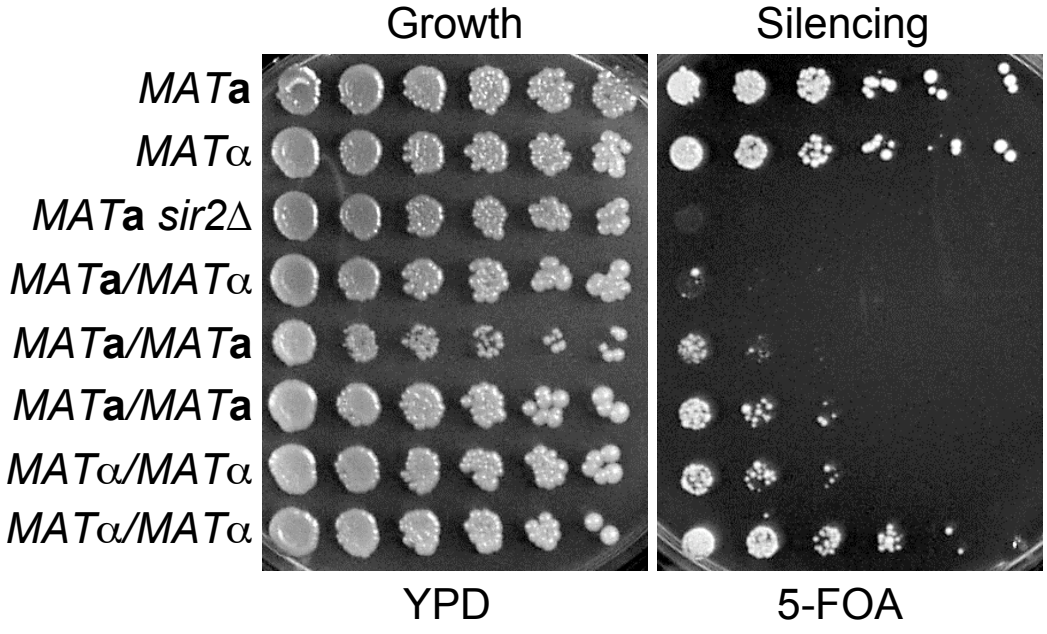
Growth
Silencing
MATa
MATα
MATa sir2Δ
MATa/MATα
MATa/MATa
MATa/MATa
MATα/MATα
MATα/MATα
YPD
5-FOA

With the TELV-R::*ADE2* reporter gene, differences were observed in telomeric silencing of wild-type diploids. Two diploids had the reporter at only one of the two chromosome V-R telomeres. Some telomeric silencing was seen in these diploids (Figure C-4). However, in a diploid with both chromosome V-R telomeres carrying the *ADE2* reporter gene, complete derepression of *ADE2* was observed, similar to the white colony color of *sir2*Δ mutants that are completely defective in telomeric silencing (Figure C-4). This suggests that the telomeric silencing defect is also a property of the number of reporters assayed in the cell.

Understanding the molecular basis for the telomeric silencing defect seen upon simultaneous expression of *MAT*a and *MAT*α. Although the exact cause of the silencing defect seen in pseudodiploids and diploids is currently unknown, cell type differences may be the answer. The decrease in telomeric silencing seen in diploid cells was also reported by an independent study (Mercier et al. 2005). The telomeric silencing defect in pseudodiploids may be caused by expression of a diploid-specific gene in a haploid cell that interferes with silencing. On the other hand, a haploid specific gene may be repressed in the pseudodiploid upon heterozygosity of *MAT*. If this haploid specific gene were critical for telomeric silencing, its loss in a pseudodiploid cell would be expected to exhibit a telomeric silencing defect. The transcriptional circuit for cell type specification has been determined (Galgoczy et al. 2004), which may include haploid specific genes contributing to telomeric silencing. In the future, experiments characterizing the telomeric silencing phenotypes of deletions of these haploid specific genes may uncover the mystery gene promoting telomeric silencing in haploid cells.

Figure C-4. Telomeric silencing is more defective in wild-type *MAT***a**/*MAT*α diploids when they are homozygous for the TELV-R::*ADE2* reporter. All of the strains shown have the TELV-R::*ADE2* reporter. The top three panels are three haploid strains, *MAT***a** WT (LPY9911), *MAT*α WT (LPY9912), and *MAT*α *sir2*Δ (LPY9961). The bottom three panels are three diploid *MAT***a**/*MAT*α strains, two with one chromosome V-R with the reporter (indicated by +/T and T/+) (LPY10953 and LPY10954), and one with both chromosomes V-R with the reporter (LPY10955). Strains were plated for single colonies on YPD and incubated at 30˚C for 3 days, then placed at 4˚C for pink/white color development. White colony color (*ADE2* expression) indicates defective silencing.

TELV-R::*ADE2*

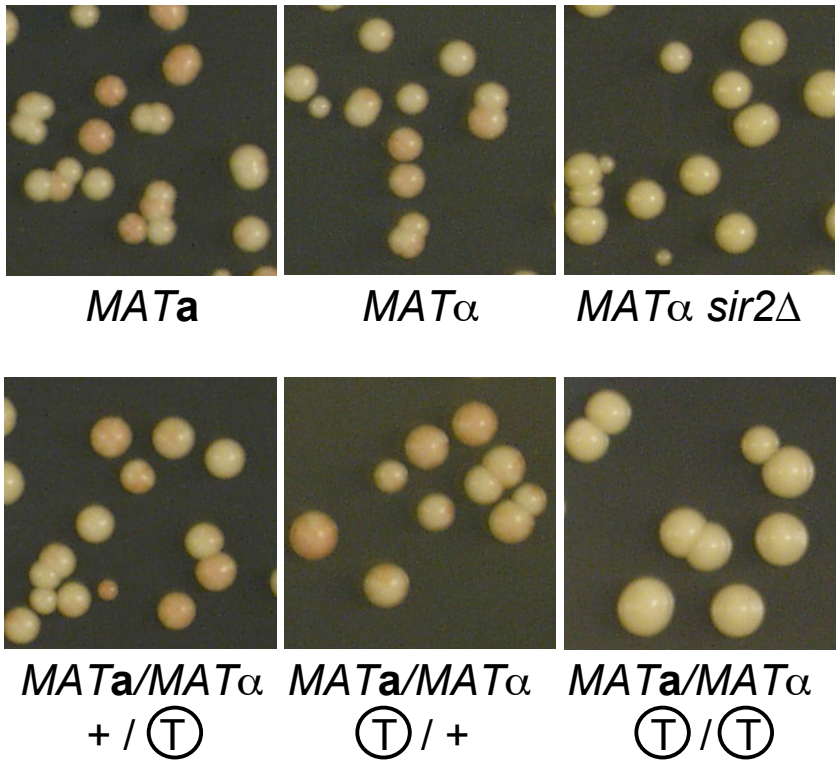

MATERIALS AND METHODS

Yeast strains and methods. Yeast strains are listed in Table C-1. Strains were constructed during this study unless otherwise noted and grown at 30˚C with standard manipulations (Amberg et al. 2005). Lithium acetate transformation was used (Ito et al. 1983). Yeast extract-peptone-dextrose (YPD) and synthetic selective media were prepared as described (Sherman 1991). 5-fluoroorotic acid (5-FOA; United States Biological, Inc., Swampscott, MA) was added at 0.1% to test for *URA3* reporter gene expression. Telomeric silencing assays were performed as described previously (van Leeuwen and Gottschling 2002). For serial-dilution assays, five-fold dilutions were plated from cultures grown at 30˚C, starting at an A_{600} of 1.0. Plates were incubated at 30˚C unless otherwise indicated for 3 days prior to digital image capture. *MAT***a**/*MAT***a** (LPY10669 and LPY10670) and *MAT*α/*MAT*α (LPY10671 and LPY10672) diploids were created by plating for single colonies on yeast extract-peptone-dextrose (YPD) media and exposing the plates to 25 μjoules UV energy to induce mitotic recombination at *MAT*. Recombination events were identified by replica plating the UV-exposed plates to lawns of *MAT***a** (LPY142) and *MAT*α (LPY78) mating type tester cells to select diploids capable of mating.

Plasmids. The plasmid pLP61, also known as pRS314 (Sikorski and Hieter 1989), served as an empty CEN *TRP1* vector. The plasmid pLP1167 contains the *MAT*α gene, inserted in pLP61 (Lowell et al. 2003). The plasmid pLP1185 contains the *MAT***a** gene, inserted in pLP61.

Table C-1. Yeast strains used in Appendix C.[a]

Strain	Genotype	Source/Reference
LPY5	W303-1a *MAT***a** *ade2-1 can1-100 his3-11,15 leu2-3,112 trp1-1 ura3-1*	R. Rothstein
LPY78	*MAT*α *his4*	P. Schatz
LPY79	W303-1b *MAT*α *ade2-1 can1-100 his3-11,15 leu2-3,112 trp1-1 ura3-1*	R. Rothstein
LPY142	*MAT***a** *his4*	P. Schatz
LPY6283	W303-1b *lys2*Δ*0 trp1*Δ*0* TELVR::*URA3*	
LPY6284	W303-1a *trp1*Δ*0* TELVR::*URA3*	
LPY9911	W303-1a TELVR::*ADE2*	
LPY9912	W303-1b TELVR::*ADE2*	
LPY9961	W303-1b *sir2::HIS3* TELVR::*ADE2*	
LPY10362	W303-1a *gas1*Δ*::kanMX* TELVR::*URA3*	
LPY10397	W303-1a *sir2::HIS3* TELVR::*URA3*	
LPY10403	W303 *MAT***a**/*MAT*α *LYS2/lys2*Δ*0 trp1*Δ*0/trp1*Δ*0* TELVR::*URA3*/TELVR::*URA3*	
LPY10404	W303 *MAT***a**/*MAT*α *LYS2/lys2*Δ*0 trp1*Δ*0/trp1*Δ*0* TELVR::*URA3*/TELVR::*URA3*	
LPY10405	W303 *MAT***a**/*MAT*α *LYS2/lys2*Δ*0 trp1*Δ*0/trp1*Δ*0* TELVR::*URA3*/TELVR::*URA3*	
LPY10406	W303 *MAT***a**/*MAT*α *LYS2/lys2*Δ*0 trp1*Δ*0/trp1*Δ*0* TELVR::*URA3*/TELVR::*URA3*	
LPY10650	LPY6284 + pLP61	
LPY10651	LPY6284 + pLP1167	
LPY10652	LPY6284 + pLP1185	
LPY10653	LPY6283 + pLP61	
LPY10654	LPY6283 + pLP1167	
LPY10655	LPY6283 + pLP1185	
LPY10669	W303 *MAT***a**/*MAT***a** *LYS2/lys2*Δ*0 trp1*Δ*0/trp1*Δ*0* TELVR::*URA3*/TELVR::*URA3*	
LPY10670	W303 *MAT***a**/*MAT***a** *LYS2/lys2*Δ*0 trp1*Δ*0/trp1*Δ*0* TELVR::*URA3*/TELVR::*URA3*	
LPY10671	W303 *MAT*α/*MAT*α *LYS2/lys2*Δ*0 trp1*Δ*0/trp1*Δ*0* TELVR::*URA3*/TELVR::*URA3*	
LPY10672	W303 *MAT*α/*MAT*α *LYS2/lys2*Δ*0 trp1*Δ*0/trp1*Δ*0* TELVR::*URA3*/TELVR::*URA3*	
LPY10953	W303 *MAT***a**/*MAT*α TELVR::*ADE2*/+	
LPY10954	W303 *MAT***a**/*MAT*α +/TELVR::*ADE2*	
LPY10955	W303 *MAT***a**/*MAT*α TELVR::*ADE2*/TELVR::*ADE2*	

[a]Unless referenced, strains are from the lab collection or were made for this study.

REFERENCES

Addinall, S.G., Downey, M., Yu, M., Zubko, M.K., Dewar, J., Leake, A., Hallinan, J., Shaw, O., James, K., Wilkinson, D.J. et al. 2008. A genomewide suppressor and enhancer analysis of *cdc13-1* reveals varied cellular processes influencing telomere capping in *Saccharomyces cerevisiae*. *Genetics* **180**(4): 2251-2266.

Ai, W., Bertram, P.G., Tsang, C.K., Chan, T.F., and Zheng, X.F. 2002. Regulation of subtelomeric silencing during stress response. *Mol. Cell* **10**(6): 1295-1305.

Akhtar, A. and Gasser, S.M. 2007. The nuclear envelope and transcriptional control. *Nat. Rev. Genet.* **8**(7): 507-517.

Al-Aidroos, K. and Bussey, H. 1978. Chromosomal mutants of *Saccharomyces cerevisiae* affecting the cell wall binding site for killer factor. *Can. J. Microbiol.* **24**(3): 228-237.

Altaf, M., Utley, R.T., Lacoste, N., Tan, S., Briggs, S.D., and Côté, J. 2007. Interplay of chromatin modifiers on a short basic patch of histone H4 tail defines the boundary of telomeric heterochromatin. *Mol. Cell* **28**(6): 1002-1014.

Amberg, D.C., Burke, D.J., and Strathern, J.N. 2005. *Methods in Yeast Genetics: A Cold Spring Harbor Laboratory Course Manual*. Cold Spring Harbor Laboratory Press, Cold Spring Harbor, NY.

Armstrong, K.A., Som, T., Volkert, F.C., Rose, A., and Broach, J.R. 1989. Propagation and expression of genes in yeast using 2-micron circle vectors. *Biotechnology* **13**: 165-192.

Axelrod, A. 1991. Role of a cell-cycle gene in transcriptional silencing. Ph.D. dissertation. University of California, Berkeley, Berkeley, CA.

Babiarz, J.E., Halley, J.E., and Rine, J. 2006. Telomeric heterochromatin boundaries require NuA4-dependent acetylation of histone variant H2A.Z in *Saccharomyces cerevisiae*. *Genes Dev.* **20**(6): 700-710.

Baum, P., Thorner, J., and Honig, L. 1978. Identification of tubulin from the yeast *Saccharomyces cerevisiae*. *Proc. Natl. Acad. Sci. USA* **75**(10): 4962-4966.

Bell, S.P., Kobayashi, R., and Stillman, B. 1993. Yeast origin recognition complex functions in transcription silencing and DNA replication. *Science* **262**(5141): 1844-1849.

Berger, S.L. 2007. The complex language of chromatin regulation during transcription. *Nature* **447**(7143): 407-412.

Bernstein, B.E., Tong, J.K., and Schreiber, S.L. 2000. Genomewide studies of histone deacetylase function in yeast. *Proc. Natl. Acad. Sci. USA* **97**(25): 13708-13713.

Berretta, J., Pinskaya, M., and Morillon, A. 2008. A cryptic unstable transcript mediates transcriptional trans-silencing of the Ty1 retrotransposon in *S. cerevisiae*. *Genes Dev.* **22**(5): 615-626.

Blander, G. and Guarente, L. 2004. The Sir2 family of protein deacetylases. *Annu. Rev. Biochem.* **73**: 417-435.

Bond, J.F., Fridovich-Keil, J.L., Pillus, L., Mulligan, R.C., and Solomon, F. 1986. A chicken-yeast chimeric beta-tubulin protein is incorporated into mouse microtubules in vivo. *Cell* **44**(3): 461-468.

Borra, M.T., O'Neill, F.J., Jackson, M.D., Marshall, B., Verdin, E., Foltz, K.R., and Denu, J.M. 2002. Conserved enzymatic production and biological effect of O-acetyl-ADP-ribose by silent information regulator 2-like NAD+-dependent deacetylases. *J. Biol. Chem.* **277**(15): 12632-12641.

Bose, M.E., McConnell, K.H., Gardner-Aukema, K.A., Muller, U., Weinreich, M., Keck, J.L., and Fox, C.A. 2004. The origin recognition complex and Sir4 protein recruit Sir1p to yeast silent chromatin through independent interactions requiring a common Sir1p domain. *Mol. Cell. Biol.* **24**(2): 774-786.

Botstein, D., Falco, S.C., Stewart, S.E., Brennan, M., Scherer, S., Stinchcomb, D.T., Struhl, K., and Davis, R.W. 1979. Sterile host yeasts (SHY): a eukaryotic system of biological containment for recombinant DNA experiments. *Gene* **8**(1): 17-24.

Boulton, S.J. and Jackson, S.P. 1996a. Identification of a *Saccharomyces cerevisiae* Ku80 homologue: roles in DNA double strand break rejoining and in telomeric maintenance. *Nucleic Acids Res.* **24**(23): 4639-4648.

Boulton, S.J. and Jackson, S.P. 1996b. *Saccharomyces cerevisiae* Ku70 potentiates illegitimate DNA double-strand break repair and serves as a barrier to error-prone DNA repair pathways. *EMBO J.* **15**(18): 5093-5103.

Boulton, S.J. and Jackson, S.P. 1998. Components of the Ku-dependent non-homologous end-joining pathway are involved in telomeric length maintenance and telomeric silencing. *EMBO J.* **17**(6): 1819-1828.

Bouwman, P. and Philipsen, S. 2002. Regulation of the activity of Sp1-related transcription factors. *Mol. Cell Endocrinol.* **195**(1-2): 27-38.

Boxem, M., Maliga, Z., Klitgord, N., Li, N., Lemmens, I., Mana, M., de Lichtervelde, L., Mul, J.D., van de Peut, D., Devos, M. et al. 2008. A protein domain-based interactome network for *C. elegans* early embryogenesis. *Cell* **134**(3): 534-545.

Brachmann, C.B., Sherman, J.M., Devine, S.E., Cameron, E.E., Pillus, L., and Boeke, J.D. 1995. The *SIR2* gene family, conserved from bacteria to humans, functions in silencing, cell cycle progression, and chromosome stability. *Genes Dev.* **9**(23): 2888-2902.

Briggs, S.D., Xiao, T., Sun, Z.W., Caldwell, J.A., Shabanowitz, J., Hunt, D.F., Allis, C.D., and Strahl, B.D. 2002. Gene silencing: trans-histone regulatory pathway in chromatin. *Nature* **418**(6897): 498.

Buck, S.W., Gallo, C.M., and Smith, J.S. 2004. Diversity in the Sir2 family of protein deacetylases. *J. Leukoc. Biol.* **75**(6): 939-950.

Buck, S.W., Sandmeier, J.J., and Smith, J.S. 2002. RNA polymerase I propagates unidirectional spreading of rDNA silent chromatin. *Cell* **111**(7): 1003-1014.

Camblong, J., Iglesias, N., Fickentscher, C., Dieppois, G., and Stutz, F. 2007. Antisense RNA stabilization induces transcriptional gene silencing via histone deacetylation in *S. cerevisiae*. *Cell* **131**(4): 706-717.

Carmen, A.A., Milne, L., and Grunstein, M. 2002. Acetylation of the yeast histone H4 N terminus regulates its binding to heterochromatin protein SIR3. *J. Biol. Chem.* **277**(7): 4778-4781.

Carotti, C., Ragni, E., Palomares, O., Fontaine, T., Tedeschi, G., Rodriguez, R., Latge, J.P., Vai, M., and Popolo, L. 2004. Characterization of recombinant forms of the yeast Gas1 protein and identification of residues essential for glucanosyltransferase activity and folding. *Eur. J. Biochem.* **271**(18): 3635-3645.

Chang, C.R., Wu, C.S., Hom, Y., and Gartenberg, M.R. 2005. Targeting of cohesin by transcriptionally silent chromatin. *Genes Dev.* **19**(24): 3031-3042.

Chen, L. and Widom, J. 2004. Molecular basis of transcriptional silencing in budding yeast. *Biochem. Cell Biol.* **82**(4): 413-418.

Chen, L. and Widom, J. 2005. Mechanism of transcriptional silencing in yeast. *Cell* **120**(1): 37-48.

Chien, C.T., Buck, S., Sternglanz, R., and Shore, D. 1993. Targeting of Sir1 protein establishes transcriptional silencing at *HM* loci and telomeres in yeast. *Cell* **75**(3): 531-541.

Chou, C.C., Li, Y.C., and Gartenberg, M.R. 2008. Bypassing Sir2 and O-acetyl-ADP-ribose in transcriptional silencing. *Mol. Cell* **31**(5): 650-659.

Christianson, T.W., Sikorski, R.S., Dante, M., Shero, J.H., and Hieter, P. 1992. Multifunctional yeast high-copy-number shuttle vectors. *Gene* **110**(1): 119-122.

Cid, V.J., Duran, A., del Rey, F., Snyder, M.P., Nombela, C., and Sanchez, M. 1995. Molecular basis of cell integrity and morphogenesis in *Saccharomyces cerevisiae*. *Microbiol. Rev.* **59**(3): 345-386.

Clarke, A.S., Samal, E., and Pillus, L. 2006. Distinct roles for the essential MYST family HAT Esa1p in transcriptional silencing. *Mol. Biol. Cell* **17**(4): 1744-1757.

Cockell, M., Palladino, F., Laroche, T., Kyrion, G., Liu, C., Lustig, A.J., and Gasser, S.M. 1995. The carboxy termini of Sir4 and Rap1 affect Sir3 localization: evidence for a multicomponent complex required for yeast telomeric silencing. *J. Cell Biol.* **129**(4): 909-924.

Coelho, P.S., Bryan, A.C., Kumar, A., Shadel, G.S., and Snyder, M. 2002. A novel mitochondrial protein, Tar1p, is encoded on the antisense strand of the nuclear 25S rDNA. *Genes Dev.* **16**(21): 2755-2760.

Darst, R.P., Garcia, S.N., Koch, M.R., and Pillus, L. 2008. Slx5 promotes transcriptional silencing and is required for robust growth in the absence of Sir2. *Mol. Cell. Biol.* **28**(4): 1361-1372.

De Rubertis, F., Kadosh, D., Henchoz, S., Pauli, D., Reuter, G., Struhl, K., and Spierer, P. 1996. The histone deacetylase Rpd3 counteracts genomic silencing in *Drosophila* and yeast. *Nature* **384**(6609): 589-591.

Dehé, P.M. and Géli, V. 2006. The multiple faces of Set1. *Biochem. Cell Biol.* **84**(4): 536-548.

Denison, C., Rudner, A.D., Gerber, S.A., Bakalarski, C.E., Moazed, D., and Gygi, S.P. 2005. A proteomic strategy for gaining insights into protein sumoylation in yeast. *Mol. Cell. Proteomics* **4**(3): 246-254.

Doering, T.L. and Schekman, R. 1997. Glycosyl-phosphatidylinositol anchor attachment in a yeast in vitro system. *Biochem. J.* **328 (Pt 2)**: 669-675.

Donze, D. and Kamakaka, R.T. 2002. Braking the silence: how heterochromatic gene repression is stopped in its tracks. *Bioessays* **24**(4): 344-349.

Douglas, C.M., Foor, F., Marrinan, J.A., Morin, N., Nielsen, J.B., Dahl, A.M., Mazur, P., Baginsky, W., Li, W., el-Sherbeini, M. et al. 1994. The *Saccharomyces cerevisiae FKS1* (*ETG1*) gene encodes an integral membrane protein which is a subunit of 1,3-beta-D-glucan synthase. *Proc. Natl. Acad. Sci. USA* **91**(26): 12907-12911.

Dubey, R.N. and Gartenberg, M.R. 2007. A tDNA establishes cohesion of a neighboring silent chromatin domain. *Genes Dev.* **21**(17): 2150-2160.

Ebert, A., Lein, S., Schotta, G., and Reuter, G. 2006. Histone modification and the control of heterochromatic gene silencing in *Drosophila*. *Chromosome Res.* **14**(4): 377-392.

Ehrenhofer-Murray, A.E., Gossen, M., Pak, D.T., Botchan, M.R., and Rine, J. 1995. Separation of origin recognition complex functions by cross-species complementation. *Science* **270**(5242): 1671-1674.

Emre, N.C., Ingvarsdottir, K., Wyce, A., Wood, A., Krogan, N.J., Henry, K.W., Li, K., Marmorstein, R., Greenblatt, J.F., Shilatifard, A. et al. 2005. Maintenance of low histone ubiquitylation by Ubp10 correlates with telomere-proximal Sir2 association and gene silencing. *Mol. Cell* **17**(4): 585-594.

Enomoto, S. and Berman, J. 1998. Chromatin assembly factor I contributes to the maintenance, but not the re-establishment, of silencing at the yeast silent mating loci. *Genes Dev.* **12**(2): 219-232.

Fillingham, J., Recht, J., Silva, A.C., Suter, B., Emili, A., Stagljar, I., Krogan, N.J., Allis, C.D., Keogh, M.C., and Greenblatt, J.F. 2008. Chaperone control of the activity and specificity of the histone H3 acetyltransferase Rtt109. *Mol. Cell. Biol.* **28**(13): 4342-4353.

Fortes, P., Bilbao-Cortes, D., Fornerod, M., Rigaut, G., Raymond, W., Seraphin, B., and Mattaj, I.W. 1999. Luc7p, a novel yeast U1 snRNP protein with a role in 5' splice site recognition. *Genes Dev.* **13**(18): 2425-2438.

Foss, M., McNally, F.J., Laurenson, P., and Rine, J. 1993. Origin recognition complex (ORC) in transcriptional silencing and DNA replication in *S. cerevisiae*. *Science* **262**(5141): 1838-1844.

Freeman-Cook, L.L., Gomez, E.B., Spedale, E.J., Marlett, J., Forsburg, S.L., Pillus, L., and Laurenson, P. 2005. Conserved locus-specific silencing functions of *Schizosaccharomyces pombe sir2+*. *Genetics* **169**(3): 1243-1260.

Fritze, C.E., Verschueren, K., Strich, R., and Easton Esposito, R. 1997. Direct evidence for *SIR2* modulation of chromatin structure in yeast rDNA. *EMBO J.* **16**(21): 6495-6509.

Fung, C.W., Mozlin, A.M., and Symington, L.S. 2009. Suppression of the Double-Strand-Break-Repair Defect of the *Saccharomyces cerevisiae rad57* Mutant. *Genetics* **181**(4): 1195-1206.

Galgoczy, D.J., Cassidy-Stone, A., Llinas, M., O'Rourke, S.M., Herskowitz, I., DeRisi, J.L., and Johnson, A.D. 2004. Genomic dissection of the cell-type-specification circuit in *Saccharomyces cerevisiae*. *Proc. Natl. Acad. Sci. USA* **101**(52): 18069-18074.

Gao, L. and Gross, D.S. 2008. Sir2 silences gene transcription by targeting the transition between RNA polymerase II initiation and elongation. *Mol. Cell. Biol.* **28**(12): 3979-3994.

Garcia, S.N. 2003. Characterization of a unique class of *sir2* mutants and novel Sir2p interactors in the yeast *Saccharomyces cerevisiae* In *Biology*. Ph.D dissertation. University of California, San Diego, La Jolla, CA.

Garcia, S.N. and Pillus, L. 1999. Net results of nucleolar dynamics. *Cell* **97**(7): 825-828.

Garcia, S.N. and Pillus, L. 2002. A unique class of conditional *sir2* mutants displays distinct silencing defects in *Saccharomyces cerevisiae*. *Genetics* **162**(2): 721-736.

Gardner, K.A. and Fox, C.A. 2001. The Sir1 protein's association with a silenced chromosome domain. *Genes Dev.* **15**(2): 147-157.

Geissenhoner, A., Weise, C., and Ehrenhofer-Murray, A.E. 2004. Dependence of ORC silencing function on NatA-mediated Nalpha acetylation in *Saccharomyces cerevisiae*. *Mol. Cell. Biol.* **24**(23): 10300-10312.

Gentzsch, M. and Tanner, W. 1996. The *PMT* gene family: protein O-glycosylation in *Saccharomyces cerevisiae* is vital. *EMBO J.* **15**(21): 5752-5759.

Girrbach, V. and Strahl, S. 2003. Members of the evolutionarily conserved PMT family of protein O-mannosyltransferases form distinct protein complexes among themselves. *J. Biol. Chem.* **278**(14): 12554-12562.

Greenall, A., Lei, G., Swan, D.C., James, K., Wang, L., Peters, H., Wipat, A., Wilkinson, D.J., and Lydall, D. 2008. A genome wide analysis of the response to uncapped telomeres in budding yeast reveals a novel role for the NAD+ biosynthetic gene *BNA2* in chromosome end protection. *Genome Biol.* **9**(10): R146.

Grewal, S.I. and Elgin, S.C. 2007. Transcription and RNA interference in the formation of heterochromatin. *Nature* **447**(7143): 399-406.

Guarente, L. 2000. Sir2 links chromatin silencing, metabolism, and aging. *Genes Dev.* **14**(9): 1021-1026.

Hampsey, M. 1997. A review of phenotypes in *Saccharomyces cerevisiae*. *Yeast* **13**(12): 1099-1133.

Hart, G.W., Housley, M.P., and Slawson, C. 2007. Cycling of O-linked beta-N-acetylglucosamine on nucleocytoplasmic proteins. *Nature* **446**(7139): 1017-1022.

Hartland, R.P., Fontaine, T., Debeaupuis, J.P., Simenel, C., Delepierre, M., and Latge, J.P. 1996. A novel beta-(1-3)-glucanosyltransferase from the cell wall of *Aspergillus fumigatus*. *J. Biol. Chem.* **271**(43): 26843-26849.

Hecht, A., Laroche, T., Strahl-Bolsinger, S., Gasser, S.M., and Grunstein, M. 1995. Histone H3 and H4 N-termini interact with Sir3 and Sir4 proteins: a molecular model for the formation of heterochromatin in yeast. *Cell* **80**(4): 583-592.

Hecht, A., Strahl-Bolsinger, S., and Grunstein, M. 1996. Spreading of transcriptional repressor SIR3 from telomeric heterochromatin. *Nature* **383**(6595): 92-96.

Hill, J.E., Myers, A.M., Koerner, T.J., and Tzagoloff, A. 1986. Yeast/E. coli shuttle vectors with multiple unique restriction sites. *Yeast* **2**(3): 163-167.

Ho, Y., Gruhler, A., Heilbut, A., Bader, G.D., Moore, L., Adams, S.L., Millar, A., Taylor, P., Bennett, K., Boutilier, K. et al. 2002. Systematic identification of protein complexes in *Saccharomyces cerevisiae* by mass spectrometry. *Nature* **415**(6868): 180-183.

Holmes, S.G., Rose, A.B., Steuerle, K., Saez, E., Sayegh, S., Lee, Y.M., and Broach, J.R. 1997. Hyperactivation of the silencing proteins, Sir2p and Sir3p, causes chromosome loss. *Genetics* **145**(3): 605-614.

Hoppe, G.J., Tanny, J.C., Rudner, A.D., Gerber, S.A., Danaie, S., Gygi, S.P., and Moazed, D. 2002. Steps in assembly of silent chromatin in yeast: Sir3-

independent binding of a Sir2/Sir4 complex to silencers and role for Sir2-dependent deacetylation. *Mol. Cell. Biol.* **22**(12): 4167-4180.

Huang, J. and Moazed, D. 2003. Association of the RENT complex with nontranscribed and coding regions of rDNA and a regional requirement for the replication fork block protein Fob1 in rDNA silencing. *Genes Dev.* **17**(17): 2162-2176.

Huh, W.K., Falvo, J.V., Gerke, L.C., Carroll, A.S., Howson, R.W., Weissman, J.S., and O'Shea, E.K. 2003. Global analysis of protein localization in budding yeast. *Nature* **425**(6959): 686-691.

Hyland, E.M., Cosgrove, M.S., Molina, H., Wang, D., Pandey, A., Cottee, R.J., and Boeke, J.D. 2005. Insights into the role of histone H3 and histone H4 core modifiable residues in *Saccharomyces cerevisiae*. *Mol. Cell. Biol.* **25**(22): 10060-10070.

Imai, S., Armstrong, C.M., Kaeberlein, M., and Guarente, L. 2000. Transcriptional silencing and longevity protein Sir2 is an NAD-dependent histone deacetylase. *Nature* **403**(6771): 795-800.

Inoue, S.B., Takewaki, N., Takasuka, T., Mio, T., Adachi, M., Fujii, Y., Miyamoto, C., Arisawa, M., Furuichi, Y., and Watanabe, T. 1995. Characterization and gene cloning of 1,3-beta-D-glucan synthase from *Saccharomyces cerevisiae*. *Eur. J. Biochem.* **231**(3): 845-854.

Ishii, K., Arib, G., Lin, C., Van Houwe, G., and Laemmli, U.K. 2002. Chromatin boundaries in budding yeast: the nuclear pore connection. *Cell* **109**(5): 551-562.

Ito, H., Fukuda, Y., Murata, K., and Kimura, A. 1983. Transformation of intact yeast cells treated with alkali cations. *J. Bacteriol.* **153**(1): 163-168.

Jackson, S.P. and Tjian, R. 1988. O-glycosylation of eukaryotic transcription factors: implications for mechanisms of transcriptional regulation. *Cell* **55**(1): 125-133.

Jacobson, S. and Pillus, L. 2004. Molecular requirements for gene expression mediated by targeted histone acetyltransferases. *Mol. Cell. Biol.* **24**(13): 6029-6039.

James, P., Halladay, J., and Craig, E.A. 1996. Genomic libraries and a host strain designed for highly efficient two-hybrid selection in yeast. *Genetics* **144**(4): 1425-1436.

Jazayeri, A., McAinsh, A.D., and Jackson, S.P. 2004. *Saccharomyces cerevisiae* Sin3p facilitates DNA double-strand break repair. *Proc. Natl. Acad. Sci. USA* **101**(6): 1644-1649.

Jiang, Y.W. 2008. An essential role of Tap42-associated PP2A and 2A-like phosphatases in Ty1 transcriptional silencing of *S. cerevisiae*. *Yeast* **25**(10): 755-764.

Jin, Y., Rodriguez, A.M., Stanton, J.D., Kitazono, A.A., and Wyrick, J.J. 2007. Simultaneous mutation of methylated lysine residues in histone H3 causes enhanced gene silencing, cell cycle defects, and cell lethality in *Saccharomyces cerevisiae*. *Mol. Cell. Biol.* **27**(19): 6832-6841.

Kaelin, W.G., Jr., Krek, W., Sellers, W.R., DeCaprio, J.A., Ajchenbaum, F., Fuchs, C.S., Chittenden, T., Li, Y., Farnham, P.J., Blanar, M.A. et al. 1992. Expression cloning of a cDNA encoding a retinoblastoma-binding protein with E2F-like properties. *Cell* **70**(2): 351-364.

Katan-Khaykovich, Y. and Struhl, K. 2005. Heterochromatin formation involves changes in histone modifications over multiple cell generations. *EMBO J.* **24**(12): 2138-2149.

Kimmerly, W.J. and Rine, J. 1987. Replication and segregation of plasmids containing cis-acting regulatory sites of silent mating-type genes in *Saccharomyces cerevisiae* are controlled by the *SIR* genes. *Mol. Cell. Biol.* **7**(12): 4225-4237.

Kimura, A., Umehara, T., and Horikoshi, M. 2002. Chromosomal gradient of histone acetylation established by Sas2p and Sir2p functions as a shield against gene silencing. *Nat. Genet.* **32**(3): 370-377.

Kirmizis, A., Santos-Rosa, H., Penkett, C.J., Singer, M.A., Vermeulen, M., Mann, M., Bahler, J., Green, R.D., and Kouzarides, T. 2007. Arginine methylation at histone H3R2 controls deposition of H3K4 trimethylation. *Nature* **449**(7164): 928-932.

Kitamura, K. and Yamamoto, Y. 1972. Purification and properties of an enzyme, zymolyase, which lyses viable yeast cells. *Arch. Biochem. Biophys.* **153**(1): 403-406.

Kobayashi, T. and Ganley, A.R. 2005. Recombination regulation by transcription-induced cohesin dissociation in rDNA repeats. *Science* **309**(5740): 1581-1584.

Krogan, N.J., Cagney, G., Yu, H., Zhong, G., Guo, X., Ignatchenko, A., Li, J., Pu, S., Datta, N., Tikuisis, A.P. et al. 2006. Global landscape of protein complexes in the yeast *Saccharomyces cerevisiae*. *Nature* **440**(7084): 637-643.

Lafon, A., Chang, C.S., Scott, E.M., Jacobson, S.J., and Pillus, L. 2007. MYST opportunities for growth control: yeast genes illuminate human cancer gene functions. *Oncogene* **26**(37): 5373-5384.

Lagorce, A., Hauser, N.C., Labourdette, D., Rodriguez, C., Martin-Yken, H., Arroyo, J., Hoheisel, J.D., and Francois, J. 2003. Genome-wide analysis of the response to cell wall mutations in the yeast *Saccharomyces cerevisiae*. *J. Biol. Chem.* **278**(22): 20345-20357.

Landry, J., Slama, J.T., and Sternglanz, R. 2000a. Role of NAD(+) in the deacetylase activity of the SIR2-like proteins. *Biochem. Biophys. Res. Commun.* **278**(3): 685-690.

Landry, J., Sutton, A., Tafrov, S.T., Heller, R.C., Stebbins, J., Pillus, L., and Sternglanz, R. 2000b. The silencing protein SIR2 and its homologs are NAD-dependent protein deacetylases. *Proc. Natl. Acad. Sci. USA* **97**(11): 5807-5811.

Laroche, T., Martin, S.G., Gotta, M., Gorham, H.C., Pryde, F.E., Louis, E.J., and Gasser, S.M. 1998. Mutation of yeast Ku genes disrupts the subnuclear organization of telomeres. *Curr. Biol.* **8**(11): 653-656.

Le, S., Davis, C., Konopka, J.B., and Sternglanz, R. 1997. Two new S-phase-specific genes from *Saccharomyces cerevisiae*. *Yeast* **13**(11): 1029-1042.

Lesage, G. and Bussey, H. 2006. Cell wall assembly in *Saccharomyces cerevisiae*. *Microbiol. Mol. Biol. Rev.* **70**(2): 317-343.

Lesage, G., Sdicu, A.M., Menard, P., Shapiro, J., Hussein, S., and Bussey, H. 2004. Analysis of beta-1,3-glucan assembly in *Saccharomyces cerevisiae* using a synthetic interaction network and altered sensitivity to caspofungin. *Genetics* **167**(1): 35-49.

Levy-Wilson, B. 1983. Glycosylation, ADP-ribosylation, and methylation of *Tetrahymena* histones. *Biochemistry* **22**(2): 484-489.

Li, C., Mueller, J.E., and Bryk, M. 2006. Sir2 represses endogenous polymerase II transcription units in the ribosomal DNA nontranscribed spacer. *Mol. Biol. Cell* **17**(9): 3848-3859.

Liang, G., Klose, R.J., Gardner, K.E., and Zhang, Y. 2007. Yeast Jhd2p is a histone H3 Lys4 trimethyl demethylase. *Nat. Struct. Mol. Biol.* **14**(3): 243-245.

Lieb, J.D., Liu, X., Botstein, D., and Brown, P.O. 2001. Promoter-specific binding of Rap1 revealed by genome-wide maps of protein-DNA association. *Nat. Genet.* **28**(4): 327-334.

Lin, Y.Y., Lu, J.Y., Zhang, J., Walter, W., Dang, W., Wan, J., Tao, S.C., Qian, J., Zhao, Y., Boeke, J.D. et al. 2009. Protein acetylation microarray reveals that NuA4 controls key metabolic target regulating gluconeogenesis. *Cell* **136**(6): 1073-1084.

Lin, Y.Y., Qi, Y., Lu, J.Y., Pan, X., Yuan, D.S., Zhao, Y., Bader, J.S., and Boeke, J.D. 2008. A comprehensive synthetic genetic interaction network governing yeast histone acetylation and deacetylation. *Genes Dev.* **22**(15): 2062-2074.

Liou, G.G., Tanny, J.C., Kruger, R.G., Walz, T., and Moazed, D. 2005. Assembly of the SIR complex and its regulation by O-acetyl-ADP-ribose, a product of NAD-dependent histone deacetylation. *Cell* **121**(4): 515-527.

Loeillet, S., Palancade, B., Cartron, M., Thierry, A., Richard, G.F., Dujon, B., Doye, V., and Nicolas, A. 2005. Genetic network interactions among replication, repair and nuclear pore deficiencies in yeast. *DNA Repair* **4**(4): 459-468.

Loo, S. and Rine, J. 1995. Silencing and heritable domains of gene expression. *Annu. Rev. Cell. Dev. Biol.* **11**: 519-548.

Lowell, J.E., Roughton, A.I., Lundblad, V., and Pillus, L. 2003. Telomerase-independent proliferation is influenced by cell type in *Saccharomyces cerevisiae*. *Genetics* **164**(3): 909-921.

Lundblad, V. 2006. *Budding Yeast Telomeres*. Cold Spring Harbor Laboratory Press.

Luo, K., Vega-Palas, M.A., and Grunstein, M. 2002. Rap1-Sir4 binding independent of other Sir, yKu, or histone interactions initiates the assembly of telomeric heterochromatin in yeast. *Genes Dev.* **16**(12): 1528-1539.

Ma, J. and Ptashne, M. 1987. A new class of yeast transcriptional activators. *Cell* **51**(1): 113-119.

Mantovani, M.S., Bellini, M.F., Angeli, J.P., Oliveira, R.J., Silva, A.F., and Ribeiro, L.R. 2008. beta-Glucans in promoting health: prevention against mutation and cancer. *Mutat. Res.* **658**(3): 154-161.

Martin, S.G., Laroche, T., Suka, N., Grunstein, M., and Gasser, S.M. 1999. Relocalization of telomeric Ku and SIR proteins in response to DNA strand breaks in yeast. *Cell* **97**(5): 621-633.

Mazur, P., Morin, N., Baginsky, W., el-Sherbeini, M., Clemas, J.A., Nielsen, J.B., and Foor, F. 1995. Differential expression and function of two homologous subunits of yeast 1,3-beta-D-glucan synthase. *Mol. Cell. Biol.* **15**(10): 5671-5681.

McBryant, S.J., Krause, C., Woodcock, C.L., and Hansen, J.C. 2008. The silent information regulator 3 protein, Sir3p, binds to chromatin fibers and assembles a hypercondensed chromatin architecture in the presence of salt. *Mol. Cell. Biol.* **28**(11): 3563-3572.

Meikle, P.J., Bonig, I., Hoogenraad, N.J., Clarke, A.E., and Stone, B.A. 1991. The location of (1→3)-β-glucans in the walls of pollen tubes of *Nicotiana alata* using a (1→3)-β-glucan-specific monoclonal antibody. *Planta* **185**(1): 1-8.

Meneghini, M.D., Wu, M., and Madhani, H.D. 2003. Conserved histone variant H2A.Z protects euchromatin from the ectopic spread of silent heterochromatin. *Cell* **112**(5): 725-736.

Mercier, G., Berthault, N., Touleimat, N., Kepes, F., Fourel, G., Gilson, E., and Dutreix, M. 2005. A haploid-specific transcriptional response to irradiation in *Saccharomyces cerevisiae*. *Nucleic Acids Res.* **33**(20):6635-6643.

Michel, A.H., Kornmann, B., Dubrana, K., and Shore, D. 2005. Spontaneous rDNA copy number variation modulates Sir2 levels and epigenetic gene silencing. *Genes Dev.* **19**(10): 1199-1210.

Micklem, G., Rowley, A., Harwood, J., Nasmyth, K., and Diffley, J.F. 1993. Yeast origin recognition complex is involved in DNA replication and transcriptional silencing. *Nature* **366**(6450): 87-89.

Millar, C.B. and Grunstein, M. 2006. Genome-wide patterns of histone modifications in yeast. *Nat. Rev. Mol. Cell. Biol.* **7**(9): 657-666.

Miller, A., Yang, B., Foster, T., and Kirchmaier, A.L. 2008. Proliferating cell nuclear antigen and *ASF1* modulate silent chromatin in *Saccharomyces cerevisiae* via lysine 56 on histone H3. *Genetics* **179**(2): 793-809.

Milne, G.T., Jin, S., Shannon, K.B., and Weaver, D.T. 1996. Mutations in two Ku homologs define a DNA end-joining repair pathway in *Saccharomyces cerevisiae*. *Mol. Cell. Biol.* **16**(8): 4189-4198.

Mitchell, L., Lambert, J.P., Gerdes, M., Al-Madhoun, A.S., Skerjanc, I.S., Figeys, D., and Baetz, K. 2008. Functional dissection of the NuA4 histone acetyltransferase reveals its role as a genetic hub and that Eaf1 is essential for complex integrity. *Mol. Cell. Biol.* **28**(7): 2244-2256.

Moazed, D., Kistler, A., Axelrod, A., Rine, J., and Johnson, A.D. 1997. Silent information regulator protein complexes in *Saccharomyces cerevisiae*: a SIR2/SIR4 complex and evidence for a regulatory domain in SIR4 that inhibits its interaction with SIR3. *Proc. Natl. Acad. Sci. USA* **94**(6): 2186-2191.

Mondoux, M.A. and Zakian, V.A. 2006. *Telomere Position Effect: Silencing Near the End*. Cold Spring Harbor Laboratory Press.

Moretti, P., Freeman, K., Coodly, L., and Shore, D. 1994. Evidence that a complex of Sir proteins interacts with the silencer and telomere-binding protein Rap1. *Genes Dev.* **8**(19): 2257-2269.

Moretti, P. and Shore, D. 2001. Multiple interactions in Sir protein recruitment by Rap1p at silencers and telomeres in yeast. *Mol. Cell. Biol.* **21**(23): 8082-8094.

Mrsa, V., Klebl, F., and Tanner, W. 1993. Purification and characterization of the *Saccharomyces cerevisiae BGL2* gene product, a cell wall endo-beta-1,3-glucanase. *J. Bacteriol.* **175**(7): 2102-2106.

Murphy, G.A., Spedale, E.J., Powell, S.T., Pillus, L., Schultz, S.C., and Chen, L. 2003. The Sir4 C-terminal coiled coil is required for telomeric and mating type silencing in *Saccharomyces cerevisiae*. *J. Mol. Biol.* **334**(4): 769-780.

Nathan, D., Ingvarsdottir, K., Sterner, D.E., Bylebyl, G.R., Dokmanovic, M., Dorsey, J.A., Whelan, K.A., Krsmanovic, M., Lane, W.S., Meluh, P.B. et al. 2006. Histone sumoylation is a negative regulator in *Saccharomyces cerevisiae* and shows dynamic interplay with positive-acting histone modifications. *Genes Dev.* **20**(8): 966-976.

Nugent, C.I., Bosco, G., Ross, L.O., Evans, S.K., Salinger, A.P., Moore, J.K., Haber, J.E., and Lundblad, V. 1998. Telomere maintenance is dependent on activities required for end repair of double-strand breaks. *Curr. Biol.* **8**(11): 657-660.

Nuoffer, C., Jeno, P., Conzelmann, A., and Riezman, H. 1991. Determinants for glycophospholipid anchoring of the *Saccharomyces cerevisiae* Gas1 protein to the plasma membrane. *Mol. Cell. Biol.* **11**(1): 27-37.

Oki, M., Valenzuela, L., Chiba, T., Ito, T., and Kamakaka, R.T. 2004. Barrier proteins remodel and modify chromatin to restrict silenced domains. *Mol. Cell. Biol.* **24**(5): 1956-1967.

Ozdemir, A., Masumoto, H., Fitzjohn, P., Verreault, A., and Logie, C. 2006. Histone H3 lysine 56 acetylation: a new twist in the chromosome cycle. *Cell Cycle* **5**(22): 2602-2608.

Palladino, F., Laroche, T., Gilson, E., Axelrod, A., Pillus, L., and Gasser, S.M. 1993. SIR3 and SIR4 proteins are required for the positioning and integrity of yeast telomeres. *Cell* **75**(3): 543-555.

Papaleo, E., Fantucci, P., Vai, M., and De Gioia, L. 2006. Three-dimensional structure of the catalytic domain of the yeast beta-(1,3)-glucan transferase Gas1: a molecular modeling investigation. *J. Mol. Model.* **12**(2): 237-248.

Parsons, X.H., Garcia, S.N., Pillus, L., and Kadonaga, J.T. 2003. Histone deacetylation by Sir2 generates a transcriptionally repressed nucleoprotein complex. *Proc. Natl. Acad. Sci. USA* **100**(4): 1609-1614.

Peng, W., Togawa, C., Zhang, K., and Kurdistani, S.K. 2008. Regulators of cellular levels of histone acetylation in *Saccharomyces cerevisiae*. *Genetics* **179**(1): 277-289.

Pillus, L. 2008. MYSTs mark chromatin for chromosomal functions. *Curr. Opin. Cell. Biol.* **20**(3): 326-333.

Popolo, L., Gilardelli, D., Bonfante, P., and Vai, M. 1997. Increase in chitin as an essential response to defects in assembly of cell wall polymers in the *ggp1*delta mutant of *Saccharomyces cerevisiae*. *J. Bacteriol.* **179**(2): 463-469.

Popolo, L. and Vai, M. 1999. The Gas1 glycoprotein, a putative wall polymer cross-linker. *Biochim. Biophys. Acta.* **1426**(2): 385-400.

Popolo, L., Vai, M., Gatti, E., Porello, S., Bonfante, P., Balestrini, R., and Alberghina, L. 1993. Physiological analysis of mutants indicates involvement of the *Saccharomyces cerevisiae* GPI-anchored protein gp115 in morphogenesis and cell separation. *J. Bacteriol.* **175**(7): 1879-1885.

Primig, M., Williams, R.M., Winzeler, E.A., Tevzadze, G.G., Conway, A.R., Hwang, S.Y., Davis, R.W., and Esposito, R.E. 2000. The core meiotic transcriptome in budding yeasts. *Nat. Genet.* **26**(4): 415-423.

Ragni, E., Coluccio, A., Rolli, E., Rodriguez-Pena, J.M., Colasante, G., Arroyo, J., Neiman, A.M., and Popolo, L. 2007a. *GAS2* and *GAS4*, a pair of developmentally regulated genes required for spore wall assembly in *Saccharomyces cerevisiae*. *Eukaryot. Cell* **6**(2): 302-316.

Ragni, E., Fontaine, T., Gissi, C., Latge, J.P., and Popolo, L. 2007b. The Gas family of proteins of *Saccharomyces cerevisiae*: characterization and evolutionary analysis. *Yeast* **24**(4): 297-308.

Ray, A., Hector, R.E., Roy, N., Song, J.H., Berkner, K.L., and Runge, K.W. 2003. Sir3p phosphorylation by the Slt2p pathway effects redistribution of silencing function and shortened lifespan. *Nat. Genet.* **33**(4): 522-526.

Reeves, R., Chang, D., and Chung, S.C. 1981. Carbohydrate modifications of the high mobility group proteins. *Proc. Natl. Acad. Sci. USA* **78**(11): 6704-6708.

Renauld, H., Aparicio, O.M., Zierath, P.D., Billington, B.L., Chhablani, S.K., and Gottschling, D.E. 1993. Silent domains are assembled continuously from the telomere and are defined by promoter distance and strength, and by *SIR3* dosage. *Genes Dev.* **7**(7A): 1133-1145.

Rine, J. and Herskowitz, I. 1987. Four genes responsible for a position effect on expression from *HML* and *HMR* in *Saccharomyces cerevisiae*. *Genetics* **116**(1): 9-22.

Roemer, T. and Bussey, H. 1991. Yeast beta-glucan synthesis: *KRE6* encodes a predicted type II membrane protein required for glucan synthesis in vivo and for glucan synthase activity in vitro. *Proc. Natl. Acad. Sci. USA* **88**(24): 11295-11299.

Roemer, T., Delaney, S., and Bussey, H. 1993. *SKN1* and *KRE6* define a pair of functional homologs encoding putative membrane proteins involved in beta-glucan synthesis. *Mol. Cell. Biol.* **13**(7): 4039-4048.

Roy, N. and Runge, K.W. 2000. Two paralogs involved in transcriptional silencing that antagonistically control yeast life span. *Curr. Biol.* **10**(2): 111-114.

Rudner, A.D., Hall, B.E., Ellenberger, T., and Moazed, D. 2005. A nonhistone protein-protein interaction required for assembly of the SIR complex and silent chromatin. *Mol. Cell. Biol.* **25**(11): 4514-4528.

Rundlett, S.E., Carmen, A.A., Kobayashi, R., Bavykin, S., Turner, B.M., and Grunstein, M. 1996. Hda1 and Rpd3 are members of distinct yeast histone deacetylase complexes that regulate silencing and transcription. *Proc. Natl. Acad. Sci. USA* **93**(25): 14503-14508.

Rusche, L.N., Kirchmaier, A.L., and Rine, J. 2002. Ordered nucleation and spreading of silenced chromatin in *Saccharomyces cerevisiae*. *Mol. Biol. Cell* **13**(7): 2207-2222.

Rusche, L.N., Kirchmaier, A.L., and Rine, J. 2003. The establishment, inheritance, and function of silenced chromatin in *Saccharomyces cerevisiae*. *Annu. Rev. Biochem.* **72**: 481-516.

Sasaki, T. and Gilbert, D.M. 2007. The many faces of the origin recognition complex. *Curr. Opin. Cell. Biol.* **19**(3): 337-343.

Schild, D. 1995. Suppression of a new allele of the yeast *RAD52* gene by overexpression of *RAD51*, mutations in *srs2* and *ccr4*, or mating-type heterozygosity. *Genetics* **140**(1): 115-127.

Schones, D.E. and Zhao, K. 2008. Genome-wide approaches to studying chromatin modifications. *Nat. Rev. Genet.* **9**(3): 179-191.

Schuldiner, M., Collins, S.R., Thompson, N.J., Denic, V., Bhamidipati, A., Punna, T., Ihmels, J., Andrews, B., Boone, C., Greenblatt, J.F. et al. 2005. Exploration of the function and organization of the yeast early secretory pathway through an epistatic miniarray profile. *Cell* **123**(3): 507-519.

Sekiya-Kawasaki, M., Abe, M., Saka, A., Watanabe, D., Kono, K., Minemura-Asakawa, M., Ishihara, S., Watanabe, T., and Ohya, Y. 2002. Dissection of upstream regulatory components of the Rho1p effector, 1,3-beta-glucan synthase, in *Saccharomyces cerevisiae*. *Genetics* **162**(2): 663-676.

Shahbazian, M.D. and Grunstein, M. 2007. Functions of site-specific histone acetylation and deacetylation. *Annu. Rev. Biochem.* **76**: 75-100.

Shen, S.H., Chretien, P., Bastien, L., and Slilaty, S.N. 1991. Primary sequence of the glucanase gene from *Oerskovia xanthineolytica*. Expression and purification of the enzyme from *Escherichia coli*. *J. Biol. Chem.* **266**(2): 1058-1063.

Sherman, F. 1991. Getting started with yeast. *Methods Enzymol.* **194**: 3-21.

Sherman, J.M., Stone, E.M., Freeman-Cook, L.L., Brachmann, C.B., Boeke, J.D., and Pillus, L. 1999. The conserved core of a human *SIR2* homologue functions in yeast silencing. *Mol. Biol. Cell* **10**(9): 3045-3059.

Shia, W.J., Li, B., and Workman, J.L. 2006. SAS-mediated acetylation of histone H4 Lys 16 is required for H2A.Z incorporation at subtelomeric regions in *Saccharomyces cerevisiae*. *Genes Dev.* **20**(18): 2507-2512.

Shia, W.J., Osada, S., Florens, L., Swanson, S.K., Washburn, M.P., and Workman, J.L. 2005. Characterization of the yeast trimeric-SAS acetyltransferase complex. *J. Biol. Chem.* **280**(12): 11987-11994.

Shilatifard, A. 2006. Chromatin modifications by methylation and ubiquitination: implications in the regulation of gene expression. *Annu. Rev. Biochem.* **75**: 243-269.

Shore, D. 1994. RAP1: a protean regulator in yeast. *Trends Genet.* **10**(11): 408-412.

Sikorski, R.S. and Hieter, P. 1989. A system of shuttle vectors and yeast host strains designed for efficient manipulation of DNA in *Saccharomyces cerevisiae*. *Genetics* **122**(1): 19-27.

Smith, J.S. and Boeke, J.D. 1997. An unusual form of transcriptional silencing in yeast ribosomal DNA. *Genes Dev.* **11**(2): 241-254.

Smith, J.S., Brachmann, C.B., Pillus, L., and Boeke, J.D. 1998. Distribution of a limited Sir2 protein pool regulates the strength of yeast rDNA silencing and is modulated by Sir4p. *Genetics* **149**(3): 1205-1219.

Smith, M.M. 1991. Histone structure and function. *Curr. Opin. Cell. Biol.* **3**(3): 429-437.

Stone, E.M. and Pillus, L. 1996. Activation of an MAP kinase cascade leads to Sir3p hyperphosphorylation and strengthens transcriptional silencing. *J. Cell Biol.* **135**(3): 571-583.

Strahl-Bolsinger, S., Immervoll, T., Deutzmann, R., and Tanner, W. 1993. *PMT1*, the gene for a key enzyme of protein O-glycosylation in *Saccharomyces cerevisiae*. *Proc. Natl. Acad. Sci. USA* **90**(17): 8164-8168.

Suka, N., Luo, K., and Grunstein, M. 2002. Sir2p and Sas2p opposingly regulate acetylation of yeast histone H4 lysine16 and spreading of heterochromatin. *Nat. Genet.* **32**(3): 378-383.

Suka, N., Suka, Y., Carmen, A.A., Wu, J., and Grunstein, M. 2001. Highly specific antibodies determine histone acetylation site usage in yeast heterochromatin and euchromatin. *Mol. Cell* **8**(2): 473-479.

Sun, Z.W. and Hampsey, M. 1999. A general requirement for the Sin3-Rpd3 histone deacetylase complex in regulating silencing in *Saccharomyces cerevisiae*. *Genetics* **152**(3): 921-932.

Sussel, L., Vannier, D., and Shore, D. 1993. Epigenetic switching of transcriptional states: cis- and trans-acting factors affecting establishment of silencing at the *HMR* locus in *Saccharomyces cerevisiae*. *Mol. Cell. Biol.* **13**(7): 3919-3928.

Suter, B., Tong, A., Chang, M., Yu, L., Brown, G.W., Boone, C., and Rine, J. 2004. The origin recognition complex links replication, sister chromatid cohesion and transcriptional silencing in *Saccharomyces cerevisiae*. *Genetics* **167**(2): 579-591.

Sutterlin, C., Doering, T.L., Schimmoller, F., Schroder, S., and Riezman, H. 1997. Specific requirements for the ER to Golgi transport of GPI-anchored proteins in yeast. *J. Cell Sci.* **110 (Pt 21)**: 2703-2714.

Tanner, K.G., Landry, J., Sternglanz, R., and Denu, J.M. 2000. Silent information regulator 2 family of NAD- dependent histone/protein deacetylases generates a unique product, 1-O-acetyl-ADP-ribose. *Proc. Natl. Acad. Sci. USA* **97**(26): 14178-14182.

Tanny, J.C., Dowd, G.J., Huang, J., Hilz, H., and Moazed, D. 1999. An enzymatic activity in the yeast Sir2 protein that is essential for gene silencing. *Cell* **99**(7): 735-745.

Tanny, J.C. and Moazed, D. 2001. Coupling of histone deacetylation to NAD breakdown by the yeast silencing protein Sir2: Evidence for acetyl transfer from substrate to an NAD breakdown product. *Proc. Natl. Acad. Sci. USA* **98**(2): 415-420.

Tomishige, N., Noda, Y., Adachi, H., Shimoi, H., and Yoda, K. 2005. *SKG1*, a suppressor gene of synthetic lethality of *kex2*Delta*gas1*Delta mutations, encodes a novel membrane protein that affects cell wall composition. *Yeast* **22**(2): 141-155.

Tompa, R. and Madhani, H.D. 2007. Histone H3 lysine 36 methylation antagonizes silencing in *Saccharomyces cerevisiae* independently of the Rpd3S histone deacetylase complex. *Genetics* **175**(2): 585-593.

Tong, A.H., Lesage, G., Bader, G.D., Ding, H., Xu, H., Xin, X., Young, J., Berriz, G.F., Brost, R.L., Chang, M. et al. 2004. Global mapping of the yeast genetic interaction network. *Science* **303**(5659): 808-813.

Toone, W.M., Aerne, B.L., Morgan, B.A., and Johnston, L.H. 1997. Getting started: regulating the initiation of DNA replication in yeast. *Annu. Rev. Microbiol.* **51**: 125-149.

Vai, M., Gatti, E., Lacana, E., Popolo, L., and Alberghina, L. 1991. Isolation and deduced amino acid sequence of the gene encoding gp115, a yeast glycophospholipid-anchored protein containing a serine-rich region. *J. Biol. Chem.* **266**(19): 12242-12248.

van Leeuwen, F. and Gottschling, D.E. 2002. Assays for gene silencing in yeast. *Methods Enzymol.* **350**: 165-186.

Vannier, D., Balderes, D., and Shore, D. 1996. Evidence that the transcriptional regulators *SIN3* and *RPD3*, and a novel gene (*SDS3*) with similar functions, are

involved in transcriptional silencing in *S. cerevisiae*. *Genetics* **144**(4): 1343-1353.

Vannier, D., Damay, P., and Shore, D. 2001. A role for Sds3p, a component of the Rpd3p/Sin3p deacetylase complex, in maintaining cellular integrity in Saccharomyces cerevisiae. *Mol. Genet. Genomics* **265**(3): 560-568.

Vasiljeva, L., Kim, M., Terzi, N., Soares, L.M., and Buratowski, S. 2008. Transcription termination and RNA degradation contribute to silencing of RNA polymerase II transcription within heterochromatin. *Mol. Cell* **29**(3): 313-323.

Venkatasubrahmanyam, S., Hwang, W.W., Meneghini, M.D., Tong, A.H., and Madhani, H.D. 2007. Genome-wide, as opposed to local, antisilencing is mediated redundantly by the euchromatic factors Set1 and H2A.Z. *Proc. Natl. Acad. Sci. USA* **104**(42): 16609-16614.

Wang, W. and Malcolm, B.A. 1999. Two-stage PCR protocol allowing introduction of multiple mutations, deletions and insertions using QuikChange Site-Directed Mutagenesis. *Biotechniques* **26**(4): 680-682.

Wang, X., Connelly, J.J., Wang, C.L., and Sternglanz, R. 2004. Importance of the Sir3 N terminus and its acetylation for yeast transcriptional silencing. *Genetics* **168**(1): 547-551.

Weake, V.M. and Workman, J.L. 2008. Histone ubiquitination: triggering gene activity. *Mol. Cell* **29**(6): 653-663.

Wilson, B., Erdjument-Bromage, H., Tempst, P., and Cairns, B.R. 2006a. The RSC chromatin remodeling complex bears an essential fungal-specific protein module with broad functional roles. *Genetics* **172**(2): 795-809.

Wilson, J.M., Le, V.Q., Zimmerman, C., Marmorstein, R., and Pillus, L. 2006b. Nuclear export modulates the cytoplasmic Sir2 homologue Hst2. *EMBO Rep.* **7**(12): 1247-1251.

Wohlschlegel, J.A., Johnson, E.S., Reed, S.I., and Yates, J.R., 3rd. 2004. Global analysis of protein sumoylation in *Saccharomyces cerevisiae*. *J. Biol. Chem.* **279**(44): 45662-45668.

Wongwisansri, S. and Laybourn, P.J. 2004. Reconstitution of yeast chromatin using yNap1p. *Methods Enzymol.* **375**: 103-117.

Wood, A., Schneider, J., and Shilatifard, A. 2005. Cross-talking histones: implications for the regulation of gene expression and DNA repair. *Biochem. Cell Biol.* **83**(4): 460-467.

Wyatt, H.R., Liaw, H., Green, G.R., and Lustig, A.J. 2003. Multiple roles for *Saccharomyces cerevisiae* histone H2A in telomere position effect, Spt phenotypes and double-strand-break repair. *Genetics* **164**(1): 47-64.

Xu, F., Zhang, Q., Zhang, K., Xie, W., and Grunstein, M. 2007. Sir2 deacetylates histone H3 lysine 56 to regulate telomeric heterochromatin structure in yeast. *Mol. Cell* **27**(6): 890-900.

Yang, B., Britton, J., and Kirchmaier, A.L. 2008a. Insights into the impact of histone acetylation and methylation on Sir protein recruitment, spreading, and silencing in *Saccharomyces cerevisiae*. *J. Mol. Biol.*

Yang, B. and Kirchmaier, A.L. 2006. Bypassing the catalytic activity of SIR2 for SIR protein spreading in *Saccharomyces cerevisiae*. *Mol. Biol. Cell* **17**(12): 5287-5297.

Yang, B., Miller, A., and Kirchmaier, A.L. 2008b. HST3/HST4-dependent deacetylation of lysine 56 of histone H3 in silent chromatin. *Mol. Biol. Cell* **19**(11): 4993-5005.

Ye, J., Ai, X., Eugeni, E.E., Zhang, L., Carpenter, L.R., Jelinek, M.A., Freitas, M.A., and Parthun, M.R. 2005. Histone H4 lysine 91 acetylation a core domain modification associated with chromatin assembly. *Mol. Cell* **18**(1): 123-130.

Zhang, L., Eugeni, E.E., Parthun, M.R., and Freitas, M.A. 2003. Identification of novel histone post-translational modifications by peptide mass fingerprinting. *Chromosoma* **112**(2): 77-86.